



**Ciências
ULisboa**

Modified gravity: from theoretical aspects to observational constraints

“Documento Definitivo”

Doutoramento em Física

Ismael Ayuso Marazuela

Tese orientada por:

Doutor José Pedro Mimoso

Doutor Francisco Lobo

Documento especialmente elaborado para a obtenção do grau de doutor

UNIVERSIDADE DE LISBOA

FACULDADE DE CIÊNCIAS



Ciências
ULisboa

Modified gravity: from theoretical aspects to observational constraints

Doutoramento em Física

Ismael Ayuso Marazuela

Tese orientada por:

Doutor José Pedro Mimoso

Doutor Francisco Lobo

Júri:

Presidente:

- José Manuel de Nunes Vicente e Rebordão, Investigador Coordenador e Presidente do Departamento de Física da Faculdade de Ciências da Universidade de Lisboa

Vogais:

- Doutor Gonzalo Olmo Alba, PDI-Titular d'Universitat Departament de Física Teòrica da Universitat de València (Espanha)
- Doutora Mariam Bouhmadi-Lopéz, Ikerbasque Research Fellow Facultad de Ciencia y Tecnología da Universidad del País Vasco
- Doutor Pedro Pina Avelino, Professor Associado Faculdade de Ciências da Universidade do Porto
- Doutor José Pedro Oliveira Mimoso, Professor Associado Faculdade de Ciências da Universidade de Lisboa (orientador)

Documento especialmente elaborado para a obtenção do grau de doutor
Trabalho financiado por IDPASC e pela Fundação para a Ciência e a Tecnologia através
da bolsa de doutoramento PD/BD/114435/2016

Me gusta que desbarren. Ése es el único privilegio de que goza el ser humano sobre los demás organismos. Desbarrando se puede llegar hasta la verdad. Porque desbarro, soy un ser humano. A ninguna verdad se ha llegado nunca sin haber errado antes catorce veces, o quizá ciento catorce veces, y eso es un honor hasta cierto punto. Pero el caso es que nosotros ni siquiera somos capaces de desbarrar por cuenta propia. Dime sandeces, pero que sean de tu propia cosecha y soy capaz de darte un beso.

Crimen y Castigo de Fiódor Dostoievski

“If you talk to a man in a language he understands, that goes to his head. If you talk to him in his own language, that goes to his heart.”

Nelson Mandela

Agradecimientos - Acknowledgments

Todo este trabajo y esta tesis no habrían salido adelante sin el apoyo y el conocimiento de muchísimas personas. Por eso, me gustaría dedicar todos los resultados a ellas y decirles GRACIAS (sí, con mayúsculas).

Quiero comenzar y agradecer en primer lugar a mis directores de tesis, José Pedro Mimoso y Francisco Lobo, que me acogieron en Lisboa, me formaron como estudiante de doctorado y sin cuyo apoyo en momentos adversos no existiría esta tesis. Además, tengo que agradecer a IDPASC (International Doctorate Network in Particle Physics, Astrophysics and Cosmology) y a la Fundação para a Ciência e a Tecnologia (FCT) por el apoyo financiero a través de la beca PD/BD/114435/2016, así como al proyecto UIDB/04434/2020 por parte del Instituto de Astrofísica de Portugal y de la FCT. Igualmente gracias a Natalia Antunes por su simpatía y disponibilidad para ayudarme con todo lo relacionado con IDPASC.

No obstante, no me puedo olvidar de mi origen, de cómo crecí en Segovia rodeado de personas con las que sonreír y mirar a las estrellas. De cómo esas personas soportaban mis muchas divagaciones sobre el Universo y temperaturas bajo cero cuando yo decidía hacer una salida astronómica. Quiero agradecer por ello a Fátima García, Mónica Sanz, Benjamín Cid, Raquel García, Beatriz López, Miriam García, Laura Esteban, Mónica Hernández, Clara Barreno, María González y Diego Chanes. También quiero agradecer a la Asociación Hespérides de Ciencia y Tecnología por darme de beber de su ilusión durante tantas noches de telescopios, cuando yo apenas levantaba un palmo del suelo.

En la Universidad Complutense este deseo por entender el Universo no hizo más que agravarse gracias a profesores como Enrique Maciá, Javier Gorgas, Luis Garay, Álvaro de la Cruz, Jose Cembranos, Jose Beltrán y Antonio Maroto; y que tantas y tantas preguntas mías han tenido que soportar sin perder en ningún momento la paciencia y la ilusión por querer enseñar. Pero

también se lo debo a mis compañeros del Grado y del Máster en Física Teórica con los que también compartíamos momentos de frustración, estrés o miedo, y que siempre eran mejor llevados con una sonrisa o un abrazo. No puedo dejar de mencionar a Elena García, Lucía Solis, Paula Santos, Félix Carrascoso, Javier Barea, María Benítez, Aleksander Kubicki y José Garre. Y por supuesto no puedo dejar en el tintero a Marina Cermeño, Yaiza Montaña y Laura Gil, que además de compañeras en la física, me soportaban en casa. No importaba lo mal que fuese el día que ellas conseguían transformarlo en un festival, en medio del salón, entre montañas de apuntes. Tampoco me puedo olvidar de mis amigos en el Colegio Mayor Jaime del Amo que fueron como hermanos para alguien que es hijo único: Jorge Luengo, Carlos Javier Serrano y Miguel Gómez.

En este recorrido que estoy haciendo por cada una de las personas que me han ayudado y enseñado algo hasta hoy tengo que pasar obligadísimo por el Instituto de Astrofísica de Canarias donde, a través de una beca de investigación, miraba al cielo en busca de exoplanetas. Lo recuerdo como uno de los veranos con más trabajo y que más aprendí de mi vida y eso fue gracias a investigadores como Sergio Velasco y Enric Pallé, además del resto de becarios que decidimos que seríamos familia aquellos meses: Noemí González, Carlos Gómez, Elena Ruiz, Leyre Nogués, Sergio Martín, Carmen Fernández y Alfonso Gijón.

Una vez comenzado el doctorado, la Universidad de Lisboa me dio a los mejores compañeros que podía tener y con los que pasar horas hablando de ciencia: Bruno Barros, Francisco Cabral, Elsa Teixeira y Rita Neves (a la que agradezco especialmente la ayuda idiomática). Pero también me ofreció compañeros de departamento y trabajo espectaculares como Diego Sáez, Iker Leanizbarrutia, Diego Rubiera, Mercedes Martín, Ángeles Moliné, Noemi Frusciante, Elisabet Galiana e Isabel Suárez. Sin olvidarme de Marta Vicente que me regaló llevarme el portugués como nueva lengua y que siempre formará parte de mí.

Tengo que hacer también mención a mi paso por la Universidad del País Vasco a través de dos estancias de investigación en las que pude compartir conocimientos con María Ortiz, Mikel Álvarez y Mariam Bouhadi. Me quiero detener especialmente en mi agradecimiento a Ruth Lazkoz, posiblemente una de las personas de las que más he aprendido, tanto de física como en lo personal, y sin la cual esta tesis nunca habría salido adelante. Gracias por compartir la ciencia y la vida conmigo. De la misma forma, quiero agradecer a Vincenzo Salzano al que, sin que hayamos coincidido nunca en el espacio-tiempo, ha sido uno de mis grandes profesores junto

con Ruth en la parte observacional y de forma totalmente altruista.

Saliendo del ámbito científico, pero siendo defensor de la justicia, tengo que agradecer encarecidamente al Hospital General de Segovia y al Hospital Clínico de Salamanca. Sin ellos no es que no hubiese tesis, sino que sin ellos no habría Ismael Ayuso para escribirla. Pasar por un cáncer durante la elaboración de esta tesis es la situación más difícil por la que he pasado en mi vida, y gracias a ellos hoy estoy aquí. Pero no sólo me salvaron, también me dieron todo el amor, ánimo y sonrisas que necesitaba. Ojalá estas líneas sirvan para transmitirles todo el cariño y admiración que les tengo.

Y por último, como no podría ser de otra forma, quiero agradecer a mi familia. Empezando por mis tíos y primos: Luis José, Olga, Nuria y Luis que me enseñaron el valor de la familia y cuyo telescopio me abrió la ventana al Universo; mis abuelos: Claudio, Consuelo, Angelines y Arsenio que me enseñaron que no hace falta tener estudios para ser las personas a las que más admiro; y a mis padres: Angelines y Juan Vicente, que me han dado la vida con más amor que podía imaginar, y que siempre han estado apoyándome con cada decisión que iba tomando, incluso cuando en pleno invierno decidía sacar el telescopio en la meseta castellana y estaban a mi lado. Porque sin todos ellos no sería nada ni nadie.

Muchas gracias.

The work outlined in this thesis would not have been possible without the support and knowledge of many people. Therefore, I would like to dedicate all the results to them and say THANK YOU (indeed, with capital letters).

I would like to begin and firstly thank my thesis supervisors, José Pedro Mimoso and Francisco Lobo, who welcomed me in Lisbon and trained me as a doctoral student and without whose support in adverse times this thesis would not exist. In addition, I should thank to IDPASC (International Doctorate Network in Particle Physics, Astrophysics and Cosmology), and to Fundação para a Ciência e a Tecnologia (FCT) for the financial support through the grant PD/BD/114435/2016, and to Instituto de Astrofísica de Portugal and FCT for the project UIDB/04434/2020. In the same way, thank to Natalia Antunes for her sympathy and availability for helping me with the IDPASC issues.

However, I cannot forget my origins, how I grew up in Segovia surrounded by people with whom I could smile and look up at the stars. How those people put up with my many ramblings about the Universe and sub-zero temperatures when I decided to go on an astronomical outing. For this I would like to thank Fátima García, Mónica Sanz, Benjamin Cid, Raquel García, Beatriz López, Miriam García, Laura Esteban, Mónica Hernández, Clara Barreno, María González and Diego Chanes. I also want to thank the Asociación Hespérides de Ciencia y Tecnología for letting me share their illusion during so many nights of telescopes, when I barely lifted an inch from the ground.

During my stay at the Complutense University, this desire to understand the Universe only worsened thanks to professors such as Enrique Maciá, Javier Gorgas, Luis Garay, Álvaro de la Cruz, José Cembranos, Jose Beltrán and Antonio Maroto; and the hardships they had to endure with so many of my questions, without ever losing patience and enthusiasm for wanting to teach. But I also owe it to my classmates from the Bachelor's and Master's in Theoretical Physics with whom we also shared moments of frustration, stress or fear that were always better handled with a smile or a hug. I cannot fail to mention Elena García, Lucía Solis, Paula Santos, Félix Carrascoso, Javier Barea, María Benítez, Aleksander Kubicki and José Garre. And of course, I cannot leave out Marina Cermeño, Yaiza Montaña and Laura Gil, who, in addition to being colleagues in physics, put up with me at home. It didn't matter how bad the day, they managed to transform it into a festival, in the middle of the room, among mountains of notes. Nor can I forget my friends at the Colegio Mayor Jaime del Amo who were like brothers to someone who is an only child: Jorge Luengo, Carlos Javier Serrano and Miguel Gómez.

In this acknowledgment tour that I am doing for each of the people who have helped me and taught me something until today, I absolutely must go through the Instituto de Astrofísica de Canarias where, through a research grant, I looked at the sky in search of exoplanets. I remember it as one of the summers with the most work and the one I learned the most from my life, and that was thanks to researchers like Sergio Velasco and Enric Pallé, in addition to the rest of the fellows who decided that we would be family during those months: Noemí González, Carlos Gómez, Elena Ruiz, Leyre Nogués, Sergio Martín, Carmen Fernández and Alfonso Gijón.

Once I started my doctorate, the University of Lisbon gave me the best classmates I could have and with whom I spent hours talking about science: Bruno Barros, Francisco Cabral, Elsa Teixeira and Rita Neves (whom I especially thank for the help with the language). But the

University of Lisbon also offered me spectacular department and work colleagues such as Diego Sáez, Iker Leanizbarrutia, Diego Rubiera, Mercedes Martín, Ángeles Moliné, Noemi Frusciante, Elisabet Galiana and Isabel Suárez. Without forgetting the support given by Marta Vicente to take on Portuguese as a new language and that will always be part of me.

I also must mention my time at the University of the Basque Country through two research stays in which I was able to share knowledge with María Ortiz, Mikel Álvarez and Mariam Bouhmadi. I want to pay a special thanks to Ruth Lazkoz, possibly one of the people from whom I have learned the most, both in physics and personally, and without whom this thesis would never have progressed. Thank you for sharing science and life with me. In the same way, I want to thank Vincenzo Salzano who, without us ever having coincided in spacetime, has been one of my great teachers along with Ruth in the observational part in a totally altruistic way.

Leaving the scientific field, but being a defender of justice, I have to dearly thank the General Hospital of Segovia and the Clinical Hospital of Salamanca. Without them it is not that there would be no thesis, but rather that without them there would be no Ismael Ayuso to write it. Going through cancer during the preparation of this thesis is the most difficult situation I have ever experienced in my life and thanks to them I am here today. But not only did they save me, but they also gave me all the love, encouragement and smiles I needed. Hopefully these lines serve to convey all the love and admiration I have for them.

Finally, and how could it be otherwise, I want to thank my family. Starting with my uncles and cousins: Luis José, Olga, Nuria and Luis who taught me the value of family and whose telescope opened the window to the Universe for me; my grandparents: Claudio, Consuelo, Angelines and Arsenio who taught me that you don't need to have studies to be the people I admire the most; and to my parents: Angelines and Juan Vicente, who have given me a life with more love than I could imagine and who have always supported me with every decision I made, even when in the middle of winter when I decided to take out the telescope on the Castilian plateau and stayed close to me. Because without all of them I would be nothing and no one.

Thank you very much.

Resumo e palavras-chave

A Relatividade Geral é um dos pilares atuais da Física. Esta teoria consegue explicar a gravidade à escala do Sistema Solar, mas não só, já que nos oferece um modelo cosmológico quando é aplicada à evolução do Universo. Não obstante, quando tentamos explicar essas escalas maiores e as suas observações, aparecem algumas perguntas desafiantes.

A primeira questão resulta da observação acelerada do Universo que, na Relatividade Geral, é resolvida (ou “remediada”) mediante a introdução de uma componente material com pressão negativa, que produz um efeito repulsivo. No entanto este tipo de matéria viola algumas das condições de energia que normalmente devem ser satisfeitas pela matéria. O exemplo mais conhecido e importante é o da constante cosmológica usualmente representada por Λ .

A segunda questão diz respeito à consideração da matéria escura. Esta nova componente é necessária para conseguirmos explicar alguns fenómenos como o da formação das estruturas no Universo ou o achatamento das curvas de velocidade de rotação das estrelas à volta do centro das galáxias. Porém, esta matéria, que apenas se manifesta gravitacionalmente, não foi ainda detetada diretamente através da sua interação com a matéria que conhecemos dos laboratórios e das experiências.

No propósito de resolvermos ou percebermos melhor estes problemas, um caminho possível é o de irmos além da Relatividade Geral e investigarmos modificações da teoria de Albert Einstein. É este o ponto de partida da presente tese.

A nossa primeira etapa neste estudo é dedicada à possibilidade de haver um acoplamento dinâmico entre um campo escalar e a geometria. Desta maneira, começamos focando-nos em teorias escalar-tensoriais, que generalizam a teoria de Brans-Dicke e que nos fornecem um enquadramento perfeito para analisar a possibilidade do acoplamento gravitacional dado por G , constante gravitacional, ser substituído por um campo escalar dinâmico, ϕ . O trabalho em que

se baseia este Capítulo 2 da tese, foi publicado em:

- **What if Newton's Gravitational Constant Was Negative?**

Ismael Ayuso, José P. Mimoso, Nelson J. Nunes, *Galaxies* 7, (2019) 1, 38;
arXiv: 1903.07604 [gr-qc].

Estuda-se um mecanismo cosmológico que possibilite definir o sinal da constante gravitacional efetiva, G . O principal resultado que se obtém é a descoberta de que modelos com um potencial quadrático estabilizam naturalmente o valor de G no ramo positivo da evolução. Esse processo é acompanhado por inflação de de-Sitter e assim um relaxamento para a Relatividade Geral é também alcançado.

Prosseguindo nesta via de modificação da gravidade no domínio das teorias escalar-tensoriais, ou seja de teorias da gravitação não-minimamente acoplada, generalizamos a ação do Capítulo 2 mediante um acoplamento mais geral entre a gravidade e o campo escalar adicional. Isso permite-nos estudar de que modo essa extensão pode afetar o acoplamento com o modelo padrão das partículas. Esta questão é abordada no Capítulo 3, baseado no artigo publicado:

- **Nonminimal scalar-tensor theories**

Ismael Ayuso, Jose A.R. Cembranos, *Physical Review D* 101, (2020) 4, 044007;
arXiv: 1411.1653 [gr-qc].

Neste artigo mostramos que os estados perturbativos destas teorias são dados por dois modos massivos de spin-0, além de um estado sem massa de spin 2. Este último modo pode ser identificado com o campo do gravitão.

No que se segue, ainda no quadro das teorias escalar-tensoriais, consideramos a teoria de Horndeski que constitui a teoria métrica da gravidade mais geral com um único campo escalar adicional, a desempenhar um papel gravitacional, que evita a instabilidade de Ostrogradsky e resulta em equações de campo de segunda ordem. Estudamos o buraco negro descrito pelo espaço-tempo de Nariai nesta teoria. Este buraco negro é caracterizado por ser o caso extremo do buraco negro Schwarzschild de-Sitter quando os dois horizontes, cosmológico e de acontecimentos, coincidem na mesma superfície. A motivação para este estudo decorre deste tipo de objetos nos oferecer um enquadramento apropriado para se testar a nova fenomenologia das teorias de gravidade modificada de Horndeski. Para entendermos melhor tanto os buracos negros

como o Lagrangiano de Horndeski, estudamos o fenômeno designado por anti-evaporação. O Capítulo 4 é baseado na publicação:

- **Extremal cosmological black holes in Horndeski gravity and the anti-evaporation regime**

Ismael Ayuso, Diego Saez-Chillon Gomez, Universe 6, (2020) 11, 210;
arXiv: 2004.10139 [gr-qc].

Mostramos que, em alguns casos do Lagrangiano de Horndeski e ao contrário do que sucede noutras teorias de gravidade modificadas, o raio do horizonte permanece estável quando perturbações de ordem linear são consideradas.

Uma maneira totalmente diferente de modificar a gravidade é exposta no Capítulo 5, onde introduzimos teorias Lagrangianas dependentes de ação e as aplicamos ao estudo de buracos de minhoca (i.e., "wormholes"). Neste capítulo investigamos se esta classe de teorias da gravidade modificada nos permite satisfazer as condições de energia para o conteúdo de matéria deste tipo de objetos exóticos. Este capítulo é baseado na publicação:

- **Wormhole geometries induced by action-dependent Lagrangian theories**

Ismael Ayuso, Francisco S.N. Lobo, José P. Mimoso, Physical Review D103, (2021) 4, 044018; arXiv: 2012.00047 [gr-qc].

No contexto deste trabalho, as equações de campo gravitacionais dependem essencialmente de um 4-vetor λ_μ , que desempenha o papel de um parâmetro de acoplamento associado à maneira como a ação depende do Lagrangiano gravitacional e que, genericamente, pode depender das coordenadas do espaço-tempo. Neste estudo, considerando diferentes buracos de minhoca, onde usamos as coordenadas de Buchdahl que, após a análise das equações de campo nos levam à constatação de que o 4-vector é dado por $\lambda_\mu = (0, 0, \lambda_\theta, 0)$, conjuntamente com algumas restrições adicionais do espaço-tempo. Para uma infinidade de exemplos de buracos de minhoca e fazendo a escolha de uma lei de potência para a função λ_θ , mostramos que esses objetos compactos possuem uma estrutura geométrica muito mais rica do que as correspondentes soluções da Relatividade Geral. No entanto, apesar dessa estrutura mais rica, todos os exemplos estudados violam alguma das condições de energia e não conseguimos avanços para obviar este problema.

Na parte subsequente desta tese exploramos a interação entre a teoria e as observações. Trata-se de um passo indispensável para contrastar qualquer modelo de gravidade modificada com as restrições dadas pelas observações, bem assim como para obter uma maneira de ajustar parâmetros livres das teorias de modo a reproduzir as observações. Com este propósito, apresentamos no Capítulo 6 o método de Markov Chain Monte Carlo (MCMC) e também alguns outros conceitos estatísticos importantes que nos ajudam a discriminar os modelos propostos. Também indicamos as diferentes fontes de dados observacionais com as quais podemos realizar as restrições e os ajustes.

Para aplicar a metodologia MCMC consideramos alguns modelos baseados no escalar de não metricidade Q , que são explicados no Capítulo 7, onde obtemos as respectivas equações de Friedmann modificadas. Este tipo de teorias de gravidade modificada ser-nos-á útil para analisar o conceito de conexão numa variedade geométrica, bem assim como para esclarecer o significado físico de cada uma das três partes em que pode ser dividida. No caso das teorias $f(Q)$ estudamos três modelos: a teoria da Relatividade Geral mimética estendida de $f(Q)$, o modelo DGP (motivado pela gravidade modificada por dimensões adicionais) e o DGPish (assim chamado pela sua semelhança com o anterior). As conclusões do primeiro modelo encontram-se expostas em:

- **Observational constraints on cosmological solutions of $f(Q)$ theories**

Ismael Ayuso, Ruth Lazkoz, Vincenzo Salzano, Physical Review D103, (2021) 6, 063505; arXiv: 2012.00046 [astro-ph.CO].

e a análise dos outros dois modelos em:

- **DGP and DGPish cosmologies from $f(Q)$ actions**

Ismael Ayuso, Ruth Lazkoz, José Pedro Mimoso, Physical Review D105, (2022) 8, 083534; arXiv: 2111.05061 [astro-ph.CO].

Nestes trabalhos, concluímos que, com a precisão das observações atuais, os melhores ajustes de nossos modelos $f(Q)$ correspondem a valores dos seus parâmetros específicos que os tornam dificilmente discerníveis do modelo Λ CDM ou, por outras palavras, esses cenários não revelam assinaturas indicando um desvio do comportamento associado a Λ CDM.

Por último, no Capítulo 8 fazemos uma discussão geral dos resultados desta tese e tiramos algumas conclusões, lembrando que os principais objetivos desta tese são a análise de algumas das principais modificações das teorias da gravidade sugeridas pelo teorema de Lovelock, o estudo da nova fenomenologia que nelas aparece e a comparação com as observações (a pensar já nas próximas missões tal como Euclid e Lisa)

Além disso, outras publicações durante a tese são:

- **Commissioning and First Observations with Wide FastCam at the Telescopio Carlos Sánchez**

Sergio Velasco, Urtats Etxegarai, Alejandro Oscoz, Roberto L. López, Marta Puga, Gaizka Murga, Antonio Pérez-Garrido, Enric Pallé, Davide Ricci, Ismael Ayuso, Mónica Hernández-Sánchez, Nicola Truant; arXiv: 1608.04807 [astro-ph.IM].

- **Prospects for Fundamental Physics with LISA**

Enrico Barausse et al; arXiv:2001.09793 [gr-qc].

Palavras-chave: gravidade modificada, teorias escalar-tensor, Lagrangianos dependentes da ação, não-metricidade, restrições observacionais.

Abstract and published works

General Relativity is one of the current pillars of physics. This theory describes gravity with flying colours at solar system scales and offers us a cosmological model when applied to the evolution of the Universe. However, when addressing these larger scales, namely, when we try to explain some observations, some challenging questions appear.

The first one is the observed acceleration of the Universe which, in General Relativity, is solved (or “patched”) introducing a component of matter with negative pressure, and supplies a repulsive effect. This exotic matter violates some energy conditions, one would expect to be satisfied by “normal” matter. A typical example is provided by the cosmological constant represented by Λ .

The second one is the consideration of Dark Matter (DM). This component is necessary to explain phenomena like the building up of structures in the Universe or the velocity curves of galaxies. It only reveals itself gravitationally and has not been detected by direct interaction with matter in experiments. Therefore, a possible way to solve these problems is to go beyond General Relativity and investigate modifications of the Einstein theory. Thus, in this thesis we will explore this possibility.

The first step in this study is devoted to the possibility of having a dynamical coupling between a scalar field and the geometry. In this sense, we will focus on scalar-tensor theories and more specifically in a generalization of the Brans-Dicke theory. This supplies us with a perfect frame to study the possibility that the gravitational coupling constant G is changed into a dynamical scalar field ϕ . The work, in which Chapter 2 of the thesis is based, was published as:

- **What if Newton’s Gravitational Constant Was Negative?**

Ismael Ayuso, José P. Mimoso, Nelson J. Nunes, *Galaxies* 7, (2019) 1, 38;

arXiv: 1903.07604 [gr-qc].

In this work, we seek a cosmological mechanism that may define the sign of the effective gravitational coupling constant, G . We find that models with a quadratic potential naturally stabilize the value of G into the positive branch of the evolution and further, that de Sitter inflation and a relaxation to General Relativity is easily attained.

Following this way of modifying gravity and the nonminimal scalar-tensor theories, we can generalize the action of Chapter 2 with a more complex coupling between gravity and the scalar field. In particular, this allows us to study how this extension would affect the coupling with the standard model of particles. This will be addressed in Chapter 3, which is based on the published paper:

- **Nonminimal scalar-tensor theories**

Ismael Ayuso, Jose A.R. Cembranos, *Physical Review D* 101, (2020) 4, 044007;
arXiv: 1411.1653 [gr-qc].

In this paper we find that the perturbative states of these theories are given by two massive spin-0 modes in addition to one massless spin-2 state. This latter mode can be identified with the standard graviton field.

Then, we will consider the so-called Horndeski theory that provides the most general metric theory of gravity with a single scalar field playing a gravitational role that avoids the Ostrogradsky instability, producing second order field equations. We will study this theory in connection to the black-hole described by the Nariai spacetime, that is, the extremal case of the Schwarzschild de-Sitter black hole (both cosmological and the black hole horizons coincide at the same surface). The motivation is that this kind of objects offer us a perfect framework to test the new phenomenology of modified gravity theories. In addition, in order to better understand both black holes as the Horndeski Lagrangian we will study the anti-evaporation phenomenon. Chapter 4 is based on the published work:

- **Extremal cosmological black holes in Horndeski gravity and the anti-evaporation regime**

Ismael Ayuso, Diego Saez-Chillon Gomez, *Universe* 6, (2020) 11, 210;
arXiv: 2004.10139 [gr-qc].

However, we show that, contrary to other frameworks of modified gravity theories, the radius of the horizon remains stable for some cases of the Horndeski Lagrangian when considering perturbations at linear order.

A different way of modifying gravity will be exposed in Chapter 5, where we introduce action-dependent Lagrangian theories and apply this to the study of wormholes. We investigate if this class of modified gravity theories allow us to satisfy the energy conditions for the matter content of this kind of exotic objects. This chapter is based on the publication:

- **Wormhole geometries induced by action-dependent Lagrangian theories**

Ismael Ayuso, Francisco S.N. Lobo, José P. Mimoso, *Physical Review D* 103, (2021) 4, 044018; arXiv: 2012.00047 [gr-qc].

We show that the generalized gravitational field equation essentially depends on a background four-vector λ_μ , that plays the role of a coupling parameter associated with the dependence of the gravitational Lagrangian upon the action, and may generically depend on the space-time coordinates. In addition, considering wormhole configurations, by using “Buchdahl coordinates”, we find that the four-vector is given by $\lambda_\mu = (0, 0, \lambda_\theta, 0)$, and some restriction of the spacetime. With a plethora of examples of wormholes and with power law choices for the function λ , we show that these compact objects possess a far richer geometrical structure than their general relativistic counterparts.

In what follows, we will explore the interplay between theory and observations. This is an indispensable step to contrast any proposed model of modified gravity against constraints given by observations. With this purpose, we will introduce in Chapter 6 the Markov Chain Monte Carlo methodology (MCMC). We will also introduce some other important statistical concepts that help us to discriminate the proposed models.

In order to apply the MCMC methodology we will consider some models based on the non-metricity scalar Q , which will be explained in Chapter 7, where we obtain their respective modified Friedmann equation. We will study three models: the extended mimetic General Relativity theory from $f(Q)$, the DGP model (coming from modified gravity with extra-dimensions), and the DGPish (so-called because its similarity with the previous one). The conclusions of the first model were exposed in:

- **Observational constraints on cosmological solutions of $f(Q)$ theories**

Ismael Ayuso, Ruth Lazkoz, Vincenzo Salzano, Physical Review D103, (2021) 6, 063505; arXiv: 2012.00046 [astro-ph.CO].

And the analysis of the other two was submitted for publication:

- **DGP and DGPish cosmologies from $f(Q)$ actions**

Ismael Ayuso, Ruth Lazkoz, José Pedro Mimoso; arXiv: 2111.05061 [astro-ph.CO].

In these works, we conclude that, at the current precision level, the best fits of our $f(Q)$ models correspond to values of their specific parameters which make them hardly distinguishable from Λ CDM, or in other words, these scenarios do not show signatures indicating a departure from the Λ CDM behaviour.

Last but not at least, in Chapter 8 we make a general discussion of the results of this thesis and, draw some conclusions.

In addition, other publications during the thesis are:

- **Commissioning and First Observations with Wide FastCam at the Telescopio Carlos Sánchez**

Sergio Velasco, Urtats Etxegarai, Alejandro Oscoz, Roberto L. López, Marta Puga, Gaizka Murga, Antonio Pérez-Garrido, Enric Pallé, Davide Ricci, Ismael Ayuso, Mónica Hernández-Sánchez, Nicola Truant; arXiv: 1608.04807 [astro-ph.IM].

- **Prospects for Fundamental Physics with LISA**

Enrico Barausse et al; arXiv:2001.09793 [gr-qc].

Keywords: Modified gravity, scalar-tensor theories, Action-dependent Lagrangians, non-metricity, observational constraints.

Contents

Agradecimientos - Acknowledgments	vii
Resumo e palavras-chave	xiii
Abstract and published works	xix
List of Figures	xxv
List of Tables	xxx
Notation and definitions	xxxiii
1 Introduction	1
1.1 General Relativity: the gravitational theory	7
1.1.1 Λ CDM model: the current cosmological model	11
1.1.2 Problems of the Λ CDM model	15
1.2 Modified Gravity	16
1.3 Energy Conditions	21
1.3.1 $T^{\mu\nu}$ as a symmetric tensor	22
1.3.2 Stress-energy tensor types: Hawking-Ellis Classification	22
1.3.3 Usual Energy Conditions	24
1.3.4 Relevant inequalities for a perfect fluid	27
1.3.5 Classical examples of violations of the Energy Conditions	30
2 About the gravitational coupling constant	35
2.1 Negative G in GR	37

2.1.1	Friedmann Models with a Single Fluid	37
2.1.2	Model with a cosmological constant	38
2.2	Scalar-Tensor Gravity Theories	42
2.2.1	Models without a Cosmological Potential	45
2.2.2	Models with a Cosmological Potential	47
2.3	Observational Features	49
2.4	Conclusions	50
3	Non-minimal Scalar tensor theories	53
3.1	Introduction	53
3.2	$f(R)$ theory of modified gravity	55
3.2.1	Conformal transformations	58
3.3	Generalized Non-minimal scalar-tensor theories	60
3.3.1	Interaction with the matter content: the Standard Model	62
3.3.2	Scalar spectrum	64
3.4	Conclusions	68
4	Extremal Black Holes in modified gravity	71
4.1	Nariai Spacetime in Horndeski Gravity	73
4.2	Reconstructing the Gravitational Action in Horndeski Gravity	81
4.2.1	Case with \mathcal{L}_2	81
4.2.2	Case \mathcal{L}_3	83
4.2.3	Case \mathcal{L}_4	87
4.3	Anti-Evaporation Regime in Horndeski Gravity	89
4.3.1	Non constant solutions with null coefficients	92
4.4	Conclusions	95
5	Wormholes in modified gravity	97
5.1	Action-dependent Lagrangian theories	100
5.2	General restrictions on wormhole geometries	105
5.3	Specific solutions	106
5.3.1	Specific wormhole solutions: Ellis-Bronnikov solution	108

5.3.2	Specific stress-energy profile	110
5.3.3	Black bounce solutions	112
5.4	Conclusions	118
6	From the theory to observations: MCMC	121
6.1	Statistical Analysis	121
6.2	MCMC	125
6.2.1	Model selection	127
6.3	Observational data and cosmological observables	128
6.3.1	Distances in Cosmology	129
6.3.2	Pantheon Supernovae data	132
6.3.3	Hubble data	134
6.3.4	Cosmic Microwave Background data	134
6.3.5	Baryon Acoustic Oscillations data	135
6.4	Summary	138
7	$f(Q)$ theories and their observational constraints.	139
7.1	Introduction	140
7.2	Symmetric Teleparallel Gravity	144
7.3	$f(Q)$ cosmologies	146
7.4	Extended mimetic GR theory from $f(Q)$	149
7.4.1	MCMC analysis and results	152
7.4.2	Cosmographic parameters	159
7.4.3	Conclusions about the extended mimetic GR theory from $f(Q)$ model	162
7.5	Building up modified gravity models based on $f(Q)$	163
7.5.1	DGP cosmologies from $f(Q)$ actions	165
7.5.2	DGPish cosmologies from $f(Q)$ actions	168
7.5.3	MCMC analysis and results	170
7.5.4	Cosmographic parameters and cosmodiagrams	175
7.5.5	Conclusions about DGP and DGPish models	178
8	General Conclusions	181

List of Figures

2.1	Phase-diagrams displaying the behaviour of the vector field (a, a') for GR with a negative G . From left to right and from top to down: (a) represents the $k = -1$ models, (b) the $k = 0$ models, and (c,d) correspond both to the $k = +1$ models with different values for the relation Ω_Λ/Ω_m . Red points are fixed points and blue points represent the starting point of the most solutions excepting those that correspond with circular orbits.	40
2.2	Behaviour of X and X' for a scalar-tensor theory without potential. The upper three phase diagrams, (a–c) , respectively, correspond to the $k = -1, 0, +1$ cases for vacuum and stiff fluid. The lower three phase diagrams, (d–f) , respectively, correspond to the $k = -1, 0, +1$ cases for radiation.	47
2.3	Behaviour of X and X' for a scalar-tensor theory with a potential λ_0 . The upper three phase diagrams, (a–c) , respectively, correspond to the $k = -1, 0, +1$ cases for vacuum and stiff fluid. The lower three phase diagrams, (d–f) , depict the qualitative behaviour of radiation models, with: (d) When $M\lambda_0 > 1$ (e) When $M\lambda_0 = 1$ (f) When $M = 1/4$ and $\lambda_0 = 2$	49
4.1	Aspect of the function $A(r)$	79

- 5.1 The plots depict the specific case of the Ellis-Bronnikov wormhole configuration with $a = 1$, for convenience, and for different choices of the function $\lambda(u)$. Depending on the sign of $\lambda(u)$, one obtains a plethora of specific symmetric or asymmetric solutions. Note that for $\lambda(u) \sim \pm u$, one obtains asymmetric solutions, where the energy density is negative at the throat and in the positive (negative) branch of u , but becomes positive in the negative (positive) branch; the radial pressure exhibits the inverse qualitative behavior. 108
- 5.2 Results for the specific stress-energy profile given by (5.58) and (5.59) with $a^2 = -1/(4\pi\rho_0(1 + \omega))$ and $\alpha = 2$. The upper plots are for the case $\rho_0 = 1$ ($\omega < -1$), and the lower plots for $\rho_0 = -1$ ($\omega > -1$). 111
- 5.3 The plots depict the Simpson-Visser black bounce solution, for the specific choices $m = 1, a = 3$. Note that one may obtain wormhole configurations with an entirely positive energy density throughout the spacetime, for negative values of the function $\lambda(u)$, and positive radial pressures in the negative branch of the u -axis. As before, it is transparent from the plots that these compact objects possess a richer geometrical structure than their general relativistic counterparts. See main text for more details. 113
- 5.4 The plots depict the stress-energy profile for the black bounce II solution, given by the metric function (5.73), where for numerical convenience we have assumed the following choices for the parameters: $m = 1, a = 1$. Recall that the parameters are restricted by the condition $a > 4m/(3\sqrt{3})$. As before these wormhole configurations possess a far richer internal structure than their general relativistic counterparts, and depending on the sign of $\lambda(u)$, specific symmetric or asymmetric solutions are obtained. However, here the tangential pressure at the wormhole throat, $p_t(u = 0) = (a - 2m)/(8\pi a^3)$, takes negative values for the parameter range $4m/(3\sqrt{3}) < a < 2m$, and positive values for $a > 2m$. . . 115

5.5 The plots depict the stress-energy profile for the black bounce III solution, given by the functions (5.77) and (5.79), for the case $n = 1$, where $a > a_{\text{ext}}$, so that there are no event horizons. We have chosen the following values for the parameters: $m = 1$ and $a = 2$. Note that for these solutions, the negative energy densities are improved, and one may also obtain positive radial pressures for positive values of the function $\lambda(u)$ 117

7.1 Contour plots for the Λ CDM model (left column) and the $f(Q)$ model with $\Omega_\Lambda \neq 0$ (right column) with the following color scheme: green - SNeIa, yellow - Hubble data, orange - *Planck 2018* CMB, blue - BAO data, black - all sets of data. As SNeIa are (of course) unable to fix the value h , their contours are missing from those plots where constraints on h is shown; for the same reason, both SNeIa and Hubble contours are absent from plots showing constraints on Ω_b . 156

7.2 Contour plots for the $f(Q)$ model with $\Omega_\Lambda \neq 0$ with the following color scheme: green - SNeIa, yellow - Hubble data, orange - *Planck 2018* CMB, blue - BAO data, black - all sets of data. 157

7.3 Contour plots for the $f(Q)$ model with $\Omega_\Lambda = 0$ using the following color scheme: green - SNeIa; yellow - Hubble data; orange - *Planck 2018* CMB; blue - BAO data; black - all sets of data. 159

7.4 Evolution of w_{eff} as function of a . The solid line is the value as drawn from the best fit, whilst the dashed lines mark the boundaries of the confidence interval. 161

7.5 Contour plots for the Λ CDM model (left column) *DGP* model (center column) and *DGPish* model (right column) with the following color scheme: green - SNeIa, yellow - Hubble data, orange - *Planck 2018* CMB, blue - BAO data, black - all sets of data. As SNeIa are not (of course) able to fix the value h their contours are missing from those plots where constraints on h are represented; for the same rationality, both SNeIa and Hubble contours are absent from plots showing constraints on Ω_b 173

- 7.6 Contour plots of the constraints on the parameter Ω_Q for the *DGP* model (left column) and *DGPish* model (right column) with the following color scheme: green - SNeIa, yellow - Hubble data, orange - *Planck 2018* CMB, blue - BAO data, black - all sets of data. 174
- 7.7 Evolution of w_{eff} as a function of the scale factor a for *DGP* (left panel) and *DGPish* (right panel) model. The solid line is the value as drawn from the best fit, whilst the dashed lines mark the boundaries of the confidence interval. . . . 176
- 7.8 Contours for the different redshift of the different models. Λ CDM (orange), DGP (blue) and DGPish (purple), all them resulting from the values of the MCMC. The red line is the theoretical behaviour of the Λ CDM model, i.e. $z_{\text{acc}} = -1 + 2^{1/3}(1 + z_{\text{eq}})$ 176

List of Tables

7.1	MCMC best fits and errors. Quantities in italic correspond to secondary parameters.	155
7.2	Best fits of the cosmographic parameters.	160
7.3	MCMC best fits and errors along with other statistical estimators for Λ CDM, DGP, and DGPish models. Quantities in italic correspond to secondary parameters.	172
7.4	Best fits and errors of the cosmographic parameters.	178

Notation and definitions

i : Latin index runs from 1 to 3

μ : Greek index runs from 0 to 3

A : Capital Latin index runs from 0 to 4

α_{EM} : Fine-structure constant

α_s : Strong coupling constant

$a(t)$: Scale factor

BAO: Baryonic Acoustic Oscillation

\square : $\nabla^\mu \nabla_\mu$

c: Speed of light

CDM: Cold Dark Matter

CMB: Cosmic Microwave Background

cte: constant

$A_{(\mu\nu)}$: Commutator among the indexes $\mu\nu$

$K^\alpha_{\mu\nu}$: Contortion

$L^\alpha_{\mu\nu}$: Disformation

dof: Degree Of Freedom

$$d\Omega^2: d\theta^2 + \sin^2 d\phi^2$$

ECs: Energy Conditions

EF: Einstein Frame

Eq.: Equation

$F_{\mu\nu}$: Gauge invariant electromagnetic field strength tensor

$f(x)_x$: Derivative of $f(x)$ with respect to x

$G_{\mu\nu}^a$: Gluon field strength tensor

Γ : Connection

g : Determinant of the metric

$g_{\mu\nu}$: Metric

$G_{\mu\nu}$: Einstein tensor

$G_i(\phi, X)$: Horndeski i function

GR: General Relativity

G : Gravitational Coupling Constant

H : Hubble parameter or Hubble function

h : Higgs Boson

$$h_0: \frac{H_0}{100}$$

H_0 : Hubble factor

JF: Jordan Frame

$$\kappa^2: 8\pi G$$

\mathcal{L}_{mat} : Matter Lagrangian

$\nabla \equiv \nabla_\mu \equiv_{;\mu}$: Covariant derivative

NMSTT: Non-Minimal Scalar-Tensor theory

$Q_{\alpha\mu\nu}$: Non-metricity tensor

$\partial \equiv \partial_\mu \equiv_{,\mu}$: Partial derivative

pdf: Probability Distribution Function

R : Scalar of curvature

ρ : Density

ρ^0 : Current density

SCDM: Standard Cold Dark Matter

SMM: Squared-Mass Matrix

STTEGR: Symmetric Teleparallel Equivalent General Relativity

\dot{A} : Time t derivative

A' : Conformal time η derivative

$\phi'(x)$: Derivative of ϕ with respect to x coordinate

$T_{\mu\nu}$: Stress-energy tensor

T : Trace of the stress-energy tensor

$T_{\mu\nu}^\alpha$: Torsion

U^μ : Four-velocity

VEVs: Vacuum Expectation Values

W^μ **and** Z^μ : Electroweak gauge bosons

Chapter 1

Introduction

It is appropriate to start a work on gravity by recalling its discoverer Isaac Newton, who proposed in 1687 that the force responsible for the fall of objects towards the Earth would also be responsible for the dynamic of stars and planets. In his words, the gravitational centripetal force should be proportional to the quantity of matter of the two bodies in interaction, as well as inversely proportional to the square of their separation [1]:

$$F \propto \frac{m_1 m_2}{r^2} . \quad (1.1)$$

However, he did not explicitly introduce the proportionality constant G [2]¹, presumably due to the lack of an internationally accepted system of units. Of course, this is required since, after all, G adjusts the dimensions of both sides of the defining equation for the strength of the gravitational interaction and the sign of this denotes the attractive or repulsive character of the force.

In 1798, H. Cavendish measured this proportionality with a torsion balance, but just as a necessary step, of secondary importance, to weigh the density of the Earth [3]. This measure was made with the remarkable accuracy of 1%. One year after, in 1799, P. S. Laplace presented his *Traité de Mécanique Céleste* [4] where he introduced explicitly the gravitational constant for the first time as

$$F = -k^2 \frac{m_1 m_2}{r^2} . \quad (1.2)$$

¹Quoting Clifford Will [2]: It is interesting to notice that the term “gravitational constant” never occurs in the *Principia*. In fact it seems that the universal constant of proportionality that we now call G does not make an appearance until well in the eighteenth century in Laplace’s “*Mécanique Céleste*”.

The subsequent success of the gravitational law in tackling the motion of the celestial bodies of the solar system is well known, and, at the beginning of the 20th century, the only major problem was the anomaly in the precession of Mercury's perihelium, a mismatch first revealed by Le Verrier in 1859.²

It was Einstein's General theory of Relativity (GR) which not only solved this puzzle with flying colours, but also revolutionized our understanding of gravitation. In this theory, gravity is perceived as the curvature of the spacetime in which particles move following the geodesics of that manifold. But this does not mean that Newton's theory was wrong, it is only valid when considering weak fields and bodies moving with low speeds when compared to the speed of light. Consequently, General Relativity must be perceived as a generalization which recovers Newtonian gravity in the appropriate limit. In others words, GR includes Newton's theory, and has a wider scope of applicability.

Modern cosmology was started in 1917 when Albert Einstein applied his theory of General Relativity of 1915 to a Universe with matter uniformly distributed over enormous space, building the first general relativistic cosmological model. He considered a finite, static, homogeneous and isotropic Universe with spherical geometry [5]. Einstein noticed that "making possible a quasi-static distribution of matter, as required by the fact of the small velocities of the stars". For this reason, in that same work, Einstein introduced the cosmological constant λ (currently denoted by Λ) into his equations of General Relativity in order to get a static Universe. This term is proportional to the metric, and it is able to counter the gravitational pull of matter. Moreover, the Universe could then be spatially closed avoiding the difficulty of establishing boundary conditions at spatial infinity.

However the prediction of the theory kept on resulting in an unstable Universe for small perturbations originated by the cosmological constant in this case. Still in 1917, after Einstein's work, Willem de Sitter applied the Einstein equations with the cosmological constant to a vacuum Universe but without considering a static Universe [6], obtaining the so-called de Sitter spacetime that allows for a dynamical evolution of the Universe, and which plays an important role in modern cosmology.

Around the same time, observations were improving. In 1914 Vesto M. Slipher presented his results about the velocity of 12 galaxies (nebulae at that moment) [7], showing that 11 of

²Nowadays, this theory is expressed by changing $-k^2$ by G as the current gravitational constant.

them were moving away from us with a magnitude of hundreds of km/s (a lot more than the star velocities measured), and using the redshift concept, as a spectroscopic measure of how galaxies were moving away from us due to a Doppler effect. Other important actors were Knut Lundmark, who added new measurements of galaxy velocities, and Carl Wilhelm Wirtz [8], who initially thought that these recession velocities were constant, around 656 km/s [9]. In 1922, Wirtz put forward a paper where he argued that the redshifts of faraway galaxies are higher than those of closer ones. These observations laid the ground for the so-called Hubble-Lemaître law which will be presented in this introduction.

Another crucial landmark subject to debate during these years, and motivated by the study of that nebulae, was the Shapley-Curtis debate, or Great Debate, in 1920. The fundamental point was the nature of the observed so-called spiral nebulae. What were they? Were they in our galaxy or out of it? On the one hand, Shapley thought that they were relatively small and belonged to the neighborhood of our galaxy. On the other hand, Curtis defended that they were other galaxies like the Milky Way and independent of it, so that they were big and distant. Therefore, the participants in the debate were actually arguing about the size of the Universe.

It seems clear that after the measurements of Wirtz and Lundmark, the position of Curtis was reinforced, but it was Hubble who ended up solving the question with the observation of the first Cepheid variable in M31 nebulae (Andromeda) in 1923-1924, published in 1924 in *The New York Times*, and formally published in a scientific journal in 1929 [10]. This would not have been possible without the work of Henrietta Leavitt who had found the pulsation period-luminosity relation for classical Cepheid variables between 1908 and 1912 [11, 12, 13]. Hubble's work confirmed that the distance to M31 seemed to be so large that it should be an independent system (or galaxy) with respect to the Milky Way.

By these years, between 1922 and 1924, Alexander Friedmann found non static solutions of the Einstein equations for a Universe in expansion, whose size is a function of time, and for different curvatures [14, 15]. Independently, in 1927 Georges Lemaître found the same solutions and understood that if the Universe were expanding, it should have had a beginning at some time in the past when all matter, spacetime, and the Universe itself appeared at once out of nothing, in a single instant [16, 17]. Nevertheless, this idea was ridiculed and harshly criticized. As an example, in the 1950s Fred Hoyle (who had an alternative proposal of a cosmological theory called the steady state theory) pejoratively named the idea of the birth of the Universe from a

point and at an instant as the “Big Bang”. Curiously, this name, which was an attempt of a joke to discredit the model was adopted as the name for the cosmological model that best fits the observations.

By 1929, Hubble had collected the distance to 24 extra-galactic nebulae, and related these with their radial velocity (change of the distance between us and the object) measured from the redshift by Vesto Slipher, and his assistant Milton L. Humason. While the recession of galaxies from us already looked like a fact, and there was an idea of expansion of the Universe, he made his second great discovery, namely the Hubble law, already mentioned before. It relates the velocity of the galaxies, and its distances with the mathematical expression: $v = H_0 d$, where v is the observed recession velocity, H_0 is the Hubble constant (which has units of $km/s/Mpc$), and d is the distance of the galaxy. Let us emphasize the linearity of the expression. It means that higher distances are translated into higher receding velocities. Therefore, the expansion of the Universe seemed almost confirmed.

At the same time, the dynamics of these galaxies continued being studied (already as external object to the Milky Way). In 1933, Fritz Zwicky applied the virial theorem to the Coma Cluster (cluster with over 1000 galaxies at 99 Mpc) [18], which relates the average of the total kinetic energy of an equilibrium system with the total potential energy of the same system. By measuring the velocity dispersion of galaxies, one should be able to obtain the gravitational potential, and consequently estimate the gravitational mass of the system. The surprise came from the great difference between the mass calculated with this theorem and that estimated from the optical luminosity of the cluster. Therefore, in agreement with the virial theorem, there was a kind of matter “invisible” to us [19], which ended up being called dark matter (in honor of Lord Kelvin, a Scots-Irish physicist who had already wondered about invisible objects in the Universe [20] by 1884).

With the evidence of the expansion of the Universe, the need for a theory for the creation of matter was introduced. George Gamow with his collaborator Ralph Alpher and with Hans Bethe³ proposed in 1948 for the first time how the synthesis of the lightest elements would

³Actually, the fact that Bethe signed the paper with Gamow and his student Alpher was a joke of Gamow who requested Bethe to do so. Bethe accepted under the condition that there would be a disclaimer on the first page of the paper saying that he didn’t collaborate with Gamow and Alpher in the work. However, let us emphasize that Bethe was an important nuclear physicist, and not a mere collaborator of Gamow, is the fact that Bethe won the Nobel prize in the 1960s for the synthesis of elements in stars.

occur in the early expanding Universe [21]. The model proposed that the elements were synthesized in a hot and very dense epoch where the primordial neutrons could decay into protons and join themselves to form heavier and heavier elements until the production was frozen by a fast expansion of the Universe. Then, Alpher and Robert Herman calculated that such high temperatures would imply that the Universe was dominated by radiation (instead of matter). But then, there should be a thermal bath remnant under the form of a background radiation which could be measured and with a temperature estimated by them to be around $5K$ [22] (today, it has been measured as $T = 2.73K$).

In 1964, Arno Penzias and Robert Woodrod Wilson (at Bell labs) built a horn antenna (7.35 cm) to use for radio astronomy and satellite communication experiments. However they encountered radio noise which they could not explain [23]. It was isotropic and had a perfect blackbody spectrum, and they thought their instrument was suffering from interference by terrestrial sources or from the bat and pigeon droppings accumulated on the antenna. But after removing the dung buildup and ruling out the possibility of terrestrial sources, the noise remained. Then, Penzias contacted Robert Dicke who was an astronomer and physicist (and one of the founders of the Brans-Dicke theory). He suggested it may be the cosmic background radiation which was predicted by the cosmological theory of Big Bang. Dicke's group (that included P.J. Peebles) was already looking for this signal, measured the second clean detection providing the total theoretical interpretation [24] and determined that the Big Bang theory and the Friedmann-Lemaître model had moved from a speculation theory into well-tested physics [25]. The measurement of the Cosmic Microwave Background (CMB) became one of the most important parts for the construction of theories about the early Universe. Let us remark at this point the importance of the combination of theory with observations and vice-versa.

At the same time, during the 1960s and 1970s, Vera Rubin was developing her work on clusters of galaxies with hundreds of spectroscopy observations, together with Kent Ford. They managed to resolve the spectra of astronomical objects, and studied the rotation curves of stars around the centers/or bulges of the galaxies, i.e., the velocity of the stars versus their distances from the galaxy center. She was able to determine the distribution of the mass observed by each star and responsible for its dynamics in the galaxy. Because most of the stars are close to the core, the radial velocity of stars was supposed to decrease as the distance increases, graphing a descendant rotation curve. Indeed, stars farther from the core should move slower than stars

closer to it. However, she discovered the unusual fact that the line of her graphics, instead of sloping down with the distance, seemed to level off. This can only be explained with additional mass distributed in the whole galaxy, which had not been observed, recovering in 1980 the already mentioned idea of dark matter [26].

Twelve years after, in 1992, the COBE satellite team discovered anisotropies in the CMB radiation at the level of 10^{-5} , and measured their sizes. This offered us an image of the primeval matter density fluctuations which would end up being the seeds for galaxies and matter cluster. The fact of finding such small variations (homogeneously distributed) of the early Universe is one of the most powerful evidences of the Cosmological Principle, claiming we are in a homogeneous and isotropic Universe. This research was improved with the evolution of technology as the COBE satellite was replaced by its descendant, the Wilkinson Microwave Anisotropy Probe satellite (WMAP) in 2001, and later by the Planck satellite in 2009. With this data, cosmologists were and are able to measure some cosmological parameters like the density of the different components of the Universe (depending on the chosen model) as we will see along this thesis.

To finish this brief introduction to the history of modern cosmology, we have to go back to 1998 for a remarkable milestone revealed by two thorough surveys of Type Ia Supernovae (SNeIa). The knowledge of this kind of Supernovae increased significantly in the years previous to the surveys so that SNeIa could be used as standard candles, which let us know higher distances. Moreover, we have already said that observations concluded that the Universe was expanding, however, it would seem logic to think that if the only force (at cosmological scale) is the gravitational force, the expansion will end up stopping and consequently the Universe would be decelerating. With the new tool of SNeIa, two separate research groups (one led by Adam G. Riess [27] and Brian P. Schmidt [28] and the other one by Saul Perlmutter [29]) tried to measure this deceleration. The surprise came when they did not observe the deceleration, but rather observed that the Universe was accelerating its expansion! The simplest explanation was, and still is, the reintroduction of the cosmological constant Λ , which had been introduced and eliminated by Albert Einstein! Nonetheless, there are other possibilities, and in general, any new component of the theory which leads to this accelerated expansion is called Dark Energy (DE). With all this information the current cosmological model is built with the introduction of Λ and the Cold Dark Matter (CDM). It is the Λ CDM model which we will comment about below.

1.1 General Relativity: the gravitational theory

General Relativity was proposed by Albert Einstein [30, 31, 32] in 1915 and provides a description of gravity as a geometric property of spacetime which is built from the matter content. Gravity is a consequence of the deformation of the spacetime by the matter and this deformation implies how the matter should move. In other words and citing John Archibald Wheeler “*Spacetime tells matter how to move; matter tells spacetime how to curve*” [33].

We should start out mentioning the main fundamental ideas on which General Relativity is based:

- Newton’s law should be recovered at Earth and solar system scales, because it was very successful to explain the so-called celestial mechanics until the middle of the nineteenth century.
- Covariance principle: the consistency of physics for different observers demands that the choice of coordinates does not affect the physical laws. If a theory is built from tensors or vectors, which are covariant by definition, the theory will be covariant. This fact seems obvious if we look for a universal theory or model which does not depend on the observer. It means that the laws are equal for all observers, even though its representation in coordinates could be different for each one.
- Special Relativity seems a good first step, but it is unable to explain the gravitational redshift of spectra lines of compact stars. So the metric tensor should be a function of the coordinates, substituting the Minkowski metric and pseudo-Euclidean geometry by a more general metric, and a Riemannian geometry.
- Associated with the previous idea, a mathematical object which describes the geometry of the manifold appears as a good candidate to be the fundamental object to describe gravity. So, all this information is encoded in the metric tensor $g_{\mu\nu}$ which is considered as the only source of geometric degrees of freedom.
- It is a four-dimensional Lorentzian manifold (special case of Pseudo-Riemannian manifold), with one temporal dimension and three spatial dimensions. In addition, the metric

is symmetric so it has only ten independent components that reduce to six due to the existence of a gauge freedom that amounts to the arbitrary specification of four conditions, reducing the actual number of degrees of freedom in the metric [34].

- This manifold is endowed with a covariant derivative ∇ (or equivalently with a connection Γ) which is assumed metric compatible ($\nabla_\alpha g_{\mu\nu} = 0$) and torsion free ($\Gamma_{\mu\nu}^\alpha = \Gamma_{\nu\mu}^\alpha$). With these two last assumptions, the connection is inevitably forced to become the Christoffel symbols.
- The energy and momentum should be conserved, since there are no experiments showing the opposite behaviour.

From a variational viewpoint, this theory is characterized by the following Einstein-Hilbert action:

$$S = \frac{c^3}{16\pi G} \int d^4x \sqrt{-g} R + \frac{1}{c} \int d^4x \sqrt{-g} \mathcal{L}_{mat}(g^{\mu\nu}, \Psi_m), \quad (1.3)$$

where c is the speed of light, R is the scalar of curvature (or Ricci scalar), g is the determinant of the metric, \mathcal{L}_{mat} is the matter Lagrangian, Ψ_m are the possible matter fields, and G is the gravitational coupling constant (from Newton's law), which defines the proportionality between the deformation of the spacetime and the matter. It is common to use the definition $8\pi G = \kappa^2$ in order to simplify the notation. The scalar of curvature is built by the Riemann and Ricci tensor respectively defined as:

$$R^\alpha_{\beta\mu\nu} = \partial_\mu \Gamma^\alpha_{\nu\beta} - \partial_\nu \Gamma^\alpha_{\mu\beta} + \Gamma^\alpha_{\mu\lambda} \Gamma^\lambda_{\nu\beta} - \Gamma^\alpha_{\nu\lambda} \Gamma^\lambda_{\mu\beta}, \quad (1.4)$$

$$R_{\mu\nu} = R^\sigma_{\mu\sigma\nu} = \partial_\sigma \Gamma^\sigma_{\nu\mu} - \partial_\nu \Gamma^\sigma_{\sigma\mu} + \Gamma^\sigma_{\sigma\gamma} \Gamma^\gamma_{\nu\mu} - \Gamma^\sigma_{\nu\gamma} \Gamma^\gamma_{\sigma\mu}, \quad (1.5)$$

$$R = g^{\mu\nu} R_{\mu\nu}, \quad (1.6)$$

with Γ being the Christoffel symbols:

$$\Gamma^\sigma_{\mu\nu} = \frac{1}{2} g^{\sigma\alpha} (\partial_\nu g_{\mu\alpha} + \partial_\mu g_{\alpha\nu} - \partial_\alpha g_{\mu\nu}). \quad (1.7)$$

Then, the total action is the contribution of the gravitational sector together with the matter sector of the form $S = S_g + S_m$. As usual in classical mechanics, the equations of motion of the theory are obtained from a variational principle, i.e. applying variations of an appropriate

functional, denoted the action, with respect to the degrees of freedom (that we have already anticipated that for GR are associated with the metric), and assessing stationarity conditions.

Let us introduce how variations apply to some terms:

$$\delta_g \sqrt{-g} = -\frac{1}{2} \sqrt{-g} g_{\mu\nu} \delta g^{\mu\nu}, \quad (1.8)$$

$$\delta_g R = \delta g^{\mu\nu} R_{\mu\nu} + g^{\mu\nu} \delta R_{\mu\nu} = \delta g^{\mu\nu} R_{\mu\nu} + \nabla_\alpha \left(g^{\mu\nu} \delta_g \Gamma^\alpha_{\mu\nu} - g^{\mu\alpha} \delta_g \Gamma^\beta_{\mu\beta} \right). \quad (1.9)$$

So metric variations of the first term of action (1.3), which describes the gravitational sector, is:

$$\delta_g S_g = \frac{c^3}{16\pi G} \int d^4x \sqrt{-g} \left[-\frac{1}{2} g_{\mu\nu} R \delta g^{\mu\nu} + \delta g^{\mu\nu} R_{\mu\nu} + \nabla_\alpha \left(g^{\mu\nu} \delta_g \Gamma^\alpha_{\mu\nu} - g^{\mu\alpha} \delta_g \Gamma^\beta_{\mu\beta} \right) \right]. \quad (1.10)$$

Focusing on the last term, it can be written as $\nabla_\alpha v^\alpha$ and its volume integral transformed into a surfaced integral by the Gauss theorem: “*the surface integral of a vector field over a closed surface, which is called the flux through the surface, is equal to the volume integral of the divergence over the region inside the surface*”. But the term v^α tends to zero at the border and consequently this term will vanish. This fact is not always true and will depend on whether it is coupled with other terms. At the end of the day, for the gravitational part of the action, one can conclude:

$$\delta_g S_g = \frac{c^3}{16\pi G} \int d^4x \sqrt{-g} \left[-\frac{1}{2} g_{\mu\nu} R + R_{\mu\nu} \right] \delta g^{\mu\nu}, \quad (1.11)$$

and consequently the equations of motion for GR in the vacuum case (for which $\mathcal{L}_{mat} = 0$) are:

$$R_{\mu\nu} - \frac{1}{2} g_{\mu\nu} R = 0. \quad (1.12)$$

The case where a cosmological constant is considered is straightforwardly obtained from the gravitational action:

$$S_g = \frac{c^3}{16\pi G} \int d^4x \sqrt{-g} (R - 2\Lambda), \quad (1.13)$$

and its equations of motion in vacuum are:

$$R_{\mu\nu} - \frac{1}{2} g_{\mu\nu} R + \Lambda g_{\mu\nu} = 0. \quad (1.14)$$

In the left hand side the first two terms constitute the Einstein tensor denoted $G_{\mu\nu}$. Additionally, one should consider variations on the matter sector, and define a stress-energy tensor

(also called the energy-momentum tensor) as follows:

$$T_{\mu\nu} = -2 \frac{\delta_g(\sqrt{-g}\mathcal{L}_{mat})}{\sqrt{-g}\delta g^{\mu\nu}}, \quad (1.15)$$

yielding the Einstein equations:

$$R_{\mu\nu} - \frac{1}{2}g_{\mu\nu}R + \Lambda g_{\mu\nu} = \frac{8\pi G}{c^4}T_{\mu\nu}. \quad (1.16)$$

In 1971, 50 years after GR was proposed, Lovelock's theorem [35, 36, 37] revealed that from a local gravitational action which contains only second derivatives of the four-dimensional spacetime metric (in order to avoid possible instabilities), the most general equations of motion are the previous ones⁴. GR has passed all precision tests to date and given us some interesting phenomenology such as: the anomalous perihelion advance of the planet Mercury [38], gravitational lensing [39], gravitational time dilation, which have been observationally checked, and which Newton's law of gravitation is unable to explain.

In spite of these successes, there are some problems with GR. Singularities are one of them, which mean that there are points where spacetime is ill-defined because the path followed by particles (the so-called geodesics) are incomplete and consequently predictability is lost. There are also problems to find a unique quantum theory of GR. Therefore, this suggests that GR is only valid for some regions and scales and then is not complete, i.e. it is not a valid theory everywhere and for any scale (in a similar form to Newton's law which is valid for small velocities and scales, or in other words, for weak fields). However, there are open questions too when one applies GR on scales greater than that of the Solar System.

But Lovelock's theorem told us that Eq. (1.16) are the most general equations, then how can physicists improve the theory? In view of the theorem (and its considerations), there are 5 main ways to go beyond GR if one considers gravity as a geometrical theory:

- Add other fields with a gravitational role rather than the metric tensor.

⁴However, these equations could come from a more general action (or Lagrangian) than the Einstein-Hilbert one, if these new terms do not change the equations of motion. Indeed, the most general Lagrangian in 4-dimensions with the previous properties is:

$$\mathcal{L}_g = a\sqrt{-g}R - 2\Lambda\sqrt{-g} + b\epsilon^{\mu\nu\rho\lambda}R^{\alpha\beta}_{\mu\nu}R_{\alpha\beta\rho\lambda} + c\sqrt{-g}\left(R^2 - 4R^{\mu\nu}R_{\mu\nu} + R^{\mu\nu\alpha\beta}R_{\mu\nu\alpha\beta}\right), \quad (1.17)$$

where a , b , Λ and c are constants and the last term will be related with a branch of modified gravity called Gauss-Bonnet gravity as it will be explained below.

- Increase or diminish the dimensions of the spacetime.
- Add terms involving derivatives of the metric of higher-order than the second.
- Consider non-locality in the fundamental action, e.g. the inverse d'Alembertian.
- Consider the idea that the field equations do not come from the action which has been dubbed *emergence*. Consequently, this idea discards the variational formulation of the action and is beyond the Lovelock theorem.

These are the major possibilities to modify gravity if one considers it as a geometrical theory.

Obviously this theory is also applied to the Cosmos when looking for a valid cosmological model. This is an essential step when we try to study the reliability of GR on large scales, where this force should dominate. As usual in physics, this allows us to create a whole new framework with new problems or questions to be solved. Consequently, it is essential to introduce the current cosmological model at this point.

1.1.1 Λ CDM model: the current cosmological model

This model is supported by two ideas:

- * GR as the gravitational theory.
- * The Cosmological Principle: the Universe can be considered homogeneous and isotropic at large scales. Therefore, one should introduce the most general spatially homogeneous and isotropic metric. It is the FLRW-metric which, in the spherical coordinate system, reads:

$$ds^2 = -c^2 dt^2 + a^2(t) \left(\frac{dr^2}{1 - kr^2} + r^2 d\theta^2 + r^2 \sin^2 \theta d\phi^2 \right). \quad (1.18)$$

where $a(t)$ is a function of the time called scale factor, which is related with the size and evolution of the Universe, and we will normalize it to unity today, while k takes account of the geometry of the space with three possibilities: $k = -1, 0, 1$. At constant time, the cases $k = 0, 1, -1$ represent hyper-surfaces which are flat, positively curved, or negatively curved, respectively.

A very important parameter defined from the metric is the Hubble factor which is written:

$$H(t) = \frac{1}{a} \frac{da}{dt}, \quad (1.19)$$

being H_0 the Hubble factor at the present time. This parameter is very useful when studying cosmology and its history because it gives the speed of expansion/contraction of the Universe, that will be a fundamental aspect to relate the models with observations.

In order to advance in cosmology, it is usual to consider a perfect fluid whose stress-energy tensor reads:

$$T^\mu{}_\nu = \left(\rho + \frac{p}{c^2} \right) U^\mu U_\nu + p g^\mu{}_\nu, \quad (1.20)$$

where ρ is the energy density, p is the pressure and U_μ is the four velocity ($U^\alpha U_\alpha = -1$). The former thermodynamic quantities are those measured by a comoving observer with the fluid.

With all this information (and assumptions), one is able to compute Einstein's field equations describing the evolution of the Universe in the comoving rest frame. The tt -component of Eq. (1.16) is called the first Friedmann equation:

$$\left(\frac{\dot{a}}{a} \right)^2 = \frac{8\pi G}{3} \rho + \frac{\Lambda c^2}{3} - \frac{kc^2}{a^2}, \quad (1.21)$$

where the dot denotes a time derivative. It is usual to define a critical density that would provide a spatially flat Universe in absence of cosmological constant:

$$\rho_c \equiv \frac{3H^2}{8\pi G}. \quad (1.22)$$

Therefore, a Universe whose total energy density was above ρ_c would be spatially closed, and spatially open in the opposite case. However, the main utility of the parameter ρ_c is that it allows us to define dimensionless density parameters for the energy density of the component i (ρ_i):

$$\Omega_i(t) \equiv \frac{\rho_i(t)}{\rho_c(t)}, \quad (1.23)$$

which, together with the next two definitions:

$$\Omega_k(t) \equiv -\frac{kc^2}{a^2 H^2}, \quad \Omega_\Lambda(t) \equiv \frac{\Lambda c^2}{3H^2}, \quad (1.24)$$

transforms the first Friedmann Eq. (1.21) into:

$$\sum_i \Omega_i(t) + \Omega_k(t) + \Omega_\Lambda(t) = 1. \quad (1.25)$$

The trace of Eq. (1.16) together with the first Friedmann equation give us the second Friedmann equation, also called the acceleration equation or the Raychaudhuri equation:

$$\frac{\ddot{a}}{a} = -\frac{4\pi G}{3} \left(\rho + \frac{3p}{c^2} \right) + \frac{\Lambda c^2}{3}. \quad (1.26)$$

From this equation it is straightforward to see that without the cosmological constant Λ , and with usual matter with positive pressure and positive energy, the Universe is condemned to be decelerated.

In addition, it is possible to use another equation from one of the previous assumptions, the conservation of the total stress-energy, $\nabla^\mu T_{\mu\nu}$, which ends up giving the continuity equation of a fluid:

$$\dot{\rho} + 3\frac{\dot{a}}{a}\left(\rho + \frac{p}{c^2}\right) = 0. \quad (1.27)$$

However, this equation can be obtained combining Eq. (1.21) and Eq. (1.26) so that only two of the three equations are independent, and the choice of which pair we should use will depend on what one is interested in studying. Eq. (1.27) informs us about the joint evolution of the species when $\rho = \sum_i \rho_i$. This is specially simplified if they do not interact with each other, which makes the continuity equation independently satisfied for each individual species. This is the case of Λ CDM where Eq. (1.27) is satisfied separately for each component, (i.e. $\dot{\rho}_i + 3\frac{\dot{a}}{a}\left(\rho_i + \frac{p_i}{c^2}\right) = 0$). In contrast, if the different species were coupled, their equations of continuity would be coupled as well and the solution could be more difficult to find or even impossible, as there will be a larger number of unknowns than equations.

For the moment, we will take perfect fluids characterized by their density and pressure. If both magnitudes are related by an equation of state of the form $p = \omega\rho$, they will be barotropic fluids⁵ and if ω were constant, one could solve equation Eq. (1.27) as follows:

$$\rho_i \propto a^{-3(1+\omega_i)}, \quad (1.28)$$

getting an expression for the evolution of the energy density of species i . There are three possibilities: if $\omega_i > -1$, the energy density decreases as the Universe expands; if $\omega_i < -1$, it increases with the Universe; and if $\omega = -1$, it remains constant, which is the important case of the cosmological constant, that can be understood as a constant energy density in Eq. (1.21).

Confronting all these assumptions and derivations with observations [40], in the present state of the art one is led to the Λ CDM model which essentially states the following:

- The Universe seems to have had a beginning at an extremely high density stage denoted as the Big Bang, from which it evolved ever since.

⁵Any fluid with a equation of state of the form $p = p(\rho)$ is barotropic.

- The Universe has undergone an early acceleration dubbed inflation in order to solve some problems. The main ones are: the horizon problem (same background radiation from any point of the sky despite the entire sky not being in causal contact and consequently not being able to achieve thermal equilibrium), the flatness problem (fine tuning problem with the density of matter and energy to get a flat Universe), and the monopole problem (absence of magnetic monopoles which should have been produced during the early epoch of the Universe, being it very hot). This phenomenon would be able to explain the very high degree of homogeneity and isotropy of the observed Universe at large scale too.

However, Λ CDM does not explain this early acceleration, although an effective Λ is usually envisaged. The majority of scenarios to produce inflation involve a self interacting scalar field, the inflaton, that under appropriate conditions exhibits a short period of “slow-roll” during which there is an exponential or quasi-exponential expansion so that the scalar field behaves as a cosmological constant Λ .

After inflation, the primordial nucleosynthesis of light elements should occur. Then, the continuous decrease of temperature of the Universe brings down the temperature of the ultra relativistic plasma to a level that enables the recombination of the atoms. This happens approximately 360000 years after the nucleosynthesis and sets the stage at which electrons and protons first became bound to form electrically neutral atoms. After this, the mean free path of photons greatly increased, photons decouple from matter and become a thermal bath dubbed the Cosmic Microwave Radiation (CMB), because it reaches us at the present in the microwave band. The release of the CMB defines what we call the Last Scattering Surface (LSS), and corresponds to the oldest “photo” of our Universe. The CMB is a perfect black body radiation, but exhibits small temperature fluctuations that we identify as the seeds for the emergence of structures. The size of the underlying baryon fluctuations is associated with the sound horizon in the plasma, and provides us with a standard ruler denoted by Baryon Acoustic Oscillation (BAO).

- It is necessary to introduce Cold Dark Matter (CDM) to explain the velocity curves of galaxies and of structure formation. However, this form of matter has not been directly observed as yet and its nature is still unknown.

- There is a fluid with negative pressure called dark energy which is associated with the cosmological constant and explains the current accelerated expansion of the Universe.
- There are three epochs depending on the component which dominates at each moment. In sequence, they are: radiation epoch Ω_r , matter epoch Ω_m and cosmological constant epoch Ω_Λ .
- Our Universe is (nearly) flat, which implies $k \simeq 0$ in (1.18).

The main success of this model is that it is able to explain almost all observations until now, so why do we need an alternative model? We expose some of the more important problems of this model in the following section.

1.1.2 Problems of the Λ CDM model

In order to explain the physics of the cosmos on larger scales, it becomes mandatory to consider more exotic kinds of energy and matter than the standard sources of geometry. In this way, and under the uncontroversial assumption of homogeneity and isotropy in a GR ruled Universe, the Λ CDM model provides a quite worthy chronicle of our Universe driven by new unusual components (as we have anticipated): dark matter and dark energy.

Nevertheless, we cannot describe the physics of our Universe by just scraping its surface: when we examine the Λ CDM model in the light of the whole assortment of evidences available, we realize that, unfortunately, its two main components lead to new problems [41, 42, 43, 44, 45, 46, 47]. In particular, volumes have been written about the shortcomings of the specific type of dark energy on which the model relies, the cosmological constant Λ .

When a cosmological constant as dark energy represented by Λ , and CDM are introduced and contrasted with observations, they are estimated to make up 69.2% and 26.8% of the total energy content of the Universe respectively at present [48, 49]. Ergo, in addition to other problems as the quantization of GR, the two main problems which we are interested in will be associated with the need of introducing these new cosmological components.

On the one hand, CDM is introduced to explain the motion of galaxies in the frame of GR, but this kind of matter or fluid has not been directly detected. It means that we observe motions or effects (around the galaxy scale) which disagree with GR (which works very well at Solar

System scales), and in order to accommodate the theory with the observations, a new kind of matter is introduced (instead of modifying gravity). The result is that the theory is able to fit the observations, including structure formation, despite the need of introducing a hypothetical dark matter particle. The main problem is that there is no success so far in the experimental search for that particle.

On the other hand, there are problems associated with the cosmological constant. The most important ones are: the cosmological constant Problem (CCP), the Coincidence Problem (CP) and the Fine-Tuning Problem (FTP). The CCP is the discrepancy (around 120 orders of magnitude) between the observational value of the cosmological constant and the predicted value of the zero-point energy of quantum field theory. The CP is associated with the question of why the late acceleration of the Universe began when it did and its connection with structure formation. In a similar way, the FTP questions the fundamental reason for such a small value of the cosmological constant [47].

We have already spoken about the problems found in GR in order to get a cosmological model in agreement with observations, which essentially are the problems of the Λ CDM model. Introducing modifications into GR opens the door to physics beyond the Λ CDM model, which tries to resolve the previous issues through modified gravity [50, 51, 52]. However, notice that the new theory must have the same behaviour as GR at the Solar System scale.

Nevertheless, there are other possibilities if one wants to maintain GR: on the one hand, one could modify the matter content, i.e. modifying the right hand side of the Einstein equations with new kinds of matter; or modifying the geometry, in which case, it is the left hand side of the Einstein equations which is modified, loosening the Cosmological Principle. However, although the cosmological problems would be resolved, the problems from singularities would remain.

1.2 Modified Gravity

There are different theoretical and experimental reasons to consider gravitational theories beyond General Relativity [53, 50, 54, 55, 55, 56, 57, 58, 59, 60, 61]. Indeed, there has been in the last years a large number of proposed gravitational theories which modify GR somehow to keep the phenomenology (with good fittings to observations), but without the problems we have

previously referred. In fact, there are so many, that the classification will depend on the author, but under our knowledge and specially focused on this work we are going to classify them in 5 big groups:

- Extra fields which are added to the theory of gravity in different ways.
- Higher derivatives and non-local theories.
- Higher (spacetime) dimensional theories.
- Alternative formulations: changes in the geometry.
- Theories arising from quantum arguments.

However, this list is only a simplification and arises depending on the motivations from which the theory emerges, as some theories may be considered to belong to more than one item. Note that these groups are practically the same ones proposed by Lovelock's theorem already explained. In addition, there are other approaches to solve problems, which maintain GR as gravitational theory, but modifying other assumptions of the Λ CDM model like the concept of homogeneity and isotropy. It does not mean that the Universe is not homogeneous and isotropic at large scales, but its structures at interstellar scales may affect the total evolution at bigger scales.

From the viewpoint of theories based on higher spacetime dimensions, the first theory proposed was the Kaluza-Klein theory between the years 1919-1926 [62, 63]. This theory tried to unify gravitation and the electromagnetic forces using 5 dimensions. The starting point of view of the theory was a 5-dimensional metric tensor which included the 4-dimensional gravitational metric plus the vector potential A_i of the electromagnetic field, together two scalar functions. Thus one was able to obtain GR on the one hand, and the Maxwell equations on the other one. This theory allowed physicists to think about the possibility of unobserved additional dimensions which would be "rolled up" to get the effective 4-dimensional spacetime of GR. Other examples of theories with extra dimensions are String Theory or Superstring Theory which go beyond gravitation.

In a different way, there are theories that go beyond Lovelock's theorem, in what concerns second derivatives in the field equations. We already said that this theorem formulates that

Einstein's equations are the most general equations from a single metric (in 4-dimensions) with at most second order derivatives. Therefore, another possibility to extend the gravitational theory is to relax this constraint letting the field equations to be higher than second order. One of the most important proposals in this respect arises from replacing R with a non-linear $f(R)$ in the Einstein-Hilbert action [57, 64]. However, even if viable examples can be found within this class of models, there seems to be no compelling reason to prefer more complicated models to the simple cosmological constant within GR. In particular the extended models do not evade the cosmological FTP. This will be briefly analyzed in Section 3.2. Other important examples are the Gauss-Bonnet models based on $f(G)$ [65, 66, 67, 68, 69] where G is the Gauss-Bonnet term defined as⁶: $G = R^2 - 4R^{\mu\nu}R_{\mu\nu} + R^{\mu\nu\alpha\beta}R_{\mu\nu\alpha\beta}$.

Of course, from this point of view, there are other possible theories which arise by adding other higher order invariants in the Lagrangian of GR. Example of these are: Lovelock theories [71, 72, 36]; extensions of $f(R)$ such as $f(R, G)$, $f(R, R_{\mu\nu}R^{\mu\nu})$, $f(R, T)$ (where T is defined by the torsion); non-local theories [73, 74, 75] like $f(\square^{-1}R)$ (where \square^{-1} is the inverse of the D'alembertian) or $f(R_{\mu\nu}\square^{-1}R^{\mu\nu})$ and the so-called conformal Weyl theory.

A different approach are the so-called scalar-tensor theories, in which one introduces a new scalar field, which can be non-minimally coupled to gravity. The first historically important example is the Brans-Dicke theory (developed in 1961) [76, 77], in which the gravitational action is defined as:

$$S_g = \frac{c^3}{16\pi G} \int d^4x \sqrt{-g} \left(\phi R - \frac{\omega}{\phi} \partial_\mu \phi \partial^\mu \phi \right), \quad (1.29)$$

where ω is the dimensionless Dicke coupling constant. Of course, if one forces to $\phi = 1$, GR is recovered. The model has been studied from different perspectives, by considering perturbations [78], or the role of the coupling in the gravitational constant [79]. This will be thoroughly studied in Chapter 2.

A generalization of the previous one, is the Horndeski theory. This theory is the most general theory of gravity with an additional scalar field (therefore it is beyond Lovelock's theorem previously mentioned) which guarantees no Ostrogradsky instabilities. These instabilities are associated with equations of motion with more than two time derivatives and a Hamiltonian

⁶This term is motivated because Lovelock's theorem allows it in the Lagrangian since in 4-dimensions, it does not contribute to the equations of motions as it vanishes (in Riemannian geometry [70]) like a boundary term. However, this term is an essential part of the generalization of Lovelock's theorem at higher dimensions.

unbounded from below. In this case, the action is:

$$S_G = \int dx^4 \sqrt{-g} \left(\frac{c^3}{16\pi G} R + \mathcal{L}_{\text{Hr}} \right), \quad (1.30)$$

where \mathcal{L}_{Hr} is the Horndeski Lagrangian given by [80]:

$$\begin{aligned} \mathcal{L}_{\text{Hr}} = & G_2(\phi, X) \\ & - G_3(\phi, X) \square \phi \\ & + G_4(\phi, X) R + G_{4X}(\phi, X) [(\square \phi)^2 - \phi_{;\mu\nu} \phi^{;\mu\nu}] \\ & + G_5(\phi, X) \phi_{;\mu\nu} G^{\mu\nu} - \frac{G_{5X}(\phi, X)}{6} [(\square \phi)^3 - 3 \square \phi \phi_{;\mu\nu} \phi^{;\mu\nu} + 2 \phi_{;\mu\nu} \phi^{;\nu\lambda} \phi_{;\lambda}^{;\mu}] , \end{aligned} \quad (1.31)$$

where each G_n is an independent free function, $;$ is the covariant derivative, $_X$ is the derivative with respect to X , and X is the kinetic term defined as: $X = -\frac{1}{2} \partial_\mu \phi \partial^\mu \phi$. This theory will be analyzed for specific spacetimes beyond FLRW-metric in Chapter 5. From Eq. (1.31) one can check that Brans-Dicke theory is a particular case. Another important specific case of this is the so-called k -essence theory, in which only function G_2 is activated like a minimal coupled case. Initially, k -essence models were proposed to explain the inflationary epoch [81, 82], but it was realized that these models could explain the late-time cosmic acceleration as well. A more specific case of this one is the quintessence model [83, 84] in which G_2 is the standard Lagrangian density $G_2 = X - V(\phi)$, where $V(\phi)$ can be a general potential, turning it into the simplest scalar field scenario introduced to explain the acceleration stages.

It is important at this stage to introduce two important concepts in modified gravity and specially in scalar-tensor theories. These are the Einstein Frame (EF) and the Jordan Frame (JF). In order to give a brief definition one could think about the JF (in scalar-tensor theories) as the frame (or the representation of the theory) in which the scalar field is coupled with gravity, as opposed to the EF where, the scalar field is coupled to the matter Lagrangian. In general, both frames can be represented as follows:

$$\begin{aligned} S_J &= \int d^4x \sqrt{-g} [\mathcal{L}_g(g_{\mu\nu}, \phi) + \mathcal{L}_{\phi_J}(\phi)] + S_m(g_{\mu\nu}), \\ S_E &= \int d^4x \sqrt{-\tilde{g}} [\mathcal{L}_g(\tilde{g}_{\mu\nu}) + \mathcal{L}_{\phi_E}(\phi)] + S_m(\tilde{g}_{\mu\nu}, \phi), \end{aligned} \quad (1.32)$$

which are usually related by a conformal or disformal transformation:

$$\tilde{g}_{\mu\nu} = C(\phi, X) g_{\mu\nu} + D(\phi, X) \partial_\mu \phi \partial_\nu \phi, \quad (1.33)$$

where $C(\phi, X)$ is the conformal factor, and $D(\phi, X)$ is the disformal factor. Therefore, this redefines the metric with the scalar field, so that the coupling appears in one sector or other. In addition, this transformation preserves causality and the number of degrees of freedom. Those theories that connect the Jordan frame with the Einstein frame by Eq. (1.33) with $D(\phi, X) \neq 0$ are so-called disformal theories of modified gravity [85, 86, 87, 88, 89, 90, 91, 92], where the main point is that they can be transformed to GR but with the matter content coupled to a scalar field. Let me add that the Horndeski action is invariant under disformal transformations [93] and in addition (and related), the Einstein frame exists only when there is no G_5 .

The natural next step from scalar-tensor theories, in the same direction, is the vector-tensor theories [94, 95, 96, 97, 98, 99, 100] (with the special mention of Einstein-æther theories [101] with the particular property that they single out a preferred reference frame and allow for the study of violations of Lorentz symmetry in gravitation), with the form:

$$S_{VT} = \int d^4x \sqrt{-g} \left[\frac{c^3}{16\pi G} R + \mathcal{L}(g^{\mu\nu}, A^\mu) \right] + S_m(g_{\mu\nu}, \Psi), \quad (1.34)$$

where A^μ is a spacetime 4-vector field and Ψ are the matter fields which are not coupled to A^μ . Obviously, other possibilities are tensor-tensor theories which involve two rank-2 tensors (such as bigravity [102] and massive gravity [103]). Finally a combination of all [104], which are called scalar-tensor-vector theories, is also possible.

Another possibility concerns the connection, which we already mentioned that in GR is considered to be metric compatible and torsionless, which forces it to become the Christoffel symbols. Therefore, another possible modified scenario is to let the connection be free, in such a way that one finds the Palatini and the metric-affine theories (many times mistakenly treated as the same). For both theories, the connection is free, but in the Palatini case one considers that the matter action does not depend on it. In opposite, in the metric-affine formulation, the matter action depends on the connection as well. In both cases, one should apply variations with respect to the degrees of freedom, i.e. the metric and the connection, but in the first one the stress-energy tensor will be the usual, whilst in the second one it will depend on the hypermomentum tensor defined from variations of the matter Lagrangian with respect to the connection and for the Hilbert-Einstein action. Both frameworks or considerations can be applied in the Hilbert-Einstein action as in modified gravitational actions. It is usual to say that if one applies the Palatini formalism in Eq. (1.12), GR is recovered, but this is only true after some assumptions,

which close the system of equations, as showed in [35]. Of course, if one imposes a torsionless theory and a null non-metricity tensor (which takes account for the metric compatible character) adding Lagrange multipliers with that parameters to the action (1.12), one recovers GR in spite of considering a metric-affine formalism. We will come back to this issue in Chapter 7, where we will also study theories built focusing on the connection and its observational constraints. An extension of the Palatini approach is the Hybrid Metric-Palatini gravity, in which it is usual to change R in the GR action by a function of $f(R, \mathcal{R})$, where R is defined with the Christoffel symbols, whilst \mathcal{R} depends on the connection and offers a richer phenomenology [105].

We will finish this brief walk in the forest of modified gravity by mentioning some other theories, either from more radical changes in the geometry, like Finsler gravity, or motivated by quantisation such as Loop Quantum gravity, Hořava-Lifschitz gravity, or some non-local theories [73, 74, 75] playing an important role the p-adic strings theory [106, 107, 108], and which will not be delved in, since they are beyond the study issue of this work.

In order to simplify our calculation, from this point on (and if we do not specify otherwise) we will take the normalization of the speed of light as $c = 1$ and keep in mind the signature of the metric $(- + ++)$.

1.3 Energy Conditions

General Relativity only informs us about the form of communication between gravity and matter, however it does not tell us anything about what kind of material content one should consider as the source of the curvature of the spacetime. In the actual Universe, the stress-energy tensor, which has to be considered in Eq. (1.16), could be made up of contributions from a large number of different matter fields:

$$T_{\mu\nu}^{total} = T_{\mu\nu}^{\phi} + T_{\mu\nu}^m + T_{\mu\nu}^V + \dots . \quad (1.35)$$

Physicists have some kind of idea of the type of matter that exists under the mild conditions we find around us, but unfortunately, we have a very little idea of the behaviour of matter under extreme conditions of density and pressure. However it is possible to make assumptions about T^{μ}_{ν} , from the identification of criteriae that should be satisfied by material fields under “normal conditions”. We speak about energy conditions that are considered as physically reasonable

assumptions on the stress-energy tensor.

1.3.1 $T^{\mu\nu}$ as a symmetric tensor

A general $T^{\mu\nu}$ is defined varying the matter action with respect to the metric, Eq. (1.15). Consequently, if one considers that $g^{\mu\nu}$ is symmetric, $T^{\mu\nu}$ should be symmetric too. Due to this symmetry, one is able to diagonalize the purely spatial part of this tensor, adopting an orthonormal basis (which is not a coordinate basis generically), $B : \{\vec{e}_0, \vec{e}_1, \vec{e}_2, \vec{e}_3\}$ and performing rotations to get:

$$T^{\mu\nu} = \begin{pmatrix} \rho & f_1 & f_2 & f_3 \\ f_1 & p_1 & 0 & 0 \\ f_2 & 0 & p_2 & 0 \\ f_3 & 0 & 0 & p_3 \end{pmatrix}, \quad (1.36)$$

where ρ is the energy density, p_i are the pressures and f_i are the energy fluxes, all measured by an observer at rest in B . It is useful to note that in the basis B , it is possible to write any timelike vector, without loss of generality, as⁷:

$$V^\mu = \gamma \begin{pmatrix} 1 \\ \beta_1 \\ \beta_2 \\ \beta_3 \end{pmatrix} \quad \text{with} \quad \sum_i \beta_i^2 < 1. \quad (1.37)$$

The energy-momentum flux 4-vector will then take the form⁸:

$$F^\mu = -T^{\mu\nu} V_\nu. \quad (1.38)$$

However, there is still a lot of freedom if we do not suppose anything about the f_i .

1.3.2 Stress-energy tensor types: Hawking-Ellis Classification

There could be as many types of matter as the imagination of physicists and gravitational theories allow. However, from a tensorial representation with a symmetric Stress Energy Tensor in

⁷ $V_\mu = \gamma(-1, \beta_1, \beta_2, \beta_3)$ because the basis is orthonormal (not flat because it is not coordinate basis)

⁸ F^μ is the energy-momentum flux seen by V^μ

4 dimensions and in an orthonormal basis (1.36), Hawking and Ellis classified it in 4 possible forms depending on the extent to which they can be diagonalised by local Lorentz transformations⁹ [110, 111]:

$$T^{\mu\nu} = (HE)^{\alpha\beta} L_\alpha^\mu L_\beta^\nu . \quad (1.39)$$

1. Type 1: It has a timelike eigenvector \vec{e}_0 . It describes almost all observed fields:

$$T_I^{\mu\nu} = \begin{pmatrix} \rho & 0 & 0 & 0 \\ 0 & p_1 & 0 & 0 \\ 0 & 0 & p_2 & 0 \\ 0 & 0 & 0 & p_3 \end{pmatrix}, \quad \sigma(\lambda) = (-\rho, p_1, p_2, p_3), \quad (1.40)$$

where $\sigma(\lambda)$ are the eigenvalues. The eigenvalues p may be equal, or not but this matrix can be diagonalised always.

2. Type 2: It has a double-null eigenvector $\equiv \vec{e}_0 + \vec{e}_1$. It describes zero rest-mass fields when they describe radiation travelling in the direction $\vec{e}_0 + \vec{e}_1$:

$$T_{II}^{\mu\nu} = \begin{pmatrix} \mu + f & f & 0 & 0 \\ f & -\mu + f & 0 & 0 \\ 0 & 0 & p_2 & 0 \\ 0 & 0 & 0 & p_3 \end{pmatrix}, \quad \sigma(\lambda) = (-\mu, -\mu, p_2, p_3). \quad (1.41)$$

3. Type 3: It has a triple-null eigenvector $\equiv \vec{e}_0 + \vec{e}_1$:

$$T_{III}^{\mu\nu} = \begin{pmatrix} \rho & f/\sqrt{2} & f/\sqrt{2} & 0 \\ f/\sqrt{2} & -\rho + f & 0 & 0 \\ f/\sqrt{2} & 0 & -\rho - f & 0 \\ 0 & 0 & 0 & p_3 \end{pmatrix}, \quad \sigma(\lambda) = (-\rho, -\rho, -\rho, p_3). \quad (1.42)$$

4. Type 4: It has no timelike or null eigenvector:

$$T_{IV}^{\mu\nu} = \begin{pmatrix} \rho & f & 0 & 0 \\ f & -\rho & 0 & 0 \\ 0 & 0 & p_2 & 0 \\ 0 & 0 & 0 & p_3 \end{pmatrix}, \quad \sigma(\lambda) = (-\rho + if, -\rho - if, p_2, p_3). \quad (1.43)$$

⁹This classification of Hawking and Ellis updates and generalizes the Segré classification [109].

In order to understand better this classification, it is easier to consider the mixed tensor¹⁰ $T^\mu{}_\nu = T^{\mu\alpha}g_{\alpha\nu}$ [111]. Now, however, $T^\mu{}_\nu$ is not symmetric. That is the reason that, although the problem is like in euclidean space, the tensor can be non-diagonalizable. It can be seen, as we already said, that the spatial matrix can be diagonalised. Therefore, there are only 4 options depending on the 4 possible sets of eigenvalues. We have taken the signs in such a way as to obtain positive energy densities. However, in principle, there is no restriction about the signs of the eigenvalues.

1.3.3 Usual Energy Conditions

The energy conditions are assumptions made on the material content to extract generic characteristics of the spacetime through the equations of the theory. Therefore, those assumptions about the energy conditions should be satisfied by the stress-energy tensor of fields that we *know* exist in nature and it should not be trivially satisfied by any. However, let us remark once more that they are only assumptions based on our experience about the matter we know, and so as they are not strictly necessary or even dogmas, one is allowed to consider alternative possibilities.

It is usual to classify ECs into two groups and one additional group if one includes purely geometrical (not energy) conditions:

1. Geometrical Conditions:

- Timelike convergence condition (TCC): It is the convergence of timelike geodesics with zero vorticity. The matter and the theory of gravity are such that they imply the convergence of timelike geodesics. This implies that *Gravity is always attractive*.

Let us consider the Raychaudhuri equation [112]:

$$\frac{d\theta}{dS} = \omega_{\mu\nu}\omega^{\mu\nu} - \sigma_{\mu\nu}\sigma^{\mu\nu} - \frac{1}{3}\theta^2 - R_{\mu\nu}u^\mu u^\nu, \quad (1.44)$$

where:

$$\omega_{\mu\nu} = \nabla_{[\alpha}u_{\beta]} \quad \text{is the vorticity.} \quad (1.45)$$

$$\theta = h^{\mu\nu}\nabla_{(\nu}u_{\mu)} = \nabla_\mu u^\mu \quad \text{is the expansion.} \quad (1.46)$$

$$\sigma_{\mu\nu} = \nabla_{(\nu}u_{\mu)} - \frac{1}{3}\theta h_{\mu\nu} = \theta_{\mu\nu} - \frac{1}{3}\theta h_{\mu\nu} \quad \text{is the shear.} \quad (1.47)$$

¹⁰It must be noted that the eigenvalue problem from this mixed tensor is similar to the usual euclidean case whereas for $T^{\mu\nu}$: $v_\alpha^\mu T_{\mu\nu} = \lambda_\alpha v_\nu \Rightarrow (T_{\mu\nu} - \lambda_\alpha g_{\mu\nu}) = 0$.

and $h^\mu_\nu = \delta^\mu_\nu + u^\mu u_\nu$ is the tensor of the projection in the tangent subspace orthogonal to the velocity of the flux u^μ . For vorticity zero we can ensure $d\theta/dS \leq 0$ if:

$$R_{\mu\nu}V^\mu V^\nu \geq 0 \quad \forall V^\nu \text{ timelike} . \quad (1.48)$$

- Null convergence condition (NCC): Convergence of null geodesics. Matter and the theory of gravity are such that they imply the convergence of null geodesics. Analogously:

$$R_{\mu\nu}k^\mu k^\nu \geq 0 \quad \forall k^\mu \text{ null vector, } k_\mu k^\mu = 0 . \quad (1.49)$$

NCC is a limit case of TCC: $V^\mu \rightarrow k^\mu$. If TCC is satisfied \rightarrow NCC is satisfied.

2. Energy conditions that assume a reasonable behaviour of matter in a given theory of gravity

- Strong Energy Condition (SEC): Gravity is attractive in GR (without a cosmological constant), and for this reason in GR the TCC must be satisfied. Let us show that SEC \rightarrow TCC + Einstein equations:

$$\begin{aligned} R_{\mu\nu} - \frac{1}{2}g_{\mu\nu}R &= 8\pi GT_{\mu\nu} \quad \rightarrow \quad R = -8\pi GT \quad \rightarrow \\ \rightarrow \quad R_{\mu\nu} &= 8\pi G \left(T_{\mu\nu} - \frac{1}{2}g_{\mu\nu}T \right) , \\ \text{TCC: } R_{\mu\nu}V^\mu V^\nu &\geq 0 \quad \Rightarrow \quad \left(T_{\mu\nu} - \frac{1}{2}g_{\mu\nu}T \right) V^\mu V^\nu \geq 0 . \end{aligned} \quad (1.50)$$

So, the condition SEC is:

$$T_{\mu\nu}V^\mu V^\nu \geq \frac{1}{2}TV^\mu V_\mu . \quad (1.51)$$

- Null Energy Condition (NEC): Matter is such that in GR the NCC ($R_{\mu\nu}k^\mu k^\nu \geq 0$) is satisfied. In this case, the NCC condition together with Einstein's equations give us the following condition:

$$T_{\mu\nu}k^\mu k^\nu \geq \frac{1}{2}Tk^\mu k_\mu = 0 \quad \Rightarrow \quad T_{\mu\nu}k^\mu k^\nu \geq 0 . \quad (1.52)$$

We should note NEC is a particular limit of SEC.

3. Energy conditions that assume properties of any reasonable material content independently of the theory of gravity.

- Dominant Energy Condition (DEC): The energy density measured by any observer is non-negative and it propagates in a casual way. There are two magnitudes related with this:
 - Energy density measured by any observer: $\rho_{obs} = T_{\mu\nu}V_{obs}^{\mu}V_{obs}^{\nu}$. This condition tell us that this magnitude should always be positive.
 - Energy-momentum flux seen by V_{obs}^{μ} : $F_{obs}^{\mu} = -T^{\mu}_{\nu}V_{obs}^{\nu}$. In this case, this condition tell us that this vector must be causal.

So, the DEC could be written in the following form:

$$T_{\mu\nu}V^{\mu}V^{\nu} \geq 0 \quad \forall V^{\mu} \text{ timelike} \quad \text{and} \quad F^{\mu} \text{ is a causal vector} . \quad (1.53)$$

In some literature, this condition is found in the following form: a stress-energy tensor satisfies DEC if, and only if, $T_{\mu\nu}V^{\mu}V^{\nu} \geq 0$, and the vector $-T^{\mu}_{\nu}V^{\nu}$ is causal and is addressed to the future for all temporal vector V^{μ} addressed to the future.

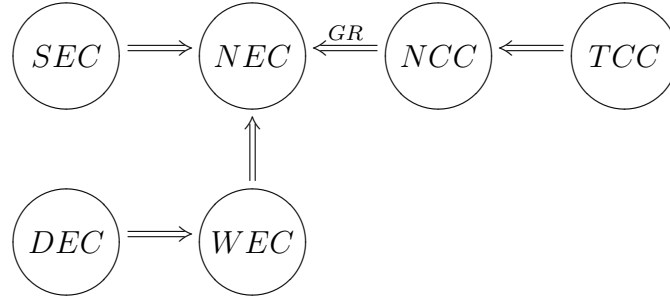
- Weak Energy Condition (WEC): The energy density measured by any observer is non-negative:

$$T^{\mu}_{\nu}V^{\nu}V_{\mu} \geq 0 . \quad (1.54)$$

Obviously, if DEC is satisfied \Rightarrow WEC is satisfied as well.

Also, the NEC is a particular limit of the WEC in which we consider $V^{\mu} \rightarrow k^{\mu}$ with $\beta \rightarrow 1$. So, if WEC is satisfied \Rightarrow NEC is satisfied too.

The relations between these conditions are:



In the diagram one can observe that if the SEC is satisfied, the NEC has to be satisfied as well. Therefore, if the NEC is not satisfied, SEC will not be satisfied. Therefore, it follows the mere violation of the NEC successively implies that the SEC, WEC and DEC are all violated (NCC and TCC too when we use GR as the gravitational theory).

During the 1960's, the trace energy condition (TEC) was also popular. It is now completely forgotten, since it is incompatible with ultra-relativistic matter and specifically focusing on stiff equations of state for neutron stars. For a signature $(-, +, +, +)$ it is [110, 113]:

$$\text{TEC: } T \leq 0 \quad \text{for type 1: } \rho - 3p \geq 0. \quad (1.55)$$

This fact teaches us the important lesson that the ECs should not be taken as fundamental and immutable conditions.

In the framework of modified gravity theories, the new degrees of freedom are usually recast as generalized effective fluids. This point of view has been intensively explored in the literature to constrain these modified theories, as for example for the case of $f(R)$ theories [114], scalar-tensor theories [115], or to find bounds on modified teleparallel gravity [116]. However, one should analyze carefully these results since the effective fluid from some modified gravity theories differ in nature with respect to the standard matter fluids [117].

1.3.4 Relevant inequalities for a perfect fluid

It is usual to find the expressions of the ECs referred to a stress-energy tensor of a perfect fluid (1.20). This is just a particular case of a type 1 stress-energy tensor which will be important throughout the present work. Recall that U^μ , in Eq. (1.20), is the fluid 4-velocity, which should not be confused with the observer's 4-velocity V^μ . In a diagonal basis comoving with the fluid,

one obtains¹¹:

$$T^\mu{}_\nu = \begin{pmatrix} -\rho & 0 & 0 & 0 \\ 0 & p & 0 & 0 \\ 0 & 0 & p & 0 \\ 0 & 0 & 0 & p \end{pmatrix}. \quad (1.56)$$

Thus, we recover the canonical expression for a type 1 with $p_1 = p_2 = p_3 = p$, without the need of using a local orthonormal basis, but only for the mixed tensor. Since this will be the main stress-energy tensor used in this work, let us write the translation of its energy conditions.

- WEC inequality

The condition is:

$$T^\mu{}_\nu V_\mu V^\nu \geq 0 \quad \forall V^\mu = (1; \vec{\beta}) \text{ such that } \beta_i \text{ satisfies } \sum_i \beta_i^2 < 1, \quad (1.57)$$

and therefore, for our kind of stress-energy tensor:

$$\rho + p \sum_i \beta_i^2 \geq 0. \quad (1.58)$$

This expression is linear in β_i^2 and it would always be satisfied by its extremal values, i.e. $\sum_i \beta_i^2 = 0$ and $\sum_i \beta_i^2 \rightarrow 1$. Therefore, on the one hand, if $\beta_1^2 + \beta_2^2 + \beta_3^2 = 0 \Rightarrow \beta_i^2 = 0$, then $\rho \geq 0$. On the other hand, if $\beta_1^2 + \beta_2^2 + \beta_3^2 \rightarrow 1$, then $\rho + p(\beta_1^2 + \beta_2^2 + \beta_3^2) \geq 0 \rightarrow \rho + p \geq 0$. Therefore, these conditions for a perfect fluid are translated into:

$$\rho \geq 0, \quad (1.59)$$

$$\rho + p \geq 0. \quad (1.60)$$

¹¹To check this one may express $U^\mu = (1, 0, 0, 0)$, $U_\mu = (-1, 0, 0, 0)$, $g^\mu{}_\nu = \delta^\mu{}_\nu$. Then:

$$\begin{aligned} T_0^0 &= (\rho + p)(-1) + p = -\rho. \\ T_j^i &= (\rho + p)(0) = 0 \text{ if } i \neq j. \\ T_j^i &= (\rho + p)(0) + p = p \text{ if } i = j = 1, 2, 3. \end{aligned}$$

- NEC inequality

The condition is:

$$T^\mu{}_\nu k^\nu k_\mu \geq 0 . \quad (1.61)$$

where, in this case, because k^μ is a null vector, $\sum_i \beta_i^2 = 1$ so we do not have the extremal case $\beta_1^2 + \beta_2^2 + \beta_3^2 = 0$ like in the previous subsection, and the only needed condition for a perfect fluid is:

$$\rho + p \geq 0 . \quad (1.62)$$

- DEC inequality

The condition is¹²:

$$T_{\mu\nu} V^\mu V^\nu \geq 0 \quad \text{and} \quad F^\mu F_\mu \leq 0 \quad \forall V^\mu \text{ timelike} . \quad (1.63)$$

As DEC implies WEC, we already know that for a perfect fluid we need the same constraint than for WEC for the first part of (1.63). Let us study the second inequality of this condition¹³.

$$F^\mu F_\mu = T^\mu{}_\nu V^\nu T_{\mu\alpha} V^\alpha = -\rho^2 + p^2(\beta_1^2 + \beta_2^2 + \beta_3^2) \leq 0 . \quad (1.64)$$

where the inequality $\rho + p_j \geq 0$ is contained. So, we express this condition for our stress-energy tensor:

$$\rho \geq 0 , \quad (1.65)$$

$$\rho \geq p \geq -\rho . \quad (1.66)$$

- SEC inequality

This condition is:

$$T^\mu{}_\nu V_\mu V^\nu \geq \frac{1}{2} T V^\mu V_\mu , \quad (1.67)$$

¹²Let us remark that a causal vector means that it is timelike or null, which for a metric with signature $(-, +, +, +)$ it is translated into $V^\mu V_\mu \leq 0$

¹³It is obvious that in this part the specific form of the metric appears, however, we will consider a sufficiently local region.

which could be translated into:

$$\frac{1}{2} (1 + \sum_i \beta_i^2) \rho + p \sum_i \beta_i^2 + \frac{3}{2} p (1 - \sum_i \beta_i^2) \geq 0 \quad , \quad (1.68)$$

and whose extremes are:

– $\sum_i \beta_i^2 \rightarrow 0$. Then:

$$\frac{1}{2} \rho + \frac{3}{2} p \geq 0 . \quad (1.69)$$

– $\sum_i \beta_i^2 \rightarrow 1$, i.e. $\beta_i^2 \rightarrow 1$ and $\beta_j^2 = \beta_k^2 \rightarrow 0$, then:

$$\rho + p \geq 0 . \quad (1.70)$$

So, in this case, the conditions are:

$$\begin{aligned} \rho + 3p &\geq 0 , \\ \rho + p &\geq 0 . \end{aligned} \quad (1.71)$$

1.3.5 Classical examples of violations of the Energy Conditions

The energy conditions or their violations are useful to extract general characteristics of the space-time. With the purpose of showing that, let us present two important examples in the frameworks of the cosmology model and scalar fields.

We showed that for the current cosmological model we need to introduce two epochs of accelerated expansion of our Universe: inflation and the current epoch. Therefore, the Time-like Convergence Condition (TCC) (which is independent of the gravitational model) cannot be satisfied during those epochs, as gravity would not be attractive in an accelerated Universe.

In order to check this fact, recall that the TCC implies:

$$R_{\mu\nu} V^\mu V^\nu \geq 0 \quad \forall V^\mu \text{ timelike} . \quad (1.72)$$

and considering a spatially flat FLRW:

$$ds^2 = -dt^2 + a^2(t)(dr^2 + r^2 d\Omega^2) , \quad (1.73)$$

where $d\Omega^2 = d\theta^2 + \sin^2\theta d\phi^2$, and whose 00–component of the Riemann tensor is¹⁴:

$$R_{00} = -3\frac{\ddot{a}}{a}. \quad (1.74)$$

On the other hand, considering the velocity of the co-moving observer $V_{co}^a = \gamma(1, \vec{0})$, one gets:

$$R_{\mu\nu}V_{co}^\mu V_{co}^\nu = \gamma^2 \left(-3\frac{\ddot{a}}{a} \right). \quad (1.75)$$

Consequently, for an accelerated ($\ddot{a} > 0$) Universe, the co-moving observer will perceive a “repulsive” gravity, and therefore the TCC is violated. In addition, putting together TCC with GR, one obtains SEC, so it should also be violated. But SEC focuses on the matter content and not on the gravitational part, so the kinds of matter that support this effect (in these specific cases dark energy and the inflation field) must violate the SEC by definition.

Thus, if one considers dark energy with a stress-energy tensor of type 1, the SEC for a comoving timelike vector is translated into $\rho \geq (\rho - 3p)/2$, and using the state equation $p = \omega\rho$, the violation of SEC becomes $\omega < -1/3$.

Another important example to show the Energy Conditions and focusing in modified gravity is the study of a non-minimally coupled scalar field (since, from the previous example, it is easy to conclude that a minimally coupled scalar field satisfies DEC, WEC and NEC, but it can violate the SEC, considering dark energy described by a quintessence model). A possible action would be then [118]:

$$S = \frac{1}{2\kappa^2} \int d^4x \sqrt{-g} R + \int d^4x \sqrt{-g} \left(-\frac{1}{2} g^{\mu\nu} \partial_\mu \phi \partial_\nu \phi - V(\phi) - \frac{\epsilon}{2} R \phi^2 \right), \quad (1.76)$$

where the non-minimal coupling is in the term: $\frac{\epsilon}{2} R \phi^2$. So, one could think about the second integral as the matter-action and use the definition of the stress-energy tensor (1.15). The first step will be to calculate the variation of the term with the non-minimally coupled term, one has to take into account that, due to the ϕ^2 factor, the variation $\delta R_{\mu\nu} / \delta g^{\alpha\beta}$ term does not vanish, as the result is not a total derivative, which we could split up from the integral and vanish it to zero in the boundary. Thus,

$$\mathcal{L}_\epsilon = -\frac{\epsilon}{2} \sqrt{-g} R_{\mu\nu} g^{\mu\nu} \phi^2. \quad (1.77)$$

¹⁴where the global sign in the metric does not affect to this result.

So,

$$\begin{aligned}
\frac{\delta \mathcal{L}_\epsilon}{\delta g^{\alpha\beta}} &= -\frac{\epsilon}{2} \frac{\delta \sqrt{-g}}{\delta g^{\alpha\beta}} R_{\mu\nu} g^{\mu\nu} \phi^2 - \frac{\epsilon}{2} \sqrt{-g} \frac{\delta R_{\mu\nu}}{\delta g^{\alpha\beta}} g^{\mu\nu} \phi^2 - \frac{\epsilon}{2} \sqrt{-g} R_{\mu\nu} \frac{\delta g^{\mu\nu}}{\delta g^{\alpha\beta}} \phi^2 \\
&= -\frac{\epsilon}{2} \left(-\frac{1}{2} \sqrt{-g} g_{\alpha\beta} \right) R_{\mu\nu} g^{\mu\nu} \phi^2 - \frac{\epsilon}{2} \sqrt{-g} \frac{\delta R_{\mu\nu}}{\delta g^{\alpha\beta}} g^{\mu\nu} \phi^2 - \frac{\epsilon}{2} \sqrt{-g} R_{\alpha\beta} \phi^2 \\
&= -\frac{\epsilon}{2} \sqrt{-g} G_{\alpha\beta} \phi^2 - \frac{\epsilon}{2} \sqrt{-g} [g_{\alpha\beta} \square \phi^2 - \nabla_\alpha \nabla_\beta (\phi^2)] , \tag{1.78}
\end{aligned}$$

where in the last step we have done an integration by parts and we have cancelled the terms which are evaluated at the boundary. We can see straightforwardly that if ϕ were a constant we would obtain the Einstein tensor with another coupled constant. So, the stress-energy tensor is¹⁵:

$$\begin{aligned}
T(\phi)_{\mu\nu} &= \nabla_\mu \phi \nabla_\nu \phi - \frac{1}{2} g_{\mu\nu} (\nabla \phi)^2 - g_{\mu\nu} V(\phi) + \epsilon G_{\mu\nu} \phi^2 + \epsilon [g_{\mu\nu} \square \phi^2 - \nabla_\mu \nabla_\nu (\phi^2)] = \\
&= \nabla_\mu \phi \nabla_\nu \phi - \frac{1}{2} g_{\mu\nu} (\nabla \phi)^2 - g_{\mu\nu} V(\phi) + \epsilon G_{\mu\nu} \phi^2 \\
&\quad + 2\epsilon [g_{\mu\nu} \nabla^\alpha (\phi \nabla_\alpha \phi) - \nabla_\mu (\phi \nabla_\nu \phi)] , \tag{1.79}
\end{aligned}$$

and therefore Einstein's equations are:

$$G_{\mu\nu} = \kappa^2 T(\phi)_{\mu\nu} , \tag{1.80}$$

where now $T(\phi)_{\mu\nu}$ contains geometrical terms. We are going to move the geometrical terms to the l.h.s:

$$G_{\mu\nu} (1 - \kappa^2 \epsilon \phi^2) = \kappa^2 \left\{ \nabla_\mu \phi \nabla_\nu \phi - \frac{1}{2} g_{\mu\nu} (\nabla \phi)^2 - g_{\mu\nu} V(\phi) + 2\epsilon [g_{\mu\nu} \nabla^\alpha (\phi \nabla_\alpha \phi) - \nabla_\mu (\phi \nabla_\nu \phi)] \right\} . \tag{1.81}$$

So, we can define an effective $T(\phi)_{\mu\nu}^{eff}$:

$$\begin{aligned}
G_{\mu\nu} &= \frac{\kappa^2}{1 - \kappa^2 \epsilon \phi^2} \left\{ \nabla_\mu \phi \nabla_\nu \phi - \frac{1}{2} g_{\mu\nu} (\nabla \phi)^2 - g_{\mu\nu} V(\phi) + 2\epsilon [g_{\mu\nu} \nabla^\alpha (\phi \nabla_\alpha \phi) - \nabla_\mu (\phi \nabla_\nu \phi)] \right\} = \\
&= \kappa^2 T(\phi)_{\mu\nu}^{eff} . \tag{1.82}
\end{aligned}$$

This is the relevant tensor for the study of the ECs, as it does not contain geometrical terms now. Let us study how the NEC (equivalently the NCC) behaves:

$$G_{\mu\nu} k^\mu k^\nu = \kappa^2 T(\phi)_{\mu\nu}^{eff} k^\mu k^\nu . \tag{1.83}$$

¹⁵Recall that for a scalar field the covariant derivative is the same as a partial derivative, i.e. $\nabla_\mu \phi = \partial_\mu \phi$.

We consider k^μ to be a null vector tangent to a geodesic $x^\mu(\lambda)$, with λ the affine parameter, i.e. $k^\mu \nabla_\mu \phi = \frac{d\phi}{d\lambda} \equiv \phi'$:

$$\begin{aligned} G_{\mu\nu} k^\mu k^\nu &= \frac{\kappa^2}{1 - \kappa^2 \epsilon \phi^2} \left\{ (\phi')^2 - 2\epsilon k^\mu k^\nu (\nabla_\mu \phi \nabla_\nu \phi + \phi \nabla_\mu \nabla_\nu \phi) \right\} \\ &= \frac{\kappa^2}{1 - \kappa^2 \epsilon \phi^2} \left\{ (\phi')^2 - \epsilon (\phi^2)'' \right\}. \end{aligned} \quad (1.84)$$

We are going to study now the three possible cases:

- $\epsilon = 0$ is the minimally coupled field. In this case: $T_{\mu\nu} k^\mu k^\nu = (\phi')^2 \geq 0$. Therefore NEC is satisfied.
- $\epsilon < 0$. In this case the coefficient $1/(1 + \kappa^2 |\epsilon| \phi^2)$ should always be positive. Let us study the minimum and maximum of ϕ^2
 1. Minimum: $\phi' = 0$ and $(\phi^2)'' > 0$ so NEC is satisfied.
 2. Maximum: $\phi' = 0$ and $(\phi^2)'' < 0$ so NEC is violated.
- $\epsilon > 0$. In this case, if $|\phi| > (\kappa^2/\epsilon)^{1/2}$ then $T_{\mu\nu}^{eff} \propto -[(\phi')^2 - \epsilon(\phi^2)']$ any local minimum of ϕ^2 would violate the NEC, and if $|\phi| < (\kappa^2/\epsilon)^{1/2}$ any local maximum would violate NEC too.

So, the conclusion is that NEC is generically violated once one introduces non-minimally couplings with the geometry.

Chapter 2

About the gravitational coupling constant

In Newton's law of gravitation, written as in Eq. (1.2) with $G = -k^2$, the gravitational constant, G , is assumed to be positive to obtain an attractive character. Of course, this character should be recovered in GR, where G plays the role of the coupling of the geometry to the matter content of the Universe. The consequence of this is to take the gravitational coupling as positive and constant. However, this fact seems to be the only reason to consider a "static" coupling. In 1938, Dirac made an astounding proposal, dubbed the Large Number Hypothesis, according to which any dimensionless ratio between two fundamental quantities of nature should be of the order unity (for a more detailed account of the motivations see [119]). This led him to put forward that if G were to evolve with the Hubble rate of expansion of the Universe this would account for the present disparity of about 40 orders of magnitude between the gravitational and electromagnetic forces at the atomic level. The possibility of a dynamical gravitational coupling was thus considered.

This was the first time the variation of some fundamental constant was explicitly and seriously envisaged. Dirac's proposal was given a field theoretical realization, first by P. Jordan within a Kaluza-Klein type approach (thus involving extra-dimensions), and then, in 1961, by R. Dicke and his student C. Brans who introduced the theory already presented in Eq. (1.29), under the motivation of accomplishing Mach's principle [2, 76]. In both cases a dynamical scalar field ϕ couples to the spacetime curvature and thus plays a gravitational role. As mentioned in the introduction, this scalar field represents new degrees of freedom and upon variational differentiation with respect to the latter implies additional field equations.

In principle, within this framework, it becomes possible for G to change sign, trading attracting into repulsive gravity, and conversely. This might happen either during the cosmological time evolution, or even conceivably it might happen at spatially separated regions of spacetime. The concern about the sign of the gravitational constant has been envisaged as a constraint to be respected by the spectrum of modified gravity theories, but the focus has never been directed to devise a mechanism to assure its positiveness. For instance, Barrow [120] proposed that the formation of primordial black holes during the early stages of the Universe might retain “memory” of the value of the gravitational constant at the time of their formation, and hence exhibit diverse values of the latter depending on the instant of their formation, around $t_{Prim} \sim 10^{-25}$ s.

Then, we will start this chapter studying the most elementary part of the gravitational theory from a relativistic point of view, this is the coupling between matter and gravity, for which one should go into the world of modified gravity and more specifically into the scalar-tensor (ST) gravity theories. In addition, we want to analyze a possible cosmological mechanism that determines the positiveness of the sign of G , even though it may exhibit transient periods in the negative region. We are going to show that this cosmological device relies on the role of a cosmological potential, which reproduces a positive cosmological constant in the so-called Einstein frame. From this latter viewpoint it can be understood as another role of paramount importance of this remarkable constant. In Refs. [121, 122], I. Roxburgh analysed the issues of the sign and magnitude of the gravitational constant, based on Einstein’s correspondence principle which demands that Newtonian gravity be recovered in the weak field limit of the theory. His analysis is done in the framework of GR and is somewhat motivated by Mach’s principle, leading him to conclude that G must be positive. Other studies which carry some relation to the present chapter are [123, 124, 125, 126, 127, 128, 129, 130].

We shall start by briefly looking at the implications of having $G < 0$ in cosmology, namely showing that inflation arises for a considerably large set of parameters, and that one obtains bouncing solutions that avoid the initial singularity when a cosmological constant is also considered. Only then will we analyze the cosmological behaviour of scalar-tensor theories to show how a subset of the solutions exhibit negative G , and how a cosmological potential provides us with a mechanism that favours positive G and eventually stabilizes its sign. In essence we will show that the presence of a cosmological constant in the Einstein frame provides such a mechanism for an extended set of varying G theories, which represents a relevant feature for the

existence of a non-vanishing cosmological constant in the Einstein frame (and of a corresponding cosmological potential in the Jordan frame). At the same time, we will use this study to introduce more deeply one of the simplest theories (but not less relevant) in modified gravity.

2.1 Negative G in GR

It must be said that if we envisage the trading of a positive G into a negative one within Einstein's General Relativity, the attractive nature of gravity will be mutating into a repulsive one, and this avoids the need to rely on exotic matter, violating the strong energy condition, to produce inflationary stages. This is therefore an alternative ad-hoc device, akin to the Albrecht and Magueijo's varying speed of light to avoid the perplexing complications of the inflationary scenarios [131]. The down side of this way of producing repulsive gravity, is that once assumed, it is forever. There would be no way of exiting inflation with canonical matter sources. The scalar-tensor scenario that we consider afterwards avoids the latter problem, since it allows a change of the sign of G along its evolution, and presents us with a natural, and theoretically consistent framework for exploring the possible negativeness of G .

2.1.1 Friedmann Models with a Single Fluid

Consider the usual FLRW universes of the standard cosmological model, and take $G = -|G|$ in Einstein's GR and without the cosmological constant in Eq. (1.21) and Eq. (1.26). We then have the following field equations¹:

$$\frac{\dot{a}^2}{a^2} + \frac{k}{a^2} = -\frac{8\pi|G|}{3} \rho, \quad (2.1)$$

$$\frac{\ddot{a}}{a} = \frac{8\pi|G|}{6} (\rho + 3p). \quad (2.2)$$

From the change of sign of G , the signs on the right hand side are the opposite with respect to the usual ones written in Eq. (1.21) and Eq. (1.26). However, the Bianchi contracted identities for a perfect fluid in thermodynamic equilibrium are immune to this change of sign and the energy conservation equation is preserved as Eq. (1.27):

$$\dot{\rho} = -3H(\rho + p). \quad (2.3)$$

¹Recall that dots denote derivatives with respect to time, a is the scale factor of the Universe, ρ and p are the energy density and pressure, respectively, and we have taken $c = 1$.

Thus, when the matter content (type I of the Hawking-Ellis Classification) satisfies the weak and strong energy conditions, $\rho > 0$, $\rho + p \geq 0$, and $\rho + 3p \geq 0$, we see from the Raychaudhuri Equation (2.2), that the expansion is accelerated, $\ddot{a} \geq 0$. Yet, this inflationary behaviour is constrained by the Friedmann Equation (2.1). It can be easily verified that the single fluid solutions are forbidden when $k = 0, +1$, and are restricted to $\rho \leq 3/8\pi|G|a^2$ when $k = -1$.

Furthermore, notice that the transformation $|G| \rightarrow -|G|$ which is performed in the Einstein field equations of the FLRW models produces a system which mimics phantom matter provided the equation of state relating the pressure and the energy density of matter is such that $p(\rho) \rightarrow -p(-\rho)$ when $\rho \rightarrow -\rho$, preserving the field equations (we remark that this happens to be the case for the barotropic equations $p = (\gamma - 1)\rho$ which are usually considered; in addition the cosmography framework, as exposed in [132, 133], also absorbs this transformation and is left unchanged).

2.1.2 Model with a cosmological constant

Now, let us introduce a cosmological constant in addition to the perfect fluid:

$$T_{\mu\nu} = -\Lambda g_{\mu\nu} . \quad (2.4)$$

The field equations now read

$$\frac{\dot{a}^2}{a^2} + \frac{k}{a^2} = \lambda - \frac{8\pi|G|}{3} \rho , \quad (2.5)$$

$$\frac{\ddot{a}}{a} = \lambda + \frac{8\pi|G|}{6} (\rho + 3p) , \quad (2.6)$$

where $\lambda = \Lambda/3$. Recasting the latter equations in conformal time η defined by $d\eta = dt/a(t)$ we get

$$(a')^2 + ka^2 = \lambda a^4 - \frac{8\pi|G|}{3} \rho a^4 , \quad (2.7)$$

$$\frac{a''}{a} = 2\lambda a^2 - k - \frac{8\pi|G|}{6} (\rho - 3p) a^2 , \quad (2.8)$$

where $'$ denotes derivative with respect to the conformal time η . Assuming that the matter content is a barotropic perfect fluid with equation of state (EOS) $p = (\gamma - 1)\rho$ where γ is a constant that takes values in the range $0 < \gamma \leq 2$, we derive the exact solutions from Eq. (2.7)

$$\int \frac{da}{(\lambda a^4 - (8\pi|G|/3)\rho_0 a^{4-3\gamma} - k a^2)^{1/2}} = \pm(\eta - \eta_0) , \quad (2.9)$$

which yields Jacobi elliptic functions. Naturally, in the latter equation η_0 is an arbitrary integration constant that sets the origin of time. There are four kinds of components that are of special interest: (i) Radiation, i.e., $\gamma = 4/3$, (ii) Dust, i.e., $\gamma = 1$, (iii) Stiff matter, i.e., $\gamma = 2$, and (iv) The coasting model $\gamma = 2/3$.

A possibility of great interest is the case where we have a combination of pressureless matter and radiation together with a cosmological constant, since these are the 3 major components that best fit the expansion history of the Universe (Λ CDM model) [40]. The corresponding dynamical system, from Eq. (2.8), reads:

$$a' = b, \quad (2.10)$$

$$b' = -ka - \frac{8\pi|G|}{6}\rho_d^0 + 2\lambda a^3 = -ka - \frac{\Omega_m H_0^2}{2} + 2\Omega_\Lambda H_0^2 a^3, \quad (2.11)$$

where ρ_d^0 is the current density of dust. In addition, the first Friedmann constraint equation becomes:

$$ka^2 + b^2 = -\frac{8\pi|G|\rho_d^0}{3}a - \frac{8\pi|G|\rho_r^0}{3} + \lambda a^4, \quad (2.12)$$

from where one can appreciate that now the cases with $k = 0, +1$ are allowed (with restriction) because of the last term λ as long as this is positive.

In Figure 2.1, we represent the phase diagrams depicting the qualitative behaviour of these negative G models for some choices of matter content (for a recent review of the methods of dynamical systems in cosmology see [134]). Analyzing the existence and nature of the fixed points, we classify the possible dynamical behaviours. Please note that we have compactified the phase diagrams using the transformation $x = \tanh a$ and $y = \tanh b$, so that the boundary lines $x = \pm 1$ and $y = \pm 1$, respectively, correspond to $a \rightarrow \pm\infty$ and $b \rightarrow \pm\infty$. This allows us to devise the asymptotic solutions at infinity.

The number and position of the fixed points in the finite region of the phase plane (a, b) is defined by the roots of Eq. (2.11) when $b = 0$. Therefore, there will be at most three fixed points on the a axis (plus the fixed points at infinity which will not be on the a axis). In Figure 2.1 we display the qualitative behaviour of the model for the three spatial curvatures and use reasonable values for the parameters in Eq. (2.11), which take into consideration the Λ CDM model. We adopt $\Omega_\Lambda H_0^2 / \Omega_m H_0^2 \approx 2$, except in Figure 2.1d.

One must be wary though that in the phase-diagrams of Figure 2.1 the half-plane corresponding to negative values of a is not physical. Yet its representation is useful, because it illustrates

the complete behavior of the mathematical dynamical system underlying the physical scenario, regardless of the physical consistency of some of its parts. Moreover, in the present case it also allows for a comparison with the posterior phase-diagrams of the scalar-tensor models we will show below.

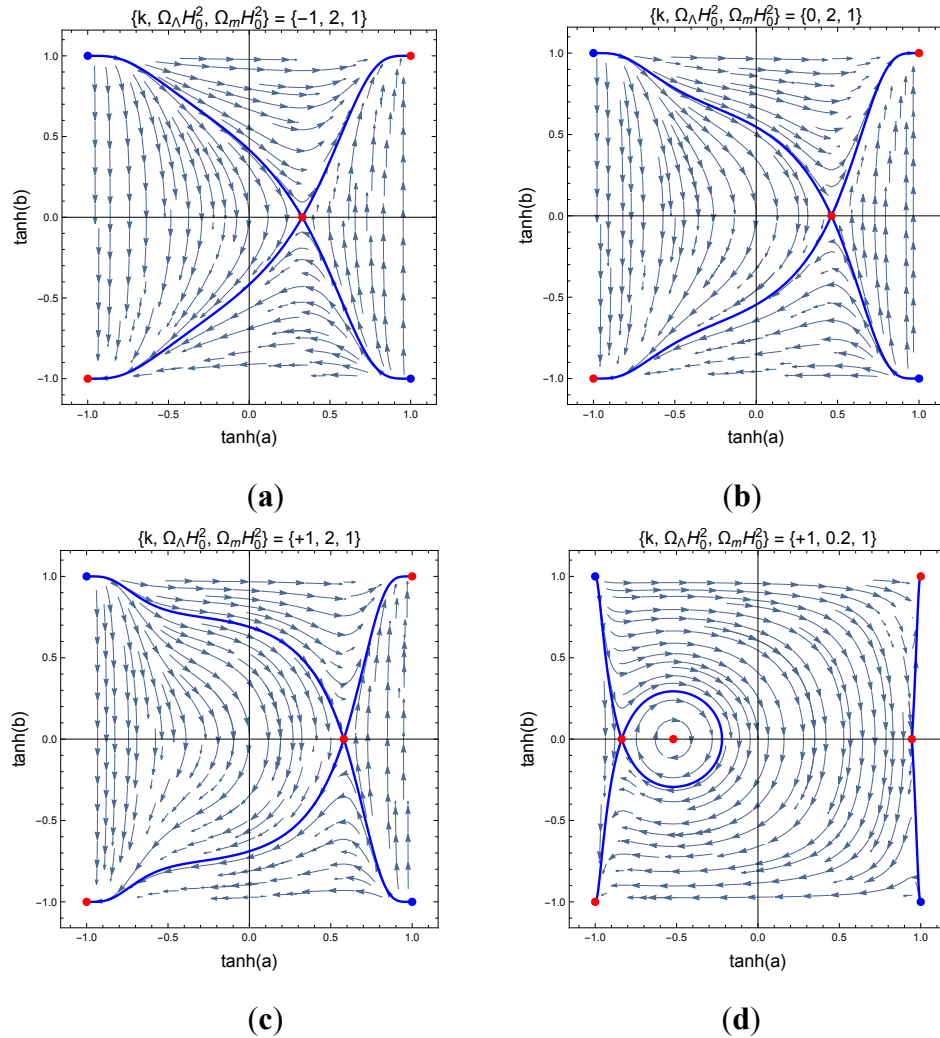


Figure 2.1: Phase-diagrams displaying the behaviour of the vector field (a, a') for GR with a negative G . From left to right and from top to down: (a) represents the $k = -1$ models, (b) the $k = 0$ models, and (c,d) correspond both to the $k = +1$ models with different values for the relation Ω_Λ/Ω_m . Red points are fixed points and blue points represent the starting point of the most solutions excepting those that correspond with circular orbits.

In Figure 2.1 (a,b) the $k = -1$ and $k = 0$ models are represented, and Figure 2.1 (c,d) correspond both to the $k = +1$ models. The lower half-planes of the various diagrams are mirror reflections from the upper ones under the $t \rightarrow -t$, $(a, b) \rightarrow (a, -b)$ symmetry. In Figure 2.1 (a) there are three fixed points, one at $\{a, b\} = \{a_*, 0\}$, where a_* is a finite root of the right-hand side of Eq. (2.11) (which for our choice of parameters corresponds to $\{a, b\} = \{0.341164, 0\}$),

and two at infinity. The former fixed point is a saddle point denoting an unstable static solution; the latter points at $b = \pm\infty$ are contracting and expanding de Sitter solutions related by the time reversal symmetry. Although the model is open, there are re-collapsing solutions at the left of the finite fixed point, and solutions collapsing from infinity and bouncing back to it. In Figure 2.1 (b) there also are three fixed points, one at $\{a, b\} = \{0.5, 0\}$, and the other two at $b = \pm\infty$. The qualitative behaviour is alike to the one found for the $k = -1$ case. The Figure 2.1 (c,d) phase diagrams display the two possible behaviours of the $k = +1$ case, which translate the existence of a bifurcation associated with two different subsets in what regards the balance of parameters (the bifurcation occurs for $8\pi|G|\rho_a^0 = 4/\sqrt{6\lambda}$). In the left one, Figure 2.1 (c), once again there are three fixed points at $\{a, b\} = \{0.662359, 0\}$ plus the two fixed points at infinity. From a qualitative viewpoint, we find the same behaviour as in the previous open models. However, in Figure 2.1 (d) there are three fixed points on the x -axis, namely two saddle points and a center in between, the latter of which corresponds to a basin of oscillatory behaviour. Yet, being located in the left-half plane, i.e., $a < 0$, its impact on the physical right-hand side is not qualitatively noticeable, apart from reducing the proportion of solutions which evolve towards the de Sitter points at $b = \pm\infty$.

Analyzing the fixed points of the compactified phase-diagrams, we find that for $k = -1$ and $k = 0$, there are only three fixed points, while for $k = +1$ there could be either three or five fixed points, counting the two critical points at infinity. In the former cases, when there are only three fixed points, the qualitative behaviour is the same independently of the value of k . Different spatial curvature indexes only distinguish through a horizontal shift of the location of the critical point on the horizontal axis. These fixed points are saddle points which correspond to unstable static solutions. In all k cases, there are solutions where a expands to infinity. This fact was foreseeable, because of the repulsive character of gravity when G is changed to $-|G|$. They correspond to asymptotic de Sitter (deS) solutions, both in the future and in the past, upon time reversal. They reflect the eventual domination of the cosmological λ -term, overcoming the impact of the sign of G , yet the swapping of the sign of G enhances this domination. Obviously, according to this behaviour, the current accelerated expansion of the Universe is not a problem, but we have a gravity which is inconsistent at small scales with the weak field limit, and thus would be at odds with the Solar System behaviour [121, 122]. However, the analysis pursued in this section is merely a first step to assess the cosmological impact of a negative gravity.

In the following section we shall consider the issue within the more appropriate framework of modified metric gravity theories which assume the variation of G .

2.2 Scalar-Tensor Gravity Theories

We now consider the scalar-tensor gravity theories given by the action

$$S = \frac{1}{16\pi} \int \sqrt{-g} \, d^4x \left[\phi R - \frac{\omega(\phi)}{\phi} \partial_\mu \phi \partial^\mu \phi - 2U(\phi) \right] + S_m, \quad (2.13)$$

which is a generalization of the Brans-Dicke theory already mentioned in Eq. (1.29), since we allow the coupling constant ω to evolve, and where a potential term $U(\phi)$ of cosmological nature is considered². We may express this potential as $U(\phi) = \phi \lambda(\phi)$ to visualize more easily the case of GR, in which this term ends up becoming the cosmological constant. Besides, one can consider that either the gravitational coupling constant G has been hidden inside the scalar field ϕ , or that it has been directly exchanged for a dynamical parameter ϕ , which generically varies, using the relation $G = 1/\phi$, allowing us to see the scalar field ϕ as the gravitational permittivity of the spacetime [135]. At last, we will say that this scalar field is non-minimally coupled to gravity. In General Relativity we can see that matter and gravity are terms completely separated in the action and in the equations of motion (excepting the metric), so we say that they are minimally coupled, but in this case, we can observe how ϕ and R are directly coupled to each other. We will denote to the theories with this sort of couplings as Non-minimal Scalar Tensor Theory (NMSTT).

The field equations are

$$R_{\alpha\beta} - \frac{1}{2} g_{\alpha\beta} R + \lambda(\phi) g_{\alpha\beta} = \frac{\omega(\phi)}{\phi^2} \left[\phi_{;\alpha} \phi_{;\beta} - \frac{1}{2} g_{\alpha\beta} \phi_{;\gamma} \phi^{;\gamma} \right] + \frac{1}{\phi} [\phi_{;\alpha\beta} - g_{\alpha\beta} \phi_{;\gamma}^{;\gamma}] + 8\pi \frac{T_{\alpha\beta}}{\phi}, \quad (2.14)$$

$$\square \phi - \frac{2\phi^2 \lambda_\phi(\phi) - 2\phi \lambda(\phi)}{2\omega(\phi) + 3} = \frac{1}{2\omega(\phi) + 3} [8\pi T - \omega_\phi(\phi) \phi_{;\gamma} \phi^{;\gamma}], \quad (2.15)$$

where $T \equiv T^\lambda{}_\lambda$ is the trace of the stress-energy tensor, $T_{\alpha\beta}$, the semicolon denotes the covariant derivative, and $A(\phi)_\phi$ means the derivative with respect ϕ of the function $A(\phi)$. When applied

²For a scalar field $\partial_\mu = \nabla_\mu$ since the connection does not interfere.

to the FLRW models we obtain

$$3 \left(\frac{\dot{a}}{a} \right)^2 + 3 \frac{\dot{a}\dot{\phi}}{a\phi} + 3 \frac{k}{a^2} = \lambda(\phi) + \frac{\omega(\phi)\dot{\phi}^2}{2\phi^2} + 8\pi \frac{\rho}{\phi}, \quad (2.16)$$

$$2 \frac{d}{dt} \left(\frac{\dot{a}}{a} \right) + 3 \left(\frac{\dot{a}}{a} \right)^2 + 2 \frac{\dot{a}\dot{\phi}}{a\phi} + \frac{k}{a^2} = \lambda(\phi) - \frac{\omega(\phi)\dot{\phi}^2}{2\phi^2} - 8\pi \frac{p}{\phi} - \frac{\ddot{\phi}}{\phi}, \quad (2.17)$$

$$\ddot{\phi} + 3 \frac{\dot{a}\dot{\phi}}{a} + \frac{2\phi^2\lambda_\phi(\phi) - 2\phi\lambda(\phi)}{2\omega(\phi) + 3} = -\frac{1}{2\omega(\phi) + 3} \left[8\pi(3p - \rho) + \omega_\phi(\phi)\dot{\phi}^2 \right]. \quad (2.18)$$

Please note that the cosmological potential $U(\phi) = \phi \lambda(\phi)$ effectively reduces to a cosmological constant when $\lambda(\phi) = \lambda_0 = \text{constant}$ in this frame. Besides if $\phi = cte = 1/G$, one recovers the action of General Relativity and consequently its system of equations.

In order to study the dynamical system let us introduce the redefined variables:

$$X = \frac{\phi}{\phi_0} a^2, \quad Y' = \sqrt{\frac{2\omega(\phi) + 3}{3}} \frac{\phi'}{\phi}, \quad (2.19)$$

and use conformal time $d\eta = dt/a = d\tilde{t}/\sqrt{X\phi_0}$, where $d\tilde{t} = \sqrt{\phi} dt$. Observe that in the definition of X , ϕ_0 is the value of ϕ at some initial condition which we shall normalize to $\phi_0 = 1$, without loss of generality. More importantly, observe that $X < 0$ when $\phi < 0$, i.e., when $G < 0$. This is in fact the crucial detail which allows us to extend the study of the dynamics into the region where $\phi = 1/G$ is negative.

The FLRW equations are then recast as

$$(X')^2 + 4kX^2 - (Y'X)^2 = 4M X \left(\frac{X}{\phi} \right)^{\frac{4-3\gamma}{2}} + \frac{4}{3} \left(\frac{\lambda(\phi)}{\phi} \right) X^3, \quad (2.20)$$

the scalar-field equation as

$$(Y'X)' = M(4 - 3\gamma) \sqrt{\frac{3}{2\omega + 3}} \left(\frac{X}{\phi} \right)^{\frac{4-3\gamma}{2}} - \frac{2X^2}{\sqrt{2\omega(\phi) + 3}} \left(\frac{d\lambda}{d\phi} - \frac{\lambda(\phi)}{\phi} \right), \quad (2.21)$$

and the generalized Raychaudhuri equation as

$$X'' + 4kX = 3M(2 - \gamma) \left(\frac{X}{\phi} \right)^{\frac{4-3\gamma}{2}} + 2X^2 \left(\frac{\lambda(\phi)}{\phi} \right), \quad (2.22)$$

where M is a constant defined by $M \equiv 8\pi\rho_0/3$. When the potential $U(\phi) = \lambda_0\phi^2$, the latter equations reduce to

$$(X')^2 + 4kX^2 - (Y'X)^2 = 4M X \left(\frac{X}{\phi} \right)^{\frac{4-3\gamma}{2}} + \frac{4}{3} \lambda_0 X^3, \quad (2.23)$$

$$(Y' X)' = M(4 - 3\gamma) \sqrt{\frac{3}{2\omega + 3}} \left(\frac{X}{\phi}\right)^{\frac{4-3\gamma}{2}}, \quad (2.24)$$

$$X'' + 4k X = 3M(2 - \gamma) \left(\frac{X}{\phi}\right)^{\frac{4-3\gamma}{2}} + 2\lambda_0 X^2. \quad (2.25)$$

These equations can be exactly integrated for the cases where the variables decouple, which are vacuum ($M = 0$), radiation ($\gamma = 4/3$) and stiff matter ($\gamma = 2$) [136, 137]. Indeed, from Eq. (2.24) for vacuum and radiation we trivially see:

$$Y' = \frac{f_0}{X(\eta)}, \quad (2.26)$$

where f_0 is an arbitrary integration constant which fixes the initial value of Y . For the stiff matter case, we should multiply Eq. (2.25) by X' and integrate the result to introduce it into Eq. (2.24), which results in $(Y' X)^2 = A - 4M\phi$, where A is an integration constant. Then, defining $\bar{Y}' = Y' / \sqrt{A - 4M\phi}$, we recover the form of the solution of (2.26).

However, for our present purposes, we only need to assess the qualitative behaviour of the dynamical system [138, 130, 139, 140, 141]. The crucial point in our analysis of the sign of the gravitational coupling ϕ is that instead of choosing either the original so-called Jordan frame or the conformally transformed Einstein frame arising from rescaling the metric with a factor ϕ/ϕ_0 , we consider the variables (X, Y) , where $X = \phi a^2/\phi_0$ reflects the actual sign of ϕ , since $a^2 \geq 0$.

An inspection of Eqs. (2.23)–(2.25) shows that, when $X \rightarrow 0$, Eq. (2.23) is dominated by the scalar field term $(Y' X)^2$, which is constant for radiation and vacuum, so that we expect the phase space trajectories to cross the $X = 0$ axes from right to left when $X' < 0$, and from left to right when $X' > 0$. Interestingly, Eq. (2.25) shows that when $X \rightarrow 0$, the dominant term is $3M(2 - \gamma) \lim_{X \rightarrow 0} (X/\phi)^{(4-3\gamma)/2}$, so that it is actually the matter term that is responsible for turning around the trajectories towards the positive side of X , and hence of $\phi > 0$. Finally, the presence of a quadratic cosmological potential eventually dominates for large values of X and consequently stabilizes the sign of ϕ . In the following subsections we perform a qualitative analysis confirming this behaviour.

2.2.1 Models without a Cosmological Potential

We begin considering the generalized case of Brans-Dicke (BD) but with a massless scalar field ϕ , i.e., the cosmological potential is absent. This will be contrasted with the case where there is a quadratic potential. By the same token it will enable us to assess whether there is any effect due to a variation of the coupling $\omega(\phi)$ with respect to the issue of determining the sign of ϕ in opposite to the canonical Brans-Dicke theory.

For this case, the previous Eq. (2.25) can be written for:

- Vacuum ($M = 0$) and a stiff fluid ($\gamma = 2$) as:

$$\begin{aligned} X' &= W, \\ W' &= -4kX. \end{aligned} \quad (2.27)$$

- Radiation ($\gamma = 4/3$) as:

$$\begin{aligned} X' &= W, \\ W' &= 2M - 4kX. \end{aligned} \quad (2.28)$$

The plots represented in Figure 2.2 show the phase diagrams of this systems (X, W) for the case without potential, i.e., $\lambda_0 = 0$. This is again done resorting to a phase space compactification where the points at $X, W \rightarrow \pm\infty$ are located at the boundaries $x = \tanh X = \pm 1$, $y = \tanh W = \pm 1$. One realizes that there are trajectories which cross the $X = 0$ dividing line in both directions, thus promoting the transition between a negative ϕ into a positive ϕ , and conversely (and hence of a swapping of the sign of G , since $\phi = G^{-1}$). Please note that as in the GR case previously considered, there is a mirror reflection between the top and lower half of the phase diagrams, arising from time reversal.

We have used the following color scheme depending on the beginning and the end of the trajectory: (i) Blue: The trajectory starts and finishes with positive value of ϕ ; (ii) Yellow: It begins and finishes with a positive value, but passes through negative values; (iii) Green: It starts with negative values, but finishes with positive values; (iv) White: The trajectory oscillates between positive and negative values; (v) Orange: It starts with positive values, but finishes with negative value; (vi) Red: It starts and finishes with a negative value of ϕ (and hence of G).

In Figure 2.2, the top three phase diagrams represent vacuum and stiff fluid models, whereas the lower three correspond to radiation models. From left to right we have $k = -1, 0$ and $k = +1$ models, respectively. It is immediately apparent that in the vacuum models the number of trajectories that cross in one direction, say from left to right, is the same as that of those which cross in the opposite direction. Once again there is a mirror symmetry with time reversal between the top half and the lower one. Therefore, assuming that a measure of the probability of the model to have a positive gravitational constant, or otherwise, is proportional to the phase space area, we realise that both signs occur with the same probability. In this sense, the same behaviour occurs for the three cases of vacuum or stiff fluid. In addition, in the case of a positive curvature, i.e. Figure 2.2 (c-top), the sign oscillates forever; while in the open models the trajectories evolve towards the Milne solution, $x = y = 1$, and are characterized by $X' = \pm f_0$ in the $k = 0$ models, which actually correspond to the solutions found in [142].

On the other hand, for radiation [136], there is a preference for the positive sign, or at least, to finish with a positive gravitational coupling, as represented by the blue, yellow and green areas. This is a reflection of the fact that the solutions are late time dominated by the matter component [143, 144]. This is more apparent in the $k = -1, 0$ cases, but the $k = +1$ cases exhibits a subset of trajectories with oscillatory behavior, confined to the $\phi > 0$ region. The impact of matter is dependent on the scalar-tensor coupling $\omega(\phi)$. When $1/\sqrt{2\omega + 3} \rightarrow 0$ the scalar-tensor theories approach GR, and this is implicit in Eq. (2.26).

We thus see that the dynamics of the vacuum or stiff matter FLRW models in ST gravity does not favour positive values of G with regard to the alternative possibility of a negative G . The dynamics is such that the upper half of the phase space corresponds to $G > 0$ and the other half to $G < 0$, and they are mirror reflections of one another. Thus both possibilities, in what concerns the sign of G , have the same probability. However, when one studies no vacuum solutions, in the case of open models specially (including $k = 0$) and for the close model ($k = +1$), there is higher probability for a positive value of G , following from of a larger proportion of solutions which evolve to become matter dominated.

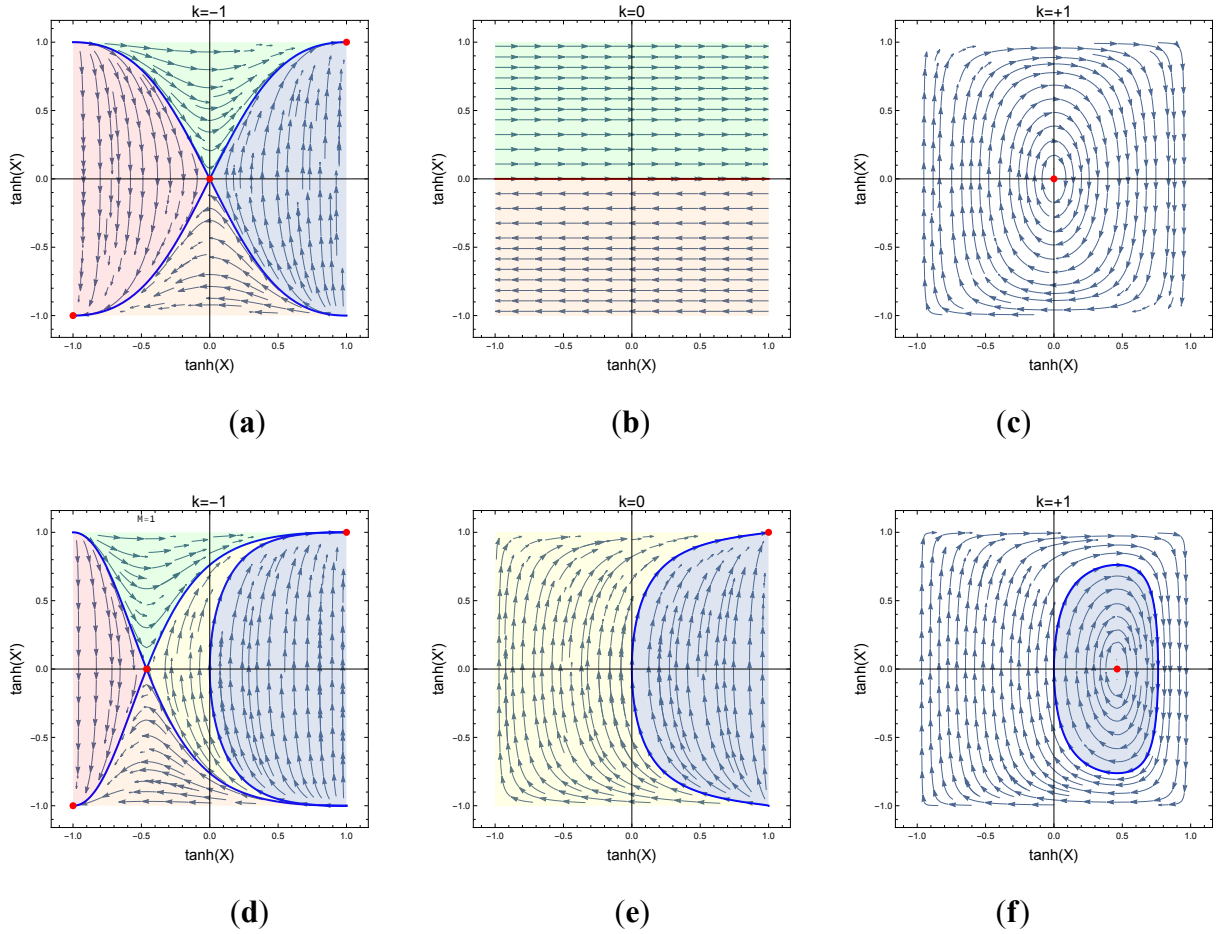


Figure 2.2: Behaviour of X and X' for a scalar-tensor theory without potential. The upper three phase diagrams, (a–c), respectively, correspond to the $k = -1, 0, +1$ cases for vacuum and stiff fluid. The lower three phase diagrams, (d–f), respectively, correspond to the $k = -1, 0, +1$ cases for radiation.

2.2.2 Models with a Cosmological Potential

When we allow for a potential with a positive λ_0 , we see that a quite different picture emerges. Indeed, the phase diagrams corresponding to this case are represented in Figure. 2.3, and we see that now there is an equilibrium point at $x = 1, x' = 1$, corresponding to $X = +\infty, X' = +\infty$, which attracts almost all trajectories of the phase plane, and this happens for all spatial curvature cases. This attractor at infinity corresponds to a de Sitter attractor, and thus to exponential behaviour of X in cosmic time. The only trajectories which do not end at this critical point are found in the closed $k = +1$ and open models $k = -1$, circling the center equilibrium point.

This is illustrated by the vacuum and radiation cases which were envisaged in the massless ST models in the previous subsection.

- Vacuum ($M = 0$) or stiff fluid $\gamma = 2$ with a cosmological potential

Recalling that $U(\phi) = \lambda_0\phi^2$, we derive for these two cases:

$$\begin{aligned} X' &= W, \\ W' &= 2\lambda_0 X^2 - 4kX. \end{aligned} \quad (2.29)$$

Please note that the case $\gamma = 2$ corresponding to stiff matter can be shown to be reducible to the vacuum case of a theory with a different coupling constant $\omega(\phi)$ (see [137]).

Now, the fixed points $\{X, X'\}$ within a finite locus will be positioned at $\{0, 0\}$ and $\{2k/\lambda_0, 0\}$. To show the graphics of the phase diagrams, λ_0 has been taken equal to 4.5 with the purpose of showing both points sufficiently separated.

- Radiation, $\gamma = 4/3$, with a cosmological potential

In this case the system is:

$$\begin{aligned} X' &= W, \\ W' &= 2M + 2\lambda_0 X^2 - 4kX, \end{aligned} \quad (2.30)$$

and the fixed points are:

$$X = \frac{k \pm \sqrt{k^2 - M\lambda_0}}{\lambda_0}, \quad W = 0.$$

Therefore, for the cases $k = \pm 1$, at the fixed points we require $M\lambda_0 < 1$. When this is not satisfied there are no fixed points, as illustrated in Figure 2.3 (d). For the case $k = 0$ there are no fixed points within the finite region of the phase plane.

The qualitative behaviour depicted in Figure 2.3 reveals that with the exception of the oscillatory solutions, confined to a closed patch, all other solutions emerge from a collapsing deS solution at $X = \infty, X' = -\infty$ and end in the deS solution at $X = \infty, X' = +\infty$, thus revealing the domination of the cosmological potential term [126, 140, 145, 146, 139, 147, 148]. More importantly, we see that the solutions are attracted to the positive G half plane. We thus conclude that the consideration of a cosmological potential³ has the power to induce the dynamics of FLRW models to favour positive values of G instead of negative G s. Thus this provides a cosmological mechanism to stabilize G in the positive sector. In addition, it happens that the deS asymptotic behaviour is accompanied with a relaxation towards GR [126, 127, 125, 129, 150].

³One possible origin for such a potential might be found from a mechanism similar to the dark fluid model of [149].

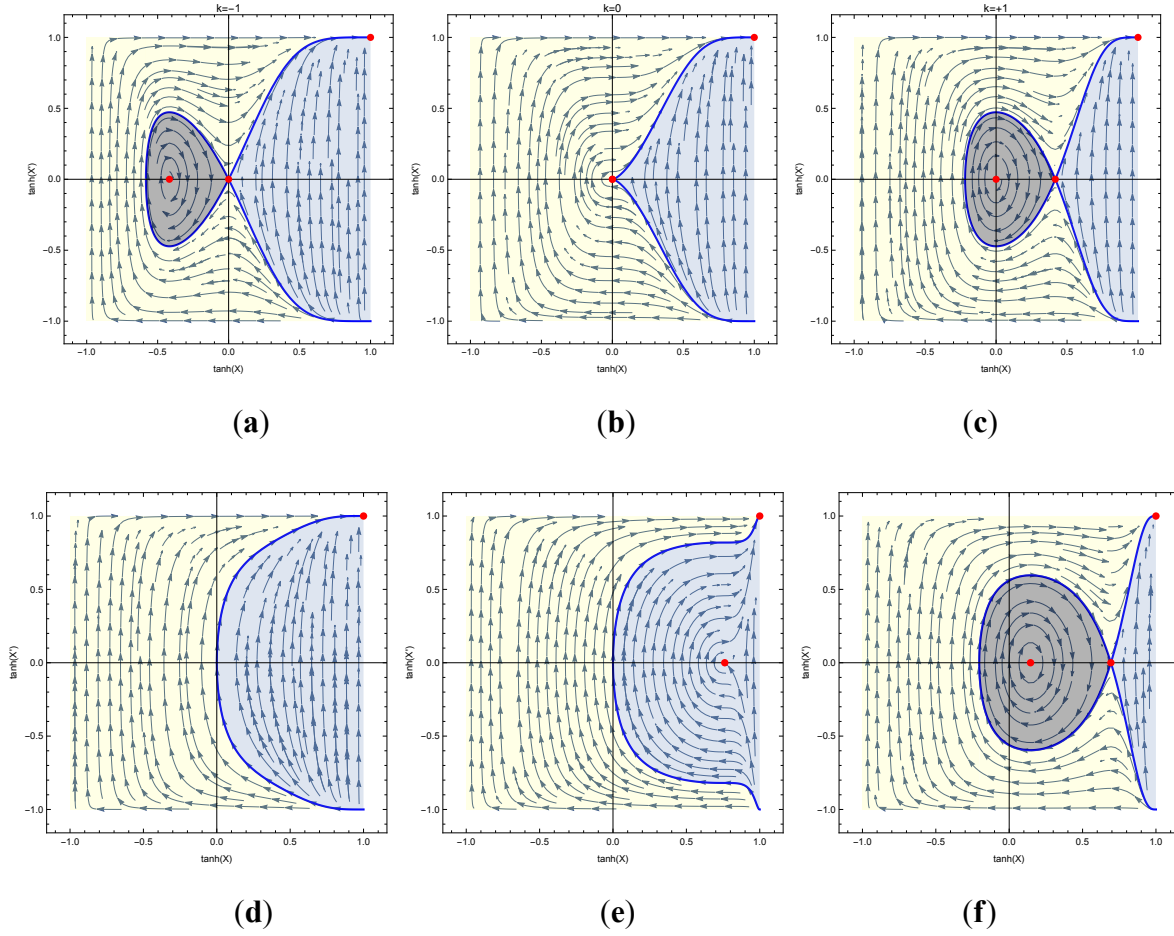


Figure 2.3: Behaviour of X and X' for a scalar-tensor theory with a potential λ_0 . The upper three phase diagrams, (a–c), respectively, correspond to the $k = -1, 0, +1$ cases for vacuum and stiff fluid. The lower three phase diagrams, (d–f), depict the qualitative behaviour of radiation models, with: (d) When $M\lambda_0 > 1$ (e) When $M\lambda_0 = 1$ (f) When $M = 1/4$ and $\lambda_0 = 2$.

2.3 Observational Features

ST gravity theories must satisfy some observational bounds, namely, the so-called Parametrized Post-Newtonian (PPN) weak field, solar system tests, bounds stemming from the cosmic microwave background (CMB), from baryonic acoustic oscillations (BAO), and from primordial Big-Bang Nucleosynthesis (BBN), as well as bounds on the time variation of the gravitational “constant” \dot{G}/G [2, 151, 152, 153].

The present state of the art tells us that at present $\omega_P \gtrsim 4 \times 10^4$, $\dot{G}/G \lesssim 10^{-10} \text{ yr}^{-1}$, and from BBN we have $\alpha_0^2 \lesssim 10^{-6.5} \beta^{-a} (\Omega_m h_0)^{-3/2}$ when $\beta > 0.5$ [154, 155, 156, 157, 158], where α and β correspond to the Damour and Nordtvedt (DN) [159] parametrization $(\sqrt{2\omega + 3})^{-1} = \alpha(\tilde{\phi})$, with $\alpha(\tilde{\phi}) = \alpha_0 + \beta_0 (\tilde{\phi} - \tilde{\phi}_0)$, $\tilde{\phi}(\phi) = \int \sqrt{(2\omega + 3)/2} \, d \ln \phi$, being the redefined BD scalar field in the so-called Einstein frame. Indeed, as shown by DN, it is possible to associate

a second internal potential $A(\tilde{\phi})$ to the running coupling $\omega(\phi)$ such that $\alpha(\tilde{\phi}) = dA/d\tilde{\phi}$ and whenever it has a minimum it drives the relaxation to GR.

The local weak field bounds can be somewhat alleviated if some chameleon or Vainshtein mechanism applies, but it is difficult to evade the other bounds on wider scales. Yet, the vast majority of these bounds pertain to models where the scalar field has no cosmological potential (see [158]).

These bounds, therefore, imply that a primordial variation of the gravitational coupling must have been severely damped before the time of BBN such that a positive coupling, satisfying mild deviations from GR [156] is not only compatible with the observations on light elements abundances, but also solves the so-called ${}^7\text{Li}$ problem. In the suite, during the following radiation and matter epochs, the cosmological approach to GR is achieved, implying that G is positive.

The mechanism investigated in this work fulfills this scenario. It tells us that the solutions approach a de Sitter behaviour, which corresponds to $X \propto (\eta_0 - \eta)^{-2}$ and $X' \propto (\eta_0 - \eta)^{-3}$, so that $X(t) \propto \exp(\sqrt{\lambda_0/3} \tilde{t})$. When we consider the radiation epoch of the Universe, we have

$$Y' = \frac{f_0}{X(\eta)}, \quad (2.31)$$

and hence, $Y' \rightarrow 0$, asymptotically with $X \rightarrow +\infty$. As $Y' = \sqrt{(2\omega(\phi) + 3)/3} \phi'/\phi$, we obtain in cosmic time (in the Einstein frame):

$$\frac{\dot{G}}{G} = \pm \sqrt{\frac{3}{2\omega + 3}} \frac{f_0}{\sqrt{X}} \equiv \pm \frac{\sqrt{3}f_0 \alpha(\phi)}{\sqrt{X}}. \quad (2.32)$$

As $Y' = f_0/X \rightarrow 0$, and the PPN parameter $\alpha \propto (\sqrt{2\omega(\phi) + 3})^{-1}$ satisfies the bound $\alpha \lesssim 10^{-8}$, since $\omega_P \gtrsim 4 \times 10^4$, we have that $\dot{G}/G \lesssim 10^{-8}/\sqrt{X(\tilde{t})}$, where $X(\tilde{t}) \rightarrow \infty$ in an exponential way, thus easily meeting the bounds on \dot{G}/G . Please note that, in this limit, $G \rightarrow G_N$ and $X(t)$ also becomes exponential in the Jordan frame.

2.4 Conclusions

The most important conclusion of this chapter is that we have investigated a cosmological mechanism that induces the value of the gravitational effective coupling “constant” to be positive. This is naturally done in the framework of scalar-tensor (ST) gravity theories, where this coupling varies, and which thus allows for the possibility of a negative coupling.

Then, we have considered the cosmological evolution of ST models both with and without the presence of a cosmological potential, and have resorted to a dynamical system analysis which enables us to put in evidence the relevant qualitative features of the models. The results are that, in the absence of the cosmological potential, the presence of radiation favours a positive value of the gravitational “constant”, when the evolution enters a phase of matter domination. This is a mild effect and it is a consequence of Damour and Nordtvedt’s relaxation mechanism towards GR [159]. However, it is when a quadratic cosmological potential, $U(\phi) = \lambda_0 \phi^2$, is present that an attracting mechanism towards a positive value of the gravitational running “constant” becomes manifest. This is accompanied by an asymptotic de Sitter behaviour.

By the same token, this system produces two additional effects: a de Sitter inflation and a relaxation towards GR. The latter effect allows, in particular, for the fulfilment of the observational bounds on $|\dot{G}/G|$, when the potential is exactly quadratic in the Jordan frame. It effectively acts as a cosmological constant in the Einstein frame and the stabilization of the gravitational constant in the positive sector, may be seen as a by-product of the cosmic no-hair theorem, which tell us that, if a cosmological spacetime obeys the Einstein equations with $\Lambda > 0$, then, the spacetime should asymptotically tend to an empty de Sitter state in the future [160]. This mechanism of stabilization of the sign of G should take place early enough, in the primordial stages of the Universe, consistently with the latest assessments of observational constraints on ST theories [161, 151]

Chapter 3

Non-minimal Scalar tensor theories from a general coupling

3.1 Introduction

In the previous section we have studied a Scalar-Tensor theory based on some generalizations of the Brans-Dicke theory and with a specific coupling between the scalar ϕ and gravity denoted by R . In this chapter we will go one step further, starting out Scalar-Tensor theory as well. We will study particular extensions of the gravitational interaction, that are defined by the addition of scalar degrees of freedom, but in this case the scalar field will present a general coupling to the scalar curvature. These new spin-0 states, which emerge from the scalar field, act as mediators of part of the total gravitational force.

From an observational point of view, there is only one candidate for a fundamental scalar particle. Its discovery was announced in 2012 by both ATLAS [162] and CMS [163] collaborations. It has associated a mass of around 125 GeV and it is consistent with the predictions for the so-called Higgs boson of the Standard Model (SM) of particles and interactions. However, many other scalar fields could be observed in the next years. Brans-Dicke theory or different low energy approaches to string theory [164], where the new scalar states are typically coupled to the matter sector through the trace of the stress-energy tensor, are examples of theories that use a scalar field non-minimally coupled to gravity.

In addition, we have already commented in (1.32) that it is possible to reexpress the extended

gravitational theory in terms of the Einstein gravity associated with General Relativity with new couplings to the matter sector, thanks to a series of field redefinitions which will be explained more carefully in this section. A similar phenomenology is associated with the so-called $f(R)$ [165, 166, 167, 168, 169, 170, 171, 172, 173, 174, 175, 176, 177, 178] theories (with some Lagrange's multiplier by the way) and which will be explained too. It is important to recall that extended models with scalar fields non-minimally coupled to gravity have some advantages such as the possibility of supporting early inflation, which exhibits non-zero vacuum expectation values (VEVs) at low energies. An example of this is the Generalized Higgs Inflation Models (GHIMs) [179, 180, 181, 182, 183, 184, 185, 186, 187, 188, 189, 190, 191, 192].

As we have briefly commented, the new interactions mediated by these scalar degrees of freedom can be interpreted as part of the gravitational force. In addition, the phenomenology associated with these new degrees of freedom themselves can be very rich and provide viable solutions to open problems in cosmology such as the mentioned inflation, dark energy or dark matter [193]. However, these new models suffer important constraints. For instance, this new field can lead to effective variations of fundamental constants, such as we have seen in the previous sections. In particular, precision tests of gravity, big bang nucleosynthesis (BBN) [194, 195, 196, 197, 198, 199, 200, 201, 202, 203, 155, 204, 205], cosmic microwave background anisotropies [206, 207] and weak-lensing [208] constrain the phenomenology of these scalar fields. In any case, different scalar models are not very sensitive to these restrictions [209, 210, 211, 212, 177].

In this chapter, we will go deeper into Scalar-Tensor theories and $f(R)$ to end up finding the bi-scalar content of a Non-minimal Scalar Tensor Theory (NMSTT) built from a general function of the scalar field and the scalar of curvature. In addition, we will enter into the Standard Model (SM) of particles, studying the explicit expressions for the masses of the scalars providing explicit expressions, their mixing and the coupling between them and with the Standard Model (SM) of particles, which give us a perspective of modified gravity theories in the framework of the SM. Finally we discuss part of the phenomenological consequences of these features, as the instabilities of GHIMs. In the previous chapter we have already studied a scalar-tensor theory, so let us start with $f(R)$ gravity as previous step for the current purpose of the chapter.

3.2 $f(R)$ theory of modified gravity

The starting point of this proposal of modified gravity is that the Einstein-Hilbert action, and consequently the scalar of curvature R , is only the dominant part of the action at solar system scales, being this a part of a more general expression in terms of R . Under this hypothesis, R is changed in the Einstein-Hilbert action (1.3) by $f(R)$ as follows:

$$S = \frac{1}{16\pi G} \int d^4x \sqrt{-g} f(R) + \int d^4x \sqrt{-g} \mathcal{L}_{mat}, \quad (3.1)$$

whose variations with respect the metric are easily obtained using the results of chapter 1.1, together with:

$$\delta_g f(R) = \frac{\partial f(R)}{\partial R} \delta_g R = F(R) \delta_g R, \quad (3.2)$$

where we have defined $\frac{\partial f(R)}{\partial R} = F(R)$. Then, variations of the gravitational part of the action reads:

$$\begin{aligned} \delta_g S_g = \frac{1}{16\pi G} \int d^4x \sqrt{-g} \left[-\frac{1}{2} g_{\mu\nu} f(R) \delta g^{\mu\nu} + F(R) \delta g^{\mu\nu} R_{\mu\nu} \right. \\ \left. + F(R) \nabla_\alpha \left(g^{\mu\nu} \delta_g \Gamma^\alpha_{\mu\nu} - g^{\mu\alpha} \delta_g \Gamma^\beta_{\mu\beta} \right) \right]. \end{aligned} \quad (3.3)$$

Note that for this case, the last term will not vanish in general, contrary to what happens in GR, and this will introduce the main modifications in the equations of motion. This last term can be written as:

$$\begin{aligned} \int d^4x \sqrt{-g} F(R) \nabla_\alpha \left(g^{\mu\nu} \delta_g \Gamma^\alpha_{\mu\nu} - g^{\mu\alpha} \delta_g \Gamma^\beta_{\mu\beta} \right) = \int d^4x \nabla_\alpha \left[\sqrt{-g} F(R) J^\alpha \right] \\ - \int d^4x J^\alpha \nabla_\alpha \left[\sqrt{-g} F(R) \right], \end{aligned} \quad (3.4)$$

where:

$$J^\alpha = \left(g^{\mu\nu} \delta_g \Gamma^\alpha_{\mu\nu} - g^{\mu\alpha} \delta_g \Gamma^\beta_{\mu\beta} \right). \quad (3.5)$$

Once again we will assume that the gravitational field vanishes at infinity and then one can eliminate the first term of the right hand side in Eq. (3.4) by the Gauss theorem. Then, at this point, we have no choice but to calculate $\delta_g \Gamma^\alpha_{\mu\nu}$. Keep in mind the definition of the Christoffel symbols:

$$\Gamma^\alpha_{\mu\nu} = \frac{1}{2} g^{\alpha\gamma} (\partial_\mu g_{\gamma\nu} + \partial_\nu g_{\mu\gamma} - \partial_\gamma g_{\mu\nu}). \quad (3.6)$$

Then:

$$\delta_g \Gamma^\alpha_{\mu\nu} = \frac{1}{2} (\delta g^{\alpha\gamma}) (\partial_\mu g_{\gamma\nu} + \partial_\nu g_{\mu\gamma} - \partial_\gamma g_{\mu\nu}) + \frac{1}{2} g^{\alpha\gamma} (\partial_\mu \delta g_{\gamma\nu} + \partial_\nu \delta g_{\mu\gamma} - \partial_\gamma \delta g_{\mu\nu}) . \quad (3.7)$$

We will also use:

$$\begin{aligned} \delta_g (g^{am} g^{de} g_{me}) &= \delta_g (g^{am}) g^{de} g_{me} + g^{am} \delta_g (g^{da}) g_{me} + g^{am} g^{de} \delta_g g_{me} \\ \delta_g g^{ad} &= 2\delta_g g^{ad} + g^{am} g^{de} \delta_g g_{me} \\ -\delta_g g^{ad} &= g^{am} g^{de} \delta_g g_{me} . \end{aligned} \quad (3.8)$$

Therefore:

$$\begin{aligned} \delta_g \Gamma^\alpha_{\mu\nu} &= -\frac{1}{2} g^{\alpha\beta} g^{\gamma\theta} (\delta_g g_{\beta\theta}) (\partial_\mu g_{\gamma\nu} + \partial_\nu g_{\mu\gamma} - \partial_\gamma g_{\mu\nu}) + \frac{1}{2} g^{\alpha\gamma} (\partial_\mu \delta g_{\gamma\nu} + \partial_\nu \delta g_{\mu\gamma} - \partial_\gamma \delta g_{\mu\nu}) \\ &= -(\delta_g g_{\gamma\theta}) g^{\alpha\gamma} \Gamma^\theta_{\mu\nu} + \frac{1}{2} g^{\alpha\gamma} (\partial_\mu \delta g_{\gamma\nu} + \partial_\nu \delta g_{\mu\gamma} - \partial_\gamma \delta g_{\mu\nu}) \\ &= \frac{1}{2} g^{\alpha\gamma} (\partial_\mu \delta g_{\gamma\nu} - \Gamma^\theta_{\mu\nu} \delta g_{\gamma\theta} - \Gamma^\theta_{\mu\gamma} \delta g_{\theta\nu}) + \frac{1}{2} g^{\alpha\gamma} (\partial_\nu \delta g_{\mu\gamma} - \Gamma^\theta_{\mu\nu} \delta g_{\gamma\theta} - \Gamma^\theta_{\nu\gamma} \delta g_{\mu\theta}) \\ &\quad + \frac{1}{2} g^{\alpha\gamma} (-\partial_\gamma \delta g_{\mu\nu} + \Gamma^\theta_{\mu\gamma} \delta g_{\theta\nu} + \Gamma^\theta_{\nu\gamma} \delta g_{\mu\theta}) \\ &= \frac{1}{2} g^{\alpha\gamma} (\nabla_\mu \delta g_{\gamma\nu} + \nabla_\nu \delta g_{\mu\gamma} - \nabla_\gamma \delta g_{\mu\nu}) , \end{aligned} \quad (3.9)$$

and:

$$\delta \Gamma^\beta_{\mu\beta} = \frac{1}{2} g^{\beta\gamma} \nabla_\mu \delta g_{\gamma\beta} . \quad (3.10)$$

which finally results in:

$$J^\alpha = -g^{\mu\nu} \nabla_\mu (g_{\gamma\nu} \delta g^{\alpha\gamma}) + g^{\gamma\alpha} \nabla_\gamma (g_{\mu\nu} \delta g^{\mu\nu}) , \quad (3.11)$$

where we have assumed a metric compatible connection, i.e. $\nabla_\alpha g_{\mu\nu} = 0$ and $\nabla_\alpha \sqrt{-g} = 0$.

Utilising this in Eq. (3.4) we derive

$$-\int d^4x J^\alpha \nabla_\alpha [\sqrt{-g} F(R)] = \int d^4x [g^{\mu\nu} \nabla_\mu (g_{\gamma\nu} \delta g^{\alpha\gamma}) - g^{\gamma\alpha} \nabla_\gamma (g_{\mu\nu} \delta g^{\mu\nu})] \nabla_\alpha (\sqrt{-g} F(R)) . \quad (3.12)$$

Returning to the use of total divergences leads to:

$$\begin{aligned} -\int d^4x J^\alpha \nabla_\alpha [\sqrt{-g} F(R)] &= -\int d^4x \delta g^{\nu\mu} \nabla_\mu \nabla_\nu (\sqrt{-g} F(R)) \\ &\quad + \int d^4x g_{\mu\nu} \delta g^{\mu\nu} \nabla_\alpha \nabla^\alpha (\sqrt{-g} F(R)) . \end{aligned} \quad (3.13)$$

Putting it all together in Eq. (3.3) we get:

$$\delta_g S = \frac{1}{16\pi G} \int d^4x \sqrt{-g} \left[-\frac{1}{2} g_{\mu\nu} f(R) + F(R) R_{\mu\nu} - \nabla_\mu \nabla_\nu F(R) + g_{\mu\nu} \nabla_\alpha \nabla^\alpha F(R) \right] \delta g^{\mu\nu}, \quad (3.14)$$

and finally:

$$F(R) R_{\mu\nu} - \frac{1}{2} g_{\mu\nu} f(R) - \nabla_\mu \nabla_\nu F(R) + g_{\mu\nu} \square F(R) = 0, \quad (3.15)$$

or with matter:

$$F(R) R_{\mu\nu} - \frac{1}{2} g_{\mu\nu} f(R) - \nabla_\mu \nabla_\nu F(R) + g_{\mu\nu} \square F(R) = 8\pi G T_{\mu\nu}, \quad (3.16)$$

where we have defined $\square = \nabla_\alpha \nabla^\alpha$. However, this theory is not so different from those already studied. Rewriting the action (3.1) with an auxiliary scalar field and a Lagrange multiplier we get:

$$S_g = \frac{1}{16\pi G} \int d^4x \sqrt{-g} [f(\psi) + \lambda(R - \psi)], \quad (3.17)$$

where the next constraint (or equation of motion) is obtained applying variations with respect to ψ :

$$f_\psi(\psi) - \lambda = 0 \quad \rightarrow \quad \lambda = f_\psi(\psi), \quad (3.18)$$

where $f_\psi = \frac{\partial f(\psi)}{\partial \psi}$, getting the action:

$$S_g = \frac{1}{16\pi G} \int d^4x \sqrt{-g} [f(\psi) + f_\psi(\psi)(R - \psi)]. \quad (3.19)$$

Taking once again variations with respect to ψ :

$$f_{\psi\psi}(\psi)(R - \psi) = 0, \quad (3.20)$$

so that if $f_{\psi\psi} \neq 0$ is satisfied, then $\psi = R$, and consequently, if one introduces this in Eq. (3.19), we will recover the starting action (3.1). But then, it is usual to apply the redefinition: $\phi = f_\psi(\psi)$ which allows us to end up writing the action as:

$$S_g = \frac{1}{16\pi G} \int d^4x \sqrt{-g} [\phi R + f(\psi(\phi)) - \phi \psi(\phi)] = \frac{1}{16\pi G} \int d^4x \sqrt{-g} [\phi R - 2U(\phi)] \quad (3.21)$$

Comparing with the Brans-Dicke action presented in Eq. (1.29), and Eq. (2.13), one can conclude that $f(R)$ theory belongs to this category with $\omega_{BD} = 0$ and a specific potential:

$$2U(\phi) = \phi\psi(\phi) - f(\psi(\phi)). \quad (3.22)$$

Consequently, the equations of motion of Eq. (3.21) reads:

$$R_{\mu\nu} - \frac{1}{2}g_{\mu\nu}R = \frac{8\pi G}{\phi}T_{\mu\nu} + \frac{1}{\phi}[\nabla_\mu\nabla_\nu - g_{\mu\nu}\square]\phi - \frac{g_{\mu\nu}}{\phi}U(\phi). \quad (3.23)$$

Let us point out that this is true if $\phi = F(R) = f_\psi(\psi)$ is invertible which allows us to express correctly the potential. In addition, the case $f_{\psi\psi} = 0$ corresponds to General Relativity plus a cosmological constant.

Summarizing, we have just checked that $f(R)$ theories are equivalent to scalar-tensor theories in the Jordan frame. However, it is possible to perform another transformation in this search of equivalences. With this purpose we will introduce the concept of conformal transformations in the next subsection.

3.2.1 Conformal transformations

A conformal transformation is a change of the rule of the metric. The simplest and most familiar example is that of a change of units, i.e. if we transform a metric, which is expressed in meters, into another one expressed in centimeters, we will be applying a scaling transformation which can be seen as a trivial conformal transformation. However, we can define more complex changes, for example, defining the change or the transformation point by point through a function $\Omega^2(x)$, which gives us a point-dependent rescaling. In addition, this function must be smooth, non-vanishing and is usually called the conformal factor. Mathematically, this rescaling reads:

$$\tilde{g}_{\mu\nu} = \Omega^2(x)g_{\mu\nu}, \quad (3.24)$$

where $g_{\mu\nu}$ is the initial metric, and $\tilde{g}_{\mu\nu}$ is the new rescaled metric. Since we want to analyze how the scalar of curvature R changes under this transformation, let us recall here the definitions of the Riemann and the Ricci tensors in function of the connection Γ :

$$R^\alpha{}_{\beta\mu\nu}(\Gamma) = \partial_\mu\Gamma^\alpha{}_{\nu\beta} - \partial_\nu\Gamma^\alpha{}_{\mu\beta} + \Gamma^\alpha{}_{\mu\lambda}\Gamma^\lambda{}_{\nu\beta} - \Gamma^\alpha{}_{\nu\lambda}\Gamma^\lambda{}_{\mu\beta}, \quad (3.25)$$

$$R_{\mu\nu}(\Gamma) = R^\sigma{}_{\mu\sigma\nu} = \partial_\sigma\Gamma^\sigma{}_{\nu\mu} - \partial_\nu\Gamma^\sigma{}_{\sigma\mu} + \Gamma^\sigma{}_{\sigma\gamma}\Gamma^\gamma{}_{\nu\mu} - \Gamma^\sigma{}_{\nu\gamma}\Gamma^\gamma{}_{\sigma\mu}, \quad (3.26)$$

where in this case we will fix the connection to be the Christoffel symbols defined in Eq. (3.6). Obviously, the conformal transformation (3.24) induces changes in the other parameters that depend on the metric. The simplest are:

$$\tilde{g}^{\mu\nu} = \Omega^{-2} g^{\mu\nu}, \quad (3.27)$$

$$\sqrt{-\tilde{g}} = \Omega^n \sqrt{-g}, \quad (3.28)$$

where n is the dimension of the manifold. For the Christoffel symbols the transformation reads:

$$\Gamma^\alpha_{\mu\alpha} = \partial_\mu \log \sqrt{-g} = \partial_\mu \log \left(\frac{1}{\Omega^n} \sqrt{-\tilde{g}} \right) = \partial_\mu \log \frac{1}{\Omega^n} + \partial_\mu \log \sqrt{-\tilde{g}} = \tilde{\Gamma}^\alpha_{\mu\alpha} - n \frac{\partial_\mu \Omega}{\Omega}, \quad (3.29)$$

$$\Gamma^\alpha_{\mu\nu} = \tilde{\Gamma}^\alpha_{\mu\nu} - \frac{1}{\Omega} (\delta^\alpha_\mu \partial_\nu \Omega + \delta^\alpha_\nu \partial_\mu \Omega - \tilde{g}_{\mu\nu} \tilde{g}^{\alpha\gamma} \partial_\gamma \Omega). \quad (3.30)$$

Other special important changes for the present work will be the ones related with R and consequently $R_{\mu\nu}$, so let us calculate them starting with each of the components of Eq. (3.26):

$$\partial_\alpha \Gamma^\alpha_{\mu\nu} = \partial_\alpha \tilde{\Gamma}^\alpha_{\mu\nu} + \frac{1}{\Omega^2} (2\partial_\mu \Omega \partial_\nu \Omega - \tilde{g}_{\mu\nu} \tilde{g}^{\alpha\gamma} \partial_\gamma \Omega \partial_\alpha \Omega) - \frac{1}{\Omega} [2\partial_\mu \partial_\nu \Omega - \partial_\alpha (\tilde{g}_{\mu\nu} \tilde{g}^{\alpha\gamma} \partial_\gamma \Omega)], \quad (3.31)$$

$$\partial_\nu \Gamma^\alpha_{\mu\alpha} = \partial_\nu \tilde{\Gamma}^\alpha_{\mu\alpha} - \frac{n}{\Omega} \partial_\nu \partial_\mu \Omega + \frac{n}{\Omega^2} \partial_\mu \Omega \partial_\nu \Omega, \quad (3.32)$$

$$\begin{aligned} \Gamma^\alpha_{\alpha\gamma} \Gamma^\gamma_{\mu\nu} &= \tilde{\Gamma}^\alpha_{\alpha\gamma} \tilde{\Gamma}^\gamma_{\mu\nu} - \frac{1}{\Omega} \tilde{\Gamma}^\alpha_{\alpha\gamma} (\delta^\gamma_\mu \partial_\nu \Omega + \delta^\gamma_\nu \partial_\mu \Omega - \tilde{g}_{\mu\nu} \tilde{g}^{\gamma\sigma} \partial_\sigma \Omega) - \frac{n}{\Omega} \partial_\gamma \Omega \tilde{\Gamma}^\gamma_{\mu\nu} \\ &\quad + \frac{n}{\Omega^2} (2\partial_\mu \Omega \partial_\nu \Omega - \tilde{g}_{\mu\nu} \tilde{g}^{\gamma\sigma} \partial_\sigma \Omega \partial_\gamma \Omega), \end{aligned} \quad (3.33)$$

$$\begin{aligned} \Gamma^\alpha_{\nu\gamma} \Gamma^\gamma_{\alpha\mu} &= \tilde{\Gamma}^\alpha_{\nu\gamma} \tilde{\Gamma}^\gamma_{\alpha\mu} - \frac{1}{\Omega} \left(\tilde{\Gamma}^\alpha_{\nu\alpha} \partial_\mu \Omega + \tilde{\Gamma}^\alpha_{\nu\mu} \partial_\alpha \Omega - \tilde{\Gamma}^\alpha_{\nu\gamma} \tilde{g}_{\alpha\mu} \tilde{g}^{\gamma\sigma} \partial_\sigma \Omega \right) \\ &\quad - \frac{\tilde{\Gamma}^\gamma_{\alpha\mu}}{\Omega} (\delta^\alpha_\nu \partial_\gamma \Omega + \delta^\alpha_\gamma \partial_\nu \Omega - \tilde{g}_{\gamma\nu} \tilde{g}^{\alpha\sigma} \partial_\sigma \Omega) \\ &\quad + \frac{1}{\Omega^2} (\delta^\alpha_\nu \partial_\gamma \Omega + \delta^\alpha_\gamma \partial_\nu \Omega - \tilde{g}_{\gamma\nu} \tilde{g}^{\alpha\sigma} \partial_\sigma \Omega) (\delta^\gamma_\mu \partial_\alpha \Omega + \delta^\gamma_\alpha \partial_\mu \Omega - \tilde{g}_{\alpha\mu} \tilde{g}^{\gamma\sigma} \partial_\sigma \Omega). \end{aligned} \quad (3.34)$$

Putting together all this information and using some equalities from the non-metricity condition $\nabla_\alpha g_{\mu\nu} = 0$ (which must be satisfied in the conformal frame as well, i.e. $\tilde{\nabla}_\alpha \tilde{g}_{\mu\nu} = 0$), such as $\partial_\alpha g_{\mu\nu} = \Gamma^\gamma_{\alpha\mu} g_{\gamma\nu} + \Gamma^\gamma_{\alpha\nu} g_{\mu\gamma}$, and $\partial_\alpha g^{\alpha\beta} = -\Gamma^\alpha_{\alpha\sigma} g^{\sigma\beta} - \Gamma^\beta_{\alpha\sigma} g^{\alpha\sigma}$, we are able to write and simplify the Ricci tensor and the scalar of curvature:

$$R_{\mu\nu} = \tilde{R}_{\mu\nu} - \frac{(n-1)}{\Omega^2} \tilde{g}_{\mu\nu} \tilde{\nabla}^\alpha \Omega \tilde{\nabla}_\alpha \Omega + \frac{1}{\Omega} \left[(n-2) \tilde{\nabla}_\mu \tilde{\nabla}_\nu \Omega + \tilde{g}_{\mu\nu} \tilde{\square} \Omega \right], \quad (3.35)$$

$$R = \Omega^2 \left[\tilde{R} - \frac{n(n-1)}{\Omega^2} \tilde{\nabla}^\alpha \Omega \tilde{\nabla}_\alpha \Omega + \frac{2(n-1)}{\Omega} \tilde{\square} \Omega \right], \quad (3.36)$$

where $\tilde{\square} = \tilde{\nabla}^\alpha \tilde{\nabla}_\alpha \Omega$. It is very usual to find in the literature these changes using the neperian logarithm \ln . Taking into account $\nabla_\alpha \Omega = \Omega \nabla_\alpha \ln \Omega$, and $\nabla^\alpha \nabla_\alpha \Omega = \Omega \nabla^\alpha \nabla_\alpha \ln \Omega + \Omega \nabla^\alpha \ln \Omega \nabla_\alpha \ln \Omega$:

$$R = \Omega^2 \left[\tilde{R} + (2-n)(n-1) \tilde{\nabla}^\alpha \ln \Omega \tilde{\nabla}_\alpha \ln \Omega + 2(n-1) \tilde{\square} \ln \Omega \right]. \quad (3.37)$$

Applying these results in the action (3.21) for $n = 4$, one can see that the term $\sqrt{-g} \phi R$ is transformed under a conformal transformation as $\Omega^{-2} \sqrt{-\tilde{g}} \phi \left(\tilde{R} + \Omega \text{terms} \right)$. Consequently, if we define the conformal factor as $\Omega^2 = \phi$, the non-minimal coupling between the scalar field and R will be undone, and action (3.21) with the matter sector reads:

$$S = \frac{1}{16\pi G} \int d^4x \sqrt{-\tilde{g}} \left[\tilde{R} - 6 \tilde{\nabla}^\alpha \ln \sqrt{\phi} \tilde{\nabla}_\alpha \ln \sqrt{\phi} + 6 \tilde{\square} \ln \sqrt{\phi} - 2 \frac{U(\phi)}{\phi^2} \right] + S_m \left(\frac{\tilde{g}_{\mu\nu}}{\phi}, \Psi_m \right). \quad (3.38)$$

However, we can eliminate the third term of the integral using Gauss theorem and the condition of null scalar fields at the boundary. Therefore, we are able to express $f(R)$ theories like General Relativity (note that we have the Einstein-Hilbert action) plus a material field ϕ , and the modification of the metric noticed by the matter sector. This latter is the Einstein frame representation of $f(R)$ theories, where the curvature and the matter are minimally coupled but the matter is coupled to the new scalar field ϕ . Of course, at the end of the day and observationally, both representations are the same, and the trajectories of the particles will be equivalent, but with a somewhat different philosophical meaning.

3.3 Generalized Non-minimal scalar-tensor theories

Following the spirit of the previous chapter and of the $f(R)$ theories, in this section we are going to study the most general action for a scalar field non-minimally coupled to the scalar curvature R , associated with the spacetime metric $g_{\mu\nu}$, which can be written in the following form:

$$S_{\text{NMSTT}} = \frac{1}{2\kappa^2} \int d^4x \sqrt{-g} [J(\varphi, R) - g^{\mu\nu} \nabla_\mu \varphi \nabla_\nu \varphi], \quad (3.39)$$

if we restrict the scalar field derivatives to the standard kinetic contribution (the second term), and where we will use reduced Planck units ($\kappa \equiv \sqrt{8\pi G} = c = \hbar = 1$) in order to simplify this study. The function $J(\varphi, R)$ takes into account the mentioned coupling, that in general, it

is non-separable. Note that this term may include a potential (mass or self interaction) for the scalar field, or a pure gravitational contribution without explicit dependence on φ .

In addition, we will assume a matter content, whose fields will be represented by the letter μ_i , minimally coupled to the spacetime metric as usual:

$$S_{\mu_i} = S_i(g_{\mu\nu}, \mu_i), \quad (3.40)$$

where by *matter*, we denote any field in the theory in addition to φ and $g_{\mu\nu}$. In such a case, we can claim that we have defined the model in the JF, in which the metric $g_{\mu\nu}$ couples in this standard way to the matter content. Although the action (3.39) did not support explicitly a kinetic term for the gravitational interaction, this could be present implicitly due to the presence of the Ricci scalar in the coupling $J(\varphi, R)$. In any case, as we already checked in the previous chapter, the gravitational interaction between matter fields can suffer important modifications, since, within the JF we have shown that this effect seems to be naturally interpreted as a modification of the Newton constant by the presence of the scalar field φ , where the scalar mode is mediating part of the gravitational interaction. Finally, we will show that the model given by Eq. (3.39) supports another scalar perturbative degree of freedom, that is also coupled to the matter content and completes the gravitational force, as it was first noted in [213].

In order to clarify the spectrum of the model, it is convenient to work in the EF, and, similarly to $f(R)$ and in order to identify the correct conformal transformation that defines the EF, it is convenient to work with an auxiliary scalar field ψ , defined by the following equation:

$$J(\varphi, R) = J(\varphi, \psi) + J_{\psi}(\varphi, \psi)(R - \psi), \quad (3.41)$$

where the sub-index ψ denotes the partial derivative of the $J(\varphi, R)$ function with respect to its second argument:

$$J_{\psi}(\varphi, \psi) = \partial_{\psi} J(\varphi, \psi). \quad (3.42)$$

We must assume that $J_{\psi\psi}(\varphi, \psi) \neq 0$ in this transformation and discuss separately the case $J_{\psi\psi}(\varphi, \psi) = 0$ in Section 3.3.2, but we can advance that, in such a case, the auxiliary field cannot be defined. By expressing $J(\varphi, R)$ in terms of ψ in the action (3.39), we can write a Lagrangian that is linear in R . Indeed, the two actions are equivalent if we also impose optimization with respect to ψ in order to obtain the equations of motion, whose solution implies $\psi = R$.

Now, it is evident to identify the proper conformal factor associated with the Einstein metric exactly as we performed in the $f(R)$ case:

$$\Omega^2 = \phi = J_\psi(\varphi, \psi), \quad (3.43)$$

where we are assuming explicitly $J_\psi(\varphi, \psi) > 0$. Of course, this turns off the possible character of a negative Newton constant which has already been studied in Section 2. In this case, we want to guarantee a positive character, i.e. an attractive gravitational interaction mediated by the expected standard spin-2 massless graviton [214]. Finally, we can define a new scalar Φ , which is based on a make-up of the conformal factor ϕ to obtain the canonical kinetic term of the field:

$$\Phi = \sqrt{3/2} \ln \phi = \sqrt{3/2} \ln J_\psi(\varphi, \psi), \quad (3.44)$$

so that, except for a boundary term, we can write the total action as:

$$S_{\text{NMSTT}} = \frac{1}{2} \int d^4x \sqrt{-\tilde{g}} \left[\tilde{R} - \tilde{g}^{\mu\nu} \tilde{\nabla}_\mu \Phi \tilde{\nabla}_\nu \Phi - \tilde{g}^{\mu\nu} e^{-\sqrt{\frac{2}{3}}\Phi} \tilde{\nabla}_\mu \varphi \tilde{\nabla}_\nu \varphi - 2V(\varphi, \Phi) \right], \quad (3.45)$$

where:

$$V = \frac{1}{2} \left[\psi(\varphi, \Phi) e^{-\sqrt{\frac{2}{3}}\Phi} - J(\varphi, \psi(\varphi, \Phi)) e^{-2\sqrt{\frac{2}{3}}\Phi} \right] \quad (3.46)$$

is the potential associated with the self-interaction of the scalar modes φ and Φ , and the interaction between them. One needs to use Eq. (3.44) in order to write ψ in terms of φ and Φ . It is interesting to remark that the third term in Eq. (3.45) not only accounts for the standard kinetic term for φ , but also for a derivative interaction with Φ . This follows, for example, from expanding the exponential factor around $\Phi = 0$, i.e. by assuming a small deviation from the two frames, a small difference between $g_{\mu\nu}$ and $\tilde{g}_{\mu\nu}$. On the other hand, the first term in Eq. (3.45) corresponds to the standard Einstein-Hilbert action and the second one is associated with a pure kinetic term for Φ . Of course, the kinetic terms include the interaction of both scalar fields with the geometry through the metric tensor $\tilde{g}_{\mu\nu}$.

3.3.1 Interaction with the matter content: the Standard Model

It is interesting to analyze in more detail the interactions associated with the different modes contained in the spectrum of the theory. Indeed, the coupling of the scalar field φ is open and not restricted by the geometrical structure of the model. In particular, its coupling with the SM

can be assumed to be absent. The opposite happens with the other scalar field Φ and the metric tensor. As we have discussed, the matter content is explicitly coupled to Φ when the action is expressed in terms of the Einstein metric:

$$S_{\mu_i} = S_i(e^{-\sqrt{\frac{2}{3}}\Phi} \tilde{g}_{\mu\nu}, \mu_i). \quad (3.47)$$

For example, we can follow [178] in order to detail the coupling of this scalar mode. This computation can be done directly with the help of the original action (JF), but it is more transparent and easier in the EF. We can study the couplings at linear order by expanding perturbatively the Jordan metric over the Minkowski background [178]:

$$g_{\mu\nu} = \eta_{\mu\nu} + \frac{1}{2}\tilde{h}_{\mu\nu} - \sqrt{\frac{2}{3}}\Phi \eta_{\mu\nu}, \quad (3.48)$$

where $\tilde{h}_{\mu\nu}$ takes into account the standard two degrees of freedom associated with the spin-2 (traceless and divergence-free) graviton. For simplification, we assume a common Minkowski background for the Jordan and Einstein geometries. In other words, we expand around $\Phi = 0$. In such a case, for computations in the linear order analysis, we do not need to specify the frame for quantities such as the stress-energy tensor.

By taking variations with respect to the metric in the matter action, it is evident that the spin-2 degree of freedom will have associated the standard interaction with the corresponding stress-energy tensor. On the other hand, the coupling of the spin-0 mode at the linear level will be given by the trace of the same stress-energy tensor, which can be calculated by expanding the exponential of Φ , that is coupled to the matter Lagrangian density, at linear order:

$$\mathcal{L}_{\Phi-T_{\mu\nu}} = \frac{1}{\sqrt{6}}\Phi T^\mu{}_\mu. \quad (3.49)$$

This means that Φ interacts with massive SM fields at tree level. In particular, the three body couplings are given by:

$$\mathcal{L}_{\Phi-\text{SM}}^{\text{tree-level}} = \frac{1}{\sqrt{6}}\Phi \left[2m_h^2 h^2 - \nabla_\mu^* h \nabla_*^\mu h + \sum_\psi m_\psi \bar{\psi}\psi - 2m_W^2 W_\mu^+ W^{-\mu} - m_Z^2 Z_\mu Z^\mu \right] \quad (3.50)$$

with the Higgs boson (h), (Dirac) fermions (ψ), and electroweak gauge bosons (W^μ and Z^μ), respectively. In addition, this scalar field interacts with photons and gluons by radiative corrections induced at one loop by charged gauge bosons and fermions (i.e. due to the *conformal*

anomaly [178]):

$$\mathcal{L}_{\Phi\text{-SM}}^{\text{one-loop}} = \frac{1}{\sqrt{6}} \Phi \left[\frac{\alpha_{\text{EM}} c_{\text{EM}}}{8\pi} F_{\mu\nu} F^{\mu\nu} + \frac{\alpha_s c_{\text{G}}}{8\pi} G_{\mu\nu}^a G_a^{\mu\nu} \right], \quad (3.51)$$

where $F_{\mu\nu}$ is the gauge invariant electromagnetic field strength tensor, $G_{\mu\nu}^a$ represents the gluon field strength tensor, α_{EM} is the fine-structure constant, and α_s is the strong coupling constant. The particular values of the couplings c_{EM} and c_{G} depend on the energy and on the complete set of particles charged with respect to these gauge interactions.

3.3.2 Scalar spectrum

Another general property given by the geometrical structure of the model is that the kinetic term for φ has the same coupling with Φ as the matter fields. Indeed, Φ can be understood as a dilaton, that parameterizes the conformal factor and couples to the trace of the stress-energy tensor. However, there is a general mixing of the scalar sector of the theory through the mass matrix that is defined by the potential function $V(\varphi, \Phi)$. If we assume that this potential reaches a minimum of value V_0 at (φ_0, Φ_0) (i.e. $V(\varphi_0, \Phi_0) = V_0$), the Squared-Mass Matrix (SMM) is given by:

$$M_{\varphi\Phi}^2 = \left(\begin{array}{cc} e\sqrt{\frac{2}{3}}\Phi_0 \partial_{\varphi\varphi}^2 V(\varphi, \Phi) & e\sqrt{\frac{1}{6}}\Phi_0 \partial_{\varphi\Phi}^2 V(\varphi, \Phi) \\ e\sqrt{\frac{1}{6}}\Phi_0 \partial_{\Phi\varphi}^2 V(\varphi, \Phi) & \partial_{\Phi\Phi}^2 V(\varphi, \Phi) \end{array} \right) \Big|_{(\varphi_0, \Phi_0)}. \quad (3.52)$$

Therefore, the mass eigenstates cannot be generally identified either with φ or with Φ , but with a linear mixing of both. This fact is not in contradiction with the dilaton nature of the couplings associated with Φ . The question is that, in general, the SMM breaks scale invariance explicitly.

In any case, a non trivial mixing and even the presence of two scalar degrees of freedom is not completely general. There are particular forms or values of the function $J(\varphi, \psi)$ that are interesting to analyze separately as we do in the following section.

Linear Couplings

If $J_{\psi\psi}(\varphi, \psi) = 0$, we find the particular case of a linear coupling of the field φ with the Ricci scalar, where action (3.39) has associated a truncated scalar spectrum. Indeed, in such a case, we can write $J(\varphi, R)$ in terms of two functions of φ : the one that parameterizes its non-minimal

interaction $H(\varphi)$, and the one that defines its potential $U(\varphi)$:

$$J(\varphi, R) = H(\varphi) R - 2U(\varphi). \quad (3.53)$$

In this case, it is not necessary to introduce any additional scalar field, since it is possible to define a conformal transformation to the EF, through a conformal factor that depends only on φ , namely:

$$\Omega^2 = H(\varphi). \quad (3.54)$$

Besides, if we redefine the scalar field in the following way [215]:

$$\frac{1}{2H(\varphi)} = \frac{1}{2} \left(\frac{d\varphi_*}{d\varphi} \right)^2 - \frac{3}{4} \left(\frac{d \ln H(\varphi)}{d\varphi} \right)^2, \quad (3.55)$$

we can write the action in the EF with a standard kinetic term for φ_* :

$$S_{\text{NMSTT}} = \int d^4x \sqrt{-\tilde{g}} \left[\frac{1}{2} \tilde{R} - \frac{1}{2} \tilde{g}^{\mu\nu} \tilde{\nabla}_\mu \varphi_* \tilde{\nabla}_\nu \varphi_* - V(\varphi_*) \right], \quad (3.56)$$

where the potential for φ_* takes into account the conformal factor and the field redefinition:

$$V(\varphi_*) = \frac{U(\varphi(\varphi_*))}{H^2(\varphi(\varphi_*))}. \quad (3.57)$$

Similarly to the previous section but for a single scalar field, by assuming a minimum for this potential at φ_*^0 , the corresponding squared-mass of the scalar mode will be given by:

$$m_{\varphi_*}^2 = \partial_{\varphi_* \varphi_*}^2 V(\varphi_*) |_{\varphi_*^0}. \quad (3.58)$$

This simple example illustrates the complexity in the identification of the scalar states. In this case, it is the field φ (or φ_*), the one that has associated the dilaton couplings with the matter content, since the conformal transformation is parameterized by φ (or φ_*):

$$S_{\mu_i} = S_i \left(\frac{\tilde{g}_{\mu\nu}}{H(\varphi(\varphi_*))}, \mu_i \right). \quad (3.59)$$

$f(R)$ theories

Another simple example of models described by Eq. (3.39) is the particular case studied in Section 3.2, i.e. the so-called $f(R)$ theories. In this case, $J(\varphi, R)$ can be written as the sum of two functions, one depending on R and another one depending on φ :

$$J(\varphi, R) = f(R) - 2U(\varphi). \quad (3.60)$$

The first one is the usual term which supports the $f(R)$ theory, and the second one constitutes a standard potential for the scalar field φ . In this case, φ is minimally coupled to gravity, and it can be interpreted directly as part of the matter content. However, recall that the non-linear dependence on R introduces an additional scalar degree of freedom as we saw in Section 3.2. Here, we can just particularize the equations derived in the previous sections. In fact, the new scalar field, when properly normalized, is defined by

$$\Phi = \sqrt{3/2} \ln f_\psi(\psi), \quad (3.61)$$

where, remember, the auxiliary field ψ verifies $\psi = R$ by taking into account the equations of motion, and the corresponding conformal factor will be $\Omega^2 = \phi = f_\psi(\psi)$ as in Eq. (3.38). Particularizing Eq. (3.46), we obtain that the total potential for the scalar sector cannot be written in general as the sum of two individual potentials associated with each one of the fields:

$$V(\varphi, \Phi) = \frac{1}{2} \left[\psi(\Phi) e^{-\sqrt{\frac{2}{3}}\Phi} - f(\psi(\Phi)) e^{-2\sqrt{\frac{2}{3}}\Phi} + 2U(\varphi) e^{-2\sqrt{\frac{2}{3}}\Phi} \right]. \quad (3.62)$$

The reason is that the conformal factor introduces a non-derivative interaction between the two scalar modes. Therefore, even in this case, the off-diagonal entries of the SMM are not necessarily zero and the mass eigenstates cannot be identified, in general, with φ or with Φ .

Generalized Higgs inflation models

Non-minimal gravitational couplings of the SM Higgs doublet have been considered in order to build viable models of inflation in the early Universe [216, 217, 218, 219, 220]. Generalizations of this idea with non-linear couplings to the Ricci scalar have been discussed in the literature with the SM Higgs working as inflaton or with a similar scalar field [179, 180, 181, 182, 183, 184, 185, 186, 187, 188, 189, 190, 191, 192]. As far as we know, the presence of a new scalar degree of freedom has been missed in these analyses. As we have shown, the non-linear couplings in the Ricci scalar introduce a new degree of freedom. We can determine its phenomenology by using the general equations deduced in this chapter. The general $J(\varphi, R)$ function that defines these models can be written as

$$J(\varphi, R) = R + \xi \varphi^a R^b - 2U(\varphi), \quad (3.63)$$

where the first term is associated with the initial Einstein-Hilbert action for the Jordan metric; the second term is the non-linear coupling parameterized by the strength constant ξ and the

exponents a and b ; and $U(\varphi)$ is the potential for the scalar field in the JF. Note that a and b need to be integer numbers to have an analytical interaction at $\varphi = 0$ and $R = 0$ respectively, but the non-minimal coupling can also be defined for any real value of both exponents. The standard potential in these models is usually assumed to be:

$$U(\varphi) = \frac{\lambda}{4} \left(\varphi^2 - \frac{\mu^2}{\lambda} \right)^2, \quad (3.64)$$

with $\mu, \lambda > 0$. It implies that $U(\varphi)$ is bounded from below, and develops a stable minimum at $\varphi_0 = \mu/\sqrt{\lambda}$ with $U(\varphi_0) = 0$, i.e. we have avoided the introduction of a vacuum energy¹. By taking into account our previous results, the conformal transformation to the EF is defined by

$$\Omega^2 = 1 + \xi b \varphi^a \psi^{b-1}, \quad (3.65)$$

with $\psi = R$ as we have commented. Therefore, provided $b \neq 1$, the coupling introduces a new scalar particle, associated with the normalized field:

$$\Phi = \sqrt{3/2} \ln(1 + \xi b \varphi^a \psi^{b-1}). \quad (3.66)$$

As we have discussed, this new degree of freedom is associated with the dynamics of the Jordan Ricci scalar through the relation: $R = \psi = \{[\exp(\sqrt{2/3} \Phi) - 1]/(\xi b \varphi^a)\}^{1/(b-1)}$. Therefore, the total action for this type of GHIMs is written in the EF as:

$$S_{\text{GHIM}} = \frac{1}{2} \int d^4x \sqrt{-\tilde{g}} \left[\tilde{R} - \tilde{g}^{\mu\nu} \tilde{\nabla}_\mu \Phi \tilde{\nabla}_\nu \Phi - \tilde{g}^{\mu\nu} e^{-\sqrt{2/3} \Phi} \tilde{\nabla}_\mu \varphi \tilde{\nabla}_\nu \varphi - 2V(\varphi, \Phi) \right], \quad (3.67)$$

where:

$$V(\varphi, \Phi) = \frac{1}{2} \left[\xi \varphi^a (b-1) \left(\frac{e^{\sqrt{2/3} \Phi} - 1}{\xi b \varphi^a} \right)^{\frac{b}{b-1}} + 2U(\varphi) \right] e^{-2\sqrt{2/3} \Phi}. \quad (3.68)$$

In order to simplify the discussion, we can fix the particular values: $a = b = 2$, and $\xi > 0$. In such a case, the total potential is bounded from below provided $U(\varphi)$ is as well. Indeed, a minimum of the scalar sector can be found at $(\varphi_0, \Phi_0) = (\mu/\sqrt{\lambda}, 0)$ if the potential (3.64) is assumed. In fact, such a minimum is global since $V(\varphi_0, \Phi_0) = 0$ and $V(\varphi, \Phi)$ is non-negative. In this case, the SMM around the minimum is given by:

$$M_{\varphi\Phi}^2 = \begin{pmatrix} 2\mu^2 & 0 \\ 0 & \frac{\lambda}{6\xi\mu^2} \end{pmatrix}. \quad (3.69)$$

¹The potential develops an analogous minimum at $\varphi_0 = -\mu/\sqrt{\lambda}$. The same discussion applies when the system chooses this other vacuum state.

Therefore, in this particular case, the mass eigenstates can be identified with φ and Φ . In other words, they do not mix. In addition, the phenomenology of Φ is decoupled since the mass scale μ is expected to be very small with respect to the Planck scale, which implies a very large mass for Φ (by assuming $\lambda, \xi \sim 1$).

It is important to comment that the original action has a parity symmetry associated with the sign of the scalar φ . However this is not the fundamental reason for the non-mixing of the scalar fields, since this discrete \mathbb{Z}_2 symmetry is broken by the VEV of φ . It means that this symmetry will not be able to protect this property, that will be potentially destroyed by radiative corrections.

Coming back to the *on-shell* analysis, the situation is different for $b = 2$ and $a < -2$. In this case, Φ is lighter than φ for $\mu \ll 1$ ($\lambda, \xi \sim 1$). Indeed, for such values of the exponents, the SMM is still diagonal, but the non-zero entries are $M_{\varphi\varphi}^2 = 2\mu^2$ and $M_{\Phi\Phi}^2 = \lambda^{a/2}/(6\xi\mu^a)$. Finally, we must mention that any other integer value of b ($b > 2$) may imply strong instabilities for the field configuration defined by $(\varphi_0, \Phi_0) = (\mu/\sqrt{\lambda}, 0)$, since the potential will develop a singularity at $\Phi = 0$. Indeed, the study of the SMM deduced in this work within the EF, is the most efficient way to analyze the stability of a NMSTT (in the same way as for $f(R)$ theories, as it was originally pointed out in [177]). This procedure is equivalent to the Hessian matrix analysis of an optimization study in two variables.

3.4 Conclusions

In this chapter, we have started reviewing the important case of $f(R)$ theories in the modified gravity background, with the purpose of explaining the equivalence of this approach with scalar-tensor theories, and passing through the study of conformal transformations applied over this to expose the way to go from the JF to the EF. After this, we have studied the phenomenology of NMSTTs, i.e. scalar field models defined by a general coupling of the scalar field with the Ricci scalar. These theories can be understood as generalizations of the gravitational interaction written in a particular JF. We have found explicitly the EF corresponding to such general theories by characterizing the conformal transformation that defines the relation between both frames. By following the general set of equations associated with the transformation between the two corresponding metric tensors, it is explicit that the spectrum of the theory contains not one,

but two (generally massive) scalar degrees of freedom, in addition to a massless spin-2 state. The latter particle can be associated with the standard mediator of Einstein gravity, whereas the second scalar mode is related to the non-linear coupling of the original (JF defined) scalar field to the Ricci scalar. Indeed, provided that the coupling is linear, we have proved that the general conformal transformation is not well defined and the spectrum of the theory is truncated by removing the second scalar degree of freedom. The situation is more involved if the Jacobian associated with the field redefinition is zero for particular values of the fields. In such a case, the effective number of degrees of freedom of the theory depends on the field configuration. This fact can be understood as if the spectrum of the theory maximizes the number of perturbative states, but the masses of the scalar modes depend on the values of the fields and can diverge for one of the modes. This fact removes effectively one of the scalar degrees of freedom as it was discussed in [177, 178] for the case of $f(R)$ theories.

Once the degrees of freedom were identified, we analyzed their couplings with the matter content. In particular, we have studied the couplings with SM particles. Under general assumptions, the spin-2 state couples as the standard GR graviton. The scalar degree of freedom associated with the conformal factor couples through the trace of the stress-energy tensor. Indeed, it can be identified with a dilaton since it parameterizes general scale transformations. On the other hand, the coupling of the other spin-0 particle is completely model dependent. It changes by depending on the definition of its interactions in the original action (JF), that is not fixed. It is interesting to remark that this factorization of the couplings associated with the scalar content of the theory is simple because it is discussed in terms of the interaction eigenstates. These modes are not necessarily the mass eigenstates. In general, there is a mixing between the two scalar modes that leads to the rich phenomenology associated with these NMSTTs.

Chapter 4

Extremal Black Holes in modified gravity

Black hole solutions have been widely studied in the literature, as they are natural solutions of GR, and have led to an important development of gravitational physics, including the famous theorems about singularities that offer a way to better understand these objects and their main features. Here we will focus on the particular black holes described by the Schwarzschild-(Anti) De Sitter spacetime as an example, which arises in GR as a solution when considering a (negative) cosmological constant, since they have been of great interest as they show a thermodynamical equilibrium when analysing Hawking radiation [221, 222, 223]. In the case of a positive cosmological constant, the Schwarzschild-de Sitter spacetime shows in general two horizons, one corresponding to the black hole event horizon and the other one to a cosmological horizon. The extreme case arises when both horizons coincide at the same hypersurface, the so-called Nariai spacetime [224], leading to an interesting structure for the spacetime and the trajectories of geodesics [225] as well as for its spectrum [226], which will be studied throughout the next sections. In addition, the stability of such an extreme spacetime has been studied in [227], but when some (quantum) corrections are included, an interesting phenomenon occurs as the radius of the horizon becomes unstable and grows, that has been called black hole anti-evaporation [228]. Despite the fact that the anti-evaporation regime was initially studied and attributed to semiclassical corrections that affect the evaporation of black holes in de Sitter spacetime when analysing the one-loop effective action [228, 229], other frameworks that lead to classical instabilities that affect the radius of the horizon have been also named antievaporation, as is the case of $f(R)$ gravity [230], Gauss–Bonnet gravities [231], bigravity theories [232, 233]

and mimetic gravity [234]. The purpose here will be the study of this phenomenon from a classical point of view, but for a generalization of the scalar-tensor theories.

As we have already seen along Chapters 2 and 3, one important branch of modified gravity is that associated with scalar fields and scalar-tensor theories. However, although a great part of these kind of theories has been extensively studied along the previous chapters, this is far from the end. Generalisations of these have been widely studied, mainly in the context of cosmology, like the so-called K-essence, which presents a non-canonical kinetic term and provides a natural explanation for dark energy [235, 236], or the so-called Galileons, that incorporate a Galilean-like symmetry and which can also reproduce in a simple way the late-time acceleration [237]. These types of models have in common that they may avoid the so-called Ostrogradsky instability that arises in higher order theories, but is absent in second order theories, such as the ones cited above. This class of scalar-tensor models are encompassed in the so-called Horndeski gravity [80], which represents the most general theory with second order field equations (for a review see [238, 239]). Horndeski gravity is shown to be a generalisation of Galileon in its covariant form [240], which is also connected to k-essence fields [241]. Nevertheless, there have been some healthy extensions of Horndeski gravity also implying second order derivatives for the field equations [242, 243, 244]. In general, Horndeski gravity is well understood in many contexts, inflationary models have been widely analysed, as well as the growth of cosmological perturbations [245, 246, 247, 248, 249]. Consequently dark energy models can be easily implemented in Horndeski gravity [250, 251], the predictions and restrictions of which have been analysed [252, 253, 254, 255]. Also, in light of the era of gravitational waves [256, 257], Horndeski gravity is shown to carry just an additional scalar mode [258], but the theory is well constrained by the speed of propagation of the graviton [259, 260, 261], which implies several restrictions on the full Lagrangian [262].

Putting together both frames, i.e. black holes (static spherically symmetric solutions) and modified gravity [263, 264, 265, 266, 267, 268, 269, 270], let us provide: a way to regularise such types of solutions [271, 272, 273, 274], a better understanding of Birkhoff's theorem [275, 276, 277], and new direct ways for testing GR [278, 279, 280]. In Horndeski gravity, there have been plenty of works where such types of solutions are studied, mainly when dealing with compact objects such as black holes [281, 282, 283, 284], but also when assuming the constraints imposed on the full Horndeski Lagrangian by the speed of propagation of gravita-

tional waves [285], and the stability of such types of spacetimes [286, 287, 288, 289, 283, 284]. The no-hair theorem is also extended in these theories [290]. Moreover, the Cauchy problem has been analysed in Horndeski gravity by studying the hyperbolicity of the system of equations, which seems to admit a well posed initial value problem [291]. Also, the stability in non perturbative cosmology has been studied [292], as well as the gauge problem in such Lagrangians [293].

The purpose of this chapter is to show an example of the study of black holes in Horndeski gravity, focusing on the anti-evaporation effect, by studying perturbations on the metric. For this goal, we will take and analyze the Nariai spacetime, in opposite to Schwarzschild black holes, where perturbations and the Cauchy problem have already been widely analysed in the literature within several gravitational theories [294, 295, 296, 270]. Then, the purpose here will be to study how perturbations of a scalar field (which should be around a constant background value as we will see) can affect the radius of the horizon of the extremal Schwarzschild-de Sitter black hole called Nariai spacetime, for the Lagrangians that compose Horndeski gravity. This also shows some implications on an extended version of Birkhoff's theorem for scalar-tensor theories. At the end, we will also try to analyse the stability of such solutions for a shorter version of the full Horndeski Lagrangian, motivated by keeping as few free functions as possible and which coincide with the viable terms restricted by the speed of GW's.

4.1 Nariai Spacetime in Horndeski Gravity

Let us start by remembering the general action that we are dealing with throughout this chapter. This is the Hilbert–Einstein action plus the so-called Horndeski Lagrangian already introduced in Eq. (1.31):

$$S = \int dx^4 \sqrt{-g} \left[\frac{R}{16\pi G} + \mathcal{L}_{\text{Hr}} + \mathcal{L}_m \right], \quad (4.1)$$

where \mathcal{L}_m is the matter Lagrangian, which encompasses all the matter species of the system under study while the Horndeski Lagrangian \mathcal{L}_{Hr} is given by:

$$\begin{aligned}
\mathcal{L}_{\text{Hr}} = & G_2(\phi, X) \\
& -G_3(\phi, X)\square\phi \\
& +G_4(\phi, X)R + G_{4X}(\phi, X) [(\square\phi)^2 - \phi_{;\mu\nu}\phi^{;\mu\nu}] \\
& +G_5(\phi, X)\phi_{;\mu\nu}G^{\mu\nu} - \frac{G_{5X}(\phi, X)}{6} [(\square\phi)^3 - 3\square\phi\phi_{;\mu\nu}\phi^{;\mu\nu} + 2\phi_{;\mu\nu}\phi^{;\nu\lambda}\phi_{;\lambda}^{;\mu}].
\end{aligned} \tag{4.2}$$

Recall that each line is an independent term labeled by the function G_n , ϕ is the scalar field, $G_{\mu\nu}$ is the Einstein tensor, $_{;\mu} = \nabla_{\mu}$ is the covariant derivative, $X = -\frac{1}{2}\partial_{\mu}\phi\partial^{\mu}\phi$ is the kinetic term, $G_i(\phi, X)$ are arbitrary functions of ϕ and X , and $_X$ is the derivative with respect to X . As it is well known, the Lagrangian (4.3) represents the most general scalar-tensor Lagrangian that leads to second order field equations despite the fact that it depends on second derivatives of the field ϕ at the level of the action as well as on non-minimally coupling terms to the Ricci scalar. As shown in Reference [241], Horndeski theory is just the generalisation of the so-called covariant Galileon field, but losing the Galilean shift symmetry that provides its name [240]. Hence, by varying the action (4.1) with respect to the metric $g_{\mu\nu}$ and with respect to the scalar field ϕ , the corresponding field equations can be obtained and one can analyse how some particular spacetimes behave within this class of theories.

The other fundamental piece here is the Nariai spacetime, i.e, as already mentioned, the extremal case of the Schwarzschild-de Sitter black hole, as is shown below. The general Schwarzschild-de Sitter metric can be expressed in spherical coordinates as follows [228]:

$$ds^2 = -A(r)dt'^2 + A(r)^{-1}dr^2 + r^2d\Omega_2^2, \tag{4.3}$$

where $d\Omega_2^2$ is the metric of a 2D sphere, and

$$A(r) = 1 - \frac{2M}{r} - \frac{\Lambda}{3}r^2. \tag{4.4}$$

Here, $\Lambda > 0$ and $M > 0$, and the latter is a mass parameter. Then, if $0 < M^2 < \frac{1}{9\Lambda}$, the function $A(r)$ has two positive roots r_{BH} and r_c , which correspond to the black hole event horizon and to the cosmological horizon, respectively:

$$r_{BH} = -\frac{2}{\sqrt{\Lambda}} \cos \left\{ \frac{1}{3} \left[\arccos \left(-\sqrt{9M^2\Lambda} \right) + \pi \right] \right\}, \tag{4.5}$$

$$r_c = \frac{2}{\sqrt{\Lambda}} \cos \left\{ \frac{1}{3} \arccos \left(-\sqrt{9M^2\Lambda} \right) \right\}. \tag{4.6}$$

It is easy to check that $A(r) > 0$ only for $r_{BH} < r < r_c$ and consequently the metric is static only in the region between both horizons. In addition, $A(r)$, given by Eq. (4.4), diverges at $r = 0$. This divergence cannot be avoided by a coordinate change and therefore it will not be a coordinate singularity, but a real singularity. It can be checked by the scalar¹ $R_{\mu\nu\alpha\beta}R^{\mu\nu\alpha\beta}$, which diverges at $r = 0$, that this is a curvature singularity. The global structure of this spacetime has been widely analysed in the literature [221, 222, 223], but Penrose's diagram give us a better idea of this spacetime. As an example of this, we introduce the Schwarzschild black hole which is essentially the same only without the de-Sitter part, i.e. with $\Lambda = 0$. It is important to remark that Penrose's diagram is useful because it does not change the casual structure but brings infinity to a finite graphic and with a slope of 45° of the light rays (which lets us know the light cone straightforwardly). For this, one should apply two steps: the first one is about choosing null coordinates to draw the light cone, the second one is a conformal compactification in order to bring the infinity to a finite region. First of all, we will focus on the region $r > 2M$ and use the null Eddington–Finkelstein coordinates, i.e:

$$u = t' - r^*, \quad v = t' + r^*, \quad \text{where} \quad r^* = r + 2M \ln \left| 1 - \frac{r}{2M} \right|. \quad (4.7)$$

Then, $r \in (2m, \infty)$, u and $v \in (-\infty, \infty)$ and one must be careful with the absolute values in $dr^* = dr/(1 - 2M/r)$. In addition, $u = cte$ and $v = cte$ respectively represent outgoing and ingoing null geodesics. This will result in the following metric:

$$ds^2 = -A(r)dudv + r^2d\Omega_2^2. \quad (4.8)$$

In addition, from Eq. (4.7) we have:

$$\frac{r^*}{2M} = \frac{r}{2M} + \ln \left| 1 - \frac{r}{2M} \right| = \frac{1}{4M}(v - u), \quad (4.9)$$

where

$$\left(\frac{r}{2M} - 1 \right) = A(r) \frac{r}{2M}, \quad (4.10)$$

and therefore:

$$A(r) = \frac{2M}{r} e^{-r/(2M)} e^{(v-u)/(4M)}, \quad (4.11)$$

¹This scalar is the so-called Kretschmann scalar and it is important because it is invariant under change of coordinates, so if it diverges at some point in some coordinate system, it will diverge at the same point for any coordinate system. For the Schwarzschild de-Sitter metric this scalar is: $K_1 = \frac{8\Lambda^2}{3} + \frac{48M^2}{r^6}$ which recovers the better known case of Schwarzschild when $\Lambda = 0$.

which transforms the metric (4.8) into:

$$ds^2 = -\frac{2M}{r} e^{-r/(2M)} e^{(v-u)/(4M)} du dv + r^2 d\Omega_2^2. \quad (4.12)$$

The next step will be the introduction of Kruskal–Szekeres coordinates defined as:

$$U = -4M e^{-u/4M}, \quad V = 4M e^{v/4M}, \quad (4.13)$$

$$dU = e^{-u/4M} du, \quad dV = e^{v/4M} dv, \quad (4.14)$$

after which the metric reads:

$$ds^2 = -\frac{2M}{r} e^{-r/(2M)} dU dV + r^2 d\Omega_2^2, \quad (4.15)$$

from where one can check that $r = 2M$ was only a coordinate singularity, which vanishes with an appropriate choose of coordinates. Besides, we can apply an extension of the coordinates. Until now, we were studying the exterior region, $r > 2M$ and $U < 0$ and $V > 0$, but now one can extend the geodesics because they do not finish their path at $U = 0$ or $V = 0$, so at the end of the day $U, V \in (-\infty, \infty)$. However we should maintain the condition $r > 0$. In addition, due to:

$$UV = -16M^2 \left(\frac{r}{2M} - 1 \right) e^{r/2M}, \quad (4.16)$$

UV will be bounded by $UV < 16M^2$. In order to finish, we will apply a compactification of the spacetime. For this purpose it is very useful to use a function as $\tan(x)$ that is infinity at a finite point. With this fact in mind, the new reparametrization is:

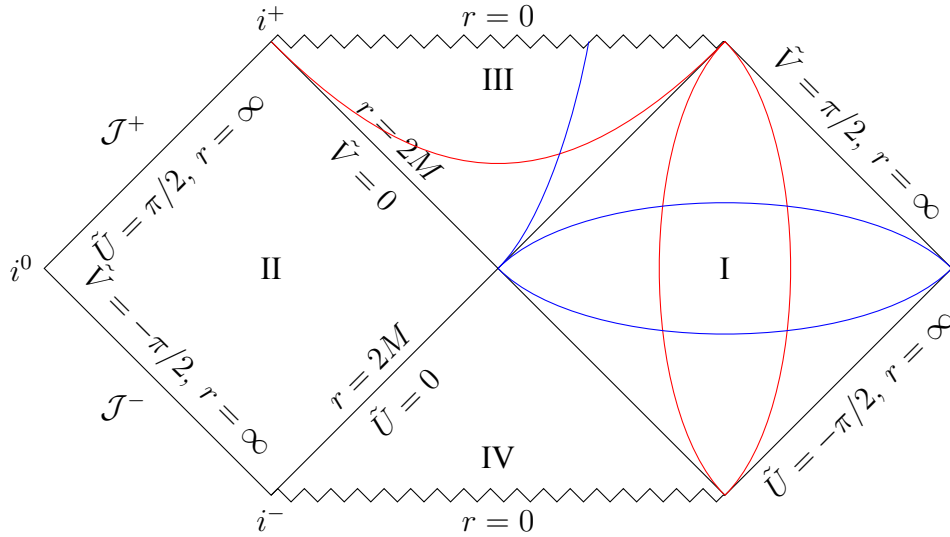
$$4M \tan(\tilde{U}) = U, \quad 4M \tan(\tilde{V}) = V, \quad (4.17)$$

$$4M \frac{d\tilde{U}}{\cos^2(\tilde{U})} = dU, \quad 4M \frac{d\tilde{V}}{\cos^2(\tilde{V})} = dV, \quad (4.18)$$

where $\tilde{U}, \tilde{V}, \tilde{U} + \tilde{V} \in (-\pi/2, \pi/2)$. Then, the resulting metric is:

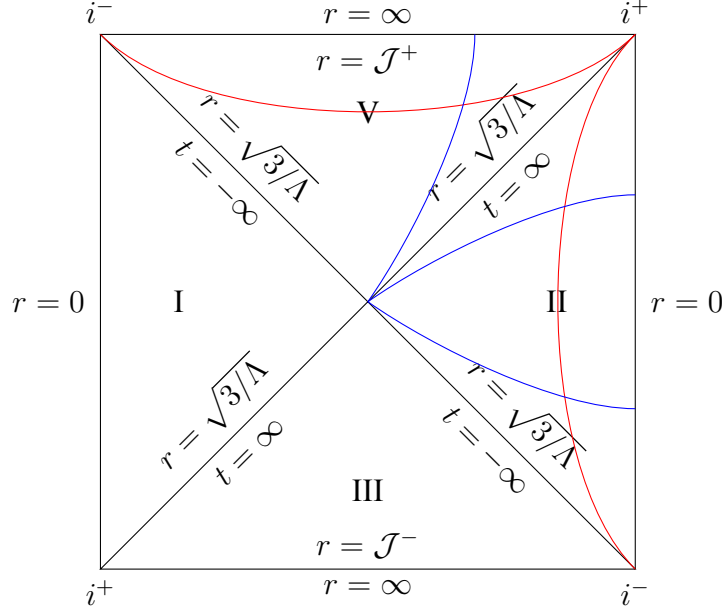
$$ds^2 = -\frac{32M^3}{r} \frac{e^{-r/(2M)}}{[\cos(\tilde{U}) \cos(\tilde{V})]^2} d\tilde{U} d\tilde{V} + r^2 d\Omega_2^2, \quad (4.19)$$

Finally, one is able to draw Penrose's diagram thinking about (\tilde{U}, \tilde{V}) as a coordinate reference system:

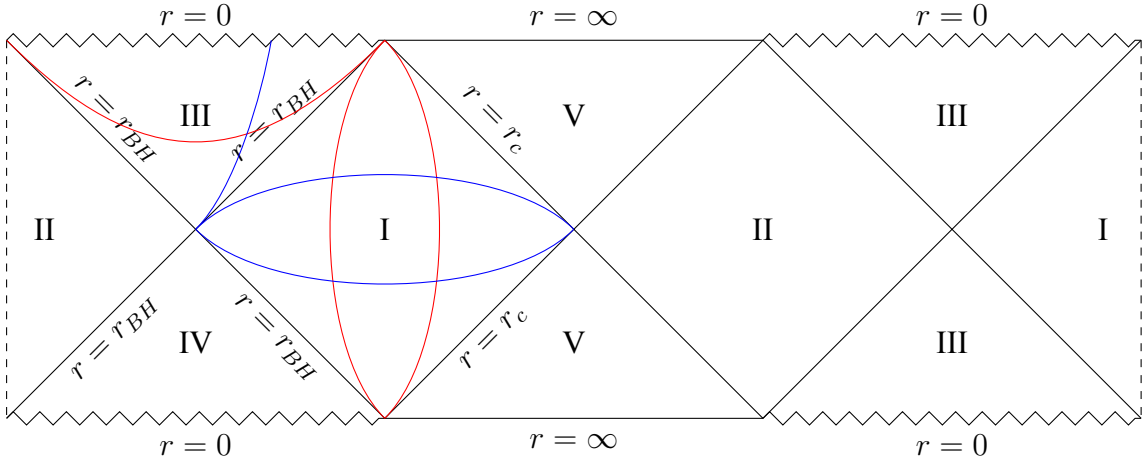


where blue lines represent $t' = cte$, red lines represent $r = cte$, i^\pm are the future (+) / past (-) timelike infinities (it means that timelike geodesics start in i^- and end up in i^+), i^0 is the spacelike infinity ($r = \infty$ with arbitrary t) and \mathcal{J}^\pm are the future (+) / past (-) null infinity, i.e. $r = \infty$ where light geodesics start or end up. Let us show that: on the one hand, $t' = cte \rightarrow u + v = cte$ and therefore $V/U = cte$, so we can represent these straight lines, transformed by the $\tan(x)$ into curves in Penrose's diagram, as can be checked. On the other hand, $r = cte \rightarrow v - u = cte \rightarrow UV = cte$. Thus $r = 0$ corresponds with $UV = 16M^2 = 16M^2 \tan \tilde{U} \tan \tilde{V}$ which corresponds to $\tilde{U} + \tilde{V} = \pm\pi/2$. The angular coordinates are not represented because they do not give us new information, but we should think about each point of the diagram as a 2-sphere of radius r . In view of the Penrose diagram, the null hypersurfaces $r = 2M$ pulls apart, for $r = cte$, time-like hypersurfaces ($r > 2M$) from space-like hypersurfaces ($r < 2M$). In addition, $r = 2M$ is called a horizon because an object which falls inside it (i.e. in area III) can never come back. In the diagram this is shown because light-like geodesics moving radially look like straight lines with an inclination of 45° . The description of the regions is as follows: I) the exterior of the black hole $r > 2M$, III) the interior of the black hole with $0 < r < 2M$, IV) the interior region of a white hole, II) the exterior of the white hole. There are no null (and much less time-like) curves which traverse from region I to region II (and vice-versa) so then they can be considered as disconnected universes.

Analogously, one could present the Penrose diagram for de-Sitter spacetime, this is the case with $M = 0$ [297]:



In this case, there is an horizon for $r = \sqrt{3/\Lambda}$ and there are no singularities. It is important to remark that a timelike observer can only access one part of the spacetime independently of their starting point. Now, it is easy to check that mixing both spacetimes in order to obtain the Schwarzschild de-Sitter spacetime, Penrose's diagram reads:



where there are two horizons at $r = r_c$ and $r = r_{BH}$. The crucial point here is that for the extreme case whenever $M \rightarrow \frac{1}{3\sqrt{\Lambda}}$, the size of the black hole event horizon r_{BH} increases and approaches the cosmological horizon r_c at $r = 3M$, such that function (4.4) tends to:

$$A(r) = -\frac{(r - 3M)^2(r + 6M)}{27M^2r}, \quad (4.20)$$

becoming the extremal case of the Schwarzschild-de Sitter black hole, which is known as the Nariai spacetime [224]. As shown in Eq. (4.20), it leads to a degenerate horizon that corresponds to the black hole one and to the cosmological one simultaneously. The causal structure of this particular case is well understood and the geodesics in such spacetime are well described in Reference [225]. Note that $A(r) \leq 0$, such that the radial coordinate becomes timelike and the time coordinate spacelike everywhere. In Fig. (4.1) we represent this function to help understand this.

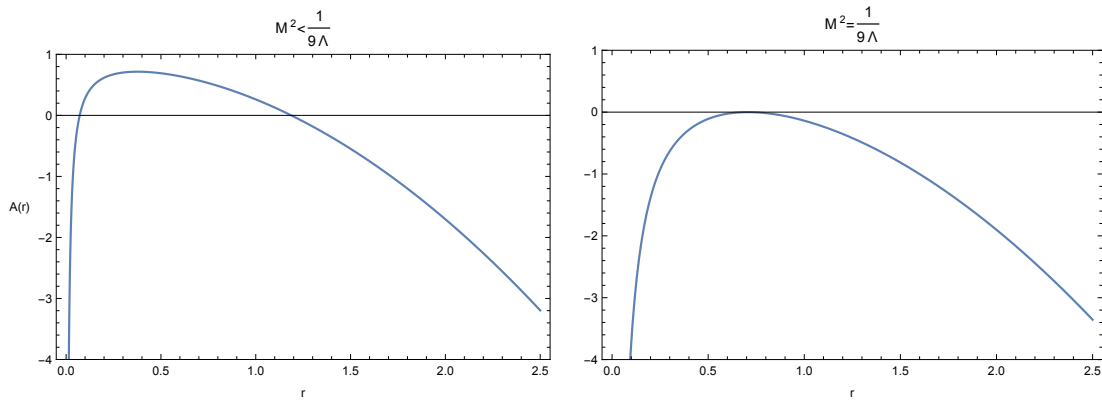
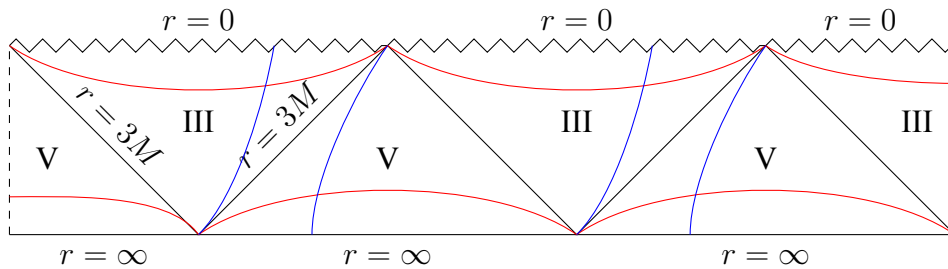


Figure 4.1: Aspect of the function $A(r)$

From the Penrose diagram point of view, one could join r_{BH} with r_c of the Schwarzschild de-Sitter case (vanishing region I and II) to obtain the extreme case. Actually, there are two possibilities, one which describes a white hole, and another one which describes a black hole. Here we are interested in the study of the latter, whose Penrose diagram is:



After this previous study of spacetimes, let us express the metric (4.3) with some more appropriate coordinates, but firstly we express the extremal case as a limit in terms of a parameter $0 < \epsilon \ll 1$, [227]:

$$9M^2\Lambda = 1 - 3\epsilon^2. \quad (4.21)$$

As $\epsilon \rightarrow 0$, both horizons approach each other, i.e. one passes from the Schwarzschild de-Sitter space time to Nariai space time, vanishing region I and II in Penrose's diagram. Then, one can choose the following coordinates [228]:

$$t' = \frac{1}{\epsilon\sqrt{\Lambda}}\psi, \quad r = \frac{1}{\sqrt{\Lambda}} \left(1 - \epsilon \cos \chi - \frac{1}{6}\epsilon^2 \right), \quad (4.22)$$

as long as one stays far away enough from spatial infinity. In these new coordinates, and expanding at first order in ϵ , the metric (4.3) becomes:

$$ds^2 = -\frac{1}{\Lambda} \left(1 + \frac{2}{3}\epsilon \cos \chi \right) \sin^2 \chi d\psi^2 + \frac{1}{\Lambda} \left(1 - \frac{2}{3}\epsilon \cos \chi \right) d\chi^2 + \frac{1}{\Lambda} (1 - 2\epsilon \cos \chi) d\Omega_2^2. \quad (4.23)$$

Here the black hole horizon is given by $\chi = 0$, whereas the cosmological one corresponds to $\chi = \pi$. The spatial topology is clearly $S_1 \times S_2$. By setting $\epsilon \rightarrow 0$, the extremal case is obtained and the metric yields (4.23):

$$ds^2 = \frac{1}{\Lambda} (-\sin^2 \chi d\psi^2 + d\chi^2) + \frac{1}{\Lambda} d\Omega_2^2. \quad (4.24)$$

Finally, we can implement another change of coordinates that simplifies the expression (4.24), which is described by the following coordinates:

$$x = \text{Log} \left(\tan \frac{\chi}{2} \right), \quad t = \frac{\psi}{4}. \quad (4.25)$$

Then the metric (4.24) for the Nariai spacetime becomes:

$$ds^2 = \frac{1}{\Lambda \cosh^2 x} (-dt^2 + dx^2) + \frac{1}{\Lambda} d\Omega_2^2. \quad (4.26)$$

The new coordinates are defined in the domain $(-\infty, \infty)$, as can be easily shown by Eq. (4.25). This metric is easily drawn in Penrose's diagram following a similar procedure from Schwarzschild case. Let us introduce some lines to check the previous diagram in the interior region of both horizons. First of all we will use the null coordinates:

$$u = t - x, \quad v = t + x, \quad (4.27)$$

and the Kruskal-Szekeres coordinates:

$$U = -e^{-u}, \quad V = e^v. \quad (4.28)$$

Then, the metric would be:

$$ds^2 = -\frac{dUdV}{\frac{\Lambda}{4}(UV+1)^2} + \frac{1}{\Lambda}d\Omega_2^2, \quad (4.29)$$

finishing with the compactification:

$$\tan(\tilde{U}) = U, \quad \tan(\tilde{V}) = V, \quad (4.30)$$

$$ds^2 = -\frac{d\tilde{U}d\tilde{V}}{\frac{\Lambda}{4}[\cos(\tilde{U} + \tilde{V})]^2} + \frac{1}{\Lambda}d\Omega_2^2, \quad (4.31)$$

where, for example, $r = cte$, corresponds to $\chi = cte$, $x = cte$, $v - u = cte$, $VU = cte$.

4.2 Reconstructing the Gravitational Action in Horndeski Gravity

In this section, we analyse the particular Lagrangians within Horndeski gravity that reproduce the Nariai solution. To do so, we use the metric as expressed in the coordinates given in Eq. (4.26). As shown, Nariai spacetime can be a solution for each of the Horndeski Lagrangians as long as some constraints are assumed on the \mathcal{L}_i functions.

4.2.1 Case with \mathcal{L}_2

As a first approximation to Horndeski gravity in Nariai spacetime, we will start studying the simplest case in which only \mathcal{L}_2 is considered for \mathcal{L}_{Hr} ,

$$\mathcal{L}_2 = G_2(\phi, X), \quad (4.32)$$

which essentially is the usual term for K-essence theory. The first step will be to solve, at the background level, the equations of motion given by the Einstein tensor plus an effective stress-energy tensor coming from metric variations of the matter Lagrangian plus the Lagrangian defined in Eq. (4.32):

$$G_{\mu\nu} = R_{\mu\nu} - \frac{1}{2}g_{\mu\nu}R = 8\pi G \left[g_{\mu\nu}G_2(\phi, X) + \frac{\partial G_2(\phi, X)}{\partial X} \partial_\mu \phi \partial_\nu \phi + T_{\mu\nu}^{(m)} \right], \quad (4.33)$$

where $T_{\mu\nu}^{(m)}$ is the stress-energy tensor of the matter Lagrangian, and which, for the case of our interest, we are going to consider zero, to focus on the vacuum, i.e., $T_{\mu\nu}^{(m)} = 0$. Therefore, this tensor equation leads to the following system of equations:

$$(tt) \quad \frac{1}{8\pi G} \frac{1}{\cosh^2 x} = -\frac{G_2(\phi, X)}{\Lambda \cosh^2 x} + \frac{\partial G_2(\phi, X)}{\partial X} \dot{\phi}^2, \quad (4.34)$$

$$(xt) \quad 0 = -\frac{\partial G_2(\phi, X)}{\partial X} \partial_t \phi \partial_x \phi, \quad (4.35)$$

$$(xx) \quad \frac{1}{8\pi G} \frac{-1}{\cosh^2 x} = \frac{G_2(\phi, X)}{\Lambda \cosh^2 x} + \frac{\partial G_2(\phi, X)}{\partial X} \phi'^2, \quad (4.36)$$

$$(\theta\theta) \quad \frac{-1}{8\pi G} = \frac{G_2(\phi, X)}{\Lambda} + \frac{\partial G_2(\phi, X)}{\partial X} \partial_\theta \phi \partial_\theta \phi, \quad (4.37)$$

$$(\Phi\Phi) \quad \frac{-\sin^2 \theta}{8\pi G} = \sin^2 \theta \frac{G_2(\phi, X)}{\Lambda} + \frac{\partial G_2(\phi, X)}{\partial X} \partial_\Phi \phi \partial_\Phi \phi. \quad (4.38)$$

Here, $\dot{\phi}$ means time derivatives (as throughout all the work) but ϕ' will represent derivatives with respect to x (and not conformal time derivatives). The two main issues that we intend to solve are the form of $G_2(\phi, X)$ and that of $\phi(t, x, \theta, \Phi)$. Combining Eq. (4.37) with Eq. (4.38) yields:

$$\partial_\Phi \phi \partial_\Phi \phi = \sin^2 \theta \partial_\theta \phi \partial_\theta \phi \quad \rightarrow \quad \partial_\Phi \phi = \pm \sin \theta \partial_\theta \phi, \quad (4.39)$$

whose solution is:

$$\phi = g(t, x) \left[\Phi \pm \ln \left(\cot \frac{\theta}{2} \right) \right] + f(t, x). \quad (4.40)$$

However, from Eq. (4.34) and Eq. (4.36) it is possible to deduce that $g(t, x)$ should vanish in order to keep the same dependence on parameters on the left and right hand side of the equations, and therefore $\phi = \phi(t, x)$, which implies that $X = \Lambda \cosh^2(x) (\dot{\phi}^2 - \phi'^2)/2$. This is the formal way for showing that the scalar field has to be spherically symmetric, as is the metric. In addition, to solve $G_2(\phi, X)$, we will use the trace of Eq. (4.33) where the scalar of curvature for the Nariai metric is $R = 4\Lambda$ and therefore:

$$-\frac{\Lambda}{4\pi G} = 2G_2(\phi, X) - \frac{\partial G_2(\phi, X)}{\partial X} X, \quad (4.41)$$

the solution of which is:

$$G_2(\phi, X) = -\frac{\Lambda}{8\pi G} + f(\phi) X^2. \quad (4.42)$$

However, by Eq. (4.35), the following condition is obtained:

$$2X f(\phi) \dot{\phi} \phi' = 0 . \quad (4.43)$$

It is straightforward to show that by combining Eq. (4.43) with xx - and tt - equations, $\phi' = \dot{\phi} = 0$, such that $\phi = cte$. Hence, the solution of the background leads to the following constraint on the action:

$$G_2(\phi_0, 0) = -\frac{\Lambda}{8\pi G} . \quad (4.44)$$

This solution mimics the one from General Relativity with a cosmological constant, but in this case induced by a constant scalar field ϕ . There is a special case when the coefficients for this system of equations become null and the background equation is satisfied also for non-constant and non-static scalar field solutions, which will be studied in Section 4.3.1. Note that despite the fact that Birkhoff's theorem is satisfied in Brans–Dicke-like theories [275, 276, 277], where a static metric implies a static scalar field, this may not be the case for other scalar-tensor theories such as Galileons or general Horndeski scenarios [283, 284].

4.2.2 Case \mathcal{L}_3

For the case \mathcal{L}_3 , the general gravitational action is given by

$$S_G = \int dx^4 \sqrt{-g} \left[\frac{R}{16\pi G} - G_3(\phi, X) \square \phi \right] . \quad (4.45)$$

By varying the action (4.45) with respect to the metric $g_{\mu\nu}$, the corresponding field equations are obtained:

$$\begin{aligned} R_{\mu\nu} - \frac{1}{2} g_{\mu\nu} R = & 8\pi G [G_{3\phi} (g_{\mu\nu} \nabla_\alpha \phi \nabla^\alpha \phi - 2 \nabla_\mu \phi \nabla_\nu \phi) \\ & + G_{3X} (-\nabla_\mu \phi \nabla_\nu \phi \square \phi - g_{\mu\nu} \nabla_\alpha \phi \nabla_\beta \phi \nabla^\alpha \phi \nabla^\beta \phi + 2 \nabla^\alpha \phi \nabla_{(\mu} \phi \nabla_{\nu)} \nabla^\alpha \phi)] . \end{aligned} \quad (4.46)$$

Here the subscript $()$ refers to a commutator among the indexes, while ϕ and X are derivatives with respect to the scalar field ϕ and its kinetic term X respectively. The equation for the scalar field is obtained by varying the action (4.45) with respect to the scalar field:

$$\begin{aligned} 2G_{3\phi} \square \phi + G_{3\phi\phi} (\nabla \phi)^2 + G_{3X\phi} [(\nabla \phi)^2 \square \phi + 2 \nabla_\mu \phi \nabla^\mu X] \\ + G_{3X} [(\square \phi)^2 - \nabla_\mu \nabla_\nu \phi \nabla^\mu \nabla^\nu \phi - R_{\mu\nu} \nabla^\mu \nabla^\nu \phi] + G_{3XX} [\nabla_\mu \phi \nabla^\mu X + (\nabla X)^2] = 0 , \end{aligned} \quad (4.47)$$

where recall that X is the kinetic term of the scalar field. As in the previous Lagrangian, a non-constant static scalar field, $\phi = \phi(x)$ is assumed. In order to show that the Nariai metric, expressed in the coordinates (4.25) as in Eq. (4.26), may be a solution for the gravitational action (4.45), we use the tt - and xx - equations, which can be easily obtained from the field Equations (4.47) and yields:

$$(tt) \quad \frac{1}{\cosh^2 x} = 8\pi G\phi'^2 [-G_{3\phi} + G_{3X}\Lambda^2 (\sinh x \cosh x\phi' + \cosh^2 x\phi'')] , \quad (4.48)$$

$$(xx) \quad -\frac{1}{\cosh^2 x} = 8\pi G\phi'^2 [-G_{3\phi} + G_{3X}\Lambda^2 \cosh x \sinh x\phi'] . \quad (4.49)$$

The $\theta\theta$ - and $\varphi\varphi$ - equations are just redundant, since the tt - equation is reproduced up to proportionality terms. In general, for an arbitrary $G_3(\phi, X)$, the system of Equation (4.49) has no solution $\phi(x)$, and consequently Nariai spacetime is not a solution for the gravitational Lagrangian (4.45). Nevertheless, Eq. (4.49) can be used for reconstructing the appropriate \mathcal{L}_3 Lagrangian that reproduces the Nariai spacetime (4.26) when assuming either a particular solution $\phi(x)$ or a particular form of $G_3(\phi, X)$. As the corresponding partial derivatives $G_{3\phi}$ and G_{3X} are in the end functions of the coordinate x , we can express both of them in terms of the scalar field and its derivatives through Eq. (4.49), which leads to:

$$G_{3\phi}(x) = \frac{1}{8\pi G} \frac{2 \tanh x \phi' + \phi''}{\phi'^2 \phi'' \cosh^2 x} , \quad (4.50)$$

$$G_{3X}(x) = \frac{1}{4\pi G\Lambda} \frac{1}{\phi'^2 \phi'' \cosh^4 x} . \quad (4.51)$$

Hence, the corresponding Lagrangian (4.45) can be reconstructed as long as the expressions (4.50) and (4.51) are well defined for $\phi(x)$, such that the integrability condition holds $G_{3\phi X} = G_{3X\phi}$. Nevertheless, it is not straightforward to obtain an analytical and exact expression for the \mathcal{L}_3 Lagrangian, but we can consider a couple of ways that lead to an analytical reconstruction of the action.

- Firstly, one may specify the form of the function $G_3(\phi, X)$, and reconstruct the corresponding action by using the system of Equation (4.49) and the integrability condition on $G_3(\phi, X)$. Let us consider the following $G_3(\phi, X)$:

$$G_3(\phi, X) = f_1(\phi) + f_2(X) . \quad (4.52)$$

The general kinetic term X is given by:

$$X = -\frac{1}{2}\Lambda \cosh^2 x \phi'^2. \quad (4.53)$$

Then, by the partial derivative with respect to X in Eq. (4.51), one obtains:

$$G_{3X} = f_{2X} = \frac{\Lambda}{4\pi G} \frac{1}{X^2} \frac{\phi'^2}{\phi''}. \quad (4.54)$$

This equation together with the assumption in Eq. (4.52) basically imposes that $\frac{\phi'^2}{\phi''} = g(X)$ must be expressed as a function of the kinetic term (4.53). As $g(X)$ is in principle arbitrary as far as providing a solution for the scalar field ϕ , we may assume $g(X) = X$ such that the scalar field becomes:

$$\phi(x) = -\frac{2 \log(\cosh x)}{\Lambda}. \quad (4.55)$$

After integrating Eq. (4.54), the function $f_2(X)$ turns out to be:

$$f_2(X) = -\frac{\Lambda}{4\pi G} \frac{1}{X^2}. \quad (4.56)$$

While the partial derivative with respect to ϕ on G_3 leads to:

$$G_{3\phi} = f_{1\phi} = \frac{\Lambda^2}{32\pi G} \frac{1 + 2 \log(\cosh x)}{\cosh^2 x} = \frac{1}{8\pi G} \frac{e^{\Lambda\phi}(1 - \Lambda\phi)}{\phi^2}, \quad (4.57)$$

which after integrating, provides the corresponding dependence on the scalar field ϕ :

$$f_1(\phi) = -\frac{1}{8\pi G} \frac{e^{\Lambda\phi}}{\phi}. \quad (4.58)$$

Then, the full gravitational action $G_3(\phi, X)$ as given in (4.52) is reconstructed.

- Nevertheless and in opposite, one may try to keep the form of $G_3(\phi, X)$ arbitrary and consider a particular solution for the scalar field in order to reconstruct the action. For illustrative purposes, we consider the following solution:

$$\phi(x) = \phi_0 e^{\mu x}. \quad (4.59)$$

Then, by following the Eq. (4.51), the following particular solutions are found in terms of the coordinate x :

$$G_{3\phi}(x) = \frac{1}{8\pi G} \frac{\operatorname{sech}^2 x (\mu + 2 \tanh x) e^{-2\mu x}}{\mu^3 \phi_0^2}, \quad (4.60)$$

$$G_{3X}(x) = \frac{1}{4\pi G} \frac{\operatorname{sech}^4 x e^{-3\mu x}}{\mu^4 \phi_0^3 \Lambda}. \quad (4.61)$$

The corresponding kinetic term $X = -\frac{1}{2}\partial_\mu\phi\partial^\mu\phi$ is given for this case by:

$$X = -\frac{1}{2}\phi_0^2\mu^2\Lambda\cosh^2 xe^{2\mu x}. \quad (4.62)$$

Hence, the partial derivative $G_{3X}(\phi, X)$ automatically leads to:

$$G_{3X}(\phi, X) = \frac{\Lambda}{16\pi G} \frac{\phi}{X^2}. \quad (4.63)$$

After integrating, it yields:

$$G_3(\phi, X) = -\frac{\Lambda}{16\pi G} \frac{\phi}{X} + f(\phi), \quad (4.64)$$

where $f(\phi)$ has to be computed by integrating the partial derivative $G_{3\phi}$, which is obtained by deriving expression (4.64) and equating to the expression in Eq. (4.61):

$$f_\phi = \frac{1}{4\pi G\phi_0^2\mu^3} \frac{\tanh x}{\cosh^2 xe^{2\mu x}} = \frac{1}{4\pi G\phi_0^2\mu^3} \frac{\tanh \left[\log \left(\frac{\phi}{\phi_0} \right)^{1/\mu} \right]}{\phi^2 \cosh^2 \left[\log \left(\frac{\phi}{\phi_0} \right)^{1/\mu} \right]}, \quad (4.65)$$

which after integrating, yields:

$$\begin{aligned} f(\phi) &= \frac{1}{8\pi G\mu^2(\mu-2)\phi} \left\{ F \left[1, 1-\mu/2, 2-\mu/2; -\left(\frac{\phi}{\phi_0} \right)^{2/\mu} \right] \right. \\ &\quad - (\mu-2)\mu F \left[1, -\mu/2, 1-\mu/2; -\left(\frac{\phi}{\phi_0} \right)^{2/\mu} \right] + \operatorname{sech}^2 \left[\log \left(\frac{\phi}{\phi_0} \right)^{1/\mu} \right] \\ &\quad \left. + \mu \tanh \left[\log \left(\frac{\phi}{\phi_0} \right)^{1/\mu} \right] \right\}. \end{aligned} \quad (4.66)$$

Here, $F(a, b, c; x)$ are hypergeometric functions, which can be computed analytically for some values of μ . For instance, $\mu = 1$ gives:

$$f(\phi) = -\frac{1}{4\pi G} \left[\frac{\phi^3 + 3\phi\phi_0^2}{(\phi^2 + \phi_0^2)^2} + \frac{\arctan \left(\frac{\phi}{\phi_0} \right)}{\phi_0} \right]. \quad (4.67)$$

Hence, the full reconstruction of the gravitational action (4.45) is explicitly shown for these two cases. The main conclusions can be obtained by analysing these two examples. As shown in the field equations, and by the expressions of $G_{3\phi}(x)$ and $G_{3X}(x)$, a constant scalar field

$\phi(x) = \phi_0$ is not a solution for Eq. (4.49), at least whenever Lagrangian (4.45) is considered as the sole action for gravity. In addition, the freedom of the function $G_3(\phi, X)$ implies that different Lagrangians can reproduce the Nariai metric, but leading to different solutions for the scalar field, as long as its partial derivatives (4.51) are well defined, as has been shown by these two examples.

4.2.3 Case \mathcal{L}_4

We now analyse the solutions when the Lagrangian \mathcal{L}_4 in (4.3) is considered as the sole Horndeski gravitational action:

$$S_G = \int dx^4 \sqrt{-g} \left[\frac{R}{16\pi G} + G_4(\phi, X)R + G_{4X} ((\square\phi)^2 - \nabla_\mu \nabla_\nu \phi \nabla^\mu \nabla^\nu \phi) \right]. \quad (4.68)$$

As usual, by varying the action (4.68) with respect to the metric $g_{\mu\nu}$, the corresponding field equations are obtained:

$$\begin{aligned} \left(\frac{1}{16\pi G} + G_4 \right) \left(R_{\mu\nu} - \frac{1}{2} g_{\mu\nu} R \right) - \nabla_\mu \nabla_\nu G_4 + g_{\mu\nu} \square G_4 - \frac{1}{2} g_{\mu\nu} G_{4X} ((\square\phi)^2 - \nabla_\mu \nabla_\nu \phi \nabla^\mu \nabla^\nu \phi) \\ + \dots \text{(second order terms)} = 0. \end{aligned} \quad (4.69)$$

We can proceed as in the previous case. However, the degree of freedom on the function $G_4(\phi, X)$ will lead to a set of infinite solutions for the scalar field, as shown above for \mathcal{L}_3 , which does not provide any new insights on Nariai spacetime in Horndeski gravity, but just some similar features as in the previous case. Concretely, for a given solution $\phi(x)$, one can in general reconstruct the appropriate action through $G_4(\phi, X)$, while the other way around is not always possible, that is, given an arbitrary $G_4(\phi, X)$ function, the field Eq. (4.69) does not have any solution for the scalar field in general, except for some special cases of the $G_4(\phi, X)$ function, as also shown for $G_3(\phi, X)$ above. In addition, note that for the general Horndeski Lagrangian, the speed of gravitational waves is given by [259]:

$$c_{GW} = \frac{G_4 - X(\ddot{\phi}G_{5X} + G_{5\phi})}{G_4 - 2XG_{4X} - X(H\dot{\phi}G_{5X} - G_{5\phi})}, \quad (4.70)$$

where H is the Hubble parameter. Hence, by assuming $G_4(\phi, X) = G_4(\phi)$ and $G_5 = 0$, analogously to [260], the speed of propagation for GW's is kept as the speed of light $c_{GW} = 1$,

satisfying the constraints obtained from the GW170817 detection [256, 257]. Hence, we explore here the case where $G_4(\phi, X) = G_4(\phi)$, such that the field eqs. (4.69) reads:

$$(tt) \quad \left(\frac{1}{16\pi G} + G_4 \right) \text{sech}^2 x - \phi'^2 G_{4\phi\phi} - (\tanh x \phi' + \phi'') G_{4\phi} = 0, \quad (4.71)$$

$$(xx) \quad - \left(\frac{1}{16\pi G} + G_4 \right) \text{sech}^2 x - \tanh x \phi' G_{4\phi} = 0, \quad (4.72)$$

$$(\theta\theta) \quad - \left(\frac{1}{16\pi G} + G_4 \right) \text{sech}^2 x - \phi'^2 G_{4\phi\phi} + \phi'' G_{4\phi} = 0. \quad (4.73)$$

By combining the xx - and $\theta\theta$ - equations, it yields:

$$\tanh x G_{4\phi} \phi' = 0 \rightarrow \phi = \text{constant}. \quad (4.74)$$

Hence, the only solution which does not modify the speed of gravitational waves leads to a constant scalar field, similarly to $G_2(\phi, X)$, unless $G_{4\phi} = 0$, which together with other conditions is analysed in Section 4.3.1. For this specific case, the only choice of G_4 that satisfies the equations of motion is:

$$G_4(\phi) = -\frac{1}{16\pi G}. \quad (4.75)$$

Nevertheless, for this choice, the gravitational effective coupling constant in Eq. (4.68) becomes null and consequently the theory is ill defined in general. Then, for the particular case (4.68) with $G_4 = G_4(\phi)$, Nariai spacetime and consequently Schwarzschild-(A)dS are not reproduced by such a Lagrangian. This is a natural consequence as Schwarzschild-(A)dS spacetime requires the presence of a cosmological constant, which cannot emerge from another term. However, such an issue can be easily sorted out by adding a scalar potential in the action,

$$S_G = \int dx^4 \sqrt{-g} \left[\frac{R}{16\pi G} + G_4(\phi) R - V(\phi) \right]. \quad (4.76)$$

The equations do not differ much from the ones above, only by a potential term,

$$(tt) \quad \left(\frac{1}{16\pi G} + G_4 \right) \text{sech}^2 x - \phi'^2 G_{4\phi\phi} - (\tanh x \phi' + \phi'') G_{4\phi} - \frac{\text{sech}^2 x}{2\Lambda} V(\phi) = 0, \quad (4.77)$$

$$(xx) \quad - \left(\frac{1}{16\pi G} + G_4 \right) \text{sech}^2 x - \tanh x \phi' G_{4\phi} + \frac{\text{sech}^2 x}{2\Lambda} V(\phi) = 0, \quad (4.78)$$

$$(\theta\theta) \quad - \left(\frac{1}{16\pi G} + G_4 \right) \text{sech}^2 x - \phi'^2 G_{4\phi\phi} + \phi'' G_{4\phi} + \frac{\text{sech}^2 x}{2\Lambda} V(\phi) = 0. \quad (4.79)$$

As in the previous case, by combining the xx - and $\theta\theta$ - equations, the constraint Eq. (4.74) is obtained, which leads to a constant scalar field $\phi(x) = \phi_0$, and by replacing it in Eq. (4.79), it leads to:

$$-G_4(\phi_0) + \frac{V(\phi_0)}{2\Lambda} = \frac{1}{16\pi G}. \quad (4.80)$$

Hence, Nariai spacetime is a solution for the gravitational action (4.76) as long as the algebraic Eq. (4.80) has at least a real solution.

Therefore, it is clear that Schwarzschild-(A)dS spacetime, and specifically Nariai spacetime is a solution for each of the Horndeski Lagrangians whereas some constraints are imposed on the Lagrangians \mathcal{L}_i . It is straightforward to show that the Nariai metric is also a solution of the full Horndeski Lagrangian as the degrees of freedom added by each \mathcal{L}_i provides a way of reconstructing the corresponding gravitational action. This will imply an infinite number of choices on the G_i functions and a degenerate solution for the scalar field, as has been shown for some of the Lagrangians above, and which will also affect the full gravitational action due to the freedom of choosing the corresponding Lagrangians. In Section 4.3, the stability of these extremal black holes for those cases for which the Nariai metric imposes real constraints on the Lagrangians will be analysed.

4.3 Anti-Evaporation Regime in Horndeski Gravity

In this section, we analyse the stability of Nariai spacetime when perturbations around the background solution are introduced. Firstly, we will focus on the cases with constant solutions of the scalar field. To do so, we focus on the first four terms of the Horndeski Lagrangian:

$$S_G = \int dx^4 \sqrt{-g} \left[\frac{R}{16\pi G} + G_2(\phi, X) - G_3(\phi, X) \square\phi + G_4(\phi) R \right]. \quad (4.81)$$

Note that action (4.81) is the most general Horndeski Lagrangian that keeps the speed of gravitational waves (4.70) as the speed of light. As shown in the previous section, for a given solution $\phi(x)$ and the Nariai metric (4.26), one can reconstruct the corresponding Horndeski Lagrangian that reproduces such solution. Nevertheless, here we are assuming for simplicity while analysing the perturbations, a constant scalar field for the background $\phi(x, t) = \phi_0$, such that following the results from the above section, Nariai spacetime is a solution for the gravitational

action (4.81) as long as the following constraint is satisfied:

$$\frac{G_{20}}{2\Lambda} + G_{40} = -\frac{1}{16\pi G}, \quad (4.82)$$

where the sub-index $_0$ denotes the background level. A useful way to define perturbations around the Nariai metric is:

$$ds^2 = e^{2\rho(x,t)} (-dt^2 + dx^2) + e^{-2\varphi(x,t)} d\Omega_2^2, \quad (4.83)$$

in which $\rho(x,t)$ and $\varphi(x,t)$ at the background level are: $\rho = -\ln \sqrt{\Lambda} \cosh x$ and $\varphi = \ln \sqrt{\Lambda}$. The perturbations on the metric and the scalar field (with spherical symmetry) can be expressed as follows:

$$\begin{aligned} \phi &\rightarrow \phi_0 + \delta\phi(t, x), \\ \rho &\rightarrow -\ln \left[\sqrt{\Lambda} \cosh x \right] + \delta\rho, \\ \varphi &\rightarrow \ln \sqrt{\Lambda} + \delta\varphi(t, x). \end{aligned} \quad (4.84)$$

Let us show how the perturbations are transformed under a gauge transformation in order to construct gauge invariants that allow us to isolate the physical perturbations from gauge artifices. We are going to consider an infinitesimal transformation of coordinates, given by

$$x'^{\mu} = x^{\mu} + \delta x^{\mu}. \quad (4.85)$$

On any generic quantity F , this implies a transformation on its perturbation:

$$\delta F' = \delta F + \mathcal{L}_{\delta x} F_0. \quad (4.86)$$

Here the prime denotes the quantity transformed in the new coordinates, F_0 is the background value and $\mathcal{L}_{\delta x}$ is the Lie derivate along the vector δx^{μ} . The corresponding perturbations on the metric are transformed as follows:

$$\begin{aligned} \delta\rho' &= \delta\rho + \mathcal{L}_{\delta x}\rho_0, \\ \delta\varphi' &= \delta\varphi + \mathcal{L}_{\delta x}\varphi_0 = \delta\varphi. \end{aligned} \quad (4.87)$$

In this case we are interested in the perturbation $\delta\varphi$, as the one that will define the perturbation on the radius of the horizon (see below). This is a gauge invariant quantity, such that we can work in an arbitrary gauge to solve the equations. Hence, introducing the perturbations (4.84) in the field equations, up to linear order, leads to:

$$\left(\frac{1}{16\pi G} + G_4 \right) \delta G_{\mu\nu} + G_{\mu\nu} G_{4\phi} \delta\phi - G_{4\phi} \nabla_{\mu} \nabla_{\nu} \delta\phi + g_{\mu\nu} G_{4\phi} \square \delta\phi - \frac{1}{2} (G_{2\phi} g_{\mu\nu} \delta\phi + G_2 \delta g_{\mu\nu}) = 0. \quad (4.88)$$

Note that the functions G_i and their derivatives are evaluated at $\phi = \phi_0$ and expanded up to first order in perturbations as follows:

$$\begin{aligned} G_2(\phi, X) &\rightarrow G_2(\phi_0, 0) + \left. \frac{\partial G_2(\phi, 0)}{\partial \phi} \right|_{\phi_0} \delta\phi, \\ G_4(\phi) &\rightarrow G_4(\phi_0) + \left. \frac{\partial G_4(\phi)}{\partial \phi} \right|_{\phi_0} \delta\phi. \end{aligned} \quad (4.89)$$

Then, we will introduce these perturbations into the field equations to study their evolution. The tt -, xx - and tx - perturbation equations are respectively:

$$\begin{aligned} -2G_{20}\text{sech}^2 x \delta\varphi + (G_{2\phi} + 2\Lambda G_{4\phi})\text{sech}^2 x \delta\phi - 2G_{20}(\tanh x \delta\varphi' + \delta\varphi'') \\ - 2G_{4\phi}\Lambda(\tanh x \delta\phi' + \delta\phi'') = 0, \end{aligned} \quad (4.90)$$

$$\begin{aligned} -2G_{20}\text{sech}^2 x \delta\varphi + (G_{2\phi} + 2\Lambda G_{4\phi})\text{sech}^2 x \delta\phi + 2G_{20}(\tanh x \delta\varphi' + \delta\ddot{\varphi}) \\ + 2G_{4\phi}\Lambda(\tanh x \delta\phi' + \delta\ddot{\phi}) = 0, \end{aligned} \quad (4.91)$$

$$G_{20}(\tanh x \delta\dot{\varphi} + \delta\dot{\varphi}') + G_{4\phi}\Lambda(\tanh x \delta\dot{\phi} + \delta\dot{\phi}') = 0, \quad (4.92)$$

from where the tx - equation can be rewritten as follows:

$$\frac{\partial}{\partial t} [G_{20}(\tanh x \delta\varphi + \delta\varphi') + G_{4\phi}\Lambda(\tanh x \delta\phi + \delta\phi')] = 0, \rightarrow g(x, t) \tanh x + g'(x, t) = h(x), \quad (4.93)$$

where $h(x)$ is an integration function to be determined, while $g(x, t) = G_{20}\delta\varphi + G_{4\phi}\Lambda\delta\phi$. Thus integrating Eq. (4.93) yields:

$$g(x, t) = G_{20}\delta\varphi + G_{4\phi}\Lambda\delta\phi = f(t) \text{sech} x + \text{sech} x \int \cosh x h(x) dx. \quad (4.94)$$

Then, by combining the tt - and xx - equations, the functions $f(t)$ and $h(x)$ are determined,

$$\begin{aligned} f(t) &= C_1 e^t + C_2 e^{-t}, \quad h(x) = C_3 \tanh x + C_4, \\ \rightarrow g(x, t) &= (C_1 e^t + C_2 e^{-t}) \text{sech} x + C_3 + C_4 \tanh x. \end{aligned} \quad (4.95)$$

Here, C_i 's are integration constants. Then, the expression for the metric perturbation $\delta\varphi$ can be easily obtained:

$$\delta\varphi = \frac{C_1 e^t + C_2 e^{-t}}{G_{20}} \text{sech} x + C_3 \frac{G_{2\phi} + 2\Lambda G_{4\phi}}{G_{20}(G_{2\phi} + 4\Lambda G_{4\phi})} + C_4 \tanh x. \quad (4.96)$$

At this point we are ready to calculate how the horizon changes when considering the above perturbations on the metric. The horizon is a null hypersurface that can be defined as follows:

$$g^{\mu\nu} \nabla_\mu \varphi \nabla_\nu \varphi = 0, \quad (4.97)$$

By introducing (4.84) and (4.96) in (4.97), the following relation is obtained:

$$C_1^2 e^{4t} + C_2^2 - (C_4^2 + 2C_1 C_2 \cosh 2x) e^{2t} + 2C_1 C_4 e^{3t} \sinh x + 2C_2 C_4 e^t \sinh x = 0, \quad (4.98)$$

which relates the x -coordinate and the t -coordinate at the horizon:

$$x = \log \left[\frac{C_4 + \sqrt{4C_1 C_2 + C_4^2}}{2C_1} e^{-t} \right]. \quad (4.99)$$

Hence, the perturbation (4.96) on the metric at the horizon leads to:

$$\delta\varphi_h = \frac{1}{G_{20}} \left[C_3 \frac{G_{2\phi} + 2\Lambda G_{4\phi}}{G_{2\phi} + 4\Lambda G_{4\phi}} + \sqrt{4C_1 C_2 + C_4^2} \right], \quad (4.100)$$

and consequently, the perturbation at the horizon remains constant. By the Nariai metric (4.83), one can identify the radius of the horizon when it is perturbed as:

$$r_h = \frac{e^{-\delta\varphi_h}}{\sqrt{\Lambda}} = \frac{e^{-\frac{1}{G_{20}} \left[C_3 \frac{G_{2\phi} + 2\Lambda G_{4\phi}}{G_{2\phi} + 4\Lambda G_{4\phi}} + \sqrt{4C_1 C_2 + C_4^2} \right]}}{\sqrt{\Lambda}}. \quad (4.101)$$

Note that this expression is time independent, such that no anti-evaporation effect arises when considering the restricted Horndeski Lagrangian (4.81) in Nariai spacetime. The only effect is a shift of the horizon, which may increase or decrease depending on the values of the integration constants (initial conditions) and on the functions G_i and their derivatives evaluated at ϕ_0 (Horndeski Lagrangian). In addition, if we set the integration constants to zero $C_i = 0$, the radius turns out to be $r_h = 1/\sqrt{\Lambda}$, i.e., the radius for the horizon in the Nariai spacetime. Moreover, by calculating the perturbation on the scalar field $\delta\phi$ through (4.94), it yields:

$$\delta\phi(x, t) = \frac{2C_3}{G_{2\phi} + 4\Lambda G_{4\phi}}. \quad (4.102)$$

Hence, the scalar field perturbation does not propagate but just introduces a perturbation on the effective cosmological constant, which explains the absence of the anti-evaporation regime and the shift of the horizon radius when considering perturbations on Nariai spacetime in the framework of Horndeski gravity.

4.3.1 Non constant solutions with null coefficients

Until now, we have worked with constant solutions to the equations for the \mathcal{L}_2 , \mathcal{L}_3 and \mathcal{L}_4 cases. Nevertheless, the full set of solutions is not completely covered by the previous analysis. Firstly,

by analysing the equations for the \mathcal{L}_2 Lagrangian given in Eq. (4.33), one could wonder about the special case in which the (in principle, non constant) coefficients of the equations become null. With the study of this case in mind, let us rewrite the Einstein tensor for an Einstein manifold, like the Nariai spacetime, as: $G_{\mu\nu} = -\Lambda g_{\mu\nu}$. This way, Eq. (4.33) acquires the form:

$$0 = \left[G_2(\phi, X) + \frac{\Lambda}{8\pi G} \right] g_{\mu\nu} + \frac{\partial G_2(\phi, X)}{\partial X} \partial_\mu \phi \partial_\nu \phi, \quad (4.103)$$

and the scalar field equation is:

$$0 = 2G_{2\phi X}(\phi, X)X - G_{2XX}(\phi, X)\nabla^\mu X \nabla_\mu \phi - G_{2X}(\phi, X)\square\phi - G_{2\phi}(\phi, X). \quad (4.104)$$

So, as long as the G_2 function satisfies the following conditions:

$$\begin{aligned} G_2(\phi_0, X_0) &= -\frac{\Lambda}{8\pi G} \equiv -A, \\ G_{2X}(\phi_0, X_0) &= G_{2\phi}(\phi_0, X_0) = G_{2\phi X}(\phi_0, X_0) = G_{2XX}(\phi_0, X_0) = 0, \end{aligned} \quad (4.105)$$

the field equations above hold. A possible reconstruction of G_2 is given by:

$$G_2(\phi, X) = \sum_{n \geq 3} c_n [g(\phi, X) - C]^n - A, \quad (4.106)$$

in which the function $g(\phi, X)$ must satisfy $g(\phi_0, X_0) = C$, which becomes the field equation for the scalar field. Some concrete examples of this can be found, but the main issue here is the possibility of solutions with $\phi_0 \neq \text{constant}$. In principle, this fact will affect the perturbations and change our conclusions since we had considered a background scalar field as a constant in order to solve the system of the perturbations above. For this case, the perturbation equations are:

$$\delta \left(8\pi G \left[g_{\mu\nu} G_2(\phi, X) + \frac{\partial G_2(\phi, X)}{\partial X} \partial_\mu \phi \partial_\nu \phi \right] \right) = \delta G_{\mu\nu}, \quad (4.107)$$

which under the constraints (4.105) at first order yield:

$$\delta G_{\mu\nu} = -\Lambda \delta g_{\mu\nu}. \quad (4.108)$$

As the perturbations on the Einstein tensor remain the same, the following system of equations for $\delta\varphi(x, t)$ is obtained:

$$\begin{aligned} (tt) \quad & \delta\varphi'' + \tanh x \delta\varphi' + \text{sech}^2 x \delta\varphi = 0, \\ (xx) \quad & \delta\ddot{\varphi} + \tanh x \delta\varphi' - \text{sech}^2 x \delta\varphi = 0, \\ (tx) \quad & \delta\dot{\varphi}' + \tanh x \delta\dot{\varphi} = 0. \end{aligned} \quad (4.109)$$

The general solution of this system of equations is:

$$\delta\varphi(x, t) = (C_1 e^t + C_1 2e^{-t}) \operatorname{sech} x + \frac{1}{2} C_3 \tanh x, \quad (4.110)$$

where C_i are integration constants.

A similar analysis can be applied for the Lagrangians \mathcal{L}_3 and \mathcal{L}_4 . For the former, the background equation can be expressed as:

$$\begin{aligned} -\frac{1}{2}\Lambda g_{\mu\nu} = & 8\pi G [G_{3\phi} (g_{\mu\nu} \nabla_\alpha \phi \nabla^\alpha \phi - 2\nabla_\mu \phi \nabla_\nu \phi) \\ & + G_{3X} (-\nabla_\mu \phi \nabla_\nu \phi \square \phi - g_{\mu\nu} \nabla_\alpha \phi \nabla_\beta \phi \nabla^\alpha \phi \nabla^\beta \phi + 2\nabla^\alpha \phi \nabla_{(\mu} \phi \nabla_{\nu)} \nabla^\alpha \phi)] . \end{aligned} \quad (4.111)$$

Then, we may impose that each term of the right hand side of this equation is expressed as follows:

$$\begin{aligned} G_{3\phi} (g_{\mu\nu} \nabla_\alpha \phi \nabla^\alpha \phi - 2\nabla_\mu \phi \nabla_\nu \phi) &= k_1 g_{\mu\nu}, \\ G_{3X} (-\nabla_\mu \phi \nabla_\nu \phi \square \phi - g_{\mu\nu} \nabla_\alpha \phi \nabla_\beta \phi \nabla^\alpha \phi \nabla^\beta \phi + 2\nabla^\alpha \phi \nabla_{(\mu} \phi \nabla_{\nu)} \nabla^\alpha \phi) &= k_2 g_{\mu\nu}, \end{aligned} \quad (4.112)$$

where k_i are constants. Nevertheless, the first condition leads to:

$$\nabla_\mu \phi \nabla_\nu \phi \propto g_{\mu\nu} f(\mathbf{x}), \quad (4.113)$$

with $f(\mathbf{x})$ being a function of the coordinates to be determined. By inspecting the tt - and xx -equations one finds

$$\dot{\phi}^2 = -\frac{1}{2} \frac{1}{\Lambda \cosh x} f(\mathbf{x}), \quad \phi'^2 = \frac{1}{2} \frac{1}{\Lambda \cosh x} f(\mathbf{x}). \quad (4.114)$$

This does not guarantee a real solution for $\phi(x, t)$. Hence, one can not find general conditions on the function G_3 and the system of equations has to be analysed step by step, as was done in Section 4.2.2.

The case for \mathcal{L}_4 is initially similar to \mathcal{L}_2 . The background Eq. (4.69) holds by imposing:

$$G_4(\phi_0, X_0) = -\frac{1}{16\pi G}, \quad (4.115)$$

$$G_{4X}(\phi_0, X_0) = G_{4\phi}(\phi_0, X_0) = G_{4\phi X}(\phi_0, X_0) = G_{4XX}(\phi_0, X_0) = 0, \quad (4.116)$$

$$G_{4XXX}(\phi_0, X_0) = G_{4XX\phi}(\phi_0, X_0) = G_{4X\phi\phi}(\phi_0, X_0) = G_{4\phi\phi\phi}(\phi_0, X_0) = 0. \quad (4.117)$$

As above, this can be satisfied by:

$$G_4(\phi, X) = \sum_{n \geq 4} c_n [g(\phi, X) - C]^n - \frac{1}{16\pi G}, \quad (4.118)$$

where $g(\phi_0, X_0) = C$. Nevertheless, all the coefficients of the perturbation equation (4.88) become also null for any background solution ϕ_0 , such that one has a degenerated equation that does not pose a well defined problem.

For the case for \mathcal{L}_2 with non-constant solutions using (4.110), the perturbation on the horizon radius (4.101) is easily obtained as:

$$r_H = \frac{e^{-\frac{1}{2}\sqrt{C_3^2+16C_1C_2}}}{\sqrt{\Lambda}}, \quad (4.119)$$

which, as in the previous case, leads to a constant such that no instability occurs.

Therefore, in both cases, the scalar field perturbation does not propagate but just introduces a perturbation on the effective cosmological constant, which explains the absence of the anti-evaporation regime and the shift of the horizon radius when considering perturbations on Nariai spacetime in the framework of Horndeski gravity.

4.4 Conclusions

Along this chapter we have analysed several aspects of Schwarzschild-de Sitter black holes, and particularly its extremal case when both horizons, the cosmological and the black hole ones, coincide at the same hypersurface of the spacetime, the so-called Nariai metric. In addition, we have focused on the framework of Horndeski gravity as a modified gravity model, showing that the existence of such type of solutions when Horndeski Lagrangians are considered can be easily achieved by the induction of an effective cosmological constant, which naturally arises when considering a constant scalar field for some of the Horndeski terms. Take into account that this case is different from GR with a cosmological constant since the constant Horndeski terms can be perturbed unlike perturbations in the cosmological constant that do not exist. However, we have also found that, not only a constant scalar field implies a Nariai spacetime as a solution of the gravitational field equations, but also a non-constant scalar field can reproduce Schwarzschild-de Sitter extremal black holes when considering the appropriate functions on the gravitational Lagrangian. However, this result may not satisfy the generalised Birkhoff's theorem as for Brans–Dicke-like theories [275, 276, 277], since, despite the fact that Nariai spacetime is a static metric, the scalar field may become non-static, as explained in Section 4.3.1.

By considering perturbations on the background scalar field, which is assumed constant, the induced perturbations on the metric turn out to be time dependent, which modifies the static regime of the metric, inducing an exponential expansion, a natural solution when considering an effective cosmological constant. Nevertheless, the linear regime just induces a slight modification on the horizon radius, keeping it constant. Contrary to other frameworks where perturbations on the Nariai spacetime have been considered [228, 229, 230, 231], which reproduce the so-called anti-evaporation regime, where the radius of the horizon may grow with time, this effect seems to be absent for the type of Horndeski Lagrangian analysed here. One obviously expects to find a non-constant scalar field perturbation by going beyond the linear regime, which will consequently induce the anti-evaporation regime. In addition, a non-constant scalar field (and no-null coefficients) for the background is also expected to produce such phenomena (turning on $G_3(\phi, X)$ in to (4.81) as an example without modifying the speed of gravitational waves), as perturbations on its propagation will naturally induce effects on the horizon radius, making the Nariai metric unstable.

Chapter 5

Wormholes in modified gravity

In the previous chapter we have spoken about black holes. However, there are other interesting spacetimes (spherically symmetrical too) that exhibit other types of exotic objects like wormholes to test modified gravity and the new phenomenology associated with new theories. The consideration of extended gravity theories has the power to introduce changes into some of these extremal gravitational phenomena that have been devised in the original framework of GR.

In the present chapter we shall investigate the implications on the existence of traversable wormholes from the consideration of an extended gravity prescription. In addition, a detailed study of the Energy Conditions for the matter content that holds this special framework will be performed. Summarizing, with this chapter we intend to understand new behaviours of the matter in modified gravity for another kind of extremal objects: wormholes.

Wormholes can be considered as tunnels from one point of spacetime to another one. If these tunnels are able to be crossed by an observer, we will name them traversable wormholes. Historically, the study of wormholes adopts the inverse starting point of GR since the spacetime is firstly built to end up finding the stress-energy tensor components which holds them. Some important properties that a traversable wormhole should have are [298]:

- By definition, a wormhole must have a throat which connects two (asymptotically flat) regions of the spacetime.
- A horizon is not permitted, since in that case the two-way travel is not possible.
- The tidal gravitational forces should be minimal to avoid the *spaghettification* effect,

which would kill any crossing observer.

- It should be possible to cross the wormhole in a finite and reasonably small time (both for the traveler, and for who await them).
- The solution must be perturbatively stable.
- The wormhole should be possible to assemble in this Universe, i.e. it must need much less energy or time than the total mass or age of the Universe.
- The stress-energy tensor that supports the wormholes should be reasonable. For example, along this section, we shall consider an anisotropic distribution of matter threading the wormhole described by the following stress-energy tensor $T_{\mu\nu}$

$$T_{\mu\nu} = (\rho + p_t)U_\mu U_\nu + p_t g_{\mu\nu} + (p_r - p_t)\chi_\mu\chi_\nu, \quad (5.1)$$

where U^μ is the four-velocity, χ^μ is the unit spacelike vector in the radial direction, i.e., $\chi^\mu = \delta^\mu_u / \sqrt{g_{uu}}$, $\rho(u)$ is the energy density, $p_r(u)$ is the radial pressure measured in the direction of χ^μ , and $p_t(u)$ is the transverse pressure measured in the orthogonal direction to χ^μ . Following the Hawking-Ellis classification (Section 1.3.2), this is a type I stress-energy tensor whose NEC inequality (recall Section 1.3.3) is:

$$\rho + p_i \geq 0 \quad \text{with } i = r, t \quad (5.2)$$

We will focus on this condition because, as we already saw, if NEC is violated, then all other conditions will be violated as well.

In order to simplify the calculations and have a tractable spacetime along this chapter, we are going to consider both spherically symmetric and static metric given by:

$$ds^2 = -f(u)dt^2 + g(u)du^2 + R^2(u)d\Omega^2, \quad (5.3)$$

where $d\Omega^2 = d\theta^2 + \sin^2\theta d\phi^2$ is the linear element of the unit sphere, and the metric functions $f(u)$, $g(u)$ and $R(u)$ are functions of the radial coordinate u . The coordinate choices used in metric (5.3) are often called ‘‘Buchdahl coordinates’’ [299, 300, 301]. Note that one possesses a freedom in choosing the radial coordinate, consequently allowing one to fix the form of one of the metric functions $f(u)$, $g(u)$ or $R(u)$, which will be considered below. Here the radial

coordinate lies in the range $u \in (-\infty, +\infty)$, so that two asymptotically flat regions exist, i.e., $u \rightarrow \pm\infty$, and are connected by the throat. The function $R(u)$ possesses a global positive minimum at the wormhole throat $u = u_0$, which one can set at $u_0 = 0$, without a loss of generality. Thus, the wormhole throat is defined as $R_0 = \min\{R(u)\} = R(0)$.

With the purpose of avoiding event horizons and singularities throughout the spacetime, one also imposes that the metric functions $f(u)$ and $g(u)$ are positive and regular everywhere. Taking into account these restrictions, namely, the necessary conditions for the minimum of the function, imposes the flaring-out conditions [298, 302], which are given by:

$$R'_0 = 0, \quad R''_0 > 0. \quad (5.4)$$

However, the flaring-out condition in General Relativity entails the violation of the null energy condition (NEC) [303]. Recall that the latter is defined as $T_{\mu\nu}k^\mu k^\nu \geq 0$, for *any* null vector k^μ [304, 305], and matter violating the NEC has been denoted as *exotic matter*. Nevertheless, it has been shown that these violations may be minimized using several procedures, such as the cut-and-paste techniques in the thin-shell formalism, where the exotic matter is concentrated at the junction interface [306, 307, 308, 309, 310, 311, 312, 313, 314, 315]. In fact, the problem is improved with evolving traversable wormholes, where it has been demonstrated that these time-dependent geometries may satisfy the energy conditions in arbitrary finite intervals of time [316, 317], and recently specific dynamical four-dimensional solutions were presented that satisfy the null and weak energy conditions everywhere and everywhen [318, 319] in the framework of modified gravity.

In fact, modified theories of gravity are an interesting avenue of research to explore traversable wormholes, where these compact objects possess a richer geometrical structure than their general relativistic counterparts. In this context, it has been shown that the NEC can be satisfied for normal matter threading the wormhole throat, where it is the higher order curvature terms that sustain the wormhole [320, 321, 322, 323, 324, 325, 326, 327, 328]. For this reason, in this chapter we are going to study this framework for an example of modified gravity, the so-called action-dependent Lagrangian theories, which are presented throughout the next section.

5.1 Action-dependent Lagrangian theories

These sort of theories have recently been proposed arising from a non-conservative gravitational theory, and tentatively denoted as action-dependent Lagrangian theories [329]. They emerge from the question: what would happen if the Lagrangian (from which the action is built up) were a function of the action? Herglotz tried to solve this question by generalizing the Action Principle [330, 331]. The Action Principle starts from the action \mathcal{S} which is defined as the integral of the Lagrangian $\mathcal{L}(t, \mathbf{x}(t), \dot{\mathbf{x}}(t))$ as follows:

$$\mathcal{S} = \int_{t_a}^{t_b} dt \mathcal{L}(t, \mathbf{x}(t), \dot{\mathbf{x}}(t)), \quad \text{with} \quad \mathbf{x} : \mathbb{R} \rightarrow \mathbb{R}^N, \quad (5.5)$$

where $\mathbf{x} = (x_1, x_2, \dots, x_N)$ represents the N generalized coordinates as functions of time. Then, the Action Principle postulates that *the path taken by the system between times t_a and t_b and configurations $\mathbf{x}(t_a)$ and $\mathbf{x}(t_b)$ is the one for which the action is stationary (no change) to first order, i.e.*

$$\delta \mathcal{S} = 0, \quad (5.6)$$

which can be compared with the GR action in an analogous way. Note that stationary action is not always a minimum, but only for sufficiently short, finite segments in the path. Applying variations in the one-dimensional case:

$$\delta \mathcal{S} = \int_{t_a}^{t_b} dt \left[\frac{\partial \mathcal{L}}{\partial x} \delta x + \frac{\partial \mathcal{L}}{\partial \dot{x}} \delta \dot{x} \right] = \int_{t_a}^{t_b} dt \left[\frac{\partial \mathcal{L}}{\partial x} - \frac{d}{dt} \frac{\partial \mathcal{L}}{\partial \dot{x}} \right] \delta x + \frac{\partial \mathcal{L}}{\partial \dot{x}} \delta x \Big|_{t_a}^{t_b} \quad (5.7)$$

one obtains the classic Euler-Lagrange equation:

$$\frac{\partial \mathcal{L}}{\partial x} - \frac{d}{dt} \frac{\partial \mathcal{L}}{\partial \dot{x}} = 0. \quad (5.8)$$

However, the proposed problem here is different and reads:

$$\dot{\mathcal{S}}(t) = \mathcal{L}(t, x(t), \dot{x}(t), \mathcal{S}(t)), \quad t \in [a, b], \quad (5.9)$$

$$\mathcal{S}(t_a) = s_a, \quad x(t_a) = x_a, \quad x(t_b) = x_b, \quad S_a, x_a, x_b \in \mathbb{R}. \quad (5.10)$$

For this case the application of variations returns us:

$$\delta \dot{\mathcal{S}}(t, x(t), \dot{x}(t), \mathcal{S}(t)) = \frac{\partial \mathcal{L}}{\partial x} \delta x + \frac{\partial \mathcal{L}}{\partial \dot{x}} \delta \dot{x} + \frac{\partial \mathcal{L}}{\partial \mathcal{S}} \delta \mathcal{S}, \quad (5.11)$$

where we have suppressed the dependence on t of δx , $\delta \dot{x}$ and δS to simplify notation, and whose solution is [332]:

$$\lambda(t_b)\delta\mathcal{S}(t_b) - \delta\mathcal{S}(t_a) = \int_{t_a}^{t_b} dt \lambda(t) \left[\frac{\partial\mathcal{L}}{\partial x} \delta x + \frac{\partial\mathcal{L}}{\partial \dot{x}} \delta \dot{x} \right], \quad (5.12)$$

where:

$$\lambda(t) = \exp \left[- \int_{t_a}^t d\tau \frac{\partial\mathcal{L}(\tau)}{\partial S} \right]. \quad (5.13)$$

Taking into account that $\delta\mathcal{S}(t_a) = \delta\mathcal{S}(t_b) = 0$ and integrating by parts the second term of Eq. (5.12), one obtains:

$$\int_{t_a}^{t_b} dt \left[\lambda(t) \frac{\partial\mathcal{L}}{\partial x} - \frac{d}{dt} \left(\lambda(t) \frac{\partial\mathcal{L}}{\partial \dot{x}} \right) \right] \delta x + \lambda(t) \frac{\partial\mathcal{L}}{\partial \dot{x}} \delta x \Big|_{t_a}^{t_b} = 0. \quad (5.14)$$

Since δx is an arbitrary function and $\delta x(t_a) = \delta x(t_b) = 0$, one can eliminate the last term. In addition, because the function $\lambda(t)$ is differentiable and different from zero, the generalized Euler-Lagrange equation for this case is:

$$\frac{\partial\mathcal{L}}{\partial x} - \frac{d}{dt} \frac{\partial\mathcal{L}}{\partial \dot{x}} + \frac{\partial\mathcal{L}}{\partial S} \frac{\partial\mathcal{L}}{\partial \dot{x}} = 0, \quad (5.15)$$

which encompasses the classical case for a non action-dependent Lagrangian, by vanishing the last term. In addition, this new term usually introduces the dissipative phenomenology. Once we have presented the point of view of classical mechanics, we are going to focus on the gravitational framework, where the Lagrangian will depend on several independent variables x^1, x^2, \dots, x^d and we will consider a curved spacetime with an associated metric $g_{\alpha\beta}$ defined on a domain $\Omega \subset \mathbb{R}^d$ and a boundary $\delta\Omega$. Then, the classical and usual gravitational action is:

$$S = \int_{\Omega} d^d x \sqrt{-g} \mathcal{L}(x^\mu, g_{\alpha\beta}, \partial_\mu g_{\alpha\beta}), \quad (5.16)$$

which we want to generalize toward the Herglotz problem. For this purpose, firstly one can suppose that there is a differentiable vector field s^μ , and that $\delta\Omega$ is an orientable Jordan surface with normal n^μ such that:

$$S(\delta\Omega) = \int d^d x \sqrt{-g} \mathcal{L}(x^\mu, g_{\alpha\beta}, \partial_\mu g_{\alpha\beta}) = \int_{\Omega} d^d x \sqrt{-g} \nabla_\nu s^\nu = \int_{\delta\Omega} d^{d-1} x \sqrt{|h|} n_\nu s^\nu, \quad (5.17)$$

where h is the determinant of the induced metric over $\delta\Omega$ by Stokes' theorem, and $\nabla_\nu s^\nu = \mathcal{L}(x^\mu, g_{\alpha\beta}, \partial_\mu g_{\alpha\beta})$. Now, in view of these previous ideas, and following the previous steps for

classical mechanics, we will generalize it as follows:

$$\begin{aligned}\nabla_\nu s^\nu &= \mathcal{L}(x^\mu, g_{\alpha\beta}, \partial_\mu g_{\alpha\beta}, s^\mu) \quad , \quad x^\mu \in \Omega \quad , \\ S &= \int_{\delta\Omega} d^{d-1}x \sqrt{|h|} n_\nu s^\nu \quad ,\end{aligned}\tag{5.18}$$

which generalizes the Action Principle. As in Eq. (5.15), there will be a dissipative effect. The novel feature when comparing with previous implementations of dissipative effects in gravity is the possible arising of such phenomena from a least action principle, so that they are of a purely geometric nature. Applications to this model have also been explored, namely, in cosmology [333], braneworld gravity [334], cosmic string configurations [335], the late-time cosmic accelerated expansion and large scale structure [336], and static spherically symmetric stellar solutions [337], amongst others.

As an example, we will study the complete set of field equations considered in the action-dependent Lagrangian theory proposed by Matheus J. Lazo in [329] which is based on the following total Lagrangian

$$\mathcal{L} = \mathcal{L}_g + \mathcal{L}_m = (R - \lambda_\mu s^\mu) + \mathcal{L}_m \quad ,\tag{5.19}$$

where the Einstein-Hilbert Lagrangian is extended with the geometrical sector dealing with the additional dissipative term $\lambda_\mu s^\mu$, while \mathcal{L}_m is the Lagrangian of the matter fields. As we already said, the field s^μ is an action-density field, which disappears after the variation of the action such that the modification to the GR counterpart is given by the four-vector λ^μ only. Note that λ^μ may be considered as a background four-vector that plays the role of a coupling parameter associated with the dependence of the gravitational Lagrangian upon the action. In the majority of the works considered above, it is assumed to be constant, however, in a more general scenario, one may assume it to be a coordinate-dependent four-vector.

In order to deduce the equations of motion for this specific case following [329], we will introduce the relation: $R = -(\tilde{L} - L)$ where $\tilde{L} = g^{\mu\nu}(\Gamma_{\mu\sigma,\nu}^\sigma - \Gamma_{\mu\nu,\sigma}^\sigma)$ and $L = g^{\mu\nu}(\Gamma_{\mu\nu}^\sigma \Gamma_{\sigma\rho}^\rho - \Gamma_{\mu\sigma}^\rho \Gamma_{\nu\rho}^\sigma)$, where $\Gamma_{\mu\nu}^\sigma$ are the Christoffel symbols following the definitions given in Eq. (1.5) and Eq. (1.6). In addition, we can write the relation:

$$\int_\Omega d^d x \sqrt{-g} \tilde{L} = 2 \int_\Omega d^d x \sqrt{-g} L + \text{surface term} \quad ,\tag{5.20}$$

so that one is able to write the effective Lagrangian equivalent to (5.19), from a point of view of the action, as follows:

$$\mathcal{L}_{eff} = -L - \lambda_\mu s^\mu + \mathcal{L}_m . \quad (5.21)$$

However, although both $-\int_\Omega d^d x \sqrt{-g} L$ and $\int_\Omega d^d x \sqrt{-g} R$ are equivalent action functions in the Hamilton variational principle sense, they are not equivalent for the Herglotz variational problem, since their Lagrangian functionals differ by a total derivative term, and we will have two different theories [338]: on the one hand the one given by Eq. (5.19), and on the other hand the one written in Eq. (5.21). Along this chapter we will study the second one as historically it was the first to appear.

Then, applying metric variations on the action associated with the Lagrangian of Eq. (5.21) one obtains:

$$\delta S = \int_\Omega d^d x \left[-\delta(\sqrt{-g} L) - \delta(\sqrt{-g} \lambda_\mu s^\mu) + \delta(\sqrt{-g} \mathcal{L}_m) \right] . \quad (5.22)$$

Using the identity $\partial_\sigma \sqrt{-g} = \sqrt{-g} \Gamma_{\sigma\alpha}^\alpha$, one gets $(\nabla_\nu s^\nu) \sqrt{-g} = \partial_\nu (s^\nu \sqrt{-g})$, and from Eq. (5.17) the variation on the action also can be written as:

$$\delta S = \delta \int_\Omega d^d x \sqrt{-g} \nabla_\nu s^\nu = \int_\Omega d^d x \partial_\nu \delta(\sqrt{-g} s^\nu) . \quad (5.23)$$

Consequently, writing together Eq. (5.22) and Eq. (5.23):

$$\int_\Omega d^d x \left[\partial_\nu \delta(\sqrt{-g} s^\nu) + \delta(\sqrt{-g} L) + \lambda_\mu \delta(\sqrt{-g} s^\mu) - \delta(\sqrt{-g} \mathcal{L}_m) \right] = 0 , \quad (5.24)$$

where we have taken into account that λ_μ is a four-vector that does not depend on the metric. This equation should be satisfied independently of the domain, which together with the redefinition $\theta^\nu = \delta(s^\nu \sqrt{-g})$ lets us obtain the analogous differential equation to Eq. (5.11):

$$\partial_\nu \theta^\nu = -\delta(\sqrt{-g} L) + \delta(\sqrt{-g} \mathcal{L}_m) - \lambda_\nu \theta^\nu , \quad (5.25)$$

whose solution is:

$$\theta^\nu(x^\mu, g_{\alpha\beta}, g_{\alpha\beta}, \mu, s^\mu) = A^\nu(x^\mu, g_{\alpha\beta}, g_{\alpha\beta}, \mu, s^\mu) e^{-\lambda_\gamma x^\gamma} , \quad (5.26)$$

where

$$\partial_\nu A^\nu = \left[-\delta(\sqrt{-g} L) + \delta(\sqrt{-g} \mathcal{L}_m) \right] e^{\lambda_\gamma x^\gamma} . \quad (5.27)$$

At this point, some considerations regarding the boundary need to be introduced. First of all, it is necessary to think about the boundary condition, which means that the metric is fixed at the extremes/boundary and therefore variations of it at the boundary vanish $\delta g_{\alpha\beta}(\delta\Omega) = 0$. On the other hand, recalling Eq. (5.17):

$$\delta S = 0 = \int d^{d-1}x \sqrt{|h|} n_\nu (\delta s^\nu), \quad (5.28)$$

since the surface $\delta\Omega$, and in consequence $\sqrt{|h|}$, are independent of variations of the metric. Therefore:

$$\delta(s^\nu)(\delta\Omega) = 0. \quad (5.29)$$

Following this with the boundary condition $\delta g_{\alpha\beta}(\delta\Omega) = 0$ and from the definition $\theta^\nu = \delta(s^\nu \sqrt{-g})$, one can say:

$$\theta^\nu|_{\delta\Omega} = A^\nu|_{\delta\Omega} e^{-\lambda_\gamma x^\gamma} = 0. \quad (5.30)$$

So, A^ν is identically zero over the boundary $\delta\Omega$ and using the Stokes' theorem:

$$0 = \int_\Omega d^d x \partial_\nu A^\nu = \int_{\delta\Omega} d^{d-1}x \frac{A^\nu}{\sqrt{-g}} |h| = 0. \quad (5.31)$$

Rewriting this last equation with Eq. (5.27), one obtains:

$$\int_\Omega d^d x [-\delta(\sqrt{-g}L) + \delta(\sqrt{-g}\mathcal{L}_m)] e^{\lambda_\gamma x^\gamma} = 0, \quad (5.32)$$

and expanding this as we would do in GR, considering $\delta\sqrt{-g}\mathcal{L}_m = -\kappa^2\sqrt{-g}T_{\mu\nu}\delta g^{\mu\nu}$:

$$\begin{aligned} & - \int_\Omega d^d x [\Gamma_{\mu\nu}^\alpha \delta(g^{\mu\nu} \sqrt{-g})_{,\alpha} - \Gamma_{\mu\alpha}^\alpha \delta(g^{\mu\nu} \sqrt{-g})_{,\nu} \\ & + (\Gamma_{\mu\alpha}^\beta \Gamma_{\nu\beta}^\alpha - \Gamma_{\alpha\beta}^\beta \Gamma_{\mu\nu}^\alpha) \delta(g^{\mu\nu} \sqrt{-g}) + \kappa^2 \sqrt{-g} T_{\mu\nu} \delta g^{\mu\nu}] e^{\lambda_\gamma x^\gamma} \\ & = \int_\Omega d^d x \sqrt{-g} \left[R_{\mu\nu} - \frac{1}{2} g_{\mu\nu} R + K_{\mu\nu} - \frac{1}{2} g_{\mu\nu} K - \kappa^2 T_{\mu\nu} \right] e^{\lambda_\gamma x^\gamma} \delta g^{\mu\nu} \\ & - \int_\Omega d^d x [(\Gamma_{\mu\nu}^\alpha \delta(g^{\mu\nu} \sqrt{-g}) - \Gamma_{\mu\nu}^\nu \delta(g^{\mu\alpha} \sqrt{-g})) e^{\lambda_\gamma x^\gamma}]_{,\alpha} = 0, \end{aligned} \quad (5.33)$$

where $K_{\mu\nu} = \lambda_\alpha \Gamma_{\mu\nu}^\alpha - \frac{1}{2}(\lambda_\nu \Gamma_{\mu\alpha}^\alpha + \lambda_\mu \Gamma_{\nu\alpha}^\alpha)$. Once more, the last term vanishes by the boundary condition and the equations of motion will be:

$$G_{\mu\nu} + Z_{\mu\nu} = \kappa^2 T_{\mu\nu}, \quad (5.34)$$

where $\kappa^2 = 8\pi$ along this chapter, since we will take $G = c = 1$ in order to simplify the results interpretation, $G_{\mu\nu}$ is the Einstein tensor, and we have grouped the new phenomenology in $Z_{\mu\nu}$ defined as:

$$Z_{\mu\nu} = K_{\mu\nu} - \frac{1}{2}g_{\mu\nu}K. \quad (5.35)$$

The quantity $K_{\mu\nu}$ (and its trace K) represents the geometric structure behind the dissipative nature of the theory. Note that the limit of a vanishing λ_μ restores the dissipationless feature of GR.

Thus, motivated by the existence of static spherically-symmetric compact objects analysed in [337], we extend this analysis to the context of wormhole physics, for which, firstly we are going to present the most general restrictions on static and spherically symmetric wormhole geometries imposed by the geometrical structure of the action-dependent Lagrangian theory, to end up considering a plethora of specific solutions of action-dependent Lagrangian induced wormhole geometries.

5.2 General restrictions on wormhole geometries

Now, rather than to write out the full gravitational field equations (5.34) for the metric (5.3), let us note that the only non-zero components of the Einstein and the stress-energy tensor are the diagonal terms. Then, the non-diagonal part of the additional tensor $Z_{\mu\nu}$, defined by Eq. (5.35), also provides additional information on the geometrical structure of the solutions of the theory, namely, that $Z_{\mu\nu} = 0$ for $\mu \neq \nu$. More specifically, the non-diagonal components of the symmetric tensor $Z_{\mu\nu}$ place restrictions on the form of the four-vector λ_μ .

The independent components of the tensor $Z_\nu^\mu = K_\nu^\mu - \frac{1}{2}\delta_\nu^\mu K$ are given by

$$Z_t^u = -\frac{\lambda_t[f g' R - g(f' R - 4f R')]}{4f g^2 R}, \quad Z_u^u = \frac{\lambda_\theta}{R^2} \cot \theta, \quad (5.36)$$

$$Z_\theta^u = -\frac{\lambda_\theta(f g)'}{4f g^2} - \frac{\lambda_u}{2g} \cot \theta, \quad Z_\phi^u = -\frac{\lambda_\phi(f g)'}{4f g^2}, \quad (5.37)$$

$$Z_\theta^\theta = Z_\phi^\phi = \frac{\lambda_u(R f' + 2f R')}{2f g R}, \quad (5.38)$$

$$Z_\phi^\theta = \frac{\lambda_\phi}{2R^2} \cot \theta, \quad Z_t^\theta = -\frac{\lambda_t}{2R^2} \cot \theta, \quad (5.39)$$

$$Z_t^t = \frac{2\lambda_u R'}{g R} + \frac{\lambda_\theta}{R^2} \cot \theta, \quad Z_\phi^t = 0. \quad (5.40)$$

From $Z_\phi^\theta = Z_t^\theta = 0$ one readily extracts the restrictions $\lambda_\phi = \lambda_t = 0$. Taking into account the assumption of the static and spherically symmetric character of the spacetime, the field equations should only depend on the radial coordinate, so that from the diagonal Z_u^u component, one readily verifies that $\lambda_\theta \propto (\cot \theta)^{-1}$, or more specifically $\lambda_\theta = \lambda(u)/(\cot \theta)$ (one may consider the simple case $\lambda(u) = \lambda_0 = \text{const}$). We emphasize that this result was also obtained in [337]. Note that if one were to consider $\lambda_\theta = 0$, then the condition $Z_\theta^u = 0$ would impose that $\lambda_u = 0$, taking us trivially back to GR. Analogously, in order for Z_t^t to only depend on the radial coordinate, from $Z_\theta^u = 0$ this imposes that $\lambda_u = 0$ and consequently places a further constraint on the metric functions, namely, $(fg)' = 0$.

Thus, the additional information on the geometrical structure of the theory, which imposes that the non-diagonal components of the symmetric tensor $Z_{\mu\nu}$ vanish, imposes the following condition on the four-vector λ_μ :

$$\lambda_\mu = \left(0, 0, \frac{\lambda(u)}{\cot \theta}, 0 \right), \quad (5.41)$$

and the additional geometric tensor Z_ν^μ takes the diagonal form $Z_\nu^\mu = (\lambda(u)/R^2) \text{diag}(1, 1, 0, 0)$. Furthermore, from the constraint on the metric functions $(fg)' = 0$, we can consider, without a loss of generality, the following choice:

$$f(u) = g^{-1}(u) = A(u). \quad (5.42)$$

5.3 Specific solutions of action-dependent Lagrangian induced wormhole geometries

The analysis outlined in the previous section imposes that the static and spherically symmetric configuration of metric Eq. (5.3) in the theory given by Eq. (5.21), can be written as

$$ds^2 = -A(u)dt^2 + A^{-1}(u)du^2 + R^2(u)d\Omega^2, \quad (5.43)$$

where, as before, the wormhole throat is defined as $R_0 = \min\{R(u)\} = R(0)$, and, in order to avoid event horizons and singularities throughout the spacetime, one imposes that the function $A(u)$ is positive and regular everywhere. These restrictions impose the flaring-out conditions, translated as Eq. (5.4).

As the metric function $A(u)$ is positive and regular for $\forall u$, it is useful to analyse its derivatives at the throat $u = 0$. In particular, the sign of A''_0 determines the type of extrema of $A(u)$, i.e., it is a minimum if $A''_0 > 0$ and a maximum if $A''_0 < 0$. The maximum (minimum) of $A(u)$ corresponds to a maximum (minimum) of the gravitational potential, so that in the vicinity of a maximum (minimum) the gravitational force is repulsive (attractive). Thus, the wormhole throat possesses a repulsive or an attractive nature that depends on the sign of A''_0 .

Now, taking into account the modified Einstein equation (5.34), the spacetime metric (5.43), and the stress-energy tensor (5.1), the gravitational field equations are finally given by:

$$8\pi\rho = -\frac{2ARR'' + AR'^2 + A'RR' - 1}{R^2} - \frac{\lambda(u)}{R^2}, \quad (5.44)$$

$$8\pi p_r = \frac{AR'^2 + A'RR' - 1}{R^2} + \frac{\lambda(u)}{R^2}, \quad (5.45)$$

$$8\pi p_t = \frac{A''R + 2AR'' + 2A'R'}{2R}. \quad (5.46)$$

Adding Eqs. (5.44) and (5.45), yields the following relation

$$R''|_{R_0} = -\frac{4\pi R}{A}(\rho + p_r)|_{R_0}, \quad (5.47)$$

and using the condition at the throat $R''_0 > 0$, one verifies that in these specific action-dependent Lagrangian theories the NEC is generically violated at the throat, i.e., $(\rho + p_r)|_{R_0} < 0$.

Taking into account the field equations (5.44)–(5.46), one has three independent equations with six unknown functions of the radial coordinate u , namely, $\rho(u)$, $p_r(u)$, $p_t(u)$, $A(u)$, $R(u)$ and $\lambda(u)$. There are several strategies that one may now follow. More specifically, one may consider specific choices for the components of the stress-energy tensor, and then solve the field equations to determine the metric functions and $\lambda(u)$; one may also take into account a plausible stress-energy tensor profile by imposing equations of state $p_r = p_r(\rho)$ and $p_t = p_t(\rho)$, and close the system by adequately choosing the energy density, or any of the metric functions. In alternative to this approach, one may use the reverse philosophy usually adopted in wormhole physics by simple choosing specific choices for the metric functions and $\lambda(u)$, and through the field equations determine the stress-energy profile responsible for sustaining the wormhole geometry. In the following, we will adopt several of the strategies outlined above, and a mixture thereof, to obtain specific exact solutions of wormhole spacetimes induced by these action-dependent Lagrangian theories.

5.3.1 Specific wormhole solutions: Ellis-Bronnikov solution

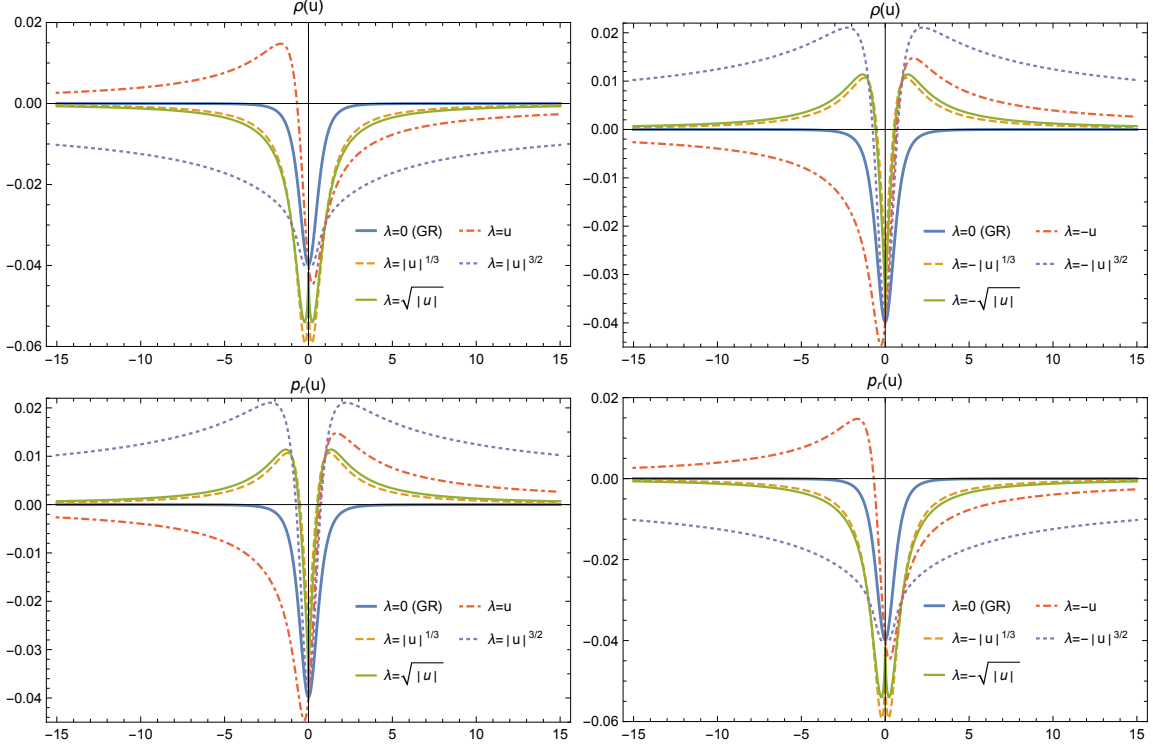


Figure 5.1: The plots depict the specific case of the Ellis-Bronnikov wormhole configuration with $a = 1$, for convenience, and for different choices of the function $\lambda(u)$. Depending on the sign of $\lambda(u)$, one obtains a plethora of specific symmetric or asymmetric solutions. Note that for $\lambda(u) \sim \pm u$, one obtains asymmetric solutions, where the energy density is negative at the throat and in the positive (negative) branch of u , but becomes positive in the negative (positive) branch; the radial pressure exhibits the inverse qualitative behavior.

Using an appropriate parametrization, we can present a solution by taking into account the reverse philosophy of solving the modified field equations. It means that firstly we build the spacetime and only after the kind of matter which sustains it is discovered, as follows [339]:

$$R(u) = e^{-\alpha(u)} \sqrt{u^2 + a^2}, \quad A(u) = e^{2\alpha(u)}, \quad (5.48)$$

with the factor $\alpha(u)$ defined as

$$\alpha(u) = \left(\frac{m}{a}\right) \arctan\left(\frac{u}{a}\right), \quad (5.49)$$

where m and a are two free parameters. Thus, the spacetime metric is given by

$$ds^2 = -e^{2\alpha} dt^2 + e^{-2\alpha} [du^2 + (u^2 + a^2)d\Omega^2]. \quad (5.50)$$

Following the previous definition of the wormhole throat, which is situated at $u_0 = 0$, we readily obtain $R'(0) = -m/a$, so that the condition $R'(0) = 0$ imposes $m = 0$. Note that

these conditions imply that the solution reduces to the well-known Ellis-Bronnikov wormhole spacetime [340, 341, 342]. It was proposed and constructed in 1973 by Ellis [343] and Bronnikov [344] independently. Both used a phantom scalar field source in GR which gives a static, spherically symmetric, geodesically complete, horizonless spacetime and with the peculiarity of a throat (called a “drainhole” by Ellis) connecting two asymptotically flat regions.¹ This does indeed simplify the analysis, such that $\alpha(u) = 0$, $A(u) = 1$, and

$$R''(u_0) = \frac{1}{|a|} > 0. \quad (5.52)$$

In addition to this, Eqs. (5.44)–(5.46) yield the following stress-energy profile:

$$\rho(u) = -\frac{(a^2 + u^2)\lambda(u) + a^2}{8\pi(a^2 + u^2)^2}, \quad (5.53)$$

$$p_r(u) = \frac{(a^2 + u^2)\lambda(u) - a^2}{8\pi(a^2 + u^2)^2}, \quad (5.54)$$

$$p_t(u) = \frac{a^2}{8\pi(a^2 + u^2)^2}. \quad (5.55)$$

For the specific case of $\lambda = 0$, where the four-vector λ^μ vanishes, this solution simply reduces to the general relativistic Ellis-Bronnikov stress-energy components. However, for the general case, one still needs to impose one more condition to close the system, and in the following we consider specific choices for the function $\lambda(u)$. Equations (5.53)–(5.54) yield the following relation:

$$\rho(u) + p_r(u) = -\frac{a^2}{4\pi(a^2 + u^2)^2}, \quad (5.56)$$

which states that the NEC is violated throughout the entire spacetime, and is independent of the function $\lambda(u)$. Therefore, one could take the specific case of $\lambda(u) = 0$ which corresponds to GR and Eq. (5.56) would still hold true. Consequently, this kind of modified gravity in the case of Ellis-Bronnikov wormhole does not improve the violation of NEC.

We are only interested in asymptotically flat solutions, so taking into account the limit of Eq. (5.53), one finds

$$\lim_{u \rightarrow \infty} \rho(u) \sim -\lim_{u \rightarrow \infty} \frac{\lambda(u)}{u^2}. \quad (5.57)$$

¹The usual form of the Ellis-Bronnikov wormhole is:

$$ds^2 = -dt^2 + \frac{dr^2}{1 - \frac{a^2}{r^2}} + r^2 d\Omega^2 \quad (5.51)$$

under the reparametrization: $r^2 = u^2 + a^2$.

For instance, assuming a power law solution for $\lambda(u) \sim u^\alpha$, the asymptotic flatness condition imposes that $\alpha < 2$, and from the regularity of the stress-energy components we have $\alpha \geq 0$, so that the parameter lies in the range $0 \leq \alpha < 2$. One may perform a similar analysis with the radial pressure $p_r(u)$, but with a change in the sign for the limit. Note that the tangential pressure, $p_t(u)$, is independent of $\lambda(u)$, possesses a maximum value at the throat, $p_t(u=0) = (8\pi a^2)^{-1}$, and tends to zero with increasing u .

Several choices for the function $\lambda(u)$ are depicted in Fig. 5.1. Depending on the sign of $\lambda(u)$, one obtains a plethora of specific symmetric or asymmetric solutions. More specifically, for the case of $\lambda(u) \sim \pm u$, one obtains asymmetric solutions where the energy density is negative at the throat and in the positive (negative) branch of u , but becomes positive in the negative (positive) branch, while the radial pressure possesses the inverse qualitative behavior, as is transparent from Fig. 5.1. Thus, it is possible to alleviate the negative energy densities needed to thread this wormhole configurations, relative to GR. The wormhole solutions obtained with $\lambda \neq 0$ possess a richer structure than their general relativistic counterparts.

5.3.2 Specific stress-energy profile

We now consider the strategy of specifying the profile of the energy density and radial pressure given by:

$$\rho(u) = \rho_0 \left(\frac{a^2}{a^2 + u^2} \right)^\alpha, \quad (5.58)$$

$$p_r(u) = p_0 \left(\frac{a^2}{a^2 + u^2} \right)^\alpha, \quad (5.59)$$

with $\alpha > 0$, so that both components tend to zero at spatial infinity. In addition to this, we close the system by considering the specific choice for the metric function

$$R(u) = \sqrt{a^2 + u^2}. \quad (5.60)$$

Note that Eqs. (5.58) and (5.59) can be written as $p_r = \omega\rho$, with $\omega = p_0/\rho_0$. Thus, this case is formally equivalent to choosing Eq. (5.60), one of Eqs. (5.58) or (5.59), and the equation of state $p_r(u) = \omega\rho(u)$.

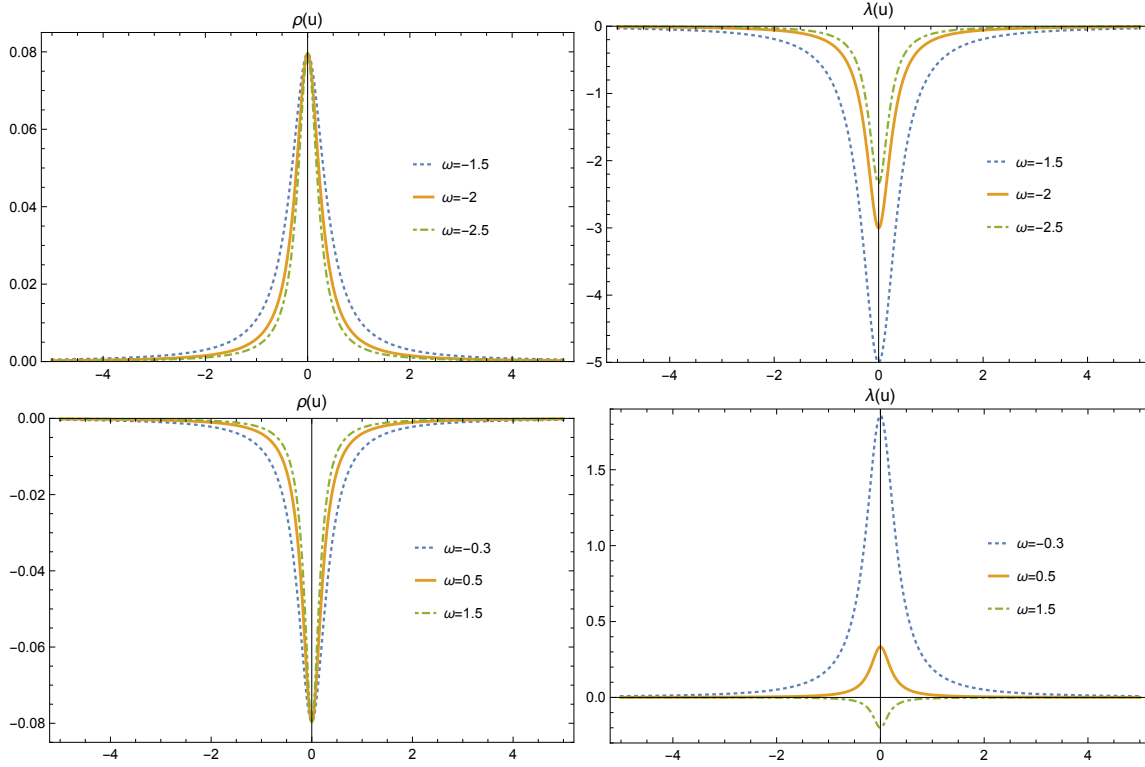


Figure 5.2: Results for the specific stress-energy profile given by (5.58) and (5.59) with $a^2 = -1/(4\pi\rho_0(1+\omega))$ and $\alpha = 2$. The upper plots are for the case $\rho_0 = 1$ ($\omega < -1$), and the lower plots for $\rho_0 = -1$ ($\omega > -1$).

The gravitational field equations (5.44)-(5.46) provide the following solutions:

$$A(u) = -4\pi a^2 \rho_0 (\omega + 1) \left(\frac{a^2}{a^2 + u^2} \right)^{\alpha-2}, \quad (5.61)$$

$$\lambda(u) = 1 + 4\pi\rho_0 [2a^2\omega - (2\alpha - 5)u^2(\omega + 1)] \left(\frac{a^2}{a^2 + u^2} \right)^{\alpha-1}. \quad (5.62)$$

As before, one should impose the asymptotic flatness condition, namely,

$$\lim_{u \rightarrow \pm\infty} A(u) \rightarrow 1, \quad (5.63)$$

and taking into account that $A(u)$ should be positive and regular $\forall u$, implies the following two stringent restrictions:

$$\alpha = 2, \quad \text{and} \quad 4\pi a^2 \rho_0 (1 + \omega) = -1, \quad (5.64)$$

where the second condition imposes:

$$\rho_0(1 + \omega) < 0. \quad (5.65)$$

This implies two specific cases depicted in Fig. 5.2: (i) $\rho_0 > 0$ and $\omega < -1$, so that, taking into account the equation of state $\omega = p_0/\rho_0$, implies a negative radial pressure at the throat; or (ii)

$\rho_0 < 0$ and $\omega > -1$, so that $p_0 > 0$ for $-1 < \omega < 0$, and $p_0 < 0$ for $\omega > 0$. Therefore, for the throat in both cases:

$$(\rho + p_r)|_{u=0} = (1 + \omega)\rho_0 < 0, \quad (5.66)$$

violating the NEC. Relative to the analysis at the throat, note that the wormhole conditions are satisfied, namely, $R'(u_0) = 0$ and $R''(0) = 1/|a| > 0$. In addition to this, for the imposition of the asymptotic flatness condition, namely, $\alpha = 2$, we readily obtain $A(u) = 1$, so that $A'(u_0) = A''(u_0) = 0$.

5.3.3 Black bounce solutions

Recently, a number of novel regular “black-bounce” spacetimes were explored [345, 346]. These are specific geometries where the “area radius” always remains non-zero, thereby leading to a “throat” that is either timelike (corresponding to a traversable wormhole), spacelike (corresponding to a “bounce” into a future Universe), or null (corresponding to a “one-way wormhole”). The regularity, the energy conditions, and the causal structure of these models were analysed in detail in Refs. [345, 346]. The main results are several new geometries with two or more horizons, with the possibility of an extremal case. Motivated by these novel solutions, in this subsection we shall analyse specific generalized “black-bounce” wormhole geometries induced by action-dependent Lagrangian theories.

Simpson–Visser black-bounce spacetime

In this section, we consider a specific black bounce geometry, which is denoted as the Simpson–Visser solution [346, 314, 345]. Consider the following parameters, which were presented in Ref. [345]:

$$R(u) = \sqrt{u^2 + a^2}, \quad A(u) = 1 - \frac{2m}{\sqrt{u^2 + a^2}}. \quad (5.67)$$

Note that the Schwarzschild solution is recovered if we take the limit $a \rightarrow 0$.

This spacetime possesses several interesting properties [345]. First, for $a > 0$ the geometry is everywhere regular, which can be verified as $R(u)$ is never zero, and is regular, as is $A(u)$. Now, one has several cases: (i) if $0 < a < 2m$, two horizons exist, namely,

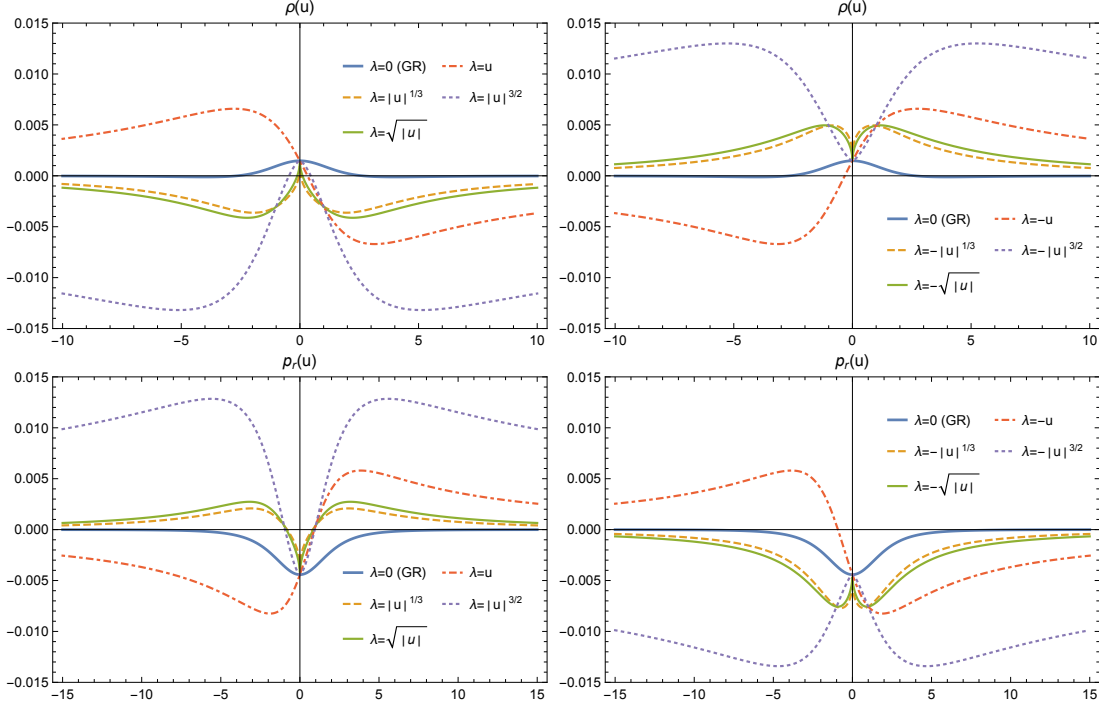


Figure 5.3: The plots depict the Simpson-Visser black bounce solution, for the specific choices $m = 1, a = 3$. Note that one may obtain wormhole configurations with an entirely positive energy density throughout the spacetime, for negative values of the function $\lambda(u)$, and positive radial pressures in the negative branch of the u -axis. As before, it is transparent from the plots that these compact objects possess a richer geometrical structure than their general relativistic counterparts. See main text for more details.

$u_{\pm} = \pm \sqrt{(2m)^2 - a^2}$, where u_+ is positive and u_- is negative; this solution corresponds to a regular black hole spacetime, where the core consists of a bounce located at $u = 0$; (ii) if $a = 2m$, a wormhole exists with a throat located at $u = 0$; this is an extremal null throat, which can only be crossed from one region to another, so that the wormhole is only one-way traversable; (iii) finally, if $a > 2m$, a two-way traversable wormhole exists, that possesses a timelike throat located at $u = 0$. Thus, only the case (iii) for $a > 2m$ interests us here. For specific details about these three cases, see Refs. [345, 346].

Taking into account the choices for the metric functions (5.67), the field equations (5.44)-(5.46) provide the following stress-energy profile:

$$\rho(u)_{SV} = -\frac{1}{8\pi} \left[\frac{a^2 (\sqrt{a^2 + u^2} - 4m)}{(a^2 + u^2)^{5/2}} + \frac{\lambda(u)}{a^2 + u^2} \right], \quad (5.68)$$

$$p_r(u)_{SV} = \frac{(a^2 + u^2) \lambda(u) - a^2}{8\pi (a^2 + u^2)^2}, \quad (5.69)$$

$$p_t(u)_{SV} = \frac{a^2 (\sqrt{a^2 + u^2} - m)}{8\pi (a^2 + u^2)^{5/2}}, \quad (5.70)$$

respectively. The asymptotic limits of the energy density and the radial pressure are given by:

$$\lim_{u \rightarrow \pm\infty} \rho(u)_{SV} \sim - \lim_{u \rightarrow \pm\infty} p_r(u)_{SV} \sim - \lim_{u \rightarrow \pm\infty} \frac{\lambda(u)}{a^2 + u^2}. \quad (5.71)$$

As before, if we assume a power law for $\lambda(u) \sim u^\alpha$, the asymptotic flatness condition and the regularity of the stress-energy components impose that $0 \leq \alpha < 2$; note that the tangential pressure $p_t(u) \rightarrow 0$ for $u \rightarrow \pm\infty$, and possesses a maximum at the wormhole throat, i.e., $p_t(u = 0) = (a - m)/(8\pi a^3)$, and is positive throughout the spacetime as we are only considering the condition $a > 2m$.

Several choices for the function are depicted in Fig. 5.3. Depending on the sign of $\lambda(u)$, one obtains a plethora of specific symmetric or asymmetric solutions. Note that these compact objects possess a richer geometrical structure than their general relativistic counterparts. It is transparent from Fig. 5.3 that one may obtain wormhole configurations with an entirely positive energy density throughout the spacetime, for negative values of the function $\lambda(u)$. In addition, for $\lambda = -u$, it is also possible to obtain positive radial pressures in the negative branch of the u -axis. However, the NEC is always violated at the wormhole throat and everywhere, as can be checked:

$$\rho(u)_{SV} + p_r(u)_{SV} = - \frac{a^2 (-2m + \sqrt{a^2 + u^2})}{4\pi (a^2 + u^2)^{5/2}} < 0, \quad \forall u, \quad \text{when } a > 2m. \quad (5.72)$$

Black bounce II

Another black bounce spacetime that exhibits interesting properties is given by the following specific metric functions [346]:

$$R(u) = \sqrt{u^2 + a^2}, \quad A(u) = 1 - \frac{2mu^2}{(u^2 + a^2)^{3/2}}. \quad (5.73)$$

Note that by solving for the roots of the function $A(u) = 0$, we have that: (i) for $a < a_{\text{ext}} = 4m/(3\sqrt{3})$, there are four real solutions, namely, $(u_+, u_C, -u_C, -u_+)$, which are symmetrical to each other, where u_+ corresponds to the event horizon and u_C to a Cauchy horizon; (ii) for $a = a_{\text{ext}}$, we have two real solutions $(u_+, -u_+)$; and (iii) for $a > a_{\text{ext}}$, no real value exists. See [346] for more details. Thus, in order to have a traversable wormhole solution, where $A(u) > 0$, only the specific case for $a > a_{\text{ext}}$ interests us here.

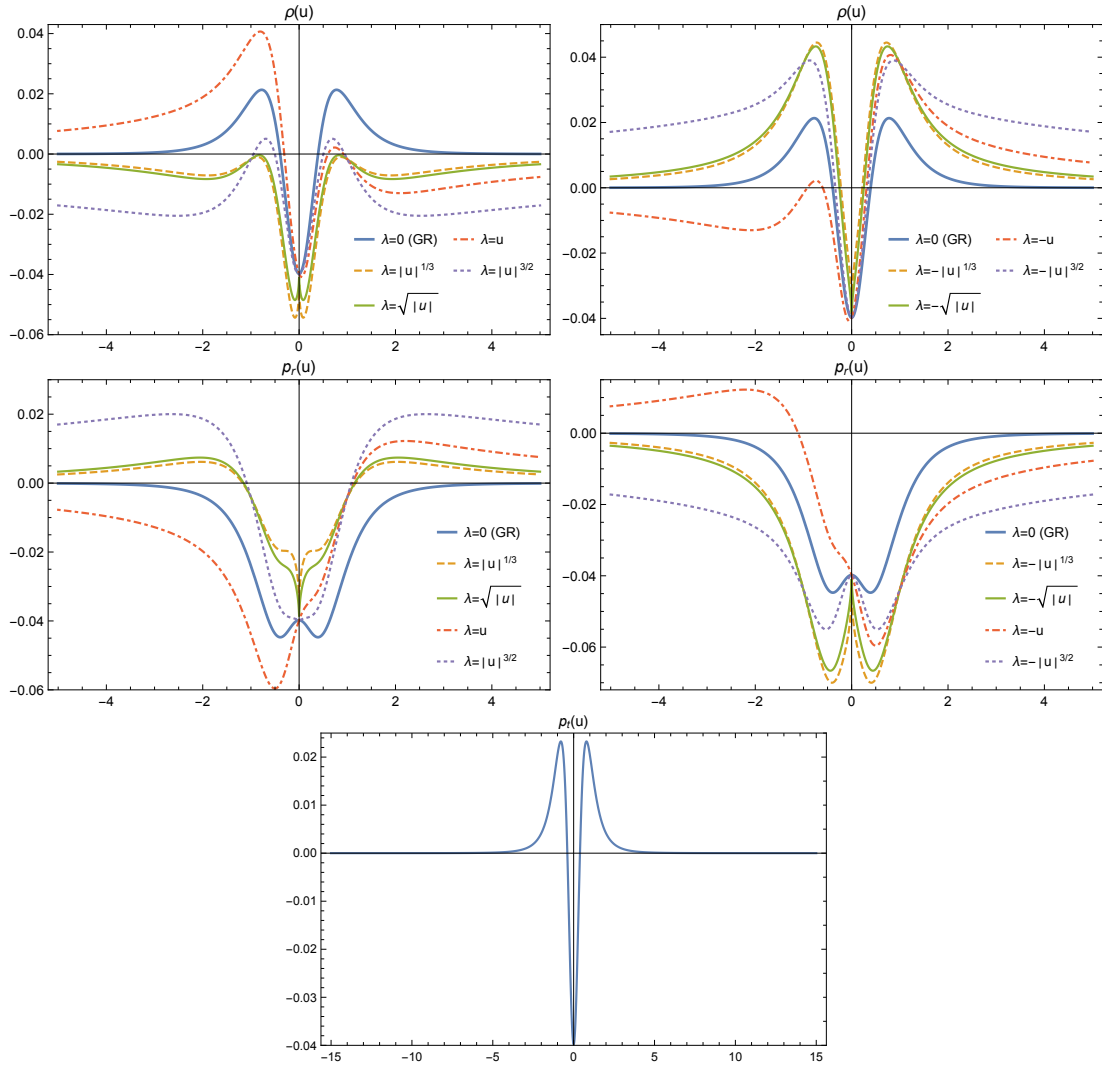


Figure 5.4: The plots depict the stress-energy profile for the black bounce II solution, given by the metric function (5.73), where for numerical convenience we have assumed the following choices for the parameters: $m = 1$, $a = 1$. Recall that the parameters are restricted by the condition $a > 4m/(3\sqrt{3})$. As before these wormhole configurations possess a far richer internal structure than their general relativistic counterparts, and depending on the sign of $\lambda(u)$, specific symmetric or asymmetric solutions are obtained. However, here the tangential pressure at the wormhole throat, $p_t(u = 0) = (a - 2m)/(8\pi a^3)$, takes negative values for the parameter range $4m/(3\sqrt{3}) < a < 2m$, and positive values for $a > 2m$.

For this case, the gravitational field equations (5.44)-(5.46) yield the stress-energy profile, given by the following relations:

$$\rho(u) = -\frac{1}{8\pi} \left[\frac{a^2 (a^2 + u^2)^{3/2} - 8ma^2 u^2}{(a^2 + u^2)^{7/2}} + \frac{\lambda(u)}{a^2 + u^2} \right], \quad (5.74)$$

$$p_r(u) = \frac{1}{8\pi} \left[-\frac{a^2 (a^2 + u^2)^{3/2} + 4ma^2 u^2}{(a^2 + u^2)^{7/2}} + \frac{\lambda(u)}{a^2 + u^2} \right], \quad (5.75)$$

$$p_t(u) = \frac{a^2 u^2 (\sqrt{a^2 + u^2} + 5m) + a^4 (\sqrt{a^2 + u^2} - 2m)}{8\pi (a^2 + u^2)^{7/2}}, \quad (5.76)$$

respectively, which are depicted in Fig. 5.4 for specific choices of the model parameters.

Assuming, once again, a power law for $\lambda(u) \sim u^\alpha$, we have that $0 \leq \alpha < 2$ by the asymptotic flatness condition and the regularity of the stress-energy components, as before. Also, as before, these wormhole geometries induced by action-dependent Lagrangian theories possess a far richer internal structure than their general relativistic counterparts, and depending on the sign of $\lambda(u)$, specific symmetric or asymmetric solutions are obtained. Let us refer the reader to Fig. 5.4 for a qualitative behaviour of the stress-energy profile; recall that taking into account the parameter range, the condition $a > 4m/(3\sqrt{3})$ is considered. Here the tangential pressure at the wormhole throat is given by $p_t(u=0) = (a-2m)/(8\pi a^3)$, and takes negative values for $4m/(3\sqrt{3}) < a < 2m$, possessing a minimum at the throat, and positive values for $a > 2m$; note that $p_t(u) \rightarrow 0$ for $u \rightarrow \pm\infty$ and from the plot it is easy to check that the NEC is violated at the throat. In fact, the value of $\rho(u) + p_r(u)$ does not depend on the chosen $\lambda(u)$, thus obtaining the same value that for GR.

Black bounce III

Finally, we consider another black bounce solution explored in [346], that also exhibits interesting properties, given by

$$R(u) = \sqrt{u^2 + a^2}, \quad (5.77)$$

and the mass function:

$$M(u) = m \left(\frac{R(u)}{u} \right) \left(\frac{2}{\pi} \right)^n \arctan^n \left(\frac{u}{a} \right), \quad (5.78)$$

so that the metric function $A(u)$ is given by

$$A(u) = 1 - \frac{2M(u)}{R(u)} = 1 - \frac{2m}{u} \left(\frac{2}{\pi} \right)^n \arctan^n \left(\frac{u}{a} \right). \quad (5.79)$$

In the limit $(a, n) \rightarrow 0$ we regain the Schwarzschild solution. However, one can fix n and regulate the presence of horizons by adjusting a . For instance, consider $n = 1$, where the extreme case is given by $a_{\text{ext}} = 4m/\pi$ [346].

The causal structure, for the specific case of $n = 1$, is the following: (i) for $a > a_{\text{ext}}$, we obtain the traditional two-way traversable wormhole; (ii) for $a = a_{\text{ext}}$, we have a one-way wormhole geometry with an extremal null throat; (iii) for $a < a_{\text{ext}}$, we have one horizon located

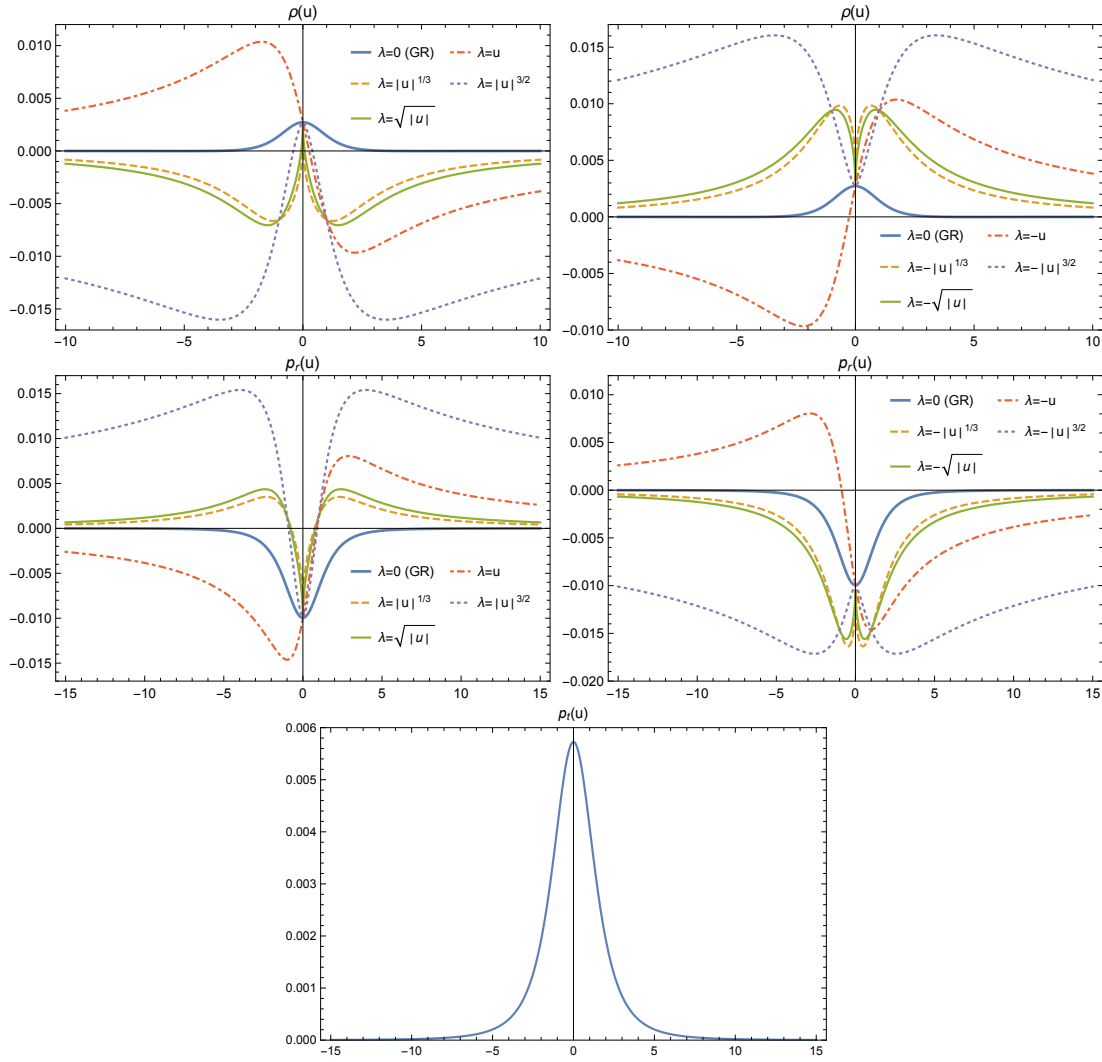


Figure 5.5: The plots depict the stress-energy profile for the black bounce III solution, given by the functions (5.77) and (5.79), for the case $n = 1$, where $a > a_{\text{ext}}$, so that there are no event horizons. We have chosen the following values for the parameters: $m = 1$ and $a = 2$. Note that for these solutions, the negative energy densities are improved, and one may also obtain positive radial pressures for positive values of the function $\lambda(u)$.

in each Universe, where one may propagate through this event horizon, located at $u = u_+$, in order to reach the spacelike “bounce” hypersurface at $u = 0$, before “bouncing” into a future version of our own Universe. Thus, we are only interested in the case $a > a_{\text{ext}}$, for $n = 1$, where there are no event horizons.

Taking into account the metric functions (5.77) and (5.79), the gravitational field equations (5.44)-(5.46) provide the following stress-energy components:

$$\rho(u) = -\frac{1}{8\pi} \left\{ \frac{a^2}{(a^2 + u^2)^2} \left[1 - \frac{2m}{ua} \left(\frac{2}{\pi} \right)^n \left(\arctan \left(\frac{u}{a} \right) \right)^{n-1} \left(a \arctan \left(\frac{u}{a} \right) + nu \right) \right] + \frac{\lambda(u)}{a^2 + u^2} \right\}, \quad (5.80)$$

$$p_r(u) = \frac{1}{8\pi} \left\{ \frac{2ma}{u(a^2 + u^2)^2} \left(\frac{2}{\pi}\right)^n \left(\arctan\left(\frac{u}{a}\right)\right)^{n-1} \left[a \arctan\left(\frac{u}{a}\right) - nu \right] + \frac{(a^2 + u^2)\lambda(u) - a^2}{(a^2 + u^2)^2} \right\}, \quad (5.81)$$

$$p_t(u) = \frac{a^2}{8\pi(a^2 + u^2)^2} \left\{ 1 - \frac{m}{au^3} \left(\frac{2}{\pi}\right)^n \left(\arctan\left(\frac{u}{a}\right)\right)^{n-2} \times \right. \quad (5.82) \\ \left. \times \left[2(a^3 + 2au^2) \left(\arctan\left(\frac{u}{a}\right)\right)^2 - 2nu(a^2 + u^2) \arctan\left(\frac{u}{a}\right) + a(n-1)nu^2 \right] \right\}.$$

respectively. Here, we will only consider, for simplicity, the specific case of $n = 1$ and $a > a_{\text{ext}}$.

If we consider, as before, a power law for $\lambda(u) \sim u^\alpha$, the asymptotic flatness and regularity conditions impose $0 \leq \alpha < 2$. Once again, one obtains a wide variety of solutions, both symmetric and asymmetric, which are depicted in Fig. 5.5. The advantage of these solutions consists essentially in that they ameliorate the negative energy densities for negative values of the function $\lambda(u)$. However, positive values of the function $\lambda(u)$ allow positive radial pressures, as is transparent in Fig. 5.5. The tangential pressure tends to zero at spatial infinity, i.e., $p_t(u) \rightarrow 0$ for $u \rightarrow \pm\infty$, and possesses a maximum at the throat, as depicted in Fig. 5.5. Also as before, the NEC condition is violated and does not depend on the chosen $\lambda(u)$.

5.4 Conclusions

Along this chapter, we have explored wormhole geometries in the recently proposed action-dependent Lagrangian theories [329], that are obtained through an action principle for action-dependent Lagrangians by generalizing the Herglotz variational problem for several independent variables. In this way, two new frameworks have been introduced: on the one hand, wormholes as an important kind of spacetime, and on the other hand, action-dependent Lagrangian theories as another example of modified gravity theories. An interesting feature of these theories as compared with previous implementations of dissipative effects in gravity is the possible arising of such phenomena from a least action principle, so they are of a purely geometric nature. It was shown that the generalized gravitational field equation essentially depends on a background four-vector λ^μ , that plays the role of a coupling parameter associated with the dependence of the gravitational Lagrangian upon the action, and may generically depend on the spacetime coordinates. In the context of wormhole configurations, we have used the ‘‘Buchdahl coordinates’’, and found that the four-vector is given generically by $\lambda_\mu = \left(0, 0, \frac{\lambda(u)}{\cot\theta}, 0\right)$. In addition to this

restriction, the spacetime geometry is also severely constrained by the condition $g_{tt}g_{uu} = -1$, where u is the radial coordinate.

More specifically, the field equations (5.44)–(5.46) impose a system of three independent equations with six unknown functions of the radial coordinate u , namely, $\rho(u)$, $p_r(u)$, $p_t(u)$, $A(u)$, $R(u)$ and $\lambda(u)$. Thus, one possesses several strategies to solve the system of equations. For instance, one may consider a plausible stress-energy tensor profile by imposing equations of state $p_r = p_r(\rho)$ and $p_t = p_t(\rho)$, and close the system by adequately choosing the energy density, or a specific metric function. However, one may also adopt the reverse philosophy approach usually used in wormhole physics, by simply choosing specific metric functions and $\lambda(u)$, and, through the field equations, determine the stress-energy profile responsible for sustaining the wormhole geometry. Here, we have found a plethora of specific asymptotically flat, symmetric and asymmetric, solutions with power law choices for the function $\lambda(u)$, for instance, by generalizing the Ellis-Bronnikov solutions and the recently proposed black bounce geometries, amongst other solutions. We have checked that these compact objects possess a far richer geometrical structure than their general relativistic counterparts. Unfortunately, we have not been able to find no-violation of the NEC condition for these spacetimes in the proposed action-dependent Lagrangian. It would be interesting to investigate time-dependent spacetimes as outlined in [318, 319] in order to explore the energy conditions. To this effect, one could consider that the metric functions in the line element (5.3) are now also time-dependent. This would imply a non-zero Einstein tensor G_u^t component, which would consequently yield the presence of flux terms. Using the modified Einstein field (5.34), one could then expect that $Z_u^t \neq 0$, which would modify the structure of λ_μ , implying a non-zero time-component, i.e., $\lambda_t \neq 0$.

In addition, let us recall that we have studied the action given by Eq. (5.21) (\mathcal{L}_{eff}) and not by Eq. (5.19) (\mathcal{L}), which would be equivalent in absence of the term $\lambda_\mu s^\mu$, but are different in the Herglotz variational problem. The case with \mathcal{L}_{eff} is interesting because of the advantage of taking a Lagrangian that depends only on first-order derivatives of the metric, but it also has the disadvantage that \mathcal{L}_{eff} is not a scalar density, which will result in a set of equations valid for specific referential frames fixed a priori. This is the reason why the geometrical term $K_{\mu\nu}$ is not covariant. Consequently, a new different theory arises by studying Eq. (5.19) (\mathcal{L}) as an actual scalar density that will end up giving truly tensorial equations that do not require us to

fix the coordinate system. The problem in this second case, studied in [338], is the necessity of imposing new boundary conditions for the variational problem as a consequence of second order derivatives of the metric.

Chapter 6

From the theory to observations: MCMC

Until now, this work has been essentially theoretical. However, as physicists, it is impossible to look for new theories without looking at Nature, i.e. at observations. For this reason, in this chapter we are going to focus on this point, introducing the Statistical Inference and the Markov Chain Monte Carlo (MCMC) which will be useful tools to fit the free parameters of a cosmological model and compare its probability of existing in opposite to other ones.

6.1 Statistical Analysis

We will start the chapter reviewing some notions about probability. It is usual to find two different approaches: On the one hand, there is the classical and usually called “frequentist” approach, based on the reproducibility of an experiment, and where the probability of an event is defined from its frequency as an outcome after many; on the other hand, there is the Bayesian approach, in which probability expresses a degree of belief in a proposition, from the available knowledge of the experimenter.

In Cosmology, where there is a unique (enormous) sample (such that it is not possible to “repeat” an experiment) the second statistical approach will be much more successful.

Some definitions will be needed in this chapter:

- $P(A)$: probability that the proposition A is true;
- $P(A, B)$ - joint probability: probability that both propositions, A and B, are true;

- $P(A|B)$ - conditional probability: probability that A is true given the proposition B is already true.

These three concepts are related by Bayes' theorem:

$$P(A|B)P(B) = P(A, B) = P(B|A)P(A) . \quad (6.1)$$

In cosmology, when a model is studied, there are two types of “propositions”: the set of experimental data, d ; and the set of free theoretical parameters to be adjusted, θ . Consequently, Bayes' theorem is translated into:

$$P(\theta|d) = \frac{P(d|\theta)P(\theta)}{P(d)} . \quad (6.2)$$

where:

- $P(\theta|d)$ is the so-called the posterior probability which tells us the probability that a specific set of values for θ are realized given the collected data d ;
- $P(d|\theta)$ is generally called the likelihood probability, and it is the conditional probability of obtaining a specific data set d when the free parameters of the model are fixed at the value θ . It is more commonly written as $L(d|\theta)$ or simply $L(\theta)$ to stress that it is a function of the model parameters;
- $P(\theta)$ is the probability of having specific (set of) value(s) of θ and which will be called the prior distribution.
- $P(d)$ is the probability of having the data d , denoted as the evidence.

Then, it is generally verified that measurements follow a normal distribution around their actual values since one must take into account that, from an experimental point of view, one measures data with mistakes and interference caused by uncontrollable phenomena.

Our next step will be the introduction of the Maximum Likelihood Principle (MLP) which tells us that given the likelihood $L(\theta)$, in order to fit the parameters θ , one must choose the values of θ that maximise $L(\theta)$, since they are the most likely ones for the observational data d . In order to exemplify this, we are going to suppose that our measurements $\{x_1, x_2, \dots, x_n\}$ have a Gaussian (or normal) distribution around the actual values. Then, the unknown parameters in

the distribution would be the mean of the distribution μ , and the standard deviation σ , and the likelihood function takes the form:

$$L(x|\mu, \sigma) = \prod_{i=1}^N \frac{1}{\sqrt{2\pi}\sigma} \exp\left(-\frac{1}{2} \frac{(x_i - \mu)^2}{\sigma^2}\right), \quad (6.3)$$

where each factor is clearly the Gaussian probability of obtaining a specific x_i given a μ and a σ . It is usual to find this likelihood written as:

$$L(x|\mu, \sigma) \propto \exp\left(-\frac{1}{2}\chi^2\right) \quad (6.4)$$

where χ^2 is the chi-square and is defined as:

$$\chi^2 = -2 \log L(x|\mu, \sigma) = \sum_{i=1}^N \frac{(x_i - \mu)^2}{\sigma^2}. \quad (6.5)$$

Now, we are going to think about a cosmological model. On the one hand, we have the measurements x_i and the standard deviation, which is usually given by the observational or experimental error (note that a smaller σ is translated into a tighter Gaussian around the true value). On the other hand, we have the value of the parameter μ which we want to fit. Following the MLP, one should maximize $\mathcal{L}(x|\mu, \sigma)$, or equivalently minimize χ^2 i.e:

$$\frac{\partial \chi^2}{\partial \mu} = 0 \quad \rightarrow \quad \frac{2}{\sigma^2} \left(\sum_i^N x_i - N\mu \right) = 0 \quad \rightarrow \quad \mu = \frac{\sum_i^N x_i}{N}, \quad (6.6)$$

which obviously is the mean of the distribution (as one could anticipate by the name). Sorrowfully, this is the simplest case which is one-dimensional and with the same σ^2 for all measurements, and real life is more complex with various parameters to fit. In order to give an idea about this, imagine a function which depends on the several parameters which we want to fit $d(\boldsymbol{\theta}) = d(x, y, \dots, z)$, and in addition we have several experimental measurements of that function with different errors. Then the definition of the χ^2 is:

$$\chi^2(\boldsymbol{\theta}) \equiv \sum_i \left(\frac{d_i^{obs} - d_i(\boldsymbol{\theta})}{\sigma_i^{obs}} \right)^2, \quad (6.7)$$

and if we have different magnitudes measured that, in addition, are usually correlated among each other by the covariance matrix \mathbf{C} we find:

$$\chi^2(\boldsymbol{\theta}) \equiv [\mathbf{d}^{obs} - \mathbf{d}(\boldsymbol{\theta})]^T \mathbf{C}^{-1} [\mathbf{d}^{obs} - \mathbf{d}(\boldsymbol{\theta})], \quad (6.8)$$

where T means transpose. If the parameters are uncorrelated, then the covariance matrix will be diagonal with the form $C_{ij} = \delta_{ij}\sigma_i^2$. Therefore, minimizing Eq. (6.8), we have a way to find the parameters θ that best reproduce the observational data sample.

Coming back to Eq. (6.2), we have defined $P(\theta)$ as the probability of having certain values of θ . It is called the prior distribution, and usually written as $\Pi(\theta)$. Then, the prior distribution introduces our previous knowledge about the parameters to fit, with the possibility of giving more probability to some values, or prohibiting other ones. Thus, we are able to introduce physical, mathematical or previous experimental information. It can also be useful to define a specific range of the free parameters.

Last but not least in Eq. (6.2), we have the term $P(d)$ which is the probability of having the data d , i.e. this term gives us an idea about how likely it is to obtain the data d from a model. In other words, this term quantifies how much the model is capable of yielding the experimentally measured data and consequently it will be a very important tool in order to compare different models. To calculate this, we should resort to Bayes' theorem once again, taking into account that:

$$\int P(\theta|d)d\theta = 1, \quad (6.9)$$

since the sum or integral of the conditional distribution for all possible values of θ has to be normalized to 1. Consequently:

$$P(d) = \mathcal{E}(d) = \int P(d|\theta)P(\theta)d\theta = \int L(d|\theta)\Pi(\theta)d\theta, \quad (6.10)$$

which is usually called the Evidence. Indeed, we can also learn about the reliability of the model by invoking the evidence \mathcal{E} , also dubbed marginal likelihood or integrated likelihood, since it estimates the support of the (measured) data d for a given model \mathcal{M} , once all possible values for the parameters θ have been considered. The evidence is generally recognized as the most reliable statistical tool for model comparison in cosmology [347], provided that wide-enough priors are chosen.

Consequently, after the redefinitions made in this section, we can translate Bayes' theorem as:

$$P(\theta|d) = \frac{L(d|\theta)\Pi(\theta)}{\mathcal{E}(d)}. \quad (6.11)$$

6.2 MCMC

In the previous section, we have presented a short theoretical and statistical introduction of fundamental concepts that we will use. Yet we need to ascertain how to translate them in practice when the system is complex, with several parameters and measurements that, in addition, are correlated with each other. Even though there are several methods to minimize the χ^2 , we are going to focus on the Markov Chain Monte Carlo algorithm (MCMC).

The starting idea is that one could build an n -dimensional grid in the space of the n free parameters, evaluating the χ^2 at each point and finding the point corresponding to its minimum. However, then the result would depend on the resolution of the grid (separation between points). Additionally, the number of the total points grows enormously with the dimension of the grid following the rule: $resolution^n$ (where the resolution is the number of points for each parameter, considering it is the same for all). Therefore, although the idea is not negligible, it has to be improved to get a real and valid method. It is at this point that MCMCs come to rescue us. The purpose of this algorithm is to build a sequence of points in the space of parameters (instead of a grid) whose distribution will depend on the posterior probability distribution function (pdf). This way the parameter space is explored in a more efficient way. A MCMC is composed of two separated pieces: On the one hand the Markov Chain, and on the other hand, a Monte Carlo method.

In order to define a Markov Chain, one should imagine a sequence of random variables $\{\theta_0, \theta_1, \dots, \theta_n\}$. We will say that this is a Markov Chain if the probability of the $(t + 1)$ -th element depends only on the value of its predecessor element, i.e. the (t) -th element, and not on the previous ones. Its main property is that a Markov chain converges to a stationary state, which will not change again with t and consequently the elements, from this state, will be samples from the target distribution $P(\theta|d)$

The jump from one point to another has a probabilistic nature, and consequently, to define a Markov Chain, one must define the transition probabilities $T(\theta^t, \theta^{t+1})$ which provide the probability of going to point θ^{t+1} from point θ^t . A sufficient condition to build a Markov Chain is the detailed balance condition [348]:

$$P(\theta^t|d)T(\theta^t, \theta^{t+1}) = P(\theta^{t+1}|d)T(\theta^{t+1}, \theta^t). \quad (6.12)$$

On the other hand, Monte Carlo methods are computational techniques that make use of

random numbers [349], or with other words, they are a broad class of computational algorithms that rely on repeated random sampling in order to obtain numerical results.

At this point, we are going to combine both procedures in the Metropolis-Hastings algorithm, which will be used in our following work. Let us expose it following [348] and explain each step of the algorithm:

- We need a starting point θ^0 , with its associated posterior probability $P(\theta^0|d)$.
- Define a proposal distribution $q(\theta^0, \theta^1)$ which will propose the next candidate point θ^1 of the Markov Chain.
- Define the function:

$$\alpha \equiv \min \left(\frac{P(\theta^1|d)q(\theta^1, \theta^0)}{P(\theta^0|d)q(\theta^0, \theta^1)}, 1 \right). \quad (6.13)$$

- We generate a random value u from the uniform distribution $[0, 1)$.
- If $u < \alpha$, we will accept the new candidate point θ^1 , add it to the chain and move to this point which will be the new θ^0 , (and reject it in the opposite case and going back to define a new proposal point).
- Repeat the process from the second item as many times as one wishes, where $\theta^0 \rightarrow \theta^t$ and $\theta^1 \rightarrow \theta^{t+1}$.

We are going to focus on the case in which the distribution q satisfies the symmetry condition, i.e. $q(x, y) = q(y, x)$ and consequently:

$$\alpha \equiv \min \left(\frac{P(\theta^1|d)}{P(\theta^0|d)}, 1 \right). \quad (6.14)$$

This particular case is that of the Metropolis algorithm. Let us analyze the logic behind it. It is clear that if the new candidate point is more likely, then $P(\theta^1|d) > P(\theta^0|d)$, and consequently $\alpha = 1$, $u < \alpha$ and we will accept the point. Otherwise, $\alpha = P(\theta^1|d)/P(\theta^0|d)$ which gets smaller as the difference $P(\theta^1|d) < P(\theta^0|d)$ gets bigger and therefore the probability of taking this as a new point will decrease. However, one may wonder why there is the possibility of taking a point such that $P(\theta^1|d) < P(\theta^0|d)$. The reason is to allow the algorithm some of freedom to explore new points in the parameter space and analyze a bigger sample. Otherwise we might

find ourselves “stuck” in a minimum too early in the chain, and not explore the parameter space truthfully. The transition probability for the Metropolis algorithm is given by:

$$T(\boldsymbol{\theta}^t, \boldsymbol{\theta}^{t+1}) = q(\boldsymbol{\theta}^t, \boldsymbol{\theta}^{t+1}) \alpha(\boldsymbol{\theta}^t, \boldsymbol{\theta}^{t+1}), \quad (6.15)$$

which satisfies the detailed balance condition (6.12).

6.2.1 Model selection

Hitherto, we have seen how we can choose the free parameters of a model, i.e. we have spoken about different values always for the same model. However, the most important part of this study is to compare different models and have enough tools to choose between all them. In other words, the essential task of this subsection will be to provide a way to assess which model (with its constraints) is the most probable one to support the observations. However, there is not a unique criterion, and we have different approaches, but they provide similar conclusions.

As a first approach, one could consider the comparison of the minimum value of χ^2 obtained for each model. This seems logical because the lower χ^2 the better the model to fit the data, and consequently the more likely to be generating the observations. However, this approach is only suitable to compare models with the same number of degrees of freedom, i.e. with the same number of parameters to fit. Of course, if we take a model with infinite free parameters, we will be able to reproduce exactly observations due to the freedom of the model, but that does not mean to have a good model. In order to solve this caveat, and to be able to compare models with different number of parameters, the reduced χ^2 is defined as:

$$\chi_{red}^2 = \frac{\chi^2}{DoF} = \frac{\chi^2}{N_{data} - k - 1}, \quad (6.16)$$

where N_{data} is the number of points in the data and k is the number of free parameters. Consequently, for a same χ^2 , the lower k the lower χ_{red}^2 and vice-versa. A normal value for χ_{red}^2 should be around 1. If $\chi_{red}^2 \ll 1$ the model fits the data too easily and a possible reason is that the errors overestimated.

The other approach which will be presented here is the Evidence, which was introduced in Eq. (6.10). The advantage of this approach is that this quantity does not need to be compared with other models, i.e. it estimates the power of a model and the goodness of fit. For model

comparison, one can define the Bayes factor as the ratio of the evidences of two different models:

$$\mathcal{B}_j^i = \frac{\mathcal{E}_i}{\mathcal{E}_j}. \quad (6.17)$$

where the sub-index denotes the evidence of each model. In gross terms if $\mathcal{B}_j^i > 1$, i.e. $\mathcal{E}_i > \mathcal{E}_j$ for the measured data d , then the model \mathcal{M}_i is preferred over model \mathcal{M}_j .

However, it is difficult to quantify how much better (or worse) is one scenario as compared to the other. Jeffreys' Scale [350] is typically adduced in this regard. According to that criterion, if $\ln \mathcal{B}_j^i < 1$, the evidence in favor of the model \mathcal{M}_i is not significant; if $1 < \ln \mathcal{B}_j^i < 2.5$, the evidence is substantial; if $2.5 < \ln \mathcal{B}_j^i < 5$, it is strong; and if $\ln \mathcal{B}_j^i > 5$, it is decisive. Nevertheless, Jeffreys' scale is not completely flawless, as discussed in [347].

From a practical point of view, the computation of the Evidences, Eq. (6.10), in this work has been performed with the nested sampling algorithm [351]. This algorithm is based on breaking up the prior volume into a large number of "equal mass" points, and ordering them by increasing likelihood. Then, one is able to calculate the Evidence as a one-dimensional integral, in which the integrand is positive and decreasing.

6.3 Observational data and cosmological observables

In this section we have a double task in mind. On the one hand, we are going to speak about the samples of data which we will use for the MCMC, and on the other hand, we will look at some cosmological observables, which are essential to understand the samples of data. In order to make this as pedagogical as possible, we will focus on every sample and from there we will see which parameters are needed.

In this work we will use 4 kinds of data:

- Type Ia Supernovae with Pantheon data;
- The expansion rate data from early-type galaxies as cosmic chronometers with *Hubble* data;
- Cosmic Microwave Background shift parameters from *Planck* 2018;
- Baryon Acoustic Oscillations data.

However, before proceeding to the characterization of these samples, we introduce important definitions about the distances which will be useful for all them.

6.3.1 Distances in Cosmology

The metric shown in (1.18) can be expressed in hyperspherical coordinates under the change:

$$d\chi^2 = \frac{dr^2}{1 - kr^2}, \quad (6.18)$$

with the form:

$$ds^2 = -c^2 dt^2 + a^2(t) [d\chi^2 + S_\kappa^2(\chi) d\Omega^2], \quad (6.19)$$

where S_κ^2 is defined depending on the value of κ :

$$S_\kappa^2 = \begin{cases} \sin(\chi) & \text{for } \kappa = 1 \\ \chi & \text{for } \kappa = 0 \\ \sinh(\chi) & \text{for } \kappa = -1 \end{cases}. \quad (6.20)$$

Take into account that in this chapter we are concerned with observable measurements, and we do not normalize the speed of light in order to analyze the actual measured parameter. Then, from metric (6.19), the definition of the distance of the path followed by a photon is defined by $ds^2 = 0$ without radial deviation, $d\Omega = 0$, and consequently: $cdt = -a(t)d\chi$. Performing the integration:

$$D_c \equiv \chi = c \int_{t_f}^{t_0} \frac{dt'}{a(t')}, \quad (6.21)$$

one is able to calculate the distance χ followed by the photon from t_0 to t_f . This distance is the so-called comoving distance, because it does not change in time due to the expansion, since an $a(t)$ term has been factored out of the definition. However, the physical distance will be given by $l = \sqrt{a^2(t)\chi^2}$, in which obviously the expansion of the Universe plays an important role.

In addition, recall that the conformal time is defined as $d\eta = dt/a(t)$, which transforms the FLRW metric into its conformal representation:

$$ds^2 = a^2(\eta) [-c^2 d\eta^2 + d\chi^2 + S_\kappa^2(\chi) d\Omega^2]. \quad (6.22)$$

So we get a coordinate system in which the expansion of the Universe is a common factor of the coordinates and consequently this does not affect their relation. Consequently, we can guarantee that in the conformal mesh two time lapses of an emitted pulse are equivalent:

$$d\eta_0 = d\eta_e, \quad (6.23)$$

which is translated into:

$$\frac{dt_0}{a(t_0)} = \frac{dt_e}{a(t_e)}, \quad (6.24)$$

and if we think of a photon flux and associate this time lapse with its frequency, t_0 with the reception and t_e with the emission, we obtain:

$$\frac{\nu_e}{\nu_0} = \frac{a(t_0)}{a(t_e)}. \quad (6.25)$$

This same procedure can be applied with the wavelength λ :

$$d\chi_0 = d\chi_e \quad \rightarrow \quad \frac{\lambda_0}{a(t_0)} = \frac{\lambda_e}{a(t_e)}. \quad (6.26)$$

Considering $a(t_0)$ as the scale factor at the present time, which from now on we normalize $a(t_0) = 1$, we define the redshift as:

$$z = \frac{\lambda_0 - \lambda_e}{\lambda_e} = \frac{1}{a(t_e)} - 1, \quad (6.27)$$

which can be used as a variable to study the evolution of the Universe, analogously to t or the scale factor $a(t)$, with the important property of being much easier to measure. At this point, one could redefine the comoving distance using the redshift¹:

$$D_c \equiv \chi = c \int_0^z \frac{dz}{H(z)}. \quad (6.28)$$

Alternatively, we can define a luminosity distance in the following way: imagine for example a light bulb in a room with luminosity L , which is the total energy emitted per unit time, and that, from our position, we measure a flux F . Then, taking into account that the emitted energy

¹A good reader could say that there is an error of the sing, but this is because χ as defined in (6.21) is $\chi_f - \chi_0$ where χ_0 is the starting point of the photon and χ_f is the receptor point, however we are interested into the modulus distance so in (6.28), where we are the receptor at $\chi_f = 0$, we can eliminate this sing

is always the same, but that it must be spread over the area of a sphere that gets bigger as the distance from the source increase, we conclude that:

$$F = \frac{L}{4\pi d^2}, \quad (6.29)$$

where d is the distance from us to the light bulb. Then one can apply this same reasoning for a star, defining the luminosity distance as:

$$D_L = \left(\frac{L}{4\pi F} \right)^{1/2}, \quad (6.30)$$

but, from a cosmological point of view (and for a Universe which is expanding), we should think that d or D_L is a little more difficult to calculate due to the expansion. For this purpose we are going to think that a star, at $r = r_1$ and $t = t_1$, emitted an energy pulse during dt_1 and we, observers at $r = 0$, $t = t_0$, measurement it during the lapse time dt_0 (all this in the FLRW metric). Then, the total energy for a sphere of radius r_1 will be:

$$\frac{L dt_1 a(t_1)}{dt_0 a(t_0)}, \quad (6.31)$$

and consequently, the flux F :

$$F = \frac{L dt_1 a(t_1)}{dt_0 a(t_0)} \frac{1}{4\pi (r_1 a(t_0))^2} = \frac{L}{4\pi ((1+z)r_1)^2}, \quad (6.32)$$

where once again we have taken $a(t_0) = 1$, the definition of the redshift $1+z = 1/a(t)$ and $dt_0/a(t_0) = dt_1/a(t_1)$. Therefore, the conclusion is that the distance d or D_L is defined as:

$$D_L = (1+z)r, \quad (6.33)$$

where r is the so-called transverse comoving distance, which takes into account the spatial curvature k and which can be written in terms of comoving distance χ using Eq. (6.20). As an example, the simplest case in which $k = 0$, which implies $r = \chi$, gets the following definition of the luminosity distance:

$$D_L = (1+z) \int_0^z \frac{c dz'}{H(z')}, \quad \text{for } k = 0, \quad (6.34)$$

Another possible cosmological ruler is the angular diameter distance D_A . In this case, it is supposed to know about the physical transverse size of the object l and the angular size α

occupied by it in the sky. Then, using trigonometry and considering a small α it is possible to define the angular diameter distance as:

$$D_A = \frac{l}{\alpha} . \quad (6.35)$$

In addition, from the metric (1.18), the physical length of a distance when all coordinates remain constant except for the angle θ is:

$$l = a r d\theta , \quad (6.36)$$

where a corresponds to the scale factor at the redshift of the observed object, and the variation of the angle θ corresponds to the sized angle α . Consequently, D_A reads:

$$D_A = \frac{r}{1+z} = \frac{D_L}{(1+z)^2} . \quad (6.37)$$

Take into account that all these distances depend on the model via $H(z)$ and consequently on their free parameters θ , such that it is possible to write explicitly this dependence $H(z) \equiv H(z, \theta)$, which will be remarked during the next subsection where the samples of data are introduced.

6.3.2 Pantheon Supernovae data

The idea here is to use the Type Ia Supernovae (SNeIa) as standard candles. This is because we are able to know their intrinsic brightness and consequently one can estimate their distance. Let us remark that this, which could seem very simple, is sometimes a hard task to calibrate and must be supported by closer standard candles, developing a cosmic distance builder. Consequently, errors in a closer object are propagated to a farther object. In this case, SNeIA are calibrated using Cepheids, that are calibrated using parallax distance measurements [352, 353]. This last one is the main method of measurements for the closest objects.

Therefore like we already said, for SNeIa the important observable from which information is extracted is brightness, which can be mathematized with the magnitudes. The apparent magnitude m is the received flux F by an observer of a celestial body compared with a zero-point as follows:

$$m = -2.5 \log_{10} \left(\frac{F}{F_0} \right) , \quad (6.38)$$

where historically the reference zero-point is the flux of the star Vega². The absolute magnitude M is defined analogously but using the intrinsic luminosity L of the object (and consequently it does not depend on the position of the observer):

$$M = -2.5 \log_{10} \left(\frac{L}{L_0} \right), \quad (6.39)$$

where in this case L_0 is defined so that $M = m$ if the object were located at a distance of 10 pc. This allows us to introduce the distance modulus μ defined as the difference between the apparent and the absolute magnitude:

$$\mu = m - M = 5 \log_{10} \left(\frac{D_L(\text{pc})}{10 \text{pc}} \right) = 5 \log_{10} D_L(\text{Mpc}) + 25. \quad (6.40)$$

From a practical point of view, we will express this as:

$$m = 5 \log_{10} \mathcal{D}_L + \mathcal{M}, \quad (6.41)$$

where \mathcal{D}_L is the Hubble-constant free luminosity distance and \mathcal{M} is the nuisance parameter which represents some combination of M of a fiducial SNeIa and the Hubble constant. Then, one can construct $\Delta m = m_{theo}(\boldsymbol{\theta}) - m_{obs}$, where $m_{theo}(\boldsymbol{\theta})$ is the theoretical apparent magnitude of a star for a specific model with parameters $\boldsymbol{\theta}$. At this point it may be thought that a possible χ_{SN}^2 is

$$\chi_{SN}^2 = (\Delta m)^T \cdot C_{SN}^{-1} \cdot \Delta m, \quad (6.42)$$

where C_{SN} is the total covariance matrix. However, the latter would contain the nuisance parameter \mathcal{M} , which in turn is a function of the Hubble constant, the speed of light c and the SNeIa absolute magnitude. In order to circumvent this dependency, χ_{SN}^2 is marginalized analytically with respect to \mathcal{M} as in [354], thus obtaining a new χ_{SN} estimator of the form:

$$\chi_{SN}^2 = (\Delta m)^T \cdot C_{SN}^{-1} \cdot \Delta m + \ln \frac{S}{2\pi} - \frac{k^2}{S}, \quad (6.43)$$

where S is the sum of all entries of C_{SN}^{-1} , which gives an estimation of the precision of the data and is independent of θ , and k is Δm but weighed by a covariance matrix as follows:

$$k = (\Delta m)^T \cdot C_{SN}^{-1}. \quad (6.44)$$

In this case, we will consider one of the latest Type Ia Supernovae (SNeIa) compilations [355], which contains the observational values of m for 1048 SNeIa at redshift $0.01 < z < 2.26$.

²Consequently, this star has an apparent magnitude $m = 0$. A negative magnitude corresponds to a brighter object (for an observer on the Earth), and a positive magnitude to a less bright object.

6.3.3 Hubble data

Early time passively evolving galaxies have some peculiar features in their spectra which have been shown to correlate with their evolving stage. Thus, direct astrophysical measurements can estimate their differential ages at different redshifts and this can finally be related to the Hubble parameter [356, 357, 358]. Then, this sample is essentially a compilation of 31 values of $H(z)$ for $0.07 < z < 1.965$ [359, 360] to assist us in fitting the free parameters of a possible theoretical setting through the construction of a χ_H^2 as follows:

$$\chi_H^2 = \sum_{i=1}^{31} \frac{[H(z_i, \boldsymbol{\theta}) - H_{obs}(z_i)]^2}{\sigma_H^2(z_i)}, \quad (6.45)$$

where $H_{obs}(z_i)$ is the observed value at z_i , $\sigma_H(z_i)$ are the observational errors, and $H(z_i, \boldsymbol{\theta})$ is the value of a theoretical H for the same z_i with the specific parameter vector $\boldsymbol{\theta}$.

6.3.4 Cosmic Microwave Background data

It is common practice to condense Cosmic Microwave Background (CMB) data into the so-called shift parameters [361] when examining the evolution of the cosmological background. This set of three quantities basically informs us about the position of the first peak in the temperature angular power spectrum through the ratio between its position in the model one wants to analyze and that of an Λ CDM model (Standard Cold Dark Matter). The set of shift parameters is formed by the exact expression of that quadrature ratio (an approximate yet quite accurate expression) and the normalized density fraction of baryons:

$$R(\boldsymbol{\theta}) \equiv \sqrt{\Omega_m H_0^2} \frac{r(z_*, \boldsymbol{\theta})}{c}, \quad l_a(\boldsymbol{\theta}) \equiv \pi \frac{r(z_*, \boldsymbol{\theta})}{r_s(z_*, \boldsymbol{\theta})}, \quad \omega_b \equiv \Omega_b h^2, \quad (6.46)$$

recalling that $r(z, \boldsymbol{\theta})$ is the transverse comoving distance to z , and $r_s(z_*, \boldsymbol{\theta})$ is the comoving sound horizon, defined as:

$$r_s(z_*, \boldsymbol{\theta}) = \int_{z_*}^{\infty} \frac{c_s(z')}{H(z', \boldsymbol{\theta})} dz', \quad (6.47)$$

where c_s is the sound speed, and z_* means the redshift at which the last scattering occurs [362], i.e. the redshift at the photon-decoupling. It is given by the expression:

$$z_* = 1048 [1 + 0.00124(\Omega_b h^2)^{-0.738}] [1 + g_1(\Omega_m h^2)^{g_2}],$$

where

$$g_1 = 0.0783(\Omega_b h^2)^{-0.238} [1 + 39.5(\Omega_b h^2)^{-0.763}]^{-1},$$

$$g_2 = 0.560 [1 + 21.1(\Omega_b h^2)^{1.81}]^{-1}.$$

In addition, the sound speed c_s is defined by the expression [363]:

$$c_s(z) = \frac{c}{\sqrt{3(1 + \hat{R}_b(1+z)^{-1})}}, \quad (6.48)$$

which obviously depends on the baryon density and its temperature as:

$$\hat{R}_b = 31500\Omega_b h^2 \left(\frac{T_{CMB}}{2.7} \right)^{-4}. \quad (6.49)$$

where $h = H_0/100$.

Finally, we are able to construct the χ_{CMB}^2 estimator for these three parameters like:

$$\chi_{CMB}^2 = (\Delta\mathcal{F}^{CMB})^T \cdot C_{CMB}^{-1} \cdot \Delta\mathcal{F}^{CMB}, \quad (6.50)$$

where $\Delta\mathcal{F}^{CMB}$ is a vector formed by the difference between experimental data and theoretical-model predictions of those three quantities mentioned above [361]. In this case, we will use for the experimental data the sample provided by *Planck* 2018 data release [364].

Let us recall that the shift parameters depend on the position of the CMB acoustic peaks, which are functions of the geometry of the model considered. For that reason, they can be used to discriminate between different models or different values of the free parameters θ , which include Ω_b in this case. A complete and detailed description of these parameters and those that follow can be found in [364, 365].

6.3.5 Baryon Acoustic Oscillations data

The last set of data addresses Baryon Acoustic Oscillations (BAO), which are fluctuations in the density of visible baryonic matter as a consequence of acoustic density waves in the primordial plasma. Accordingly, there is a distance associated with the maximum distance that acoustic waves could travel through this medium until the plasma cooled at the recombination moment, where it became a soup of neutral atoms and the expansion of plasma density waves stopped and they got frozen. That being so, the mentioned distance can be used as a standard ruler.

We will use five sets of data, collected by different observational missions. Let us give now relevant details.

- WigggleZ: these are data coming from the WigggleZ Dark Energy survey [366], which are evaluated at redshifts $z_w = (0.44, 0.66, 0.73)$ as shown in Table 1 of [367]. Following that work, we will consider two quantities: the acoustic parameter given by

$$A(z, \boldsymbol{\theta}) = 100 \sqrt{\Omega_m} h^2 \frac{D_V(z, \boldsymbol{\theta})}{cz}, \quad (6.51)$$

and the Alcock-Paczynski distortion parameter:

$$F(z, \boldsymbol{\theta}) = (1+z) \frac{D_A(z, \boldsymbol{\theta}) H(z, \boldsymbol{\theta})}{c}, \quad (6.52)$$

where D_A is the angular diameter distance, and D_V is the geometric mean of the longitudinal (D_A) and radial ($c/H(z)$) BAO modes, defined as

$$D_V(z, \boldsymbol{\theta}) = \left[(1+z)^2 D_A^2(z, \boldsymbol{\theta}) \frac{cz}{H(z, \boldsymbol{\theta})} \right]^{1/3}. \quad (6.53)$$

Consequently, we have two observational parameters, i.e. $A(z_w)$ and $F(z_w)$, which can be compared with the theoretical value drawn from the model under study with a specific $\boldsymbol{\theta}$, allowing us to construct a new $\Delta\mathcal{F}_w$. In this case we define χ_w^2 as

$$\chi_w^2 = (\Delta\mathcal{F}_w)^T \cdot C_w^{-1} \cdot \Delta\mathcal{F}_w, \quad (6.54)$$

where C_w^{-1} is a matrix given in Table 2 of [367].

- BOSS: in this case, we consider the data from the SDSS-III Baryon Oscillation Spectroscopy Survey (BOSS) DR12 described in [368]. We proceed analogously to the WigggleZ case but now we have $z_B = (0.38, 0.51, 0.61)$, whereas the fundamental parameters are

$$D_M(z, \boldsymbol{\theta}) \frac{r_s^{fid}(z_d)}{r_s(z_d, \boldsymbol{\theta})}, \quad H(z, \boldsymbol{\theta}) \frac{r_s(z_d, \boldsymbol{\theta})}{r_s^{fid}(z_d)}, \quad (6.55)$$

where $D_M(z) = r(z)$, $r_s(z_d, \boldsymbol{\theta})$ denotes the sound horizon defined as Eq. (6.47) but evaluated at the dragging redshift z_d , and $r_s^{fid}(z_d)$ is the same parameter but calculated for a given fiducial cosmological model and it is equal to 147.78 Mpc in this specific case.

Clearly, the first step involves calculating the redshift of the drag epoch z_d , which can be done considering the following approximation, like in [369]:

$$z_d = \frac{1925(\Omega_m h^2)^{0.251}}{1 + 0.659(\Omega_m h^2)^{0.828}} [1 + b_1(\Omega_b h^2)^{b_2}] , \quad (6.56)$$

where b_1 and b_2 are factors calculated as follows:

$$b_1 = 0.313(\Omega_m h^2)^{-0.419} [1 + 0.607(\Omega_m h^2)^{0.6748}] , \quad (6.57)$$

$$b_2 = 0.238(\Omega_m h^2)^{0.223} . \quad (6.58)$$

Once more, we will define:

$$\chi_B^2 = (\Delta\mathcal{F}_B)^T \cdot C_B^{-1} \cdot \Delta\mathcal{F}_B , \quad (6.59)$$

where $\Delta\mathcal{F}_B$ is the difference between the observational data and the resulting value for θ , and C_B^{-1} is the inverse of the covariance matrix given in Table 8 of [368].

- eBOSS: the extended Baryon Oscillation Spectroscopy Survey (eBOSS) gives us one more data point [370]:

$$D_V(z = 1.52) = 3843 \pm 147 \frac{r_s(z_d)}{r_s^{fid}(z_d)} \text{ Mpc} . \quad (6.60)$$

Our function χ_{eB}^2 gets a simpler expression that in other cases, as the matrix notation is not necessary, and we simply have

$$\chi_{eB}^2 = \frac{\Delta\mathcal{F}_{eB}^2}{\sigma_{eB}^2} , \quad (6.61)$$

where σ_{eB}^2 is the error in the datum.

- BOSS-Lyman α : another set of data is Quasar-Lyman α Forest from SDSS-III BOSS DR11 [371], which contributes two new data points to the analysis:

$$\frac{D_M(z = 2.34, \theta)}{r_s(z_d, \theta)} = 36.98_{-1.18}^{+1.26} , \quad (6.62)$$

$$\frac{c}{H(z = 2.34, \theta)r_s(z_d, \theta)} = 9.00_{-0.22}^{+0.22} , \quad (6.63)$$

and its χ^2 is defined as: $\chi_{BL}^2 = (\Delta\mathcal{F}_{BL})^T C_{BL}^{-1} \Delta\mathcal{F}_{BL}$.

- Finally, we consider the voids-galaxy cross-correlation data from [372]. This set gives us two new data points at $z = 0.57$ which are

$$\frac{D_A(z = 0.57, \boldsymbol{\theta})}{r_s(z_d, \boldsymbol{\theta})} = 9.383 \pm 0.077, \quad (6.64)$$

$$H(z = 0.57, \boldsymbol{\theta})r_s(z_d, \boldsymbol{\theta}) = (14.05 \pm 0.14) \frac{10^3 \text{ km}}{\text{s}}, \quad (6.65)$$

and the same usual definition applies to $\chi_{vg}^2 = (\Delta\mathcal{F}_{vg})^T C_{vg}^{-1} \Delta\mathcal{F}_{vg}$.

6.4 Summary

In this section we have presented the statistical analysis needed to study a cosmological model focusing on the MCMC methodology. In addition, we have featured some tools for a correct model selection (among the vast expanse of possibilities) which are the most usual ones without great differences between them. In this way, some important concepts are the likelihood $L(\theta)$ related with the chi-squared χ^2 , the priors $\Pi(\theta)$, the evidence $\mathcal{E}(d)$, and the Bayes factor \mathcal{B}_j^i . From a practical viewpoint, we have also shown the specific Monte Carlo method we use, based on the Metropolis-Hastings algorithm.

Besides, we have exposed several samples of data based on SNeIa, cosmic chronometers, CMB and BAO and the methodology to build the important χ^2 in order to be able to fit the free parameters of a cosmological model through the MCMC.

Hence, with all this information, we are now able to study the proposed cosmological models. In fact, this will be the main purpose of the next section, where we will study some examples of cosmological models based on modified gravitational theories.

Chapter 7

$f(Q)$ theories and their observational constraints.

Until now, we have considered modified theories of gravity that change or add terms to the gravitational action. However, another more ambitious approach from a mathematical and geometrical point of view is to treat the connection as a new degree of freedom. As a matter of fact a spacetime can be built from its metric tensor $g_{\mu\nu}$, that provides the prescription to measure distances, and its affine structure determined by the connection $\Gamma_{\mu\nu}^{\alpha}$, that governs how objects move about the manifold. As we will see, this consideration in GR does not lead to any new phenomenology, but on the contrary it does so in the cases of modified gravity theories.

In this chapter, among the different starting points considered in the vast literature on modified gravity theories, we will embrace that of the metric-affine geometry, that generalizes the Riemannian geometry approach adopted in GR.

The connection then becomes a non-standard free variable at the same level as the metric, and hence it is not necessarily of the Levi-Civita type. Broadly speaking, this freedom in the features of the connection brings a rich phenomenology related to the transformations that objects of physico-mathematical nature undergo in a displacement [373, 374].

This will be translated into the study of some cosmological models based on the non-metricity scalar [375], a quantity that measures how the length of a vector changes when it is transported, and which will be defined shortly. The motivation behind this chapter is that in recent years a lot of interest has been gathered by $f(Q)$ theories, which are new candidates to replace Einstein's

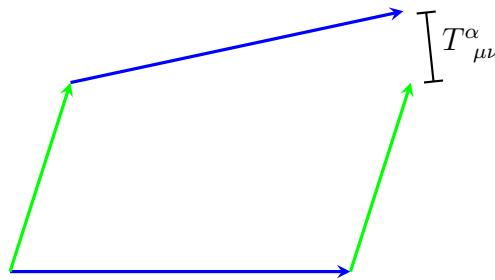
prescription for gravity. In addition, these theories give us a particularly illustrative framework to apply the knowledge acquired in the previous chapter. This will eventually be translated into observational constraints and fittings for some examples we shall address here. So, we will resort to observational tests to draw conclusions about the (statistical and physical) reliability of some specific models.

7.1 Introduction

As we anticipated, our final purpose of this section will be the study of $f(Q)$ theories. However, it is not possible to delve into these theories without a brief previous study of the connection, and of its role both in GR and in modified gravity theories. Provided that the connection will not be (so to speak) geometrically trivial, we must define two further fundamental objects conveying additional information about it which is relevant [376]. The first one is the torsion, which stems from the antisymmetric part of the connection:

$$T_{\mu\nu}^{\alpha} \equiv \Gamma_{\mu\nu}^{\alpha} - \Gamma_{\nu\mu}^{\alpha}, \quad (7.1)$$

and which obviously vanishes for any symmetric connection, i.e. $\Gamma_{\mu\nu}^{\alpha} = \Gamma_{\nu\mu}^{\alpha}$. From a pictorial point of view, it can be seen as the following diagram:

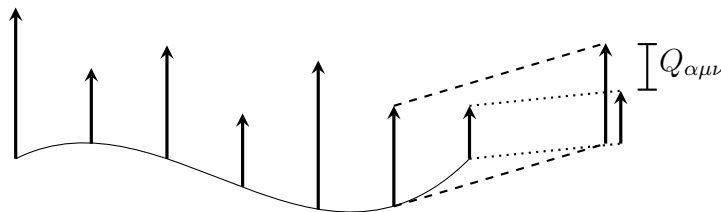


Concretely, the torsion measures the difference between the parallel transport of the blue vector along the green vector and the parallel transport of the green vector along the blue vector. If there is no torsion, we will say that this is a torsionless connection, i.e. $T_{\mu\nu}^{\alpha}(\Gamma) = 0$ and consequently, the parallelogram will be closed.

The second fundamental object will be the non-metricity tensor:

$$Q_{\alpha\mu\nu} \equiv \nabla_{\alpha} g_{\mu\nu}, \quad (7.2)$$

which informs us about the failure of the connection to be metric, and which can be represented as:



since non-metricity informs us about the change of the length of vectors when they are parallel transported. Thus, if the connection is metric compatible, i.e. $Q_{\alpha\mu\nu}(\Gamma, g) = 0$, the length of vectors is conserved, and we will say that this is a metric space.

Both objects allow us to define the proper decomposition of any general connection [376, 373] as:

$$\Gamma_{\mu\nu}^{\alpha} = \{\mu\nu\}^{\alpha} + K_{\mu\nu}^{\alpha} + L_{\mu\nu}^{\alpha}, \quad (7.3)$$

where $\{\mu\nu\}^{\alpha}$ is the usual Christoffel symbol, $K_{\mu\nu}^{\alpha}$ is called the contortion, and $L_{\mu\nu}^{\alpha}$ is the disformation. The last two are built from the torsion and the non-metricity respectively as follows:

$$K_{\mu\nu}^{\alpha} = \frac{1}{2}T_{\mu\nu}^{\alpha} + T_{(\mu}^{\alpha}{}_{\nu)}, \quad (7.4)$$

$$L_{\mu\nu}^{\alpha} = \frac{1}{2}Q_{\mu\nu}^{\alpha} - Q_{(\mu}^{\alpha}{}_{\nu)}. \quad (7.5)$$

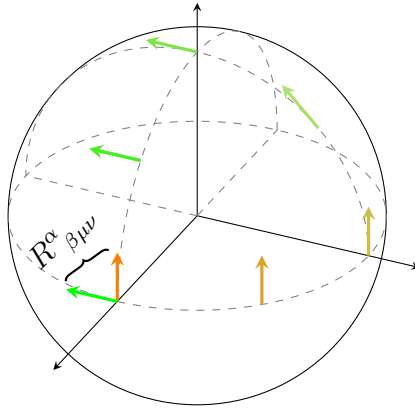
The disformation will be the relevant quantity for this chapter, as it measures how much the symmetric part of the (general) connection deviates from the Levi-Civita connection $\{\mu\nu\}^{\alpha}$.

Let us remark an important change of notation to be in agreement with the literature: when we are not in the framework of metric-affine theories, it is usual to express the Christoffel symbols as $\Gamma_{\mu\nu}^{\alpha}$, and in fact this is true because the contortion and disformation vanish; however, when we wish to study the connection as a free parameter we must distinguish the Christoffel symbols from the general connection. Summarizing, the definitions of the Riemann tensor in Eq. (1.4) and the Ricci tensor in (1.5) tensors are still valid, but, Eq. (1.7) will no longer be valid, i.e:

$$\Gamma_{\mu\nu}^{\sigma} \neq \frac{1}{2}g^{\sigma\alpha} (\partial_{\nu}g_{\mu\alpha} + \partial_{\mu}g_{\alpha\nu} - \partial_{\alpha}g_{\mu\nu}) = \{\mu\nu\}^{\sigma}. \quad (7.6)$$

In addition, it is also possible to have a connection whose Riemann tensor vanishes, ($R^\alpha_{\beta\mu\nu}(\Gamma) = 0$). In this case we will say that the connection is not curved or, in others words, that the spacetime is flat. The curvature measures the change of direction of a vector which has undergone parallel transport along a closed curve.

In order to show this concept, we will use the famous example of a sphere, like the Earth, where if we consider a tangent vector at, say, the upper pole, and we parallel transport it along the closed triangle path whose sides are maximum circles, and hence geodesics of the sphere, we will obtain a change in direction between the start and end vector, as illustrated below.



In flat spaces, vectors do not rotate when they are parallel transported and one gets a better notion of parallelism at a distance. The theories formulated in these frameworks are referred to as teleparallel due to a well-defined notion of parallelism¹ as a consequence of the vanishing of total curvature [381, 382, 373].

Equipped with this information, we write the Einstein-Hilbert action as:

$$S_{GR} = \frac{1}{16\pi G} \int d^4x \sqrt{-g} R(\{\}), \quad (7.7)$$

where $R(\{\})$ is the curvature scalar that results from a specific choice of the Levi-Civita connection in the definition of the Riemann tensor of Eq. (1.4), which follows from considering a Riemannian geometry. It is usual to find in many works that this action has the special property of producing the same equations of motion when it is promoted to the metric-affine formalism. However, this sentence is only true under some assumptions that will be explained here.

For this purpose, we recast Eq. (7.7) in terms of the general scalar of curvature $R(\Gamma)$, instead of $R(\{\})$, and we study this “alternative action” in the metric-affine formalism for other possible

¹As a bonus, this formulation can be regarded as a “translational gauge theory” [377, 378, 379, 380].

kinds of geometries, together with the matter content:

$$S = \frac{1}{16\pi G} \int d^4x \sqrt{-g} R(\Gamma) + \int d^4x \mathcal{L}_{mat}(g, \Gamma, \Psi). \quad (7.8)$$

Consequently, we should define similar tensors to the metric formalism for variations with respect to the connection. For the gravitational sector it is:

$$P_{\mu}^{\alpha\beta} = \frac{1}{\sqrt{-g}} \frac{\delta(\sqrt{-g}R)}{\delta\Gamma_{\alpha\beta}^{\mu}}, \quad (7.9)$$

which is the Palatini tensor with 64 components and 60 of them are independent components (because it is identically traceless $P_{\alpha}^{\alpha\beta} = 0$). For the matter sector it is:

$$\Delta_{\mu}^{\alpha\beta} = -\frac{1}{\sqrt{-g}} \frac{\delta\mathcal{L}_{mat}}{\delta\Gamma_{\alpha\beta}^{\mu}}, \quad (7.10)$$

which is usually called hypermomentum tensor. Then, the equations of motion read:

$$G_{(\mu\nu)} = 8\pi G \tilde{T}_{\mu\nu} \quad (7.11)$$

$$P_{\mu}^{\alpha\beta} = 8\pi G \Delta_{\mu}^{\alpha\beta}, \quad (7.12)$$

where $\tilde{T}_{\mu\nu}$ has to be defined at constant Γ . In the Palatini approach, a simpler case when we consider that matter is only coupled to the metric and not to the connection, the hypermomentum vanishes ($\Delta_{\mu}^{\alpha\beta} = 0$), and Eq. (7.12) gives us 60 constraints among the 64 independent components of the connection. In fact, these constraints can be summarized by the following form of the connection, which is a result of $P_{\mu}^{\alpha\beta} = 0$ [383, 35]²:

$$\Gamma_{\beta\alpha}^{\mu} = \{\}_{\alpha\beta}^{\mu} - \frac{1}{2} g^{\gamma\nu} Q_{\alpha\gamma\nu} \delta_{\mu\beta} = \{\}_{\alpha\beta}^{\mu} + \frac{1}{3} T^{\gamma}_{\gamma\alpha} \delta_{\beta}^{\mu}. \quad (7.13)$$

Then, there are 4 additional degrees of freedom which cannot be determined by the field equations but they can be related with either $Q^{\mu}_{\mu\nu}$ or $T^{\beta}_{\beta\alpha}$. Consequently, imposing one of these two terms to vanish is enough to produce a consistent theory where the connection will be defined by the Christoffel symbols, recovering the usual GR.

Summarizing, if GR is our gravitational theory, both formalisms are able to provide the same equations of motion after some constraints to close the system. Nevertheless, this is but an exception of GR, it will not be true for theories of modified gravity in general, and yet it can be

²Notice the important change in the definition of the Riemann tensor of these works which induces some changes in Eq. (7.13)

used to our advantage. Indeed, incorporating the connection as a new d.o.f. on the framework of modified gravity opens a complete new range of theoretical paths to explore.

Coming back to the case of flat spaces or to the notion of teleparallelism, one is able to relate the three components of the decomposition of the connection. This fact will have important consequences as it allows the possibility of rewriting General Relativity as a theory based on the torsion, or on the non-metricity when we take either the contortion or the disformation to vanish respectively. Because the purpose of this chapter is the study of theories based on the non-metricity, along the next section, we will analyze the latter case, which is the so-called Symmetric Teleparallel Gravity. It is characterised by the fact that the connection is torsionless, and consequently symmetric. In any case the underlying reasoning is exactly the same as for the other case based on the torsion, and with a vanishing non-metricity.

7.2 Symmetric Teleparallel Gravity

As we anticipated, Symmetric Teleparallel Gravity encompasses all theories where there is neither torsion $T^\alpha_{\mu\nu} = 0$, nor curvature $R^\alpha_{\beta\mu\nu}(\Gamma) = 0$. Our immediate goal is to construct an equivalent theory to General Relativity, but based on the non-metricity. Such a theory is denoted as Symmetric Teleparallel Equivalent General Relativity (STEGR) [373]. For this purpose, we need to ascertain how the Riemann tensor is transformed by a general shift of the connection of the form $\hat{\Gamma}^\alpha_{\beta\mu\nu} = \Gamma^\alpha_{\mu\nu} + \Omega^\alpha_{\mu\nu}$ where $\Omega^\alpha_{\mu\nu}$ is an arbitrary tensor which encodes the transformation. Specifically

$$\hat{R}^\alpha_{\beta\mu\nu}(\hat{\Gamma}) = R^\alpha_{\beta\mu\nu}(\Gamma) + T^\lambda_{\mu\nu}\Omega^\alpha_{\lambda\beta} + 2\nabla_{[\mu}\Omega^\alpha_{\nu]\beta} + 2\Omega^\alpha_{[\mu|\lambda|}\Omega^\lambda_{\nu]\beta}, \quad (7.14)$$

where ∇ is the covariant derivative associated to Γ . Upon inspection of the latter, one ends up realising the existence of a theory that is fully equivalent to GR (as obtained from the Levi-Civita connection), but otherwise coming only from the disformation (i.e., from the part of the connection related to the non-metricity)³. This requirement translates into $\Gamma = \{\}$, $T^\lambda_{\mu\nu} = 0$ and $\Omega^\alpha_{\mu\nu} = L^\alpha_{\mu\nu}$. If we replace those expressions in Eq. (7.14) it becomes

$$R^\alpha_{\beta\mu\nu}(\hat{\Gamma}) = R^\alpha_{\beta\mu\nu}(\{\}) + 2\nabla_{[\mu}\{L^\alpha_{\nu]\beta} + 2L^\alpha_{[\mu|\lambda|}L^\lambda_{\nu]\beta}, \quad (7.15)$$

³Note that in this theory the torsion plays no role whatsoever.

where the super-index in $\nabla^{\{\}}$ specifies the covariant derivative defined from the Levi-Civita connection.

At this step, we resort to the parallel condition of a flat spacetime that is given by the constraint $R^\alpha_{\beta\mu\nu}(\hat{\Gamma}) = 0$, which reduces the connection to the Weitzenböck form [384, 385]. Consequently, in this symmetric teleparallel framework [386], it is possible to write the Riemann tensor based on the Levi-Civita connection through the non-metricity tensor, $Q_{\alpha\mu\nu}$. Casting further light into this, one may perform a contraction of Eq. (7.15), which can be used to rewrite $R(\{\})$ (the piece we eventually need to show the equivalence at the Lagrangian level):

$$0 = R(\{\}) + \nabla_\alpha^{\{\}} \left(Q^\alpha - \tilde{Q}^\alpha \right) + \frac{1}{4} Q^{\alpha\beta\gamma} Q_{\alpha\beta\gamma} - \frac{1}{2} Q^{\gamma\alpha\beta} Q_{\alpha\gamma\beta} - \frac{1}{4} Q^\alpha Q_\alpha + \frac{1}{2} \tilde{Q}^\alpha Q_\alpha, \quad (7.16)$$

where $Q_\alpha = Q_\alpha^\mu{}_\mu$ and $\tilde{Q}_\alpha = Q^\mu{}_{\alpha\mu}$.

It is convenient now to simplify the latter expression by defining the non-metricity scalar Q as⁴:

$$Q = \frac{1}{4} Q^{\alpha\beta\gamma} Q_{\alpha\beta\gamma} - \frac{1}{2} Q^{\gamma\alpha\beta} Q_{\alpha\gamma\beta} - \frac{1}{4} Q^\alpha Q_\alpha + \frac{1}{2} \tilde{Q}^\alpha Q_\alpha. \quad (7.18)$$

Therefore, for symmetric (torsionless) and flat constraints we get:

$$R(\{\}) = -Q - \nabla_\alpha^{\{\}} (Q^\alpha - \tilde{Q}^\alpha), \quad (7.19)$$

where $\nabla_\alpha^{\{\}}$ is a total divergence term. Continuing with this lengthy scheme we can verify that, if we take the scalar of curvature obtained from the Levi-Civita connection appearing in Eq. (7.7) and we replace it with Eq. (7.19), we do as a matter of fact build a theory that is equivalent to GR up to a total derivative in the action, which, in any case, does not contribute to the equations of motion:

$$S_{GR} = \frac{1}{16\pi G} \int d^4x \sqrt{-g} R(\{\}) = -\frac{1}{16\pi G} \int d^4x \sqrt{-g} Q = S_{\text{STTEGR}}. \quad (7.20)$$

Thus, the STEGR theory and GR are equivalent frameworks of gravity, but formulated with R and Q respectively. Obviously, cosmological models following from these two settings are

⁴However, the most general even-parity second order quadratic form of the non-metricity is:

$$Q = \frac{c_1}{4} Q_{\alpha\mu\nu} Q^{\alpha\mu\nu} - \frac{c_2}{2} Q_{\alpha\mu\nu} Q^{\mu\alpha\nu} - \frac{c_3}{4} Q_\alpha Q^\alpha + \frac{c_4}{2} Q_\alpha \tilde{Q}^\alpha + (c_5 - 1) \tilde{Q}_\alpha \tilde{Q}^\alpha, \quad (7.17)$$

which is a generalisation of Eq. (7.18) that gets recovered by setting $c_1 = c_2 = c_3 = c_4 = c_5 = 1$.

completely identical, and cosmological observations would not offer any hints as to which is the underlying theory. However, we are now in a position that allows us to go one step beyond, and build $f(Q)$ models close enough to GR to make sense, but at the same time, different enough so that small modifications could ideally be spotted. In this sense we want to stress that theories stemming from actions based on Q have only begun to be explored in what regards observations. For instance, previous works like [387] adopted a more phenomenological perspective by putting forward expressions for $f(Q)$ directly as functions of the redshift with some parameters which cannot be readily associated to a specific matter/energy content. Of course, both routes are complementary, and for this reason, we feel that continuing to explore statistical examinations of the free parameters of $f(Q)$ cosmologies in the light of astrophysical data could help us discuss the suitability of $f(Q)$ in general.

7.3 $f(Q)$ cosmologies

Following the justification offered in the previous sections, and similarly to $f(R)$ theories, we are able to generalize the STEGR action to rise it to the modified gravity field with the action:

$$S = \int d^4x \sqrt{-g} \left[-\frac{1}{2}f(Q) + \mathcal{L}_M \right], \quad (7.21)$$

where STEGR is directly recovered for $f(Q) = Q/8\pi G$. Analogously to [388], we can work in the coincident gauge as the preferred reference system, which allows us to use a null connection, i.e.

$${}_{cg}\Gamma_{\mu\nu}^{\alpha} = 0 \quad \rightarrow \quad \nabla_{\alpha}g_{\mu\nu} = \partial_{\alpha}g_{\mu\nu}. \quad (7.22)$$

Besides and as usual, we will consider a spatially flat FLRW spacetime (1.18), as the homogeneous and isotropic standard spacetime to describe the Universe at large scales. However, because we have already chosen the coincident gauge, we should not forget the lapse function $N(t)$, since the diffeomorphism gauge symmetry is lost when we choose the coincident gauge (7.22), and consequently the time parametrization cannot be chosen arbitrarily [389]. Explicitly the metric will read:

$$ds^2 = -N^2(t)dt^2 + a^2(t) [dx^2 + dy^2 + dz^2]. \quad (7.23)$$

Using the definition of the non-metricity scalar (7.18), we are going to calculate it term by term. For this purpose it is important to remark that metric terms only depend on time and consequently

$$\partial_\alpha g_{\mu\nu} \rightarrow \delta_\alpha^t \partial_t g_{\mu\nu}:$$

$$\begin{aligned} Q_{\alpha\beta\gamma} Q^{\alpha\beta\gamma} &= g^{\alpha\mu} g^{\beta\omega} g^{\gamma\nu} (\partial_\alpha g_{\beta\gamma}) (\partial_\mu g_{\omega\nu}) = -\frac{1}{N^2} g^{\beta\omega} g^{\gamma\nu} (\partial_t g_{\beta\gamma}) (\partial_t g_{\omega\nu}) \\ &= -\frac{1}{N^6} (-2N\dot{N})^2 - 3\frac{1}{N^2} \frac{1}{a^4} (2a\dot{a})^2 = -4\frac{\dot{N}^2}{N^4} - 12\frac{\dot{a}^2}{N^2 a^2}, \end{aligned} \quad (7.24)$$

$$Q_{\alpha\beta\gamma} Q^{\beta\alpha\gamma} = g^{\beta\mu} g^{\alpha\omega} g^{\gamma\nu} (\partial_\alpha g_{\beta\gamma}) (\partial_\mu g_{\omega\nu}) = g^{tt} g^{tt} g^{tt} (\partial_t g_{tt}) (\partial_t g_{tt}) = -4\frac{\dot{N}^2}{N^4}, \quad (7.25)$$

$$\begin{aligned} Q_\alpha Q^\alpha &= g^{\mu\lambda} \partial_\alpha (g_{\lambda\mu}) g^{\alpha\epsilon} g^{\omega\nu} \partial_\epsilon (g_{\omega\nu}) = -\frac{1}{N^2} [g^{\mu\lambda} \partial_t (g_{\mu\lambda})]^2 \\ &= -\frac{1}{N^2} \left(4\frac{\dot{N}^2}{N^2} + 36\frac{\dot{a}^2}{a^2} + 24\frac{\dot{N}\dot{a}}{Na} \right), \end{aligned} \quad (7.26)$$

$$\tilde{Q}^\alpha = g^{\mu\lambda} Q_{\mu\lambda\alpha} = -\frac{1}{N^2} \partial_t (g_{t\alpha}), \quad (7.27)$$

$$\begin{aligned} Q_\alpha \tilde{Q}^\alpha &= g^{\mu\lambda} \partial_\alpha (g_{\lambda\mu}) g^{\alpha\epsilon} \left(-\frac{1}{N^2} \right) \partial_t (g_{t\epsilon}) = \frac{1}{N^4} g^{\mu\lambda} \partial_t (g_{\lambda\mu}) \partial_t (g_{tt}) \\ &= -4\frac{\dot{N}^2}{N^4} - 12\frac{\dot{a}\dot{N}}{aN^3}. \end{aligned} \quad (7.28)$$

Finally, putting together all these terms with the coefficients given in the definition of Q , Eq. (7.18):

$$Q = 6\frac{H^2}{N^2}. \quad (7.29)$$

Note that the terms with time derivatives of the lapse function $N(t)$ cancel each other. In addition, if we study the action of the linear case $f(Q) \propto Q$ and its equations of motion, we will see that, for the specific definition of Q with its coefficients given in (7.18), the lapse function $N(t)$ does not play any role, and the equations will be satisfied for any choice of it [389]. This fact only occurs for the specific prescription of the non-metricity scalar given in (7.18) and this will not always be true for the general expression of the non-metricity scalar \mathcal{Q} , given in (7.17). However, one wonders what happens to a general function of $f(Q)$? In order to answer this, let us write the gravitational part of (7.21) with the result of Eq. (7.29):

$$S_g = -\frac{1}{2} \int d^3x dt N(t) a^3(t) f\left(6\frac{\dot{a}^2}{N^2(t)a^2(t)}\right), \quad (7.30)$$

and we take the time reparameterization: $t \rightarrow \chi(t)$, $N(t) \rightarrow N(t)/\dot{\chi}(t)$:

$$S_g = -\frac{1}{2} \int d^3x \dot{\chi}(t) dt \frac{N(t)}{\dot{\chi}(t)} a^3(t) f\left(6\frac{1}{a^2(t)} \frac{\dot{\chi}^2(t)}{N^2(t)} \frac{\dot{a}(t)^2}{\dot{\chi}^2(t)}\right), \quad (7.31)$$

recovering the initial action of Eq. (7.30). Therefore, $f(Q)$ theories let us fix a particular lapse function, because they retain this residual time-reparameterization invariance, despite having already used diffeomorphisms to select the coincident gauge. Therefore, and for the sake of simplicity, we will take this into our advantage and choose $N(t) = 1$. After this great simplification, the cosmological equations become:

$$6f_Q H^2 - \frac{1}{2}f = \rho, \quad (7.32)$$

$$(12H^2 f_{QQ} + f_Q)\dot{H} = -\frac{1}{2}(\rho + p), \quad (7.33)$$

where in this case the sub-index denotes derivatives with respect to Q . Also, from now on the presence or the absence of the cosmological constant is encoded in ρ which takes into account all the matter species we wish to have, in a similar way to ρ_m and ρ_r under the definition: $\rho_\Lambda \equiv \Lambda c^2/(8\pi G)$. Examination of this system of equations shows that we can reproduce exactly the GR background behaviour using its Friedmann equation $H_{GR}^2 = 8\pi G\rho/3$ as in (1.21):

$$Qf_Q - \frac{1}{2}f = \frac{3H_{GR}^2}{8\pi G} = \frac{Q}{16\pi G}. \quad (7.34)$$

Solving this differential equation, one obtains an $f(Q)$ theory which mimics General Relativity:

$$f(Q) = \frac{1}{8\pi G} \left(Q + M\sqrt{Q} \right), \quad (7.35)$$

where M is a constant which can be interpreted as a mass scale [388]. The analogy between the particular case with $M = 0$ and GR should not be surprising at all, because it corresponds to the STEGR framework which was already discussed in the previous section. But the $M \neq 0$ case represents a whole class of theories with the same background as GR, whose differences do not show up at the background level, although they do at the perturbation level [390].

An alternative route is to put forward an ansatz for $f(Q)$ that includes Eq. (7.35) as a particular case in the hope that this analytical extension will let us integrate Eq. (7.32) and Eq. (7.33), but with some differences in the phenomenology at the background level. With this in mind, we are going to propose some cosmological models created from different $f(Q)$ theories in the next sections.

7.4 Extended mimetic GR theory from $f(Q)$

In this section, we are going to study the model proposed in [388], which is characterized by:

$$f(Q) = \frac{1}{8\pi G} \left[Q - 6\lambda M^2 \left(\frac{Q}{6M^2} \right)^\alpha \right], \quad (7.36)$$

where λ and α are dimensionless parameters and $M \neq 0$. Interestingly, different values of α can be chosen to construct solutions depicting new early or late Universe behaviours. It is clear that for the values $\alpha = 1/2$ and $\lambda = -1/\sqrt{6}$ one recovers the exact function of the mimetic General Relativity (7.35), and the case $\lambda = 0$ will recover General Relativity at all levels. From Eq. (7.36) and using Eq. (7.29), the Friedmann equation (7.32) can be integrated to yield

$$H^2 \left[1 + (1 - 2\alpha)\lambda \left(\frac{H^2}{M^2} \right)^{\alpha-1} \right] = \frac{8\pi G}{3} \rho. \quad (7.37)$$

Note that from this last expression of the Hubble function one is able to recognize an identical background evolution to that of GR for either $\lambda = 0$, or $\alpha = 1/2$, as expected. In addition, the case for $\alpha = 1$ follows the same dynamics as GR after a redefinition of G .

In this section, though, we will follow [388] and set the focus on the $\alpha = -1$ case, which leads to a solution with two possible branches:

$$H_{\pm}^2 = \frac{4\pi G}{3} \rho \left(1 \pm \sqrt{1 - \frac{27\lambda M^4}{(4\pi G\rho)^2}} \right), \quad (7.38)$$

where ρ is the sum of all energy densities (as customary it will be regarded as positive). The correction with respect to the GR case becomes larger as ρ decreases, so the new degree of freedom plays the effective role of dark energy. Note the considerable level of non-linearity at play in Eq. (7.38). As we already anticipated, in order to be able to exploit the predicting capabilities of an assortment of cosmological data sets, we consider that our Universe's evolution is driven by the three usual kinds of matter-energy: cosmic dust, radiation and a cosmological constant.

The explicit presence of a cosmological constant might seem redundant or unnecessary, as we rather want to explore geometric corrections that mimic its effect. However, it will become clear that, as far as statistical comparisons are concerned, the presence of such a term renders the whole analysis far more palpable.

Additionally, the whole lot of standard matter-energy fields will satisfy the continuity equation (1.27):

$$\dot{\rho} = -3H(\rho + p) , \quad (7.39)$$

With our choices of (barotropic) matter and additionally to the evolution of the energy densities (1.28), one is able to express:

$$\frac{\rho_i(a_t)}{\rho_i(a_0)} = \frac{a_t^{-3(1+\omega_i)}}{a_0^{-3(1+\omega_i)}} = \frac{1}{a_t^{3(1+\omega_i)}} , \quad (7.40)$$

where a_0 is the normalized scale factor at the present time, and a_t is the scale factor at some time t . In addition, using (1.23) we can define Ω_i at the present time as:

$$\Omega_i(a_0) = \frac{8\pi G}{3H_0^2} \rho_i(a_0) . \quad (7.41)$$

In order to save notation, and as usual in the literature, from now on we do not write the argument a_0 of Ω_i when it is referred to at the present time, i.e. $\Omega_i(a_0) \equiv \Omega_i$ (and this argument will be explicitly written at a different $a(t)$). At the end of the day, we obtain the important definition:

$$\rho_i(a_t) = \frac{3H_0^2}{8\pi G} \Omega_i (1+z)^{3(1+\omega_i)} , \quad (7.42)$$

in which we can include the parametrization of the cosmological constant as we already said in the previous section. Specifically, for the three components usually considered, namely dust-matter ($\omega_m = 0$), radiation ($\omega_r = 1/3$), and cosmological constant ($\omega_\Lambda = -1$):

$$\rho_m(z) = \frac{3H_0^2 \Omega_m}{8\pi G} (1+z)^3, \quad \rho_r(z) = \frac{3H_0^2 \Omega_r}{8\pi G} (1+z)^4, \quad \rho_\Lambda = \frac{3H_0^2 \Omega_\Lambda}{8\pi G}, \quad (7.43)$$

with the sum of the three defining ρ :

$$\rho(z) = \frac{3H_0^2}{8\pi G} [\Omega_\Lambda + \Omega_m (1+z)^3 + \Omega_r (1+z)^4] , \quad (7.44)$$

where we let Ω_Λ , Ω_m and Ω_r stand for current values of the fractional densities of the three cosmological fluids comprising our matter-energy lot. Under this whole set of prescriptions, the way to recover the Λ CDM setting, for the positive branch, is to take

$$H_+^2|_{\Omega_Q=0} = H_{\Lambda\text{CDM}}^2 \equiv \frac{8\pi G}{3} \rho(z) , \quad (7.45)$$

where Ω_Q must encode all the new phenomenology. To calculate it, we can resort to usual “normalization” of the Hubble parameter, which will also allow us to lighten the notation whenever possible:

$$E(z = 0) = \frac{H_{\pm}(z = 0)}{H_0} = 1. \quad (7.46)$$

This gives us the ligature

$$-\frac{M^4\lambda}{H_0^4} = \frac{1}{3}(1 - \Omega_{\Lambda} - \Omega_m - \Omega_r) \equiv \frac{\Omega_Q}{3}, \quad (7.47)$$

which can be seen to hold for both branches (obviously, the standard Λ CDM normalization condition follows from choosing $\Omega_Q = 0$). Besides, we will say that Ω_{Λ} , Ω_m and Ω_r are primary parameters, in contrast to Ω_Q which is a derived one.

In addition, let us remark a peculiarity from the previous normalization. When it is carried out for the positive branch, one of the intermediate steps is:

$$\sqrt{1 - \frac{12\lambda M^4}{H_0^4(\Omega_{\Lambda} + \Omega_m + \Omega_r)^2}} = \frac{2 - \Omega_{\Lambda} - \Omega_m - \Omega_r}{\Omega_{\Lambda} + \Omega_m + \Omega_r}. \quad (7.48)$$

Because the left hand side of this equation is positive, the right hand side must be positive as well. Therefore, it is also necessary to impose the condition $0 < \Omega_{\Lambda} + \Omega_m + \Omega_r < 2$, and this condition lets Ω_Q take negative values. By contrast, a healthy behaviour enabling the normalization in the negative branch would demand either $\Omega_{\Lambda} + \Omega_m + \Omega_r > 2$ or $\Omega_{\Lambda} + \Omega_m + \Omega_r < 0$ (clearly the second condition makes no sense physically).

After these convenient remarks, we can use Eq. (7.47) to rewrite the Hubble function as a function of the free parameters that will be fitted at a later stage in this section:

$$H_{\pm}^2 = \frac{H_0^2}{2} [\Omega_{\Lambda} + \Omega_m(1+z)^3 + \Omega_r(1+z)^4] \left(1 \pm \sqrt{1 + \frac{4\Omega_Q}{[\Omega_{\Lambda} + \Omega_m(1+z)^3 + \Omega_r(1+z)^4]^2}} \right), \quad (7.49)$$

recalling that Ω_Q will be constrained by the ligature (7.47).

Up to this point, we have kept our discussion as general as possible, but in the remainder we will consider the positive branch only, because the negative one depicts a Hubble parameter which decreases as z increases, and therefore seems quite unlikely to match observational evidences.

Obviously, at high redshifts the contribution of Ω_Q becomes negligible and one recovers the usual Λ CDM Hubble parameter, as we have already mentioned. However, at the asymptotic future one rather has

$$\lim_{\rho_m, \rho_r \rightarrow 0} H_+^2 = \frac{1}{2} H_0^2 \left[\Omega_\Lambda + \sqrt{\Omega_\Lambda^2 + 4\Omega_Q} \right], \quad (7.50)$$

and for the extremal case without a cosmological constant, i.e. $\Omega_\Lambda = 0$, we have $H_{ds}^2 = H_0^2 \sqrt{\Omega_Q}$.

It is clear that in order to guarantee the physicality of our expression in this particular regime, we should impose more restrictive conditions (which are translated into priors), as for instance the positivity of Ω_Q for the case without cosmological constant, or $\Omega_\Lambda^2 > -4\Omega_Q$ for the general case. This subject is related to the possible appearance of sudden cosmological singularities. Interestingly, if such singularities were to occur, then the above physicality conditions would no longer be necessary, as the singularity would happen earlier than the asymptotic future above considered. Again, the parameter space could be restricted through priors to preclude such singular behaviour. However, we will rather let data speak for themselves, and see whether observations end up favouring parameter values capable of causing trouble in the negative redshift region (where they really offer no control).

From a wider perspective, one could also wonder about the particular case of the $f(Q)$ model studied in this section that follows from setting $\Omega_\Lambda = 0$, thus letting the effects of non-metricity account entirely for the dark energy sector allowing us to waive the presence of a cosmological constant or any other form of dark energy altogether. Although this scenario might seem too optimistic, we will examine it too.

7.4.1 MCMC analysis and results

The connection between theory and observations arises from the possibility to write useful prescriptions for cosmological applications. In this case, we have been able to compute the Hubble parameter analytically for a class of non-metricity spacetime geometries [388], which we have decided to call here the extended mimetic GR theory.

The main objective of this section is to perform a statistical analysis in order to obtain the tightest possible constraints on the parameters of the $f(Q)$ model given in the positive branch of (7.49) and under the previous assumptions of matter-energy content, to be able to describe

the cosmological background. Results will shed some light as to whether non-metricity effects are compatible with observations, thus opening a new window of interest on the possibility of an underlying modified gravity description of our Universe. Interestingly, the GR limit of the modified gravity framework will be easily recognisable, thus allowing for a neat statistical analysis.

The tests will be implemented using an MCMC code [391, 392] (see Section 6), which, upon minimization of a total χ^2 , will produce proficient fits of the values of Ω_m , h , Ω_Λ , Ω_Q and Ω_b ; and, by the same token, this analysis will also produce selection criteria permitting us to draw unimpaired conclusions. In order to narrow down our conclusions we will combine the different background astrophysical probes of known statistical relevance exposed in Section 6.3.

However, we should refer some more statistical considerations before applying the MCMC. Let us bring back the prior concept at this point. Recall that the prior distribution encodes the previous knowledge about the probability that a free parameter takes a certain value. Therefore, our results are forced to be obtained under the assumption of some priors, which give some room to modified gravity features, enforce the choice of the right branch and preclude nonphysical behaviour and pronounced departures from the well established standard evolution (the Λ CDM golden pattern). For this case, the flat priors will be:

- $0 < \Omega_r < \Omega_b < \Omega_m$,
- $0 < h < 1$,
- $0 < \Omega_m + \Omega_\Lambda + \Omega_r < 2$.

Thus, we can appreciate that the first two priors have the purpose of obtaining a model close to Λ CDM, whilst the last one is the mathematical condition to guarantee the physicality of the Hubble parameter. We stress again that according to our earlier discussion, and in view of these priors, Ω_Q can be either positive or negative.

In addition, it seems logical that we prefer priors that have the least possible influence in our results, i.e. we want to guarantee a certain framework but without forcing the fit of the parameters to any given value. This is the reason why we have taken flat priors, where the probability of a parameter is the same within a range of values, and zero outside of it.

Once we have laid the groundwork of the MCMC for this cosmological model, we will only

have to apply the algorithm. The convergence of the results is checked by applying the MCMC three times with 50.000, 100.000 and 200.000 iterations respectively, after which we check if the jump factors are small enough and almost do not change in the last two chains, and if the form of the posterior probability is sufficiently Gaussian.

We will also perform the same study (with the same previous knowledge, i.e. the same priors, whenever possible) for the Λ CDM model and for the $f(Q)$ model but imposing $\Omega_\Lambda = 0$ to check whether this scenario is capable of reproducing the observations without the need of a cosmological constant. Of course, it is not possible to apply the last prior in the Λ CDM model where $\Omega_m + \Omega_\Lambda + \Omega_r = 1$, being this the only difference as far as the priors are concerned. The scenario of $f(Q)$ with $\Omega_\Lambda = 0$ would be of interest as to avoid the problems associated with the cosmological constant. Although some insight into this particular setting can be easily drawn from the more general $f(Q)$ one, we treat it in full so that our conclusions are more complete and precise.

Consequently, at the end of the day, we will be able to compare the three models/cases and say something about the preferred one. Recall that the cosmological data used in the MCMC analysis for an observational scrutiny of both Λ CDM and the $f(Q)$ given by Eq. (7.49) are Type Ia Supernovae with Pantheon data, the expansion rate data from early-type galaxies as cosmic chronometers with *Hubble* data, Cosmic Microwave Background shift parameters from *Planck* 2018, and Baryon Acoustic Oscillations data. With the purpose of being as pedagogical as possible, we will show the MCMC fittings for each set of data separately with their respective χ^2 , and the sum of all them which build the total χ^2 . Then we will find the values of the parameters which minimize each of those individual contributions (with the pertinent errors) in order to appreciate the contribution of each data set, and after this we will repeat the procedure but using the total χ^2 .

However, strictly speaking, our “best fits” will be drawn from the median of the posterior, so that we account for deviations from perfect Gaussianity, which will also be reflected in asymmetrical errors. Thus, even though we will loosely talk about “best-fits”, the remark we just made will have to be taken into account at all times. Our best fits report of the (three) models are arranged in Table 7.1, so as to make the conclusions readier to be drawn. Let us emphasize that Ω_Q is a characteristic parameter of the $f(Q)$ scenario, a signature of it that does not appear at all in the Λ CDM setting.

Table 7.1: MCMC best fits and errors. Quantities in italic correspond to secondary parameters.

		Pantheon	Hubble	CMB	BAO	Total
Ω_m	Λ CDM	$0.298^{+0.022}_{-0.021}$	$0.327^{+0.066}_{-0.056}$	$0.316^{+0.007}_{-0.007}$	$0.320^{+0.016}_{-0.015}$	$0.323^{+0.005}_{-0.005}$
	$f(Q)_{\Omega_\Lambda \neq 0}$	$0.337^{+0.075}_{-0.073}$	$0.341^{+0.070}_{-0.060}$	$0.346^{+0.092}_{-0.080}$	$0.323^{+0.020}_{-0.017}$	$0.325^{+0.007}_{-0.007}$
	$f(Q)_{\Omega_\Lambda = 0}$	$0.400^{+0.024}_{-0.024}$	$0.350^{+0.057}_{-0.049}$	$0.238^{+0.006}_{-0.006}$	$0.348^{+0.016}_{-0.016}$	$0.285^{+0.004}_{-0.004}$
Ω_b	Λ CDM	—	—	$0.0491^{+0.0006}_{-0.0006}$	$0.063^{+0.012}_{-0.031}$	$0.0496^{+0.0004}_{-0.0004}$
	$f(Q)_{\Omega_\Lambda \neq 0}$	—	—	$0.057^{+0.014}_{-0.012}$	$0.081^{+0.019}_{-0.036}$	$0.0501^{+0.0010}_{-0.0010}$
	$f(Q)_{\Omega_\Lambda = 0}$	—	—	$0.0371^{+0.0005}_{-0.0005}$	$0.042^{+0.011}_{-0.021}$	$0.0407^{+0.0004}_{-0.0004}$
h	Λ CDM	—	$0.678^{+0.031}_{-0.031}$	$0.675^{+0.005}_{-0.005}$	> 0.65	$0.670^{+0.003}_{-0.003}$
	$f(Q)_{\Omega_\Lambda \neq 0}$	—	$0.674^{+0.039}_{-0.054}$	$0.645^{+0.090}_{-0.071}$	> 0.62	$0.667^{+0.007}_{-0.007}$
	$f(Q)_{\Omega_\Lambda = 0}$	—	$0.703^{+0.029}_{-0.030}$	$0.777^{+0.007}_{-0.007}$	> 0.70	$0.730^{+0.004}_{-0.004}$
Ω_Λ	Λ CDM	$0.701^{+0.021}_{-0.022}$	$0.673^{+0.056}_{-0.066}$	$0.684^{+0.007}_{-0.007}$	$0.680^{+0.015}_{-0.016}$	$0.677^{+0.005}_{-0.005}$
	$f(Q)_{\Omega_\Lambda \neq 0}$	$0.43^{+0.47}_{-0.49}$	$0.64^{+0.59}_{-0.60}$	$0.87^{+0.43}_{-0.57}$	$1.11^{+0.21}_{-0.18}$	$0.701^{+0.054}_{-0.053}$
	$f(Q)_{\Omega_\Lambda = 0}$	—	—	—	—	—
Ω_Q	Λ CDM	—	—	—	—	—
	$f(Q)_{\Omega_\Lambda \neq 0}$	$0.23^{+0.42}_{-0.40}$	$0.03^{+0.58}_{-0.61}$	$-0.22^{+0.65}_{-0.52}$	$-0.43^{+0.18}_{-0.22}$	$-0.027^{+0.057}_{-0.058}$
	$f(Q)_{\Omega_\Lambda = 0}$	$0.599^{+0.023}_{-0.024}$	$0.650^{+0.049}_{-0.057}$	$0.762^{+0.006}_{-0.006}$	$0.651^{+0.016}_{-0.016}$	$0.715^{+0.004}_{-0.004}$
χ^2	Λ CDM	1035.77	14.49	0.001	16.55	1072.19
	$f(Q)_{\Omega_\Lambda \neq 0}$	1035.72	14.40	0.005	11.34	1072.01
	$f(Q)_{\Omega_\Lambda = 0}$	1036.48	14.53	0.003	51.34	1207.96
χ^2_{red}	Λ CDM	—	—	—	—	0.98
	$f(Q)_{\Omega_\Lambda \neq 0}$	—	—	—	—	0.98
	$f(Q)_{\Omega_\Lambda = 0}$	—	—	—	—	1.10
$\mathcal{B}_{\Lambda CDM}^i$	Λ CDM	—	—	—	—	1
	$f(Q)_{\Omega_\Lambda \neq 0}$	—	—	—	—	0.76
	$f(Q)_{\Omega_\Lambda = 0}$	—	—	—	—	$3 \cdot 10^{-30}$
$\ln \mathcal{B}_{\Lambda CDM}^i$	Λ CDM	—	—	—	—	0
	$f(Q)_{\Omega_\Lambda \neq 0}$	—	—	—	—	-0.27
	$f(Q)_{\Omega_\Lambda = 0}$	—	—	—	—	-68

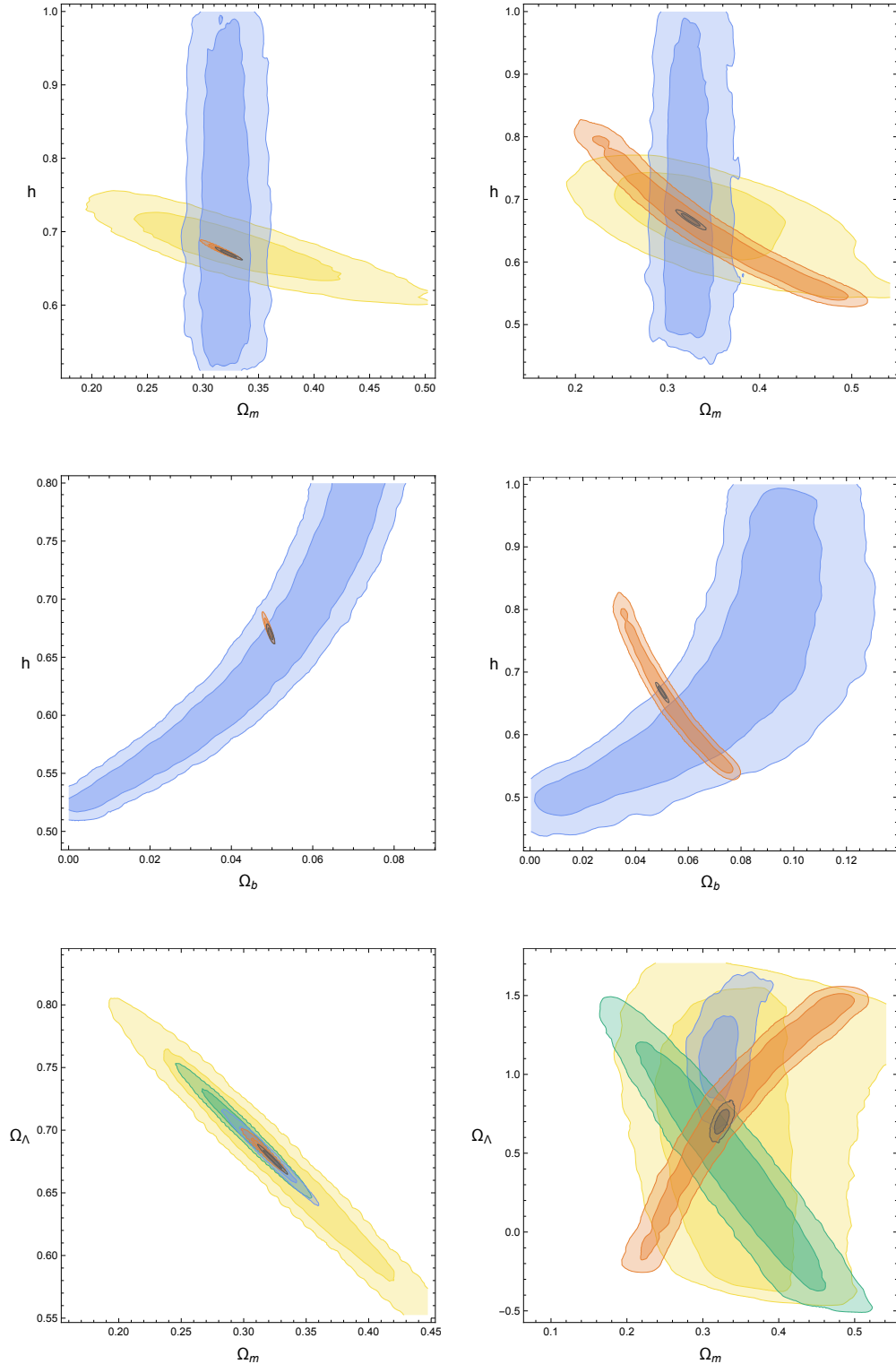


Figure 7.1: Contour plots for the Λ CDM model (left column) and the $f(Q)$ model with $\Omega_\Lambda \neq 0$ (right column) with the following color scheme: green - SNeIa, yellow - Hubble data, orange - *Planck 2018* CMB, blue - BAO data, black - all sets of data. As SNeIa are (of course) unable to fix the value h , their contours are missing from those plots where constraints on h is shown; for the same reason, both SNeIa and Hubble contours are absent from plots showing constraints on Ω_b .

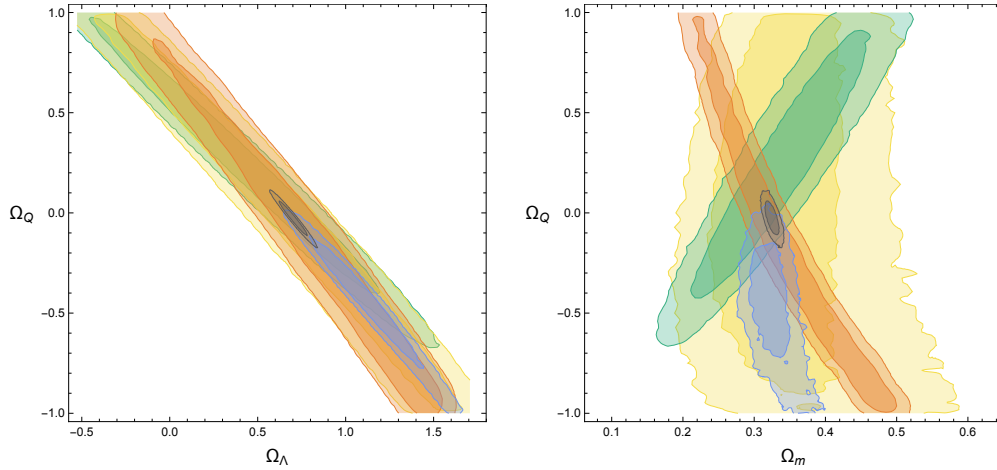


Figure 7.2: Contour plots for the $f(Q)$ model with $\Omega_\Lambda \neq 0$ with the following color scheme: green - SNeIa, yellow - Hubble data, orange - *Planck 2018* CMB, blue - BAO data, black - all sets of data.

For additional discernment, we present the marginalized confidence contours directly as drawn from the MCMC procedure providing our best fits. This supplies visual hints of the complementarity of different data sets, their constraining power, and correlation among parameters. The comparison of the contour plots for Λ CDM and $f(Q)$ with $\Omega_\Lambda \neq 0$ can be found in Fig. 7.1, while specific results of the $f(Q)$ model are presented separately in Fig. 7.2. Finally, results for $f(Q)$ with $\Omega_\Lambda = 0$ are shown in Fig. 7.3. For each individual data set or data set combination we draw the contours by choosing two shades of a single colour, and we let the dark and light hues represent the 1σ and 2σ regions respectively.

One of the main conclusions of the MCMC analysis is that in the case of $f(Q)$ with $\Omega_\Lambda \neq 0$ the combination of data sets yields a tiny negative value of Ω_Q . Specifically it lies in a significantly wide uncertainty range that makes it compatible with a null value at the 1σ level (see Table 7.1 and the black contour in Fig. 7.2). This compatibility with a vanishing Ω_Q applies for all the separate data sets except for BAO, which not only bet on a larger negative value only compatible with $\Omega_Q = 0$ at the 2σ level, but also exhibit much lower errors (at least twice smaller) than other probes. The large uncertainty in Ω_Q can undoubtedly be associated to that in Ω_Λ . It is visually manifest that the two parameters are mutually quite (anti)correlated for all data sets, as the inclination of the contours is very close to -45° . This significant negative correlation, expected from Eq. (7.47), makes the large degree of uncertainty in the Ω_Λ induce the same behaviour on Ω_Q . Interestingly, the negative best fit value of Ω_Q hints at the interest of

exploring and characterizing sudden future singularities in these models.

A second outcome is that, independently of the values of Ω_Λ and Ω_Q , the fits of the other two parameters, Ω_m and h , are very similar in the $f(Q)$ and Λ CDM scenarios. This makes sense considering previous arguments, since shifts in Ω_Λ are reabsorbed into Ω_Q and vice-versa, affecting quite little the rest of parameters. A reflection of this fact are the very similar χ^2 values displayed by both models in Table 7.1.

But we may also note that, although the Λ CDM and $f(Q)$ with $\Omega_\Lambda \neq 0$ models yield similar best fits of Ω_m and Ω_Λ , the distinctive feature encoded in Ω_Q changes quite significantly the correlations between those two parameters (see the bottom row of Fig. 7.1).

However the behaviour of Ω_m and h is approximately similar in both models (see top row of Fig. 7.1) in a broad sense and in particular in what concerns the correlation among the two parameters. Still there is a noticeable difference, which is the quite larger uncertainty on Ω_m as associated with CMB data in the case of $f(Q)$ with $\Omega_\Lambda \neq 0$. We infer accordingly that the roles of Ω_m and h seem to be quite similar at low redshifts, but the same does not apply at high redshifts for what Ω_m is concerned.

Recalling the Bayes factors, the conclusion is (again) that, within the current data sets, we are not able to distinguish one model from the other. This reasoning is obviously drawn from a background examination, a perturbative one might propound more refined pieces of information (some results along this route were sketched in [388]).

We now may come back to the possibility of imposing $\Omega_\Lambda = 0$. Fig. 7.2 provides insight on this matter as it shows that Ω_Λ is enormously correlated with Ω_Q ; for that reason that parameter could in principle take the role of the cosmological constant, and thus gives the same evolution. In such case though the model would be irreducible to Λ CDM, as it can be seen inspecting Eq. (7.49). However, a look at the contours of Fig. 7.2 that corresponds to $\Omega_\Lambda = 0$ suggests that this value is clearly disfavoured. Nevertheless, we perform a direct MCMC analysis to confirm such concerns.

The strong tension among all single data sets in this restricted scenario becomes manifest in Fig. 7.3. Paradoxically, the CMB constraints are much better than those derived in the $f(Q)$ case with $\Omega_\Lambda \neq 0$, but they require an abnormally low value for Ω_m which is not consistent with any of the other probes considered. Moreover, although the single χ^2 are comparable with those from other frameworks, we must note that BAO impose very poor constraints, and that

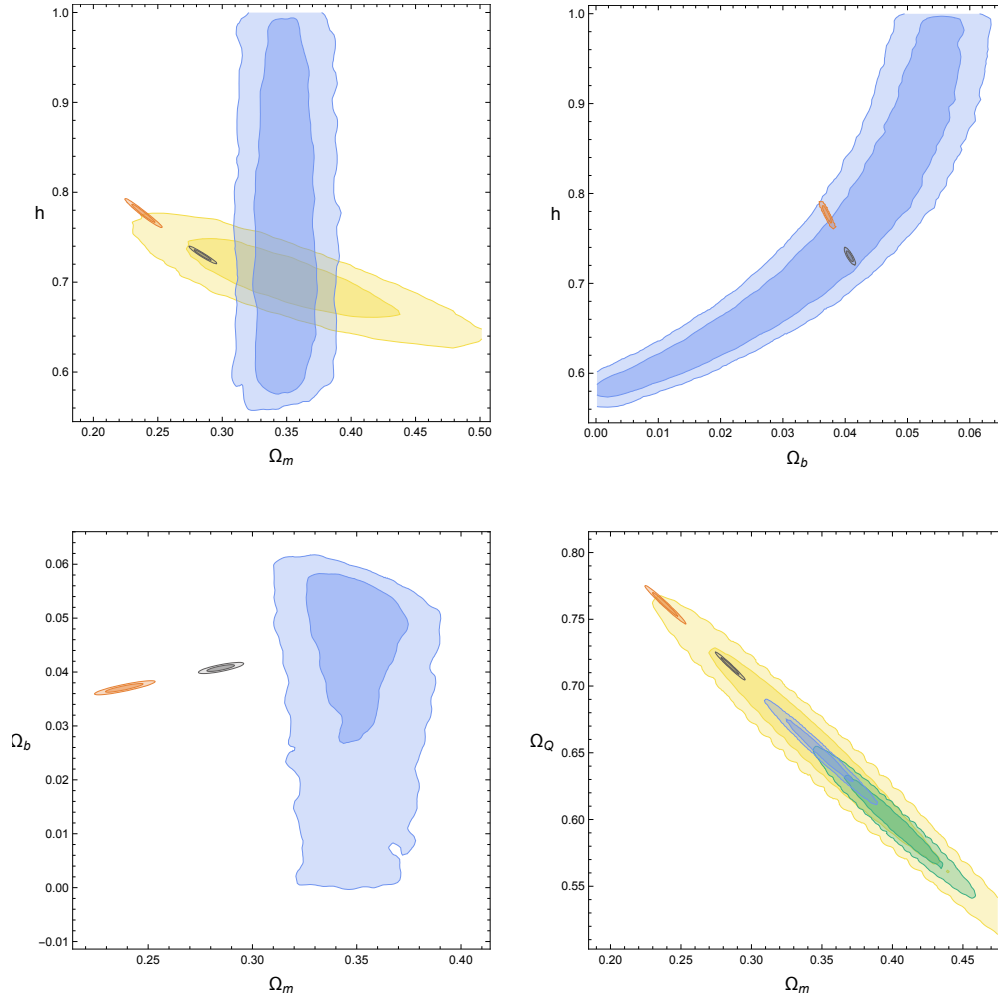


Figure 7.3: Contour plots for the $f(Q)$ model with $\Omega_\Lambda = 0$ using the following color scheme: green - SNIa; yellow - Hubble data; orange - *Planck 2018* CMB; blue - BAO data; black - all sets of data.

the best χ^2 fit coming from the joint use of all the probes is much larger. If we finally look at the values of the Bayes factors, we can see how this scenario is frankly statistically disfavoured with respect to the other cases.

7.4.2 Cosmographic parameters

It is useful to examine other quantities which offer a clearer picture of the evolutionary features of the particular FLRW spacetime under study. In fact, once constraints on Ω_m , h , Ω_Λ , Ω_Q and Ω_b are obtained through our MCMC procedure, we can also draw inferences on the well-known

cosmographic parameters, which follow from the Taylor expansion of the scale factor:

$$a(t) = a_0 \left[1 + H_0 \Delta t - \frac{q_0}{2} H_0^2 \Delta t^2 + \frac{j_0}{3!} h_0^3 \Delta t^3 + \frac{s_0}{4!} h_0^4 \Delta t^4 + O(\Delta t^5) \right]. \quad (7.51)$$

In the latter we have defined $\Delta t = t - t_0$ while q_0 , j_0 and s_0 are the so-called deceleration, jerk and snap parameters respectively evaluated at t_0 (present time) [393, 394]. Explicit expressions to evaluate them at any given t (or redshift z) are:

$$q(t) = -\frac{a\ddot{a}}{\dot{a}^2} \rightarrow q(z) = -1 + (1+z) \frac{E'(z)}{E(z)}, \quad (7.52)$$

$$j(t) = \frac{a^2 \dot{\ddot{a}}}{\dot{a}^3} \rightarrow j(z) = (1+z)^2 \frac{E''(z)}{E(z)} + q^2(z), \quad (7.53)$$

$$s(t) = \frac{a^3 \ddot{\ddot{a}}}{\dot{a}^4} \rightarrow s(z) = -(1+z)j'(z) - 2j(z) - 3q(z)j(z), \quad (7.54)$$

where in this case the dot and the prime denote differentiation with respect to cosmic time and z respectively.

Thus, following these expressions and using the results of the MCMC, we can compute the cosmographic parameters deceleration q_0 , jerk j_0 , and snap s_0 to add more elements to the comparison between the kinematics of the two models, where the sub-index 0 means the value at the present time. Table 7.2 summarizes our findings: All best fits share a small uncertainty which is much larger in the $f(Q)$ case than in the Λ CDM case. In addition, the values for the $f(Q)$ model fall completely within the 1σ region of their respective counterparts in the former ones.

Table 7.2: Best fits of the cosmographic parameters.

	q_0	j_0	s_0
Λ CDM	$-0.515^{+0.007}_{-0.007}$	$1.000186^{+2 \cdot 10^{-6}}_{-2 \cdot 10^{-6}}$	$-0.454^{+0.021}_{-0.021}$
$f(Q)_{\Omega_\Lambda \neq 0}$	$-0.499^{+0.040}_{-0.035}$	$0.973^{+0.053}_{-0.081}$	$-0.453^{+0.029}_{-0.039}$

Finally, to close the analysis of this model, we confront once again our modified gravity scenario with the Λ CDM model by rewriting it as a model fuelled by dark matter, radiation and dark energy following for instance [395, 396, 397, 398], by setting

$$p_{\text{eff}} = w_{\text{eff}} \rho_{\text{eff}}, \quad (7.55)$$

and

$$H^2 = H_0^2 [\Omega_m(1+z)^3 + \Omega_r(1+z)^4] + \frac{8\pi G}{3}\rho_{\text{eff}}. \quad (7.56)$$

If we combine the last two expressions with the continuity equation, Eq. (7.39), we finally write the general expression:

$$w_{\text{eff}}(z) = \frac{2(1+z)\frac{d \ln E(z)}{dz} - E^{-2}(z)\Omega_r(1+z)^4 - 3}{3(1 - E^{-2}(z)[\Omega_m(1+z)^3 + \Omega_r(1+z)^4])}. \quad (7.57)$$

The explicit expression of w_{eff} for our modified gravity model is too complicated for it to convey readily usable information, so we resort to plot it as a function of a in Fig. 7.4, using the best fit values coming from the MCMC analysis. In addition, we are able to calculate the value of w_{eff} at the present day for the $f(Q)$ model consistent with the MCMC results:

$$w_{\text{eff}}|_{z=0} = -0.987^{+0.032}_{-0.027} \quad (7.58)$$

Once again we find an indication that the best fit values of the parameters of our model are very similar to those of Λ CDM, in fact, $w_{\text{eff}} = -1$ is perfectly inside the 1σ interval.

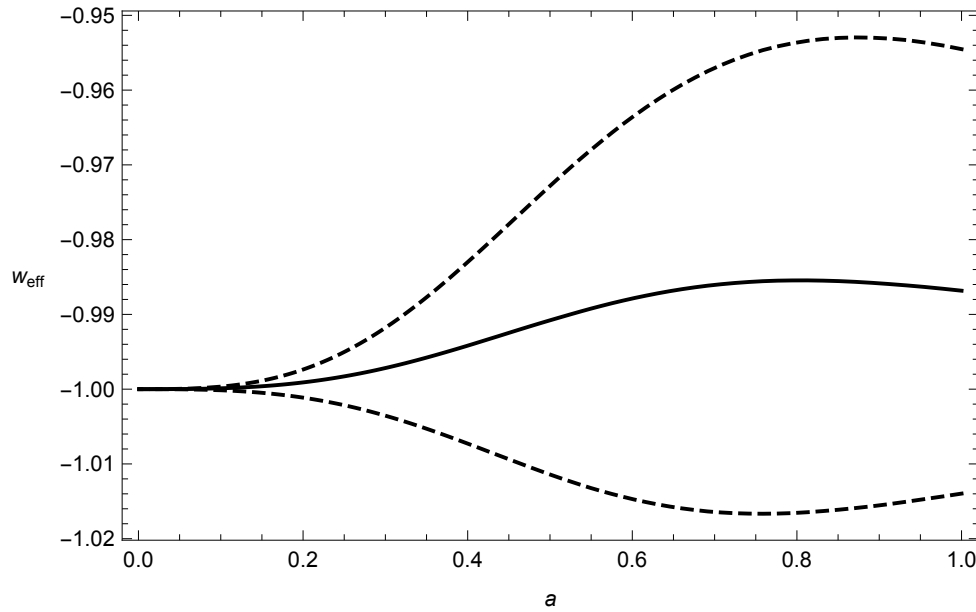


Figure 7.4: Evolution of w_{eff} as function of a . The solid line is the value as drawn from the best fit, whilst the dashed lines mark the boundaries of the confidence interval.

7.4.3 Conclusions about the extended mimetic GR theory from $f(Q)$ model

Recent works in the field have been inspired by the realization that, in the symmetric teleparallel framework, the GR Lagrangian density can be written⁵ by basically replacing the scalar of curvature built from the Levi-Civita connection with the non-metricity Q .

The former framework can be generalized upon replacement of Q with a specific $f(Q)$ given by Eq. (7.35), which reproduces the GR background behavior (and the Λ CDM model when we consider dust, radiation and the cosmological constant). Interestingly, the fact that this new setup is not exactly that of GR might have implications at the perturbative level, which is (also) beyond our specific concerns.

The particular action considered at this level allows us to make progress towards yet another form for $f(Q)$ that becomes the core of this section. We present it in Eq. (7.36) and it lets us derive an exact expression for the Hubble parameter under some parameter specifications. The grand picture is then that it resembles the standard evolution and therefore is worthing to be observationally tested. To that end we resort to the MCMC method to constraint the free parameters in the theory, and compare the values obtained with those of the Λ CDM scenario.

Our main conclusion is that the parameter which encodes the difference between the two evolutions at the background level is very close to zero when all data sets are combined. This parameter, which we have dubbed Ω_Q , gets positive best fit values for some data sets while it is negative for others, but in all cases the errors make the best fit perfectly compatible with a null value; thus an overall smaller best fit (almost zero value) is the most admissible consequence. The same conclusion follows from the Bayesian evidence: According to the Jeffreys' scale no model is preferred over the other.

A complementary study of the cosmographic parameters yields values which, once more, only reflect the striking similarity of the best fits between Λ CDM and our $f(Q)$. Notice in this respect that, for the modified gravity model, these parameters are more poorly constrained as their complexity penalizes error propagation. Finally, and for the sake of further interpretation of the kind of evolution our best fit scenario depicts, we have computed the corresponding w_{eff} . As expected, the value is very close to -1 .

For all these reasons we have seen that a yet another (promising/intriguing) cosmological

⁵Up to small details which are not really relevant at a summary level of discussion

candidate to become an alternative to Λ CDM cannot be considered a real challenger, at least at the background level.

7.5 Building up modified gravity models based on $f(Q)$

One of the great features of the Friedmann equation (7.32) is that it allows us to write the energy density ρ as a function of Q to mimic some models of modified gravity as follows:

$$Qf_Q - \frac{1}{2}f = b(Q) . \quad (7.59)$$

So, we can propose generic $b(Q)$ functions so that the latter equation can be integrated, similarly to the case where we mimicked the background of General Relativity (7.34) showed in the previous section. As Eq. (7.59) is a first order non-homogeneous ordinary differential equation, it is not difficult to reduce its solution to a quadrature for any ansatz:

$$f(Q) = \sqrt{Q} \int \frac{b(Q)}{Q^{3/2}} . \quad (7.60)$$

Although this formal result may in principle serve as a guidance to propose other ansätze, we just regard it as anecdotal information, because only judicious choices of $f(Q)$, combined with (7.32), render results which are invertible, and thus lead to expressions of H^2 as explicit functions of ρ .

This strategy sets off by proposing a form of $b(Q)$ which, upon integration of Eq. (7.59), produces an explicit expression of $f(Q)$ that we insert back into (7.32). Then, using Eq. (7.29) we finally can relate H^2 to ρ through an implicit equation. In general these equations will not be solvable for H , thus making it very complicated to significantly progress, as we already discussed. Fortunately, an array of cases can be found where this difficulty is overcome.

In this section, we are going to present two new such scenarios based on DGP models of modified gravity, and examine them. Those two cases will be found by putting forward ansätze for $f(Q)$ which include the General Relativity as a particular case ($b(Q) = Q/16\pi G$), and assess whether this may prove a promising route.

However, let us briefly introduce at this point the DGP models independently of the $f(Q)$ bodywork to understand them in the framework of modified gravity. These models are based on one of the extensions of gravity that we have not yet analyzed in depth: extra-dimensions.

We should start this brief introduction by saying that DGP refers to the authors of this model: G. Dvali, G. Gabadadze, and M. Porrati, who introduced the theory in [399] with the action:

$$S = -\frac{1}{2\kappa^2} \int d^5 X \sqrt{G} \mathcal{R}_{(5)} - \frac{1}{2\mu^2} \int d^4 x \sqrt{|g|} R + \int d^5 X \sqrt{G} \mathcal{L}_m , \quad (7.61)$$

for a $D = (4 + 1)$ dimensional theory with a 3-brane embedded in the total 5-dimensional spacetime, and where $\kappa^2 = 8\pi G_{(5)}$, $\mu^2 = 8\pi G_{(4)}$ being $G_{(5)}$ and $G_{(4)}$ the gravitational coupling constants, G_{AB} is the 5D metric with the 5D scalar of curvature $\mathcal{R}_{(5)}$, and where capital letters run from 0 to 5, and $g_{\mu\nu}$ is the induced metric on the brane with the scalar of curvature R .

In addition, we will introduce the 5D metric:

$$\begin{aligned} ds^2 &= g_{AB} dx^A dx^B = g_{\mu\nu} dx^\mu dx^\nu + b^2 dy^2 \\ &= -N^2(t, y) dt^2 + a^2(t, y) \gamma_{ij} dx^i dx^j + b^2(t, y) dy^2 , \end{aligned} \quad (7.62)$$

where y is the new coordinate of the fifth dimension and γ_{ij} is a maximally symmetric 3-dimensional metric where $k = -1, 0, 1$ parametrizes the spatial curvature as in the FLRW metric (1.18). Moreover, we will assume that the brane is the hypersurface defined by $y = 0$. Then, the 5D Einstein equations read:

$$R_{AB} - \frac{1}{2} R_{(5)} g_{AB} = \kappa^2 S_{AB} , \quad (7.63)$$

where S_{AB} is the combination of the stress-energy tensor T_{AB} from \mathcal{L}_m with the scalar of curvature of the brane (the second term in (7.61)). The stress-energy tensor T_{AB} can be decomposed into two parts: one from the bulk content and another one from the brane. Assuming that the stress-energy tensor of the bulk is that of a cosmological constant, we can write:

$$T^A_B|_{bulk} = \text{diag}(-\rho_B, -\rho_B, -\rho_B, -\rho_B, -\rho_B) , \quad (7.64)$$

$$T^A_B|_{brane} = \frac{\delta(y)}{b} \text{diag}(-\rho_b, p_b, p_b, p_b, 0) , \quad (7.65)$$

where ρ_B is a constant and ρ_b and p_b depend only on time. In addition, it is usual to assume that there is no flow of matter along the fifth dimension, i.e. $T_{05} = 0$. Then, using Israel's junction conditions [400, 401] which relate the jump of the derivative of the metric across the brane to the stress-energy tensor inside the brane to be continuous, and using for that the extrinsic curvature tensor. Then, we obtain the generalized Friedmann equation [402]:

$$\epsilon \sqrt{H^2 - \frac{\kappa^2}{6} \rho_B - \frac{C}{a(y=0)^4} + \frac{k}{a(y=0)^2}} = \frac{\kappa^2}{2\mu^2} \left(H^2 + \frac{k}{a^2(y=0)} \right) - \frac{\kappa^2}{6} \rho_b , \quad (7.66)$$

where $\epsilon = \pm 1$ is the sign of the jump of the function da/dy across $y = 0$, corresponding to the two possibilities with different embeddings of the brane into the bulk spacetime, \mathcal{C} is a constant of integration, and the Hubble parameter H has to be defined as:

$$H = \frac{\dot{a}(y=0)}{a(y=0)N(y=0)}. \quad (7.67)$$

Then, if we take $\mathcal{C} = 0$, and consider that the bulk cosmological constant ρ_B vanishes, we get

$$H^2 + \frac{k}{a(y=0)^2} - \frac{2\epsilon}{\kappa^2} \sqrt{H^2 + \frac{k}{a(y=0)^2}} = \frac{\mu^2}{3} \rho_b, \quad (7.68)$$

which, for the flat case $k = 0$, simplifies into:

$$H^2 - 2\epsilon \frac{G_{(4)}}{G_{(5)}} H = \frac{8\pi G_{(4)}}{3} \rho_b. \quad (7.69)$$

This equation for the Hubble parameter will be one of the fundamental pieces throughout the next section.

7.5.1 DGP cosmologies from $f(Q)$ actions

Coming back to (7.59), the choice $b(Q) \propto Q$ would be responsible for the appearance of the prescriptive H^2 term in the left hand side (lhs) of the Friedmann equation [388, 403]. For this reason it may be expected that adding a term proportional to \sqrt{Q} will make an H term appear alongside H^2 , thus leading to the sort of modified Friedmann equation characterizing several modified gravity scenarios.

Let us show this is indeed the case by proposing

$$b(Q) = \frac{1}{16\pi G} \left(\alpha \sqrt{Q} + \beta Q \right) \quad (7.70)$$

in Eq. (7.59), where α and β are arbitrary constants. This equation can be integrated to give:

$$f(Q) = \frac{1}{16\pi G} \left(\alpha \sqrt{Q} \log Q + 2\beta Q \right), \quad (7.71)$$

where we have set to zero an integration constant, that would give us a term proportional to \sqrt{Q} as in General Relativity again, which really does not induce any background dynamics. Using the form that the Friedman equation takes for this $f(Q)$ setting, and translating the non-metricity

scalar into the Hubble factor through the (above mentioned and) known relation $Q = 6H^2$, we arrive at

$$H \left(\sqrt{6}\alpha + 6\beta H \right) = 16\pi G\rho. \quad (7.72)$$

Alternatively, if we opt for a more enlightening rendering of the same relation, we can write

$$H^2 + \frac{\alpha}{\sqrt{6}\beta}H = \frac{8\pi G}{3\beta}\rho. \quad (7.73)$$

An exact GR framework is recovered for the simultaneous choice $\alpha = 0$, $\beta = 1$. In addition, we obtain the solution proposed by the DGP model in Eq. (7.69) if $\beta = 1$, and $\alpha = -2\epsilon\sqrt{6}G_{(4)}/G_{(5)}$. So we have just connected two theories, independent in principle, based on extra dimensions and on the non-metricity scalar. The $\alpha < 0$ case is self accelerated, i.e acceleration will occur even if its only matter content would not produce acceleration on its own, for instance cosmic dust [404]. In opposite, the $\alpha > 0$ case is not self-accelerated, but needs dark energy on the brane. We will try to explore both models simultaneously, as long as it is possible while fixing $\beta = 1$, and to study both theories (with the same H parameter) together following a way similar to that of Section (7.4).

With this purpose, we solve either of the former two expressions for H and select the branch that corresponds to an expanding Universe ($H > 0$) to conclude:

$$H = \frac{\sqrt{6}}{12} \left(\sqrt{\alpha^2 + 64\pi G\rho} - \alpha \right). \quad (7.74)$$

Let us now make the same typical assumption for the matter-energy content of the previous section, in which it is described by a sum of the barotropic fluids of cosmic dust, cosmological constant and radiation ($\rho = \rho_m + \rho_r + \rho_\Lambda$), and where each one of them satisfies separately the standard conservation equation: $\dot{\rho}_i + 3H(1 + w_i)\rho_i = 0$, where the additional assumption of simple equations of state mediated by constant w_i parameters has been made as well.

In addition, we are able to draw some easy conclusions about the behaviour of the model, following [404], and assuming the physical condition $\rho_m, \rho_r, \rho_\Lambda \geq 0$, since upon differentiation of Eq. (7.73), we obtain:

$$\dot{H} = -\frac{4\pi G}{3}(3\rho_m + 4\rho_r) \left(1 - \frac{\alpha}{\sqrt{\alpha^2 + 64\pi G\rho}} \right), \quad (7.75)$$

from where it is clear that $\dot{H} < 0$ regardless of the sign of α .

As the Universe expands the linear term in H appearing in Eq. (7.73) ceases to be negligible as compared to the quadratic one, and the $f(Q)$ effects cannot be waived any longer. Actually, a screening of the cosmological constant arises, and an effective dark energy turns out to offer a good description. For this, we will use Eq. (7.56) or its equivalent equation expressed in terms of ρ :

$$H^2 = \frac{8\pi G}{3} (\rho_m + \rho_r + \rho_{\text{eff}}) , \quad (7.76)$$

which allows us to define:

$$\rho_{\text{eff}} = \rho_\Lambda - \frac{\sqrt{6}\alpha H}{16\pi G} . \quad (7.77)$$

Here ρ_{eff} offers a convenient way to encode the modification in a general relativistic fashion, together with an effective equation of state parameter w_{eff} :

$$\dot{\rho}_{\text{eff}} + 3H(1 + w_{\text{eff}})\rho_{\text{eff}} = 0 . \quad (7.78)$$

Combining Eq. (7.78) and Eq. (7.77) we arrive at

$$(1 + w_{\text{eff}}) = \frac{\sqrt{6}\alpha \dot{H}}{48\pi G \rho_{\text{eff}} H} , \quad (7.79)$$

which can be evaluated using the reformulation

$$\rho_{\text{eff}} = \rho_\Lambda + \frac{\alpha}{32\pi G} \left(\alpha - \sqrt{\alpha^2 + 64\pi G \rho} \right) . \quad (7.80)$$

It can be seen that for $\alpha < 0$ a phantom behaviour is excluded (as a consequence of ρ_{eff} being positive, which gets translated into $w_{\text{eff}} > -1$), whereas for $\alpha > 0$ there is no such guarantee.

The following necessary step consists in recasting our expressions as functions of redshift, thus paving the way for an observational analysis. Using the definition of ρ as a function of the redshift expressed in Eq. (7.44), as well as⁶

$$\Omega_Q \equiv \frac{\alpha}{2\sqrt{6}H_0} , \quad (7.81)$$

we arrive at the expression

$$E(z) = \sqrt{\Omega_\Lambda + \Omega_m(1+z)^3 + \Omega_r(1+z)^4 + \Omega_Q^2} - \Omega_Q , \quad (7.82)$$

⁶Alternative definitions of this parameter so that dimensionally/aesthetically would stand on the same grounds as, say, Ω_Λ will force the need to consider sign duplicities and square roots which will induce less transparency in the geometry of the space of parameters and will complicate unnecessarily the codes to perform observational tests.

recalling the prescription $H(z) = H_0 E(z)$. It is obvious then that the following applies for H as given by Eq. (7.82):

$$\lim_{\Omega_Q \rightarrow 0} H^2 = H_0^2 [\Omega_\Lambda + \Omega_m(1+z)^3 + \Omega_r(1+z)^4] , \quad (7.83)$$

recovering then the Λ CDM case. Furthermore, from Eq. (7.82) it can be seen that the non-metricity features encoded in the parameter Ω_Q are somewhat screened: explicitly, the choice $\Omega_m = \Omega_\Lambda = \Omega_r = 0$ gives a null H function for any value of Ω_Q .

On the other hand, the customary normalization condition $E(z=0) = 1$ enforces an extra condition:

$$\Omega_Q = \frac{1}{2}(\Omega_m + \Omega_\Lambda + \Omega_r - 1) . \quad (7.84)$$

Note that (from Eq. (7.82) once again) a positive Ω_Q value will slow down the expansion as compared to the Λ CDM case, whereas a negative one will exert the contrary effect. An alternative way to see this is to check that for $\alpha < 0$ the effective dark energy term is bigger than a bare cosmological constant, as Eq. (7.77) suggests. In any case, an observational inference of a large absolute value of Ω_Q would be extremely unexpected if we take into account the mounting evidence of a Universe extremely agreeable with the Λ CDM behaviour.

7.5.2 DGPish cosmologies from $f(Q)$ actions

We may explore other routes compatible with a $b(Q) \propto Q$ behaviour in an appropriate limit and thus leading to the standard H^2 term on the left hand side of the Friedmann equations, while reproducing a different behaviour in other regimes. We propose now a new case inspired by our first case, which explicitly stems from the assumption:

$$b(Q) = \frac{1}{16\pi G} \sqrt{\gamma Q + \beta^2 Q^2} , \quad (7.85)$$

where γ and β are, in principle, two arbitrary constants, even though from early lessons we may anticipate that we will have to fix $\beta = 1$ along the road. Upon integration of Eq. (7.59) we arrive at:

$$f(Q) = \frac{Q \sqrt{u(Q)} \left(\sqrt{u(Q)} - \sqrt{\gamma} \operatorname{arctanh} \left(\frac{\sqrt{u(Q)}}{\sqrt{\gamma}} \right) \right)}{8\pi G \sqrt{Qu(Q)}} , \quad (7.86)$$

where $u(Q) = \gamma + \beta^2 Q$. Keeping our discussion general for the time being, and following the same recipe as before, we obtain

$$H \sqrt{\gamma + 6\beta^2 H^2} = \frac{16\pi G}{\sqrt{6}} \rho, \quad (7.87)$$

whose solution for the positive branch of H^2 is:

$$H^2 = \frac{\sqrt{\gamma^2 + (32\pi G\beta\rho)^2} - \gamma}{12\beta^2}. \quad (7.88)$$

Besides, if the physical branch is chosen, we can go further and write:

$$H = \frac{\sqrt{\sqrt{\gamma^2 + (32\pi G\beta\rho)^2} - \gamma}}{2\sqrt{3}\beta}. \quad (7.89)$$

We can follow the same sequence of steps as for the previous case so as to shed some light on the evolution of this model, where once again we assume $\rho = \rho_m + \rho_r + \rho_\Lambda$ and $\beta = 1$. Under this assumption and upon differentiation of Eq. (7.88) we obtain

$$\dot{H} = -\frac{128\pi^2 G^2 (3\rho_m + 4\rho_r)\rho}{3\sqrt{\gamma^2 + 1024\pi^2 G^2 \rho^2}}, \quad (7.90)$$

which is definite negative under our hypotheses on the positivity of the various densities, regardless of the sign of γ . In this case, finding the explicit expression of ρ_{eff} is not so straightforward, but we can find that it reads

$$\rho_{\text{eff}} = \rho_\Lambda + \frac{3H}{8\pi G} \left(H - \frac{\sqrt{\gamma + 6H^2}}{\sqrt{6}} \right). \quad (7.91)$$

We then process our definitions and equations and eventually get:

$$(1 + w_{\text{eff}}) = \frac{\dot{H}\sqrt{6} \left[\sqrt{\gamma^2 + (32\pi G\rho)^2} - 32\pi G\rho \right]}{48\pi G\rho_{\text{eff}}H\sqrt{\gamma + 6H^2}}, \quad (7.92)$$

which can be evaluated using the reformulation:

$$\rho_{\text{eff}} = \rho_\Lambda - \rho + \frac{\sqrt{\gamma^2 + (32\pi G)^2 \rho^2} - \gamma}{32\pi G}. \quad (7.93)$$

It is clear from Eq. (7.91) that for positive ρ_Λ and H we can guarantee $\rho_{\text{eff}} > 0$ if $\gamma < 0$ (for the case with $\gamma > 0$ it is not possible to conclude the sign of ρ_{eff}), and whatever the sign of γ it follows that $\dot{H} < 0$. Consequently, we can conclude that $1 + w_{\text{eff}} < 0$ for $\gamma < 0$ necessarily.

Let us go on building from Eq. (7.89) by choosing again Eq. (7.44) as our expression for ρ as a function of redshift. For this case the normalized Hubble function reads:

$$E(z) = \sqrt{\sqrt{\left(\Omega_\Lambda + \frac{8\pi G}{3H_0^2}(\rho_m + \rho_r)\right)^2 + \Omega_Q^2} - \Omega_Q}, \quad (7.94)$$

where now

$$\Omega_Q = \frac{\gamma}{12H_0^2}, \quad (7.95)$$

and from the normalization, we obtain

$$\Omega_Q = \frac{1}{2} [(\Omega_\Lambda + \Omega_m + \Omega_r)^2 - 1]. \quad (7.96)$$

Again, for our new expression describing H^2 we see that the limit of Eq. (7.83) also happens to recover GR for $\gamma = 0$.

7.5.3 MCMC analysis and results

We apply a MCMC for these two new cases as in the previous section to fit the free parameters of both $f(Q)$ models and the Λ CDM case. Once again, we will find the values of the free parameters which maximize the posterior (probability density) produced by combining a prior (probability density) with hypothetical Gaussian likelihoods associated with a χ^2 function built for each dataset and then a combined one through the product of likelihoods or the sum of χ^2 (of course, priors can be combined as well). The only thing we should change here with respect the previous section is the respective flat priors:

- $0 \leq \Omega_m + \Omega_\Lambda + \Omega_r,$
- $0 < (\Omega_m, \Omega_\Lambda, h) < 1,$
- $\Omega_m > \Omega_b > \Omega_r.$

Take into account that the MCMC analysis for the Λ CDM is repeated because it should be done in the same statistical background in order to be compared to the new cases. This lets us draw conclusions about the statistical admissibility of our proposals. We can check that the specific constraint of Λ CDM, $\Omega_m + \Omega_r + \Omega_\Lambda = 1$, does not violate any of the priors.

Therefore, having presented the statistical course of action and having chosen the astrophysical probes, we can set forth the results of our analysis. Throughout the discussion we will often compare our findings to those in the Λ CDM case. The corresponding best fits along with those of our two $f(Q)$ models are shown on Table 7.3. Recall that the Ω_Q parameter is a signature of the $f(Q)$ scenarios alone.

As in the previous model, the reason why we will explore individual χ^2 values and their best fits is that of the possibility of estimating the contribution of each data set to the final result and conclusions. Besides, let us remember that our fits will be drawn from the median of the posterior probability to better expose deviations from perfect Gaussianity, and complementary and very relevant information will be provided through confidence contours addressing again the separate and joint data set analyses. They give us visual indications on data set complementarity, tightness of constraints, and parameter correlation. As in the previous section, in the corresponding plots (Figs. 7.5-7.6) we choose two different hues of several single colours to represent the 1σ (dark) and 2σ (light) regions, and then we associate each single colour to an individual data set or data set combination (see figure captions).

For the most standard parameters, that is, Ω_m , Ω_b and h , we conclude (mainly from Table 7.3 and Fig. 7.5) that best fits, uncertainty and data set complementarity are very much the same in the three scenarios (Λ CDM, DGP and DGPish). The most noticeable discrepancies arise when CMB data are considered alone, but for the combination of data sets differences are minimal. Stronger disagreements arise (mainly in the size of errors) in Ω_Λ due to its blurring with the new parameter Ω_Q . In any case, it would be worth exploring the effects of generalizations of our models with additional parameters, in particular if the generalizations give non-phantom models; but we leave this for future prospects.

Now, even though Ω_Λ belongs in the classical category of parameters, we must consider it separately due to its non-trivial mixing with the new parameter. From the third row of Fig. 7.5 we notice that Ω_Λ displays more uncertainty in the modified gravity models than in Λ CDM, which again, we put down to the fact that Ω_Q acts as Ω_Λ somehow, which is otherwise obvious from the Hubble function. In the DGPish case the uncertainty is way bigger than in the other two cases, there is practical no correlation whatsoever among Ω_Λ and Ω_m as shown in the contours, and the huge size of the errors makes us declare that Ω_Λ is basically unconstrained in this case.

Along the same vein, the upper row on Fig. 7.6 tells us there is indeed a high correlation

Table 7.3: MCMC best fits and errors along with other statistical estimators for Λ CDM, DGP, and DGPish models. Quantities in italic correspond to secondary parameters.

		Pantheon	Hubble	CMB	BAO	Total
Ω_m	Λ CDM	$0.297^{+0.023}_{-0.023}$	$0.328^{+0.065}_{-0.056}$	$0.316^{+0.007}_{-0.007}$	$0.320^{+0.016}_{-0.015}$	$0.323^{+0.005}_{-0.005}$
	DGP	$0.277^{+0.048}_{-0.051}$	$0.316^{+0.076}_{-0.065}$	$0.358^{+0.057}_{-0.053}$	$0.301^{+0.019}_{-0.018}$	$0.326^{+0.006}_{-0.006}$
	DGPish	$0.307^{+0.027}_{-0.026}$	$0.326^{+0.066}_{-0.055}$	$0.310^{+0.009}_{-0.014}$	$0.320^{+0.016}_{-0.015}$	$0.322^{+0.005}_{-0.005}$
Ω_b	Λ CDM	—	—	$0.0490^{+0.0006}_{-0.0006}$	$0.057^{+0.010}_{-0.024}$	$0.0496^{+0.0004}_{-0.0004}$
	DGP	—	—	$0.0557^{+0.0089}_{-0.0083}$	$0.066^{+0.013}_{-0.027}$	$0.051^{+0.001}_{-0.001}$
	DGPish	—	—	$0.0483^{+0.0009}_{-0.0021}$	$0.056^{+0.010}_{-0.025}$	$0.0494^{+0.0005}_{-0.0005}$
h	Λ CDM	—	$0.677^{+0.031}_{-0.031}$	$0.675^{+0.005}_{-0.005}$	$0.70^{+0.18}_{-0.15}$	$0.670^{+0.003}_{-0.003}$
	DGP	—	$0.673^{+0.030}_{-0.031}$	$0.634^{+0.053}_{-0.045}$	$0.69^{+0.17}_{-0.16}$	$0.665^{+0.006}_{-0.006}$
	DGPish	—	$0.682^{+0.032}_{-0.032}$	$0.681^{+0.015}_{-0.008}$	$0.70^{+0.18}_{-0.16}$	$0.671^{+0.004}_{-0.004}$
Ω_Λ	Λ CDM	$0.702^{+0.022}_{-0.023}$	$0.672^{+0.056}_{-0.065}$	$0.684^{+0.007}_{-0.007}$	$0.680^{+0.015}_{-0.016}$	$0.677^{+0.005}_{-0.005}$
	DGP	$0.58^{+0.27}_{-0.32}$	$0.53^{+0.30}_{-0.31}$	$0.43^{+0.32}_{-0.28}$	$0.38^{+0.18}_{-0.15}$	$0.629^{+0.047}_{-0.047}$
	DGPish	$0.53^{+0.30}_{-0.31}$	$0.50^{+0.32}_{-0.31}$	$0.51^{+0.30}_{-0.31}$	$0.64^{+0.19}_{-0.19}$	$0.64^{+0.19}_{-0.19}$
Ω_Q	Λ CDM	—	—	—	—	—
	DGP	$-0.07^{+0.16}_{-0.19}$	$-0.08^{+0.17}_{-0.17}$	$-0.10^{+0.13}_{-0.11}$	$-0.161^{+0.093}_{-0.082}$	$-0.022^{+0.022}_{-0.022}$
	DGPish	$-0.16^{+0.29}_{-0.19}$	$-0.16^{+0.32}_{-0.22}$	$-0.16^{+0.29}_{-0.22}$	$-0.04^{+0.20}_{-0.17}$	$-0.04^{+0.20}_{-0.16}$
χ^2	Λ CDM	1035.77	14.49	0.0013	16.55	1072.19
	DGP	1035.75	14.50	0.0022	13.58	1071.20
	DGPish	1035.77	14.33	0.016	16.55	1072.22
χ^2_{red}	Λ CDM	—	—	—	—	0.98
	DGP	—	—	—	—	0.98
	DGPish	—	—	—	—	0.98
\mathcal{B}_j^i	Λ CDM	—	—	—	—	1
	DGP	—	—	—	—	1.16
	DGPish	—	—	—	—	0.83
$\ln \mathcal{B}_j^i$	Λ CDM	—	—	—	—	0
	DGP	—	—	—	—	0.15
	DGPish	—	—	—	—	-0.18

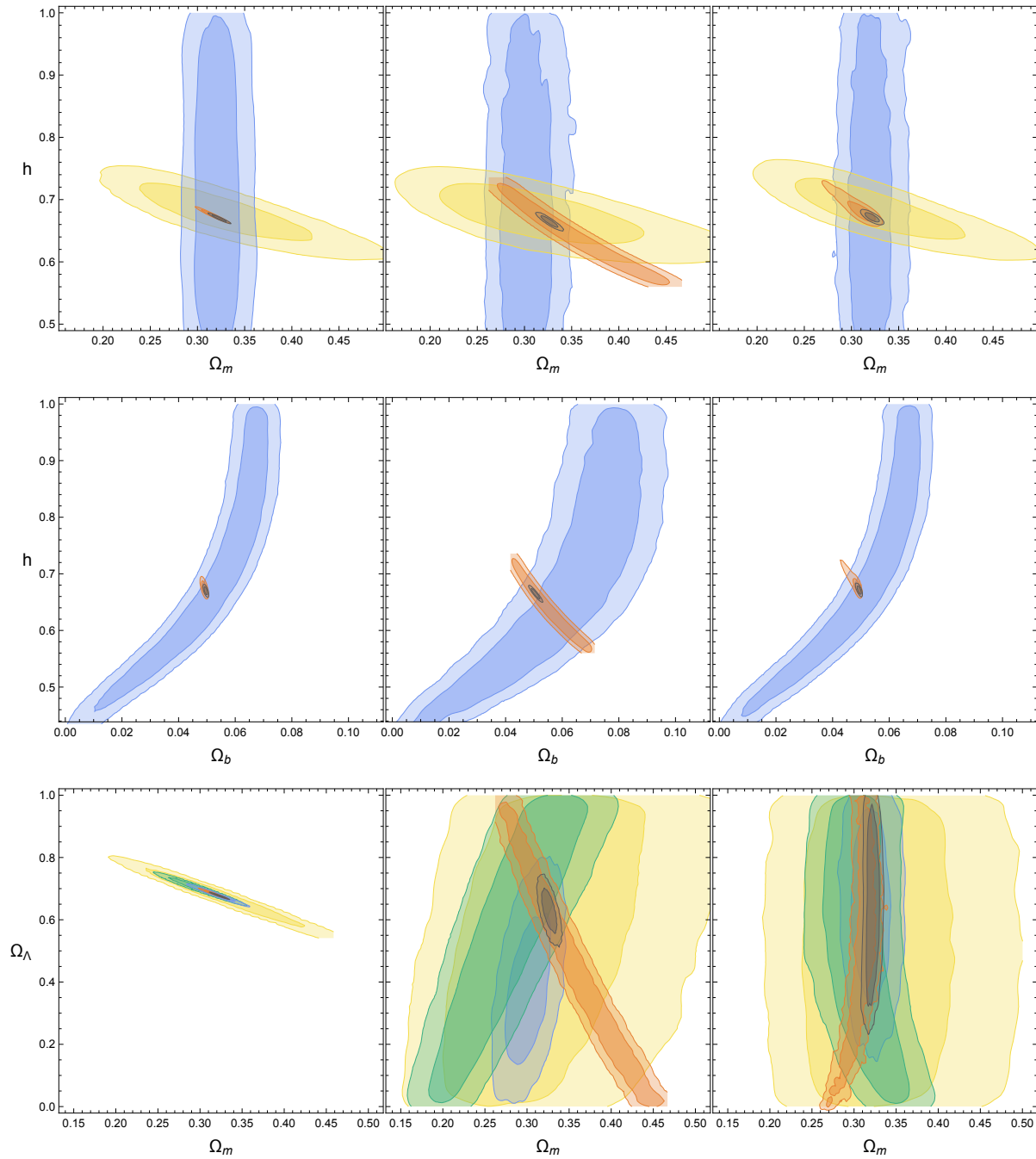


Figure 7.5: Contour plots for the Λ CDM model (left column) DGP model (center column) and $DGPish$ model (right column) with the following color scheme: green - SNeIa, yellow - Hubble data, orange - *Planck 2018* CMB, blue - BAO data, black - all sets of data. As SNeIa are not (of course) able to fix the value h their contours are missing from those plots where constraints on h are represented; for the same rationality, both SNeIa and Hubble contours are absent from plots showing constraints on Ω_b .

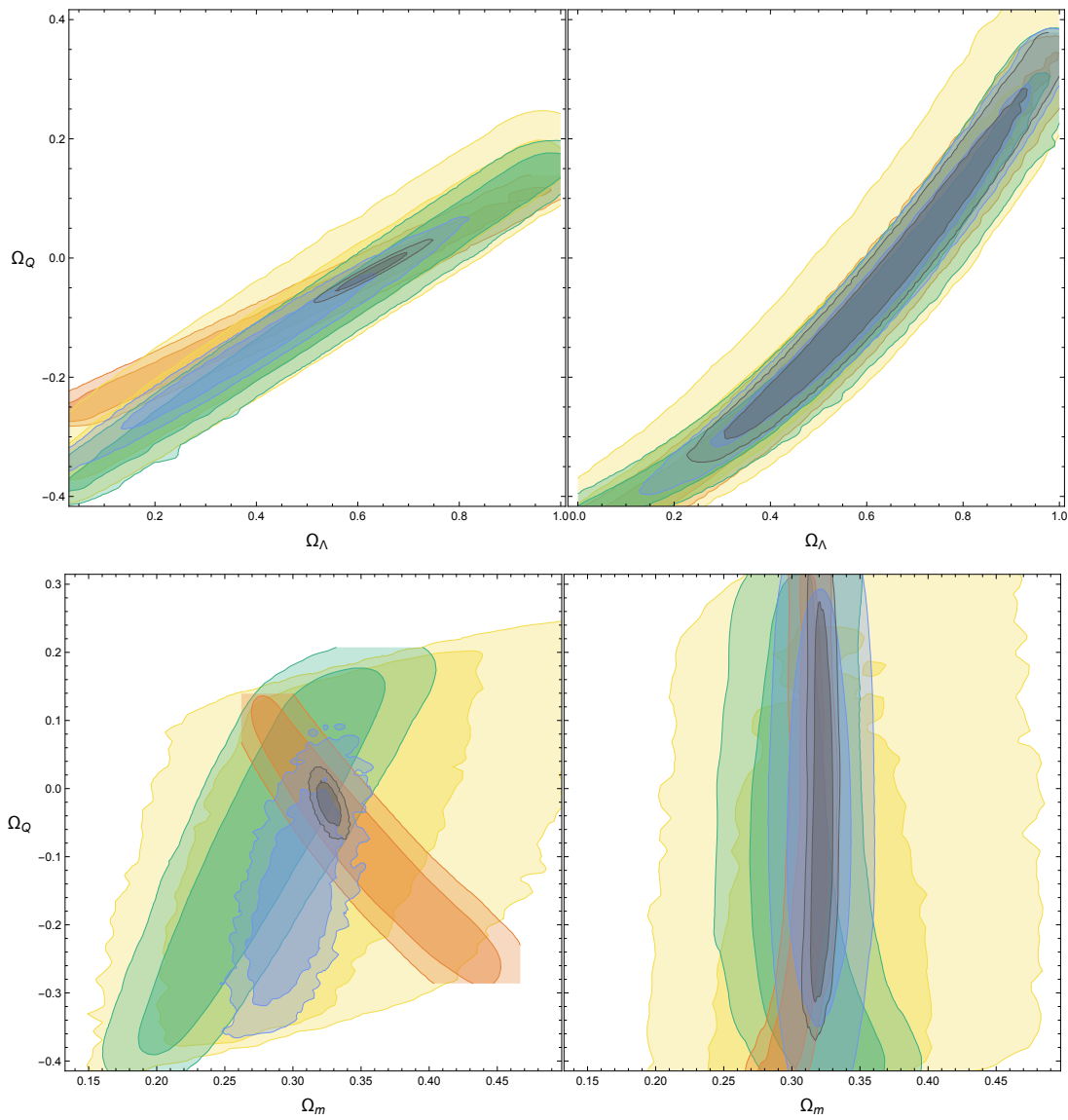


Figure 7.6: Contour plots of the constraints on the parameter Ω_Q for the DGP model (left column) and $DGPish$ model (right column) with the following color scheme: green - SNeIa, yellow - Hubble data, orange - *Planck* 2018 CMB, blue - BAO data, black - all sets of data.

between Ω_Q and Ω_Λ . Note, however that the combination of all data sets gives a far smaller contour in the DGP case, and therefore, as we have already stated, Ω_Q is better fitted.

The conclusions on constraints on Ω_Q and its role in relation to Ω_Λ are strengthened by the contour which confronts Ω_Q with Ω_m (see Fig. 7.6 again). In the DGPish case we get a very large almost vertical contour, that is, a very narrow fit in Ω_m is compatible with a very wide range of Ω_Q values, that is the modified gravity parameter Ω_Q is almost blind to the matter density. In contrast in the DGP case constraints are much more significant.

7.5.4 Cosmographic parameters and cosmodiagrams

Determining the values of parameters in the so-to-say “cosmographic spectrum” is quite a relevant task given their implications for the evolution and final fate of the Universe as shown in Sec. 7.4.2. For instance, we know that if (in the Λ CDM model) the cosmological constant had become dominant earlier than it seems to have then structures would not have formed. Insights into these matters may put us on the track of a solution of puzzles like the coincidence problem, in the sense that it would be good to find some physical mechanism associating the beginning of the dark ages with the onset of non-linear structures.

Our first task will go back to the previous discussion in which an effective dark energy density ρ_{eff} and corresponding equation of state w_{eff} were defined. The explicit expressions for the two cases considered are formidable and they really do not add readily usable information to the discussion. For this reason we just rely on graphical representations of w_{eff} drawn from its best fit and errors (see Table 7.4). The plots we thus obtain confirm our earlier conclusions for all redshifts that in the DGP case (with $\alpha < 0$) we are to expect a non-phantom behavior, whereas in the DGPish case (with $\gamma < 0$) we have exactly the opposite, a purely phantom evolution.

Next we will determine numerically the redshift value signaling the beginning of dark energy domination: z_{eq} . To this end we rest on our earlier definition of ρ_{eff} and we then define z_{eq} implicitly as:

$$\rho_{\text{eff}}(z_{\text{eq}}) = \rho_m(z_{\text{eq}}) . \quad (7.97)$$

As discussed in [405], evidences of considerable dark energy proportions at $z \sim 1$ or larger would favor some scalar field based models, as for those redshifts the contribution of a cosmological constant to the matter-energy budget would be negligible. On the contrary, and according

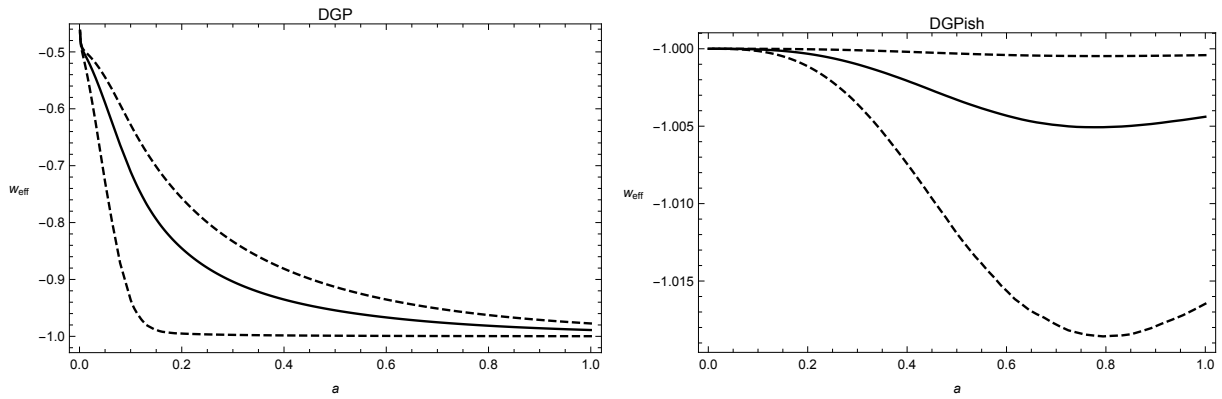


Figure 7.7: Evolution of w_{eff} as a function of the scale factor a for *DGP* (left panel) and *DGPish* (right panel) model. The solid line is the value as drawn from the best fit, whilst the dashed lines mark the boundaries of the confidence interval.

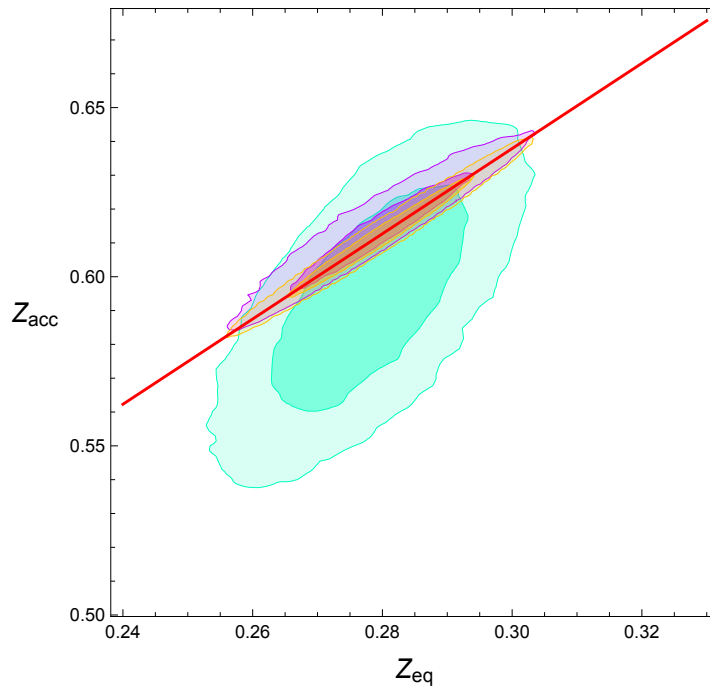


Figure 7.8: Contours for the different redshift of the different models. Λ CDM (orange), DGP (blue) and DGPish (purple), all them resulting from the values of the MCMC. The red line is the theoretical behaviour of the Λ CDM model, i.e. $z_{\text{acc}} = -1 + 2^{1/3}(1 + z_{\text{eq}})$.

to [405] again, a beginning of dark energy domination occurring at $z \sim 0.2$ or lower seems to indicate phantom dark energy. These assertions depend of course on the value of Ω_m , and, in general, the discussion may branch out into the specifics of the effects of the various parameters entering our dark energy description.

Likewise, it might be interesting to learn not only when does dark energy domination begin, but also when do its effects become manifest, that is, which is the redshift value for which acceleration begins (z_{acc}). This occurs when the so called deceleration parameter q vanishes:

$$q(z_{acc}) = 0 . \quad (7.98)$$

For Λ CDM, and provided that the contribution from radiation is considered to be negligible (at z_{eq} and z_{acc}), the pertinent expressions for the beginning of the acceleration $q(z_{acc}) = 0$ (which implies $z_{acc} = -1 + (2\Omega_\Lambda/\Omega_m)^{1/3}$) and the condition of the onset of dark energy domination $\Omega_\Lambda = (1 + z_{eq})^3\Omega_m$ can be combined to conclude that $z_{acc} = -1 + 2^{1/3}(1 + z_{eq})$. In addition, we will be able to calculate the deceleration parameter q and the jerk j following equations (7.52) and (7.53) respectively. Sadly, once more for the $f(Q)$ models, the explicit expressions are too lengthy and convoluted to be worth presenting here, and again we report our findings numerically and graphically.

In addition, it is customary to evaluate q and j at $z = 0$ along with equivalent values of the other parameters in the (standard) cosmographic cascade. For this, we take into account that the normalization condition can be used to eliminate from expressions the parameters that are less convenient/important for our discussion. In the case of the effect of the $f(Q)$ correction on the deceleration factor and the jerk of each model we choose to eliminate Ω_Λ . More specifically at $z = 0$:

$$q_0 = q_0^{\Lambda\text{CDM}} - \begin{cases} \frac{3}{2}(3\Omega_m + 4\Omega_r)\Omega_Q + \mathcal{O}(Q^2) & \text{for the DGP model,} \\ \frac{1}{4}(3\Omega_m + 4\Omega_r)\Omega_Q^2 + \mathcal{O}(Q^3) & \text{for the DGPish model,} \end{cases} \quad (7.99)$$

$$\text{where } q_0^{\Lambda\text{CDM}} = -1 + \frac{1}{2}(3\Omega_m + 4\Omega_r) ,$$

$$j_0 = j_0^{\Lambda\text{CDM}} - \begin{cases} \frac{1}{4} [24\Omega_r + (3\Omega_m + 4\Omega_r)^2] \Omega_Q + \mathcal{O}(Q^2) & \text{for the DGP model,} \\ \frac{1}{2} [2\Omega_r - (3\Omega_m + 4\Omega_r)^2] \Omega_Q^2 + \mathcal{O}(Q^3) & \text{for the DGPish model,} \end{cases} \quad (7.100)$$

where $j_0^{\Lambda\text{CDM}} = 1 + 2\Omega_r$.

Using the latter expression we can compare analytically the deceleration factor for both modified gravity models and a ΛCDM one with the same values of the parameters Ω_m and Ω_r . As it can be noticed, for the DGP model with negative Ω_Q , the deceleration parameter gets bigger, i.e. $q_0 > q_0^{\Lambda\text{CDM}}$ and consequently the acceleration is smaller. However, for the DGPish model the sign of Ω_Q does not matter any more, the deceleration parameter will always be smaller than in ΛCDM which gives comparably a more pronounced acceleration.

All the previous results are summarized in Table 7.4.

Table 7.4: Best fits and errors of the cosmographic parameters.

	q_0	j_0	s_0	w_{eff}	z_{ac}	z_{eq}
ΛCDM	$-0.515^{+0.007}_{-0.007}$	$1.000186^{+2*10^{-6}}_{-2*10^{-6}}$	$-0.455^{+0.022}_{-0.022}$	-1	$0.612^{+0.012}_{-0.012}$	$0.280^{+0.009}_{-0.009}$
<i>DGP</i>	$-0.499^{+0.018}_{-0.017}$	$0.994^{+0.006}_{-0.007}$	$-0.480^{+0.033}_{-0.034}$	$-0.989^{+0.012}_{-0.011}$	$0.593^{+0.022}_{-0.022}$	$0.278^{+0.010}_{-0.010}$
<i>DGPish</i>	$-0.523^{+0.010}_{-0.015}$	$1.009^{+0.029}_{-0.008}$	$-0.463^{+0.023}_{-0.025}$	$-1.004^{+0.004}_{-0.012}$	$0.614^{+0.012}_{-0.012}$	$0.279^{+0.010}_{-0.009}$

7.5.5 Conclusions about DGP and DGPish models

In this section we have analyzed two cosmological models stemming from modified gravity proposals in the $f(Q)$ arena. One of them has an evolution which is identical to that of the DGP models, although the different Lagrangians they are derived from point out in the direction of

differences at the level of perturbations, which are beyond our scope. The second model bears a considerable resemblance to the former, and for that reason we have branded it as DGPish. We offer some details regarding the prescription to generate new $f(Q)$ cosmological models from a few simple assumptions with some physical guidance.

Through the MCMC best fits of their free parameters, encoding the new features of the models into a single parameter dubbed as Ω_Q , and using selection criteria in a analogous way to previous Section (7.4), we are able to discern whether these models can be viewed as contenders to the Λ CDM evolution.

Results indicate a statistical preference of negligible values of Ω_Q of both $f(Q)$ models, so much so for individual data as for data set combined. The only case in which Ω_Q seems to be most comfortable a little away from zero is when the analysis is performed with BAO data for the DGP model. All in all, the possible new phenomenology associated with the $f(Q)$ features finds room between possible evolutions for our Universe but does not seem to be preferred, at least along the two routes we have explored. This fact gets reinforced by values we obtain for the Bayesian evidence, which according to Jeffreys' scale, tell us again these models are not preferred over the Λ CDM one.

However the mildly better agreement on Ω_m , Ω_b and h values between the DGPish and the Λ CDM suggests that perhaps a generalization with extra parameters could offer an even better agreement while retaining some modified gravity character.

In addition, we have performed a cosmographic study with similar results which reflect the striking similarity of the best fits between Λ CDM and our $f(Q)$ models once more, with similar or bigger errors due to their complexity, which penalizes error propagation.

Therefore, at the end of the day, both models are as good as Λ CDM at the background level, but only when they fall upon Λ CDM, which is obvious but does not turn on the new phenomenology. In other words, this new phenomenology is not necessary. Hence, neither of these $f(Q)$ models can be considered as better models, at least as far as the background considerations.

Chapter 8

General Conclusions

In this final chapter we present the major conclusions of our work. The main concern of the present work are the possible benefits of considering modifications (or equivalently extensions) of Einstein's Theory of General Relativity. The study of extensions of the theory was addressed soon after GR was put forward, and was originally devoted to the search of a unification of gravitation and electromagnetism; this endeavour was based on an aesthetic goal of also geometrising electromagnetic forces, and was later extended to include the weak and strong nuclear forces as well.

In this thesis we have investigated theoretical and observational issues of extensions of GR in order to foster a better understanding of questions that should be addressed when we go beyond GR. For instance, in the framework of GR the coupling between the geometry and matter is conveyed by the Newton gravitational constant, and hence it does make a sense to ask ourselves how this coupling became not only constant, but acquired the sign and value we measure. In fact, if we consider scalar-tensor gravity the aforementioned endeavour finds a natural theoretical framework to be addressed, as these theories are characterised by a dynamical evolution of the coupling between geometry and matter.

In the literature it is not uncommon to find the idea that GR fails. However, from our viewpoint this is a wrong approach, since almost all the extended gravity theories share the framework of metric theories, that is the paradigm introduced by GR. Then, why do we find this idea of failure in gravitational physics? Is it because we need to resort to two dark components in astrophysics and cosmology? Should we consider these dark components, as a problem with GR,

or should we rather consider it as a problem with our understanding of the types of energy that gravitate? The only actual argument is about the existence of singularities, which in general are also not resolved in other metric theories. Moreover don't we have singularities or infinities throughout physics? For example: what happens at the location of charges?

Summing up, the simple goal of pushing the limits of the geometrization of physics (that is the trademark of Einstein's GR) is a sufficiently reasonable argument. This goal leads us to a better understanding of the limits of GR, and also to ascertain whether any of its extensions provides a better fit to some observational issues. What is done in this thesis is the tackling of questions in this line of research.

Briefly recapping what we have done in this thesis, we recall that we started classifying the possible forms of modifying gravity in possible 5 ways, most of them motivated by the Lovelock theorem. In this thesis we have sought to supply a wide analysis of almost all these ways, covering several topics from theoretical issues (including extremal objects) to observational tests.

One of the paths to go beyond GR involves the consideration of extra fields which are added to the theory of gravity in different ways. In this class of theories we find the Brans-Dicke theory, and more generally the Scalar-Tensor theories which we have studied in Chapters 2, 3, and 4.

The first question we have addressed was the inspection of scalar-tensor theories starting out with the possibility of a dynamical gravitational coupling instead of the usual "constant" G . It is clear that this dynamics in the coupling gives us a whole new phenomenology that may contribute to explain some problems as, for instance, the early inflation. However there is no doubt that the coupling should end up with a positive value to reproduce gravity at human and solar system scales. In Chapter 2 we obtained a simple mechanism to enforce this positiveness, which consists in the introduction of a quadratic potential. Therefore, this potential attracts the gravitational coupling towards a positive value, with some exceptions that maintain an oscillatory behaviour, but with a lower probability than without the potential.

Then, in Chapter 3 we have considered a more general kind of scalar-tensor theories characterised by the generalization of the coupling between the scalar field, and the curvature scalar, using a function of them $J(\varphi, R)$ in the action. We have introduced the study of this kind of theories, and their representation both on the Einstein Frame and on the Jordan Frame in order

to analyse how the coupling with the matter is presented. The spectrum of this theory contains two scalar degrees of freedom, together with a massless spin-2 state. The two scalar degrees of freedom come from the introduction of a scalar field φ with a non-linear coupling to the Ricci scalar (in the original Jordan Frame), whereas the massless spin-2 state can be related to the standard mediator of Einstein gravity, and couples to matter like the standard GR graviton. The scalar degree of freedom associated with the conformal factor couples to the trace of the stress-energy tensor, and, as this parameterizes general scale transformations, it can be identified to be a dilaton. However, the coupling of the other scalar field is model dependent and we should specify the form of the function $J(\varphi, R)$ to get conclusions.

In addition, in Chapter 3 we introduced the $f(R)$ theory, more specifically in Section 3.2. This class of gravity can also be framed as a theory with higher derivatives which is another way of going beyond GR motivated by Lovelock's theorem. However, for this specific theory the Ostrogradsky's instability is not present, since we showed that the $f(R)$ theory is equivalent to a specific scalar-tensor theory which is included in the Horndeski theory. In Section 3.3.2 we have studied this sort of theory including a scalar potential $U(\varphi)$. After a conformal transformation based on a new scalar field Φ in order to get the Einstein Frame, the conclusion was that, in general, the resulting potential cannot be written as the sum of two individual potentials associated with each of the fields. This fact means that the mass eigenstates cannot be identified with φ or with Φ .

To finish our study of scalar-tensor theories, in Chapter 4 we have presented the Horndeski theory, which is characterized by being the most general theory with an unique additional scalar field without Ostrogradsky's instability. We have applied this theory to black holes and more specifically to the Nariai spacetime to observe whether the antievaporation effect occurs. We have found solutions for some of the Horndeski terms, and we have focused on the cases for which the speed of gravitational waves is equal to the speed of light. The perturbations of the scalar field induce time dependent perturbations on the metric. However, these perturbations just create a slight modification on the horizon radius, keeping it constant, which is translated into the vanishing of the anti-evaporation effect.

Another theoretical scenario beyond GR are the Action-dependent Lagrangian theories studied in Chapter 5. These theories have been considered to study the impact of new theories of gravity in what concerns wormholes, and the possibility of a modification of the energy con-

ditions that are required. The effective theory studied here is characterized by the Lagrangian: $\mathcal{L}_{eff} = -L - \lambda_\mu s^\mu + \mathcal{L}_m$, where s^μ is a differentiable vector field or an action-density field and $L = g^{\mu\nu}(\Gamma_{\mu\nu}^\sigma \Gamma_{\sigma\rho}^\rho - \Gamma_{\mu\sigma}^\rho \Gamma_{\nu\rho}^\sigma)$, where $\Gamma_{\mu\nu}^\sigma$ are the Christoffel symbols. The main result for this kind of theories in wormholes is that the generalized gravitational field equation essentially depends on the background four-vector λ_μ , which is given generically by $\lambda_\mu = \left(0, 0, \frac{\lambda(u)}{\cot\theta}, 0\right)$. With respect to the energy conditions, unfortunately, we have not been able to find examples with the non-violation of the NEC.

In the last chapters of the thesis, we have addressed the observational impact of modified gravity theories introducing a statistical analysis, and the so-called MCMC machinery in Chapter 6. The corresponding methods and tools were used to test three models based on the non-metricity scalar Q , denoted $f(Q)$ models, which introduce changes in the geometry corresponding to yet another way of modifying gravity from Lovelock's theorem. In this sense we have studied changes in the connection in Chapter 7. On the one hand, we have shown that there is an equivalent theory to GR at all levels (STTEGR), and also an equivalent theory to GR, but just at the background level (mimetic GR). On the other hand, we have studied some models with new phenomenology associated with Q , in particular: extended mimetic GR, DGP, and DGPish models. However, we found that the best fits of the latter models impose the vanishing of the new phenomenology, and hence recover the background of GR.

In addition, we have also considered the case of the DGP theory in Section 7.5.1 based on an extra-dimensional theory. This is yet another form of modifying gravity from Lovelock's theorem. In this section we have shown how the Hubble parameter of the DGP theory can be obtained from a $f(Q)$ model. The main characteristic of this class of theories is how the 3-brane is embedded in a n -dimensional spacetime with the need of junction conditions in the border of the brane.

Therefore, this thesis arises from the necessity of assessing the implications of going beyond General Relativity. In this sense, we have studied and explored several (and different) theories to better understand the phenomenology of some case studies representative of the main classes of modifications. In other words, we have analyzed different approaches to Lovelock's theorem in order to improve the knowledge of fundamental, and mathematical aspects or objects, while providing general view of the state of the art in gravity. To assess how extensions of gravity may bring improvements with respect to GR, we have studied some of these theories in extreme

frameworks such as wormholes and black holes.

But besides the investigation of theoretical issues, we kept in sight that the success of models, is gauged by their success in fitting observations. With the purpose of obtaining observational tests, we have used the MCMC machinery, and have found models that are as good as GR, but not better, from a statistical point of view.

However, as a new generation of observational missions, namely the Euclid and the Lisa missions, as well as new ground breaking telescopes like the James Webb and the Extremely Large Telescope (ELT), will come soon into play, this brings new auspicious prospects to improve our current observations, and thus present a real possibility of better scrutinising modified gravity theories.

Bibliography

- [1] Isaac Newton. Philosophiæ Naturalis Principia Mathematica. Royal Society (Great Britain), England, 1687.
- [2] C. M. Will. Experimental gravitation from Newton's Principia to Einstein's general relativity, pages 80–127. Cambridge, UK, 1987.
- [3] Isobel Falconer. Henry cavendish: the man and the measurement. Measurement Science and Technology, 10(6):470–477, jan 1999.
- [4] P.S. Laplace. Traité de Mécanique Céleste. A Paris : De L'Imprimerie de Crapelet, 1799.
- [5] Albert Einstein. Kosmologische Betrachtungen zur allgemeinen Relativitätstheorie. Sitzungsberichte der Königlich Preußischen Akademie der Wissenschaften (Berlin), pages 142–152, January 1917.
- [6] W. de Sitter. Einstein's theory of gravitation and its astronomical consequences, Third Paper. Mon. Not. Roy. Astron. Soc., 78:3–28, 1917.
- [7] Vesto M. Slipher. Nebulae. Proc. Am. Phil. Soc., 56:403–409, 1917.
- [8] Øyvind Grøn. The discovery of the expansion of the universe. Galaxies, 6(4), 2018.
- [9] Michael J. Way. Dismantling Hubble's Legacy? ASP Conf. Ser., 471:97, 2013.
- [10] E. P. Hubble. A spiral nebula as a stellar system, Messier 31. apj, 69:103–158, March 1929.
- [11] Henrietta S. Leavitt. Ten variable stars of the Algol type. Harvard Obs. Annals, 60:109–146, 1908.

- [12] Henrietta S. Leavitt. 1777 variables in the Magellanic Clouds. Harvard Obs. Annals, 60:87–108, 1908.
- [13] Henrietta S. Leavitt and Edward C. Pickering. Periods of 25 Variable Stars in the Small Magellanic Cloud. Harvard Obs. Circ., 173:1–3, 1912.
- [14] A. Friedman. On the Curvature of space. Z. Phys., 10:377–386, 1922.
- [15] A. Friedmann. On the Possibility of a world with constant negative curvature of space. Z. Phys., 21:326–332, 1924.
- [16] Georges Lemaitre. A Homogeneous Universe of Constant Mass and Growing Radius Accounting for the Radial Velocity of Extragalactic Nebulae. Annales Soc. Sci. Bruxelles A, 47:49–59, 1927.
- [17] G. Lemaitre. The expanding universe. Annales Soc. Sci. Bruxelles A, 53:51–85, 1933.
- [18] F. Zwicky. Die Rotverschiebung von extragalaktischen Nebeln. Helv. Phys. Acta, 6:110–127, 1933.
- [19] F. Zwicky. On the Masses of Nebulae and of Clusters of Nebulae. Astrophys. J., 86:217–246, 1937.
- [20] Gianfranco Bertone and Dan Hooper. History of dark matter. Rev. Mod. Phys., 90(4):045002, 2018.
- [21] R. A. Alpher, H. Bethe, and G. Gamow. The origin of chemical elements. Phys. Rev., 73:803–804, 1948.
- [22] Ralph A. Alpher and Robert Herman. Evolution of the Universe. Nature, 162(4124):774–775, 1948.
- [23] A. A. Penzias and R. W. Wilson. A Measurement of Excess Antenna Temperature at 4080 Mc/s. apj, 142:419–421, July 1965.
- [24] R. H. Dicke, P. J. E. Peebles, P. G. Roll, and D. T. Wilkinson. Cosmic Black-Body Radiation. Astrophys. J., 142:414–419, 1965.

- [25] P. G. Roll and David T. Wilkinson. Cosmic Background Radiation at 3.2 cm-Support for Cosmic Black-Body Radiation. Phys. Rev. Lett., 16:405–407, 1966.
- [26] V. C. Rubin, N. Thonnard, and W. K. Ford, Jr. Rotational properties of 21 SC galaxies with a large range of luminosities and radii, from NGC 4605 /R = 4kpc/ to UGC 2885 /R = 122 kpc/. Astrophys. J., 238:471, 1980.
- [27] Adam G. Riess et al. Observational evidence from supernovae for an accelerating universe and a cosmological constant. Astron. J., 116:1009–1038, 1998.
- [28] Brian P. Schmidt et al. The High Z supernova search: Measuring cosmic deceleration and global curvature of the universe using type Ia supernovae. Astrophys. J., 507:46–63, 1998.
- [29] S. Perlmutter et al. Measurements of Ω and Λ from 42 high redshift supernovae. Astrophys. J., 517:565–586, 1999.
- [30] Albert Einstein. On the General Theory of Relativity. Sitzungsber. Preuss. Akad. Wiss. Berlin (Math. Phys.), 1915:778–786, 1915. [Addendum: Sitzungsber. Preuss. Akad. Wiss. Berlin (Math. Phys.)1915,799(1915)].
- [31] Albert Einstein. The Field Equations of Gravitation. Sitzungsber. Preuss. Akad. Wiss. Berlin (Math. Phys.), 1915:844–847, 1915.
- [32] Albert Einstein. The Foundation of the General Theory of Relativity. Annalen Phys., 49(7):769–822, 1916.
- [33] John Wheeler and Kenneth Ford. Geons, black holes and quantum foam: A life in physics. American Journal of Physics, 68, 06 2000.
- [34] L. D. Landau and E. M. Lifschits. The Classical Theory of Fields, volume Volume 2 of Course of Theoretical Physics. Pergamon Press, Oxford, 1975.
- [35] Timothy Clifton, Pedro G. Ferreira, Antonio Padilla, and Constantinos Skordis. Modified Gravity and Cosmology. Phys. Rept., 513:1–189, 2012.

- [36] D. Lovelock. The Einstein tensor and its generalizations. J. Math. Phys., 12:498–501, 1971.
- [37] D. Lovelock. The four-dimensionality of space and the einstein tensor. J. Math. Phys., 13:874–876, 1972.
- [38] Albert Einstein. Explanation of the Perihelion Motion of Mercury from the General Theory of Relativity. Sitzungsber. Preuss. Akad. Wiss. Berlin (Math. Phys.), 1915:831–839, 1915.
- [39] Albert Einstein. Lens-Like Action of a Star by the Deviation of Light in the Gravitational Field. Science, 84:506–507, 1936.
- [40] N. Aghanim et al. Planck 2018 results. VI. Cosmological parameters. Planck, 2018.
- [41] Sean M. Carroll. The Cosmological constant. Living Rev. Rel., 4:1, 2001.
- [42] P. J. E. Peebles and Bharat Ratra. The Cosmological constant and dark energy. Rev. Mod. Phys., 75:559–606, 2003. [,592(2002)].
- [43] Steven Weinberg. The Cosmological Constant Problem. Rev. Mod. Phys., 61:1–23, 1989. [,569(1988)].
- [44] T. Padmanabhan. Cosmological constant: The Weight of the vacuum. Phys. Rept., 380:235–320, 2003.
- [45] Sean M. Carroll. Why is the universe accelerating? eConf, C0307282:TTH09, 2003. [AIP Conf. Proc.743,no.1,16(2004)].
- [46] Eugenio Bianchi and Carlo Rovelli. Why all these prejudices against a constant? Why all these prejudices against a constant?, 2010.
- [47] Philip Bull et al. Beyond Λ CDM: Problems, solutions, and the road ahead. Phys. Dark Univ., 12:56–99, 2016.
- [48] P.A.R. Ade et al. Planck 2013 results. I. Overview of products and scientific results. Astron. Astrophys., 571:A1, 2014.

- [49] P.A.R. Ade et al. Planck 2015 results. XIII. Cosmological parameters. Astron. Astrophys., 594:A13, 2016.
- [50] Shin'ichi Nojiri and Sergei D. Odintsov. Introduction to modified gravity and gravitational alternative for dark energy. eConf, C0602061:06, 2006. [Int. J. Geom. Meth. Mod. Phys.4,115(2007)].
- [51] Emanuele Berti et al. Testing General Relativity with Present and Future Astrophysical Observations. Class. Quant. Grav., 32:243001, 2015.
- [52] Ismael Ayuso and Jose A.R. Cembranos. Nonminimal scalar-tensor theories. Phys. Rev. D, 101(4):044007, 2020.
- [53] A. Dobado and Antonio Lopez Maroto. Some consequences of the effective low-energy Lagrangian for gravity. Phys. Lett. B, 316:250–256, 1993. [Erratum: Phys.Lett.B 321, 435–435 (1994)].
- [54] Shin'ichi Nojiri and Sergei D. Odintsov. Dark energy, inflation and dark matter from modified $F(R)$ gravity. TSPU Bulletin, N8(110):7–19, 2011.
- [55] Shin'ichi Nojiri and Sergei D. Odintsov. Unified cosmic history in modified gravity: from $F(R)$ theory to Lorentz non-invariant models. Phys. Rept., 505:59–144, 2011.
- [56] Salvatore Capozziello and Mauro Francaviglia. Extended Theories of Gravity and their Cosmological and Astrophysical Applications. Gen. Rel. Grav., 40:357–420, 2008.
- [57] Thomas P. Sotiriou and Valerio Faraoni. $f(R)$ Theories Of Gravity. Rev. Mod. Phys., 82:451–497, 2010.
- [58] Francisco S. N. Lobo. The Dark side of gravity: Modified theories of gravity. Dark Energy-Current Advances and Ideas, 7 2008.
- [59] Valerio Faraoni and Salvatore Capozziello. Beyond Einstein Gravity: A Survey of Gravitational Theories for Cosmology and Astrophysics. Springer, Dordrecht, 2011.
- [60] Salvatore Capozziello. Curvature quintessence. Int. J. Mod. Phys., D11:483–492, 2002.

- [61] Tiberiu Harko and Francisco S. N. Lobo. Extensions of $f(R)$ Gravity. Cambridge University Press, 2018.
- [62] Th. Kaluza. Zum Unitätsproblem der Physik. Sitzungsber. Preuss. Akad. Wiss. Berlin (Math. Phys.), 1921:966–972, 1921.
- [63] Oskar Klein. Quantum Theory and Five-Dimensional Theory of Relativity. (In German and English). Z. Phys., 37:895–906, 1926.
- [64] Shin’ichi Nojiri and Sergei D. Odintsov. Modified gravity with negative and positive powers of the curvature: Unification of the inflation and of the cosmic acceleration. Phys. Rev. D, 68:123512, 2003.
- [65] Guido Cognola, Emilio Elizalde, Shin’ichi Nojiri, Sergei D. Odintsov, and Sergio Zerbini. Dark energy in modified Gauss-Bonnet gravity: Late-time acceleration and the hierarchy problem. Phys. Rev. D, 73:084007, 2006.
- [66] Shin’ichi Nojiri and Sergei D. Odintsov. Modified Gauss-Bonnet theory as gravitational alternative for dark energy. Phys. Lett. B, 631:1–6, 2005.
- [67] E. Elizalde, R. Myrzakulov, V. V. Obukhov, and D. Saez-Gomez. LambdaCDM epoch reconstruction from $F(R,G)$ and modified Gauss-Bonnet gravities. Class. Quant. Grav., 27:095007, 2010.
- [68] Ratbay Myrzakulov, Diego Saez-Gomez, and Anca Tureanu. On the Λ CDM Universe in $f(G)$ gravity. Gen. Rel. Grav., 43:1671–1684, 2011.
- [69] Alvaro de la Cruz-Dombriz and Diego Saez-Gomez. On the stability of the cosmological solutions in $f(R, G)$ gravity. Class. Quant. Grav., 29:245014, 2012.
- [70] Zahra Haghani, Nima Khosravi, and Shahab Shahidi. The Weyl–Cartan Gauss–Bonnet gravity. Class. Quant. Grav., 32(21):215016, 2015.
- [71] T. Padmanabhan and D. Kothawala. Lanczos-Lovelock models of gravity. Phys. Rept., 531:115–171, 2013.

- [72] Cornelius Lanczos. A Remarkable property of the Riemann-Christoffel tensor in four dimensions. Annals Math., 39:842–850, 1938.
- [73] Tirthabir Biswas, Tomi Koivisto, and Anupam Mazumdar. Towards a resolution of the cosmological singularity in non-local higher derivative theories of gravity. JCAP, 11:008, 2010.
- [74] Tirthabir Biswas, Erik Gerwick, Tomi Koivisto, and Anupam Mazumdar. Towards singularity and ghost free theories of gravity. Phys. Rev. Lett., 108:031101, 2012.
- [75] Tirthabir Biswas, Alexey S. Koshelev, Anupam Mazumdar, and Sergey Yu. Vernov. Stable bounce and inflation in non-local higher derivative cosmology. JCAP, 08:024, 2012.
- [76] C. Brans and R.H. Dicke. Mach’s principle and a relativistic theory of gravitation. Phys. Rev., 124:925–935, 1961.
- [77] C. H. Brans. Mach’s Principle and a Relativistic Theory of Gravitation. II. Phys. Rev., 125:2194–2201, 1962.
- [78] J. A. R. Cembranos, A. de la Cruz Dombriz, and L. Olano Garcia. Complete density perturbations in the Jordan-Fierz-Brans-Dicke theory. Phys. Rev. D, 88:123507, 2013.
- [79] Juan Garcia-Bellido, Andrei D. Linde, and Dmitri A. Linde. Fluctuations of the gravitational constant in the inflationary Brans-Dicke cosmology. Phys. Rev. D, 50:730–750, 1994.
- [80] Gregory Walter Horndeski. Second-order scalar-tensor field equations in a four-dimensional space. Int. J. Theor. Phys., 10:363–384, 1974.
- [81] C. Armendáriz-Picón, T. Damour, and V. Mukhanov. k-inflation. Physics Letters B, 458(2-3):209–218, Jul 1999.
- [82] Jaume Garriga and V.F. Mukhanov. Perturbations in k-inflation. Physics Letters B, 458(2-3):219–225, Jul 1999.
- [83] Shinji Tsujikawa. Quintessence: a review. Classical and Quantum Gravity, 30(21):214003, Oct 2013.

- [84] Roland de Putter and Eric V. Linder. Kinetic k-essence and Quintessence. Astropart. Phys., 28:263–272, 2007.
- [85] Jacob D. Bekenstein. The Relation between physical and gravitational geometry. Phys. Rev. D, 48:3641–3647, 1993.
- [86] M. Zumalacarregui, T. S. Koivisto, D. F. Mota, and P. Ruiz-Lapuente. Disformal Scalar Fields and the Dark Sector of the Universe. JCAP, 05:038, 2010.
- [87] Tomi S. Koivisto, David F. Mota, and Miguel Zumalacarregui. Screening Modifications of Gravity through Disformally Coupled Fields. Phys. Rev. Lett., 109:241102, 2012.
- [88] Miguel Zumalacarregui, Tomi S. Koivisto, and David F. Mota. DBI Galileons in the Einstein Frame: Local Gravity and Cosmology. Phys. Rev. D, 87:083010, 2013.
- [89] Shinji Tsujikawa. Cosmological disformal transformations to the Einstein frame and gravitational couplings with matter perturbations. Phys. Rev. D, 92(6):064047, 2015.
- [90] Jose A. R. Cembranos and Antonio L. Maroto. Disformal scalars as dark matter candidates: Branon phenomenology. Int. J. Mod. Phys., 31(14n15):1630015, 2016.
- [91] Philippe Brax and Clare Burrage. Constraining disformally coupled scalar fields. Physical Review D, 90(10), Nov 2014.
- [92] Tomi S. Koivisto, David F. Mota, and Miguel Zumalacárregui. Screening modifications of gravity through disformally coupled fields. Physical Review Letters, 109(24), Dec 2012.
- [93] Dario Bettoni and Stefano Liberati. Disformal invariance of second order scalar-tensor theories: Framing the Horndeski action. Phys. Rev. D, 88:084020, 2013.
- [94] L. H. Ford. INFLATION DRIVEN BY A VECTOR FIELD. Phys. Rev. D, 40:967, 1989.
- [95] Jose Beltran Jimenez and Antonio Lopez Maroto. A cosmic vector for dark energy. Phys. Rev. D, 78:063005, 2008.
- [96] Jose Beltran Jimenez and Antonio L. Maroto. Cosmological evolution in vector-tensor theories of gravity. Phys. Rev. D, 80:063512, 2009.

- [97] Tomi Koivisto and David F. Mota. Vector Field Models of Inflation and Dark Energy. JCAP, 0808:021, 2008.
- [98] J. A. R. Cembranos, C. Hallabrin, A. L. Maroto, and S. J. Nunez Jareno. Isotropy theorem for cosmological vector fields. Phys. Rev. D, 86:021301, 2012.
- [99] J. A. R. Cembranos, A. L. Maroto, and S. J. Núñez Jareño. Isotropy theorem for cosmological Yang-Mills theories. Phys. Rev. D, 87(4):043523, 2013.
- [100] J. A. R. Cembranos, A. L. Maroto, and S. J. Núñez Jareño. Isotropy theorem for arbitrary-spin cosmological fields. JCAP, 03:042, 2014.
- [101] Ted Jacobson. Einstein-aether gravity: A Status report. PoS, QG-PH:020, 2007.
- [102] Yashar Akrami, Philippe Brax, Anne-Christine Davis, and Valeri Vardanyan. Neutron star merger gw170817 strongly constrains doubly coupled bigravity. Physical Review D, 97(12), Jun 2018.
- [103] Claudia de Rham, Gregory Gabadadze, and Andrew J. Tolley. Resummation of massive gravity. Physical Review Letters, 106(23), Jun 2011.
- [104] J. W. Moffat. Scalar-tensor-vector gravity theory. JCAP, 03:004, 2006.
- [105] Bogdan Dănilă, Tiberiu Harko, Francisco S. N. Lobo, and Man Kwong Mak. Spherically symmetric static vacuum solutions in hybrid metric-Palatini gravity. Phys. Rev. D, 99(6):064028, 2019.
- [106] Tirthabir Biswas, Jose A. R. Cembranos, and Joseph I. Kapusta. Thermal Duality and Hagedorn Transition from p-adic Strings. Phys. Rev. Lett., 104:021601, 2010.
- [107] Tirthabir Biswas, Jose A. R. Cembranos, and Joseph I. Kapusta. Thermodynamics and Cosmological Constant of Non-Local Field Theories from p-Adic Strings. JHEP, 10:048, 2010.
- [108] Tirthabir Biswas, Jose A. R. Cembranos, and Joseph I. Kapusta. Finite Temperature Solitons in Non-Local Field Theories from p-Adic Strings. Phys. Rev., D82:085028, 2010.

- [109] Hans Stephani, Dietrich Kramer, Malcolm MacCallum, Cornelius Hoenselaers, and Eduard Herlt. Exact Solutions of Einstein's Field Equations. Cambridge Monographs on Mathematical Physics. Cambridge University Press, 2 edition, 2003.
- [110] Prado Martin-Moruno and Matt Visser. Classical and semi-classical energy conditions. Fundam. Theor. Phys., 189:193–213, 2017.
- [111] Prado Martin-Moruno and Matt Visser. Essential core of the Hawking–Ellis types. Class. Quant. Grav., 35(12):125003, 2018.
- [112] Sayan Kar and Soumitra SenGupta. The Raychaudhuri equations: A Brief review. Pramana, 69:49, 2007.
- [113] Carlos Barcelo and Matt Visser. Twilight for the energy conditions? Int. J. Mod. Phys. D, 11:1553–1560, 2002.
- [114] Santiago Esteban Perez Bergliaffa. Constraining $f(R)$ theories with the energy conditions. Phys. Lett. B, 642:311–314, 2006.
- [115] Salvatore Capozziello, Francisco S. N. Lobo, and José P. Mimoso. Energy conditions in modified gravity. Phys. Lett. B, 730:280–283, 2014.
- [116] Di Liu and M. J. Reboucas. Energy conditions bounds on $f(T)$ gravity. Phys. Rev. D, 86:083515, 2012.
- [117] Salvatore Capozziello, Francisco S. N. Lobo, and José P. Mimoso. Generalized energy conditions in Extended Theories of Gravity. Phys. Rev. D, 91(12):124019, 2015.
- [118] Carlos Barcelo and Matt Visser. Scalar fields, energy conditions, and traversable wormholes. Class. Quant. Grav., 17:3843–3864, 2000.
- [119] John D. Barrow and Frank J. Tipler. The Anthropic Cosmological Principle. Oxford U. Pr., Oxford, 1988.
- [120] John D. Barrow. Gravitational memory? Phys. Rev. D, 46:3227–3230, 1992. [Erratum: Phys.Rev.D 47, 1730 (1993)].

- [121] I Roxburgh. The Sign and Magnitude of the Constant of Gravity in General Relativity;, 1980.
- [122] I Roxburgh. The Constant of Gravity in General Relativity;, 1980.
- [123] N.N. Khuri. The Sign of the Induced Gravitational Constant. Phys. Rev. D, 26:2664, 1982.
- [124] B. M. Barker. General scalar-tensor theory of gravity with constant G . apj, jan 1978.
- [125] José Pedro Mimoso and Ana Nunes. A Qualitative Analysis of the Attractor Mechanism of General relativity. Astrophys. Space Sci., 283(4):661–666, 2003.
- [126] J.P. Mimoso and A.M. Nunes. General relativity as a cosmological attractor of scalar tensor gravity theories. Phys. Lett. A, 248:325–331, 1998.
- [127] Jose P. Mimoso and Ana Nunes. General relativity as an attractor to scalar tensor gravity theories. Astrophys. Space Sci., 261:327–330, 1999.
- [128] José Pedro Mimoso. The Dynamics of Scalar Fields in Cosmology. Springer Proc. Math., 2:543–547, 2011.
- [129] Laur Jarv, Piret Kuusk, and Margus Saal. Potential dominated scalar-tensor cosmologies in the general relativity limit: phase space view. Phys. Rev. D, 81:104007, 2010.
- [130] Laur Jarv, Piret Kuusk, and Margus Saal. Scalar-tensor cosmologies with a potential in the general relativity limit: time evolution. Phys. Lett. B, 694:1–5, 2011.
- [131] Andreas Albrecht and Joao Magueijo. A Time varying speed of light as a solution to cosmological puzzles. Phys. Rev. D, 59:043516, 1999.
- [132] Peter K. S. Dunsby and Orlando Luongo. On the theory and applications of modern cosmography. Int. J. Geom. Meth. Mod. Phys., 13(03):1630002, 2016.
- [133] Alejandro Aviles, Christine Gruber, Orlando Luongo, and Hernando Quevedo. Cosmography and constraints on the equation of state of the Universe in various parametrizations. Phys. Rev. D, 86:123516, 2012.

- [134] Sebastian Bahamonde, Christian G. Böhmer, Sante Carloni, Edmund J. Copeland, Wei Fang, and Nicola Tamanini. Dynamical systems applied to cosmology: dark energy and modified gravity. *Phys. Rept.*, 775-777:1–122, 2018.
- [135] José A.R. Cembranos, Mario Coma Díaz, and Prado Martín-Moruno. Modified gravity as a diagravitational medium. *Phys. Lett. B*, 788:336–340, 2019.
- [136] John D. Barrow. Scalar - tensor cosmologies. *Phys. Rev. D*, 47:5329–5335, 1993.
- [137] Jose P. Mimoso and David Wands. Massless fields in scalar - tensor cosmologies. *Phys. Rev. D*, 51:477–489, 1995.
- [138] Valerio Faraoni. Phase space geometry in scalar-tensor cosmology. *Annals Phys.*, 317:366–382, 2005.
- [139] Tiago C. Charters, Ana Nunes, and Jose P. Mimoso. Stability analysis of cosmological models through Liapunov’s method. *Class. Quant. Grav.*, 18:1703–1714, 2001.
- [140] Caroline Santos and Ruth Gregory. Cosmology in Brans-Dicke theory with a scalar potential. *Annals Phys.*, 258:111–134, 1997.
- [141] S. Carloni, S. Capozziello, J.A. Leach, and P.K.S. Dunsby. Cosmological dynamics of scalar-tensor gravity. *Class. Quant. Grav.*, 25:035008, 2008.
- [142] J. O’ Hanlon and B.O.J. Tupper. Vacuum-field solutions in the Brans-Dicke theory. *Nuovo Cim. B*, 7:305–312, 1972.
- [143] Hidekazu Nariai. On the Green’s Function in an Expanding Universe and Its Role in the Problem of Mach’s Principle. *Progress of Theoretical Physics*, 40(1):49–59, 07 1968.
- [144] John D. Barrow and J.P. Mimoso. Perfect fluid scalar - tensor cosmologies. *Phys. Rev. D*, 50:3746–3754, 1994.
- [145] S. Capozziello, R. de Ritis, and P. Scudellaro. Nonminimal coupling and cosmic no hair theorem. *Phys. Lett. A*, 188:130–136, 1994.
- [146] S. Capozziello, R. de Ritis, C. Rubano, and P. Scudellaro. Nonminimal coupling, no hair theorem and matter cosmologies. *Phys. Lett. A*, 201:145–150, 1995.

- [147] Orest Hrycyna and Marek Szydlowski. Dynamical complexity of the Brans-Dicke cosmology. JCAP, 12:016, 2013.
- [148] Ricardo García-Salcedo, Tame González, and Israel Quiros. Brans-Dicke cosmology does not have the Λ CDM phase as a universal attractor. Phys. Rev. D, 92(12):124056, 2015.
- [149] Orlando Luongo and Marco Muccino. Speeding up the universe using dust with pressure. Phys. Rev. D, 98(10):103520, 2018.
- [150] Piret Kuusk, Laur Jarv, and Margus Saal. Scalar-tensor cosmologies: General relativity as a fixed point of the Jordan frame scalar field. Int. J. Mod. Phys. A, 24:1631–1638, 2009.
- [151] Junpei Ooba, Kiyotomo Ichiki, Takeshi Chiba, and Naoshi Sugiyama. Cosmological constraints on scalar–tensor gravity and the variation of the gravitational constant. PTEP, 2017(4):043E03, 2017.
- [152] Clifford M. Will. The Confrontation between General Relativity and Experiment. Living Rev. Rel., 17:4, 2014.
- [153] Kazuya Koyama. Cosmological Tests of Modified Gravity. Rept. Prog. Phys., 79(4):046902, 2016.
- [154] J.P. Mimoso. Primordial cosmology in Jordan-Brans-Dicke theory: Nucleosynthesis. In 1st Iberian Meeting on Gravity (IMG-1), pages 243–246, 1992.
- [155] Thibault Damour and Bernard Pichon. Big bang nucleosynthesis and tensor - scalar gravity. Phys. Rev. D, 59:123502, 1999.
- [156] Julien Larena, Jean-Michel Alimi, and Arturo Serna. Big Bang nucleosynthesis in scalar tensor gravity: The key problem of the primordial Li-7 abundance. Astrophys. J., 658:1–10, 2007.
- [157] Fabio Iocco, Gianpiero Mangano, Gennaro Miele, Ofelia Pisanti, and Pasquale D. Serpico. Primordial Nucleosynthesis: from precision cosmology to fundamental physics. Phys. Rept., 472:1–76, 2009.

- [158] Alain Coc, Pierre Descouvemont, Keith A. Olive, Jean-Philippe Uzan, and Elisabeth Vangioni. The variation of fundamental constants and the role of $A=5$ and $A=8$ nuclei on primordial nucleosynthesis. Phys. Rev. D, 86:043529, 2012.
- [159] T. Damour and K. Nordvedt. Tensor - scalar cosmological models and their relaxation toward general relativity. Phys. Rev. D, 48:3436–3450, 1993.
- [160] Sean M. Carroll and Aidan Chatwin-Davies. Cosmic equilibration: A holographic no-hair theorem from the generalized second law. Phys. Rev. D, 97:046012, Feb 2018.
- [161] Seokcheon Lee. Constraints on scalar-tensor theories of gravity from observations. JCAP, 03:021, 2011.
- [162] Georges Aad et al. Observation of a new particle in the search for the Standard Model Higgs boson with the ATLAS detector at the LHC. Phys. Lett. B, 716:1–29, 2012.
- [163] Serguei Chatrchyan et al. Observation of a New Boson at a Mass of 125 GeV with the CMS Experiment at the LHC. Phys. Lett. B, 716:30–61, 2012.
- [164] Joseph Polchinski. String Theory, volume 1 of Cambridge Monographs on Mathematical Physics. Cambridge University Press, 1998.
- [165] K. S. Stelle. Classical Gravity with Higher Derivatives. Gen. Rel. Grav., 9:353–371, 1978.
- [166] Alexei A. Starobinsky. A New Type of Isotropic Cosmological Models Without Singularity. Phys. Lett. B, 91:99–102, 1980.
- [167] Milan B. Mijić, Michael S. Morris, and Wai-Mo Suen. The R^2 cosmology: Inflation without a phase transition. Phys. Rev. D, 34:2934–2946, Nov 1986.
- [168] Sean M. Carroll, Vikram Duvvuri, Mark Trodden, and Michael S. Turner. Is cosmic speed - up due to new gravitational physics? Phys. Rev. D, 70:043528, 2004.
- [169] Naureen Goheer, Julien Larena, and Peter K. S. Dunsby. Power-law cosmic expansion in $f(R)$ gravity models. Phys. Rev. D, 80:061301, 2009.

- [170] S. Carloni, P. K. S. Dunsby, and A. Troisi. The Evolution of density perturbations in $f(R)$ gravity. Phys. Rev. D, 77:024024, 2008.
- [171] Kishore N. Ananda, S. Carloni, and P. K. S. Dunsby. The Evolution of cosmological gravitational waves in $f(R)$ gravity. Phys. Rev. D, 77:024033, 2008.
- [172] Kishore N. Ananda, Sante Carloni, and Peter K. S. Dunsby. A detailed analysis of structure growth in $f(R)$ theories of gravity. Class. Quant. Grav., 26:235018, 2009.
- [173] J. A. R. Cembranos, A. de la Cruz-Dombriz, and P. Jimeno Romero. Kerr-Newman black holes in $f(R)$ theories. Int. J. Geom. Meth. Mod. Phys., 11:1450001, 2014.
- [174] Amare Abebe, Mohamed Abdelwahab, Alvaro de la Cruz-Dombriz, and Peter K. S. Dunsby. Covariant gauge-invariant perturbations in multifluid $f(R)$ gravity. Class. Quant. Grav., 29:135011, 2012.
- [175] Amare Abebe, Alvaro de la Cruz-Dombriz, and Peter K. S. Dunsby. Large Scale Structure Constraints for a Class of $f(R)$ Theories of Gravity. Phys. Rev. D, 88:044050, 2013.
- [176] Alvaro de la Cruz-Dombriz, Peter K. S. Dunsby, Vinicius C. Busti, and Sulona Kandhai. On tidal forces in $f(R)$ theories of gravity. Phys. Rev. D, 89(6):064029, 2014.
- [177] J. A. R. Cembranos. The Newtonian limit at intermediate energies. Phys. Rev. D, 73:064029, 2006.
- [178] Jose A. R. Cembranos. Dark Matter from R^2 -gravity. Phys. Rev. Lett., 102:141301, 2009.
- [179] Michael Atkins and Xavier Calmet. Remarks on Higgs Inflation. Phys. Lett. B, 697:37–40, 2011.
- [180] Girish Chakravarty, Subhendra Mohanty, and Naveen K. Singh. Higgs Inflation in $f(\Phi, R)$ Theory. Int. J. Mod. Phys. D, 23(4):1450029, 2014.
- [181] Ichiro Oda. Classically Scale-invariant B-L Model and Dilaton Gravity. Phys. Rev. D, 87(6):065025, 2013.

- [182] Ichiro Oda. Higgs Mechanism in Scale-Invariant Gravity. *Adv. Stud. Theor. Phys.*, 8:215–249, 2014.
- [183] Renata Kallosh and Andrei Linde. Superconformal generalization of the chaotic inflation model $\frac{\lambda}{4}\phi^4 - \frac{\xi}{2}\phi^2 R$. *JCAP*, 06:027, 2013.
- [184] Renata Kallosh and Andrei Linde. Superconformal generalizations of the Starobinsky model. *JCAP*, 06:028, 2013.
- [185] Renata Kallosh and Andrei Linde. Universality Class in Conformal Inflation. *JCAP*, 07:002, 2013.
- [186] Itzhak Bars, Paul J. Steinhardt, and Neil Turok. Cyclic Cosmology, Conformal Symmetry and the Metastability of the Higgs. *Phys. Lett. B*, 726:50–55, 2013.
- [187] Itzhak Bars, Paul Steinhardt, and Neil Turok. Local Conformal Symmetry in Physics and Cosmology. *Phys. Rev. D*, 89(4):043515, 2014.
- [188] Mark P. Hertzberg. Inflation, Symmetry, and B-Modes. *Phys. Lett. B*, 745:118–124, 2015.
- [189] Renato Costa and Horatiu Nastase. Conformal inflation from the Higgs. *JHEP*, 06:145, 2014.
- [190] Jing Ren, Zhong-Zhi Xianyu, and Hong-Jian He. Higgs Gravitational Interaction, Weak Boson Scattering, and Higgs Inflation in Jordan and Einstein Frames. *JCAP*, 06:032, 2014.
- [191] Girish Kumar Chakravarty and Subhendra Mohanty. Power law Starobinsky model of inflation from no-scale SUGRA. *Phys. Lett. B*, 746:242–247, 2015.
- [192] Ichiro Oda and Takahiko Tomoyose. Conformal Higgs Inflation. *JHEP*, 09:165, 2014.
- [193] Jose A. R. Cembranos. Dark Matter from R²-gravity. *Phys. Rev. Lett.*, 102:141301, 2009.
- [194] John D. Barrow. A cosmological limit on the possible variation of G. *Monthly Notices of the Royal Astronomical Society*, 184(4):677–682, 10 1978.

- [195] J. Yang, D. N. Schramm, G. Steigman, and R. T. Rood. Constraints on cosmology and neutrino physics from big bang nucleosynthesis. *apj*, 227:697–704, January 1979.
- [196] Frank S. Accetta, Lawrence M. Krauss, and Paul Romanelli. New limits on the variability of G from big bang nucleosynthesis. *Phys. Lett. B*, 248:146–150, 1990.
- [197] K. Arai, M. Hashimoto, and T. Fukui. Primordial nucleosynthesis in the Brans-Dicke theory with a variable cosmological term. *aap*, 179(1-2):17–22, June 1987.
- [198] Thibault Damour and Carsten Gundlach. Nucleosynthesis constraints on an extended Jordan-Brans-Dicke theory. *Phys. Rev. D*, 43:3873–3877, Jun 1991.
- [199] J. A. Casas, J. Garcia-Bellido, and M. Quiros. Nucleosynthesis bounds on Jordan-Brans-Dicke theories of gravity. *Mod. Phys. Lett. A*, 7:447–456, 1992.
- [200] J. A. Casas, J. Garcia-Bellido, and M. Quiros. Updating nucleosynthesis bounds on Jordan-Brans-Dicke theories of gravity. *Phys. Lett. B*, 278:94–96, 1992.
- [201] Timothy Clifton, John D. Barrow, and Robert J. Scherrer. Constraints on the variation of G from primordial nucleosynthesis. *Phys. Rev. D*, 71:123526, 2005.
- [202] A. Serna and J. M. Alimi. Scalar - tensor cosmological models. *Phys. Rev. D*, 53:3074–3086, 1996.
- [203] D. I. Santiago, D. Kalligas, and R. V. Wagoner. Nucleosynthesis constraints on scalar - tensor theories of gravity. *Phys. Rev. D*, 56:7627–7637, 1997.
- [204] Alain Coc, Keith A. Olive, Jean-Philippe Uzan, and Elisabeth Vangioni. Big bang nucleosynthesis constraints on scalar-tensor theories of gravity. *Phys. Rev. D*, 73:083525, 2006.
- [205] Alain Coc, Keith A. Olive, Jean-Philippe Uzan, and Elisabeth Vangioni. Non-universal scalar-tensor theories and big bang nucleosynthesis. *Phys. Rev. D*, 79:103512, 2009.
- [206] Alain Riazuelo and Jean-Philippe Uzan. Cosmological observations in scalar - tensor quintessence. *Phys. Rev. D*, 66:023525, 2002.

- [207] Alain Riazuelo and Jean-Philippe Uzan. Quintessence and gravitational waves. Phys. Rev. D, 62:083506, 2000.
- [208] Carlo Schimd, Jean-Philippe Uzan, and Alain Riazuelo. Weak lensing in scalar-tensor theories of gravity. Phys. Rev. D, 71:083512, 2005.
- [209] Thibault Damour and Kenneth Nordtvedt. General relativity as a cosmological attractor of tensor scalar theories. Phys. Rev. Lett., 70:2217–2219, 1993.
- [210] T. Damour and Alexander M. Polyakov. The String dilaton and a least coupling principle. Nucl. Phys. B, 423:532–558, 1994.
- [211] Justin Khoury and Amanda Weltman. Chameleon fields: Awaiting surprises for tests of gravity in space. Phys. Rev. Lett., 93:171104, 2004.
- [212] Philippe Brax, Carsten van de Bruck, Anne-Christine Davis, Justin Khoury, and Amanda Weltman. Detecting dark energy in orbit: The cosmological chameleon. Phys. Rev. D, 70:123518, 2004.
- [213] Kei-ichi Maeda. Towards the Einstein-Hilbert Action via Conformal Transformation. Phys. Rev. D, 39:3159, 1989.
- [214] Steven Weinberg. Photons and gravitons in perturbation theory: Derivation of Maxwell’s and Einstein’s equations. Phys. Rev., 138:B988–B1002, 1965.
- [215] Jose A. R. Cembranos, Keith A. Olive, Marco Peloso, and Jean-Philippe Uzan. Quantum Corrections to the Cosmological Evolution of Conformally Coupled Fields. JCAP, 07:025, 2009.
- [216] Fedor L. Bezrukov and Mikhail Shaposhnikov. The Standard Model Higgs boson as the inflaton. Phys. Lett. B, 659:703–706, 2008.
- [217] A. O. Barvinsky, A. Yu. Kamenshchik, and A. A. Starobinsky. Inflation scenario via the Standard Model Higgs boson and LHC. JCAP, 11:021, 2008.
- [218] F. Bezrukov, D. Gorbunov, and M. Shaposhnikov. On initial conditions for the Hot Big Bang. JCAP, 06:029, 2009.

- [219] Fedor L. Bezrukov, Amaury Magnin, and Mikhail Shaposhnikov. Standard Model Higgs boson mass from inflation. *Phys. Lett. B*, 675:88–92, 2009.
- [220] Fedor Bezrukov. The Higgs field as an inflaton. *Class. Quant. Grav.*, 30:214001, 2013.
- [221] G.W. Gibbons and S.W. Hawking. Cosmological Event Horizons, Thermodynamics, and Particle Creation. *Phys. Rev. D*, 15:2738–2751, 1977.
- [222] K. Lake and R.C. Roeder. Effects of a Nonvanishing Cosmological Constant on the Spherically Symmetric Vacuum Manifold. *Phys. Rev. D*, 15:3513–3519, 1977.
- [223] S.W. Hawking and Don N. Page. Thermodynamics of Black Holes in anti-De Sitter Space. *Commun. Math. Phys.*, 87:577, 1983.
- [224] Hidekaz Nariai. On a New Cosmological Solution of Einstein’s Field Equations of Gravitation. *General Relativity and Gravitation*, 31:963–971, 1999.
- [225] Jiri Podolsky. The Structure of the extreme Schwarzschild-de Sitter space-time. *Gen. Rel. Grav.*, 31:1703–1725, 1999.
- [226] Alec Maassen van den Brink. Approach to the extremal limit of the Schwarzschild-de Sitter black hole. *Phys. Rev. D*, 68:047501, 2003.
- [227] Paul H. Ginsparg and Malcolm J. Perry. Semiclassical Perdurance of de Sitter Space. *Nucl. Phys. B*, 222:245–268, 1983.
- [228] Raphael Bousso and Stephen W. Hawking. (Anti)evaporation of Schwarzschild-de Sitter black holes. *Phys. Rev. D*, 57:2436–2442, 1998.
- [229] Shin’ichi Nojiri and Sergei D. Odintsov. Effective action for conformal scalars and anti-evaporation of black holes. *Int. J. Mod. Phys. A*, 14:1293–1304, 1999.
- [230] Shin’ichi Nojiri and Sergei D. Odintsov. Anti-Evaporation of Schwarzschild-de Sitter Black Holes in $F(R)$ gravity. *Class. Quant. Grav.*, 30:125003, 2013.
- [231] L. Sebastiani, D. Momeni, R. Myrzakulov, and S.D. Odintsov. Instabilities and (anti)-evaporation of Schwarzschild–de Sitter black holes in modified gravity. *Phys. Rev. D*, 88(10):104022, 2013.

- [232] Taishi Katuragawa. Anti-Evaporation of Black Holes in Bigravity. *Universe*, 1(2):158–172, 2015.
- [233] Taishi Katuragawa and Shin’ichi Nojiri. Stability and antievaporation of the Schwarzschild–de Sitter black holes in bigravity. *Phys. Rev. D*, 91(8):084001, 2015.
- [234] G.G. L. Nashed. Spherically symmetric black hole solution in mimetic gravity and anti-evaporation. *Int. J. Geom. Meth. Mod. Phys.*, 15(09):1850154, 2018.
- [235] C. Armendariz-Picon, Viatcheslav F. Mukhanov, and Paul J. Steinhardt. A Dynamical solution to the problem of a small cosmological constant and late time cosmic acceleration. *Phys. Rev. Lett.*, 85:4438–4441, 2000.
- [236] C. Armendariz-Picon, Viatcheslav F. Mukhanov, and Paul J. Steinhardt. Essentials of k essence. *Phys. Rev. D*, 63:103510, 2001.
- [237] Alberto Nicolis, Riccardo Rattazzi, and Enrico Trincherini. The Galileon as a local modification of gravity. *Phys. Rev. D*, 79:064036, 2009.
- [238] Tsutomu Kobayashi. Horndeski theory and beyond: a review. *Rept. Prog. Phys.*, 82(8):086901, 2019.
- [239] Cédric Deffayet and Danièle A. Steer. A formal introduction to Horndeski and Galileon theories and their generalizations. *Class. Quant. Grav.*, 30:214006, 2013.
- [240] C. Deffayet, Gilles Esposito-Farese, and A. Vikman. Covariant Galileon. *Phys. Rev. D*, 79:084003, 2009.
- [241] C. Deffayet, Xian Gao, D.A. Steer, and G. Zahariade. From k-essence to generalised Galileons. *Phys. Rev. D*, 84:064039, 2011.
- [242] Miguel Zumalacárregui and Juan García-Bellido. Transforming gravity: from derivative couplings to matter to second-order scalar-tensor theories beyond the Horndeski Lagrangian. *Phys. Rev. D*, 89:064046, 2014.
- [243] Jibril Ben Achour, David Langlois, and Karim Noui. Degenerate higher order scalar-tensor theories beyond Horndeski and disformal transformations. *Phys. Rev. D*, 93(12):124005, 2016.

- [244] Jérôme Gleyzes, David Langlois, Federico Piazza, and Filippo Vernizzi. Healthy theories beyond Horndeski. Phys. Rev. Lett., 114(21):211101, 2015.
- [245] Tsutomu Kobayashi, Masahide Yamaguchi, and Jun'ichi Yokoyama. Generalized G-inflation: Inflation with the most general second-order field equations. Prog. Theor. Phys., 126:511–529, 2011.
- [246] Antonio De Felice and Shinji Tsujikawa. Inflationary non-Gaussianities in the most general second-order scalar-tensor theories. Phys. Rev. D, 84:083504, 2011.
- [247] Xian Gao and Daniele A. Steer. Inflation and primordial non-Gaussianities of 'generalized Galileons'. JCAP, 12:019, 2011.
- [248] Antonio De Felice, Tsutomu Kobayashi, and Shinji Tsujikawa. Effective gravitational couplings for cosmological perturbations in the most general scalar-tensor theories with second-order field equations. Phys. Lett. B, 706:123–133, 2011.
- [249] Xian Gao, Tsutomu Kobayashi, Masahide Yamaguchi, and Jun'ichi Yokoyama. Primordial non-Gaussianities of gravitational waves in the most general single-field inflation model. Phys. Rev. Lett., 107:211301, 2011.
- [250] Christos Charmousis, Edmund J. Copeland, Antonio Padilla, and Paul M. Saffin. General second order scalar-tensor theory, self tuning, and the Fab Four. Phys. Rev. Lett., 108:051101, 2012.
- [251] Edmund J. Copeland, Antonio Padilla, and Paul M. Saffin. The cosmology of the Fab-Four. JCAP, 12:026, 2012.
- [252] Tsutomu Kobayashi. Generic instabilities of nonsingular cosmologies in Horndeski theory: A no-go theorem. Phys. Rev. D, 94(4):043511, 2016.
- [253] Luca Amendola, Martin Kunz, Mariele Motta, Ippocratis D. Saltas, and Ignacy Sawicki. Observables and unobservables in dark energy cosmologies. Phys. Rev. D, 87(2):023501, 2013.

- [254] Miguel Zumalacárregui, Emilio Bellini, Ignacy Sawicki, Julien Lesgourgues, and Pedro G. Ferreira. h_i class: Horndeski in the Cosmic Linear Anisotropy Solving System. JCAP, 08:019, 2017.
- [255] Jose María Ezquiaga and Miguel Zumalacárregui. Dark Energy After GW170817: Dead Ends and the Road Ahead. Phys. Rev. Lett., 119(25):251304, 2017.
- [256] B.P. Abbott et al. GW170817: Observation of Gravitational Waves from a Binary Neutron Star Inspiral. Phys. Rev. Lett., 119(16):161101, 2017.
- [257] B.P. Abbott et al. Gravitational Waves and Gamma-rays from a Binary Neutron Star Merger: GW170817 and GRB 170817A. Astrophys. J. Lett., 848(2):L13, 2017.
- [258] Cedric Deffayet, Gilles Esposito-Farese, and Daniele A. Steer. Counting the degrees of freedom of generalized Galileons. Phys. Rev. D, 92:084013, 2015.
- [259] Dario Bettoni, Jose María Ezquiaga, Kurt Hinterbichler, and Miguel Zumalacárregui. Speed of Gravitational Waves and the Fate of Scalar-Tensor Gravity. Phys. Rev. D, 95(8):084029, 2017.
- [260] Cedric Deffayet, Oriol Pujolas, Ignacy Sawicki, and Alexander Vikman. Imperfect Dark Energy from Kinetic Gravity Braiding. JCAP, 10:026, 2010.
- [261] Nicola Bartolo, Purnendu Karmakar, Sabino Matarrese, and Mattia Scomparin. Cosmic structures and gravitational waves in ghost-free scalar-tensor theories of gravity. JCAP, 05:048, 2018.
- [262] Ryotaro Kase and Shinji Tsujikawa. Dark energy in Horndeski theories after GW170817: A review. Int. J. Mod. Phys. D, 28(05):1942005, 2019.
- [263] A. de la Cruz-Dombriz, A. Dobado, and A.L. Maroto. Black Holes in $f(R)$ theories. Phys. Rev. D, 80:124011, 2009. [Erratum: Phys.Rev.D 83, 029903 (2011)].
- [264] Gonzalo J. Olmo and D. Rubiera-Garcia. Palatini $f(R)$ Black Holes in Nonlinear Electrodynamics. Phys. Rev. D, 84:124059, 2011.

- [265] Gonzalo J. Olmo, D. Rubiera-Garcia, and Helios Sanchis-Alepuz. Geonic black holes and remnants in Eddington-inspired Born-Infeld gravity. *Eur. Phys. J. C*, 74:2804, 2014.
- [266] A. de la Cruz-Dombriz and D. Saez-Gomez. Black holes, cosmological solutions, future singularities, and their thermodynamical properties in modified gravity theories. *Entropy*, 14:1717–1770, 2012.
- [267] Thomas P. Sotiriou and Shuang-Yong Zhou. Black hole hair in generalized scalar-tensor gravity. *Phys. Rev. Lett.*, 112:251102, 2014.
- [268] T. Clifton. Spherically Symmetric Solutions to Fourth-Order Theories of Gravity. *Class. Quant. Grav.*, 23:7445, 2006.
- [269] Nicolas Yunes and Carlos F. Sopuerta. Perturbations of Schwarzschild Black Holes in Chern-Simons Modified Gravity. *Phys. Rev. D*, 77:064007, 2008.
- [270] Vitor Cardoso and Leonardo Gualtieri. Perturbations of Schwarzschild black holes in Dynamical Chern-Simons modified gravity. *Phys. Rev. D*, 80:064008, 2009. [Erratum: *Phys.Rev.D* 81, 089903 (2010)].
- [271] Gonzalo J. Olmo, D. Rubiera-Garcia, and A. Sanchez-Puente. Geodesic completeness in a wormhole spacetime with horizons. *Phys. Rev. D*, 92(4):044047, 2015.
- [272] Gonzalo J. Olmo, D. Rubiera-Garcia, and A. Sanchez-Puente. Classical resolution of black hole singularities via wormholes. *Eur. Phys. J. C*, 76(3):143, 2016.
- [273] Cecilia Bejarano, Gonzalo J. Olmo, and Diego Rubiera-Garcia. What is a singular black hole beyond General Relativity? *Phys. Rev. D*, 95(6):064043, 2017.
- [274] Shin’ichi Nojiri and S.D. Odintsov. Regular multihorizon black holes in modified gravity with nonlinear electrodynamics. *Phys. Rev. D*, 96(10):104008, 2017.
- [275] Valerio Faraoni. The Jebsen-Birkhoff theorem in alternative gravity. *Phys. Rev. D*, 81:044002, 2010.
- [276] Kristin Schleich and Donald M. Witt. A simple proof of Birkhoff’s theorem for cosmological constant. *J. Math. Phys.*, 51:112502, 2010.

- [277] Salvatore Capozziello and Diego Saez-Gomez. Scalar-tensor representation of $f(R)$ gravity and Birkhoff's theorem. *Annalen Phys.*, 524:279–285, 2012.
- [278] J.W. Moffat. Modified Gravity Black Holes and their Observable Shadows. *Eur. Phys. J. C*, 75(3):130, 2015.
- [279] Anne-Christine Davis, Ruth Gregory, Rahul Jha, and Jessica Muir. Astrophysical black holes in screened modified gravity. *JCAP*, 08:033, 2014.
- [280] Minyong Guo, Niels A. Obers, and Haopeng Yan. Observational signatures of near-extremal Kerr-like black holes in a modified gravity theory at the Event Horizon Telescope. *Phys. Rev. D*, 98(8):084063, 2018.
- [281] Eugeny Babichev, Christos Charmousis, and Antoine Lehébel. Asymptotically flat black holes in Horndeski theory and beyond. *JCAP*, 04:027, 2017.
- [282] Oliver J. Tattersall and Pedro G. Ferreira. Quasinormal modes of black holes in Horndeski gravity. *Phys. Rev. D*, 97(10):104047, 2018.
- [283] Eugeny Babichev, Christos Charmousis, and Antoine Lehébel. Black holes and stars in Horndeski theory. *Class. Quant. Grav.*, 33(15):154002, 2016.
- [284] Eugeny Babichev, Christos Charmousis, Antoine Lehébel, and Tetiana Moskalets. Black holes in a cubic Galileon universe. *JCAP*, 09:011, 2016.
- [285] Oliver J. Tattersall, Pedro G. Ferreira, and Macarena Lagos. Speed of gravitational waves and black hole hair. *Phys. Rev. D*, 97(8):084005, 2018.
- [286] Eugeny Babichev, Christos Charmousis, Gilles Esposito-Farèse, and Antoine Lehébel. Stability of Black Holes and the Speed of Gravitational Waves within Self-Tuning Cosmological Models. *Phys. Rev. Lett.*, 120(24):241101, 2018.
- [287] Apratim Ganguly, Radouane Gannouji, Manuel Gonzalez-Espinoza, and Carlos Pizarro-Moya. Black hole stability under odd-parity perturbations in Horndeski gravity. *Class. Quant. Grav.*, 35(14):145008, 2018.

- [288] Jeremy Sakstein, Eugeny Babichev, Kazuya Koyama, David Langlois, and Ryo Saito. Towards Strong Field Tests of Beyond Horndeski Gravity Theories. *Phys. Rev. D*, 95(6):064013, 2017.
- [289] Hiromu Ogawa, Tsutomu Kobayashi, and Teruaki Suyama. Instability of hairy black holes in shift-symmetric Horndeski theories. *Phys. Rev. D*, 93(6):064078, 2016.
- [290] Antoine Lehébel, Eugeny Babichev, and Christos Charmousis. A no-hair theorem for stars in Horndeski theories. *JCAP*, 07:037, 2017.
- [291] Áron D. Kovács and Harvey S. Reall. Well-posed formulation of Lovelock and Horndeski theories. *Phys. Rev. D*, 101(12):124003, 2020.
- [292] Anna Ijjas, Frans Pretorius, and Paul J. Steinhardt. Stability and the Gauge Problem in Non-Perturbative Cosmology. *JCAP*, 01:015, 2019.
- [293] Anna Ijjas. Space-time slicing in Horndeski theories and its implications for non-singular bouncing solutions. *JCAP*, 02:007, 2018.
- [294] Karl Martel and Eric Poisson. Gravitational perturbations of the Schwarzschild space-time: A Practical covariant and gauge-invariant formalism. *Phys. Rev. D*, 71:104003, 2005.
- [295] Masashi Kimura. Stability analysis of Schwarzschild black holes in dynamical Chern-Simons gravity. *Phys. Rev. D*, 98(2):024048, 2018.
- [296] Pei-Ken Hung, Jordan Keller, and Mu-Tao Wang. Linear Stability of Schwarzschild Spacetime: Decay of Metric Coefficients. *J. Diff. Geom.*, 116(3):481–541, 2020.
- [297] E. Abdalla, K. H. C. Castello-Branco, and A. Lima-Santos. Support of dS / CFT correspondence from space-time perturbations. *Phys. Rev. D*, 66:104018, 2002.
- [298] M. S. Morris and K. S. Thorne. Wormholes in space-time and their use for interstellar travel: A tool for teaching general relativity. *Am. J. Phys.*, 56:395, 1988.
- [299] M. R. Finch and J. E. F. Skea. A review of the relativistic static fluid sphere. unpublished, 1998.

- [300] P. Boonserm and M. Visser. Buchdahl-like transformations for perfect fluid spheres. Int. J. Mod. Phys. D, 17:135–163, 2008.
- [301] P. Boonserm and M. Visser. Buchdahl-like transformations in general relativity. Thai Journal of Mathematics, 5 # 2:209–223, 2007.
- [302] M. S. Morris, K. S. Thorne, and U. Yurtsever. Wormholes, time machines, and the weak energy condition. Phys. Rev. Lett., 61, 1988.
- [303] David Hochberg and Matt Visser. General dynamic wormholes and violation of the null energy condition. In Advanced School on Cosmology and Particle Physics (ASCPP 98), 6 1998.
- [304] M. Visser. Lorentzian wormholes: From Einstein to Hawking. AIP, Woodbury, USA, 1995.
- [305] F. S. N. Lobo. Wormholes, Warp Drives and Energy Conditions. Fundam. Theor. Phys. **189**, pp. (formerly Lecture Notes in Physics), Springer Nature Switzerland AG, 2017.
- [306] M. Visser. Traversable wormholes from surgically modified schwarzschild space-times. Nucl. Phys. B, 328, 1989.
- [307] M. Visser. Traversable wormholes: Some simple examples. Phys. Rev. D, 39, 1989.
- [308] E. Poisson and M. Visser. Thin shell wormholes: Linearization stability. Phys. Rev. D, 52, 1995.
- [309] F. S. N. Lobo and P. Crawford. Linearized stability analysis of thin shell wormholes with a cosmological constant. Class. Quant. Grav., 21:391–404, 2004.
- [310] F. S. N. Lobo. Energy conditions, traversable wormholes and dust shells. Gen. Rel. Grav., 37:2023–2038, 2005.
- [311] F. S. N. Lobo and P. Crawford. Stability analysis of dynamic thin shells. Class. Quant. Grav., 22:4869–4886, 2005.

- [312] N. Montelongo-García, F. S. N. Lobo, and M. Visser. Generic spherically symmetric dynamic thin-shell traversable wormholes in standard general relativity. *Phys. Rev. D*, 86, 2012.
- [313] M. Bouhmadi-López, F. S. N. Lobo, and P. Martín-Moruno. Wormholes minimally violating the null energy condition. *JCAP*, 11, 2014.
- [314] F. S. N. Lobo, A. Simpson, and M. Visser. Dynamic thin-shell black-bounce traversable wormholes. *Phys. Rev. D*, 101(12), 2020.
- [315] T. Berry, F. S. N. Lobo, A. Simpson, and M. Visser. Thin-shell traversable wormhole crafted from a regular black hole with asymptotically minkowski core. *Phys. Rev. D*, 102, 2020.
- [316] S. Kar. Evolving wormholes and the weak energy condition. *Phys. Rev. D*, 49:862–865, 1994.
- [317] S. Kar and D. Sahdev. Evolving lorentzian wormholes. *Phys. Rev.D*, 53, 1996.
- [318] Mahdi Kord Zangeneh, Francisco S. N. Lobo, and Hooman Moradpour. Evolving traversable wormholes satisfying the energy conditions in the presence of pole dark energy. *Phys. Dark Univ.*, 31:100779, 2021.
- [319] Mahdi Kord Zangeneh and Francisco S. N. Lobo. Dynamic wormhole geometries in hybrid metric-Palatini gravity. *Eur. Phys. J. C*, 81(4):285, 2021.
- [320] F. S. N. Lobo. General class of wormhole geometries in conformal weyl gravity. *Class. Quant. Grav.*, 25, 2008.
- [321] F. S. N. Lobo and M. A. Oliveira. Wormhole geometries in $f(r)$ modified theories of gravity. *Phys. Rev. D*, D80, 2009.
- [322] N. Montelongo-García and F. S. N. Lobo. Wormhole geometries supported by a nonminimal curvature-matter coupling. *Phys. Rev. D*, D82, 2010.
- [323] N. Montelongo-García and F. S. N. Lobo. Nonminimal curvature-matter coupled wormholes with matter satisfying the null energy condition. *Class. Quant. Grav.*, 28, 2011.

- [324] C. G. Boehmer, T. Harko, and F. S. N. Lobo. Wormhole geometries in modified teleparallel gravity and the energy conditions. *Phys. Rev. D*, 85, 2012.
- [325] T. Harko, F. S. N. Lobo, M. K. Mak, and S. V. Sushkov. Modified-gravity wormholes without exotic matter. *Phys. Rev. D*, 87(6), 2013.
- [326] M. R. Mehdizadeh, M. Kord Zangeneh, and F. S. N. Lobo. Einstein-gauss-bonnet traversable wormholes satisfying the weak energy condition. *Phys. Rev. D*, 91(8), 2015.
- [327] M. Kord Zangeneh, F. S. N. Lobo, and M. H. Dehghani. Traversable wormholes satisfying the weak energy condition in third-order loveclock gravity. *Phys. Rev. D*, 92(12), 2015.
- [328] J. L. Rosa, J. P. S. Lemos, and F. S. N. Lobo. Wormholes in generalized hybrid metric-palatini gravity obeying the matter null energy condition everywhere. *Phys. Rev. D*, 98(6), 2018.
- [329] M. J. Lazo, J. Paiva, J. T. S. Amaral, and G. S. F. Frederico. Action principle for action-dependent lagrangians toward nonconservative gravity: Accelerating universe without dark energy. *Phys. Rev. D*, 95(10), 2017.
- [330] G. Herglotz and Lectures Berührungstransformationen. at the university of göttingen. Göttingen, 1930.
- [331] R.B. Guenther, C.M. Guenther, and J.A. Gottsch. The Herglotz Lectures on Contact Transformations and Hamiltonian Systems. Lecture Notes in Nonlinear Analysis. Juliusz Schauder Center for Nonlinear Studies. Nicholas Copernicus University, 1995.
- [332] Ricardo Almeida. A scale variational principle of herglotz, 2016.
- [333] J. C. Fabris, H. Velten, T. R. P. Caramês, M. J. Lazo, and G. S. F. Frederico. Cosmology from a new nonconservative gravity. *Int. J. Mod. Phys. D*, 27(6), 2018.
- [334] J. C. Fabris, T. R. P. Caramês, and J. M. Hoff Da Silva. Braneworld gravity within non-conservative gravitational theory. *Eur. Phys. J. C*, 78(5), 2018.
- [335] E. A. F. Bragança, T. R. P. Caramês, J. C. Fabris, and A. d. Santos. Some effects of non-conservative gravity on cosmic string configurations,. *Eur. Phys. J. C*, 79(2), 2019.

- [336] T. R. P. Caramês, H. Velten, J. C. Fabris, and M. J. Lazo. Dark energy with zero pressure: Accelerated expansion and large scale structure in action-dependent lagrangian theories. Phys. Rev. D, 98(10), 2018.
- [337] J. C. Fabris, H. Velten, and A. Wojnar. Existence of static spherically-symmetric objects in action-dependent lagrangian theories. Phys. Rev. D, 99(12), 2019.
- [338] Juilson A. P. Paiva, Matheus J. Lazo, and Vilson T. Zanchin. Generalized nonconservative gravitational field equations from Herglotz action principle. 8 2021.
- [339] S. V. Sushkov and R. Korolev. Scalar wormholes with nonminimal derivative coupling. Class. Quant. Grav., 29, 2012.
- [340] H. G. Ellis. Ether flow through a drainhole: A particle model in general relativity. J. Math. Phys., 14:104, 1973.
- [341] H. G. Ellis. The evolving, flowless drain hole: a nongravitating particle model in general relativity theory. Gen. Rel. Grav., 10:105–123, 1979.
- [342] K. A. Bronnikov. Scalar-tensor theory and scalar charge. Acta Phys. Pol. B, 4:251, 1973.
- [343] H. G. Ellis. Ether flow through a drainhole - a particle model in general relativity. J. Math. Phys., 14:104–118, 1973.
- [344] K. A. Bronnikov. Scalar-tensor theory and scalar charge. Acta Phys. Polon. B, 4:251–266, 1973.
- [345] A. Simpson and M. Visser. Black-bounce to traversable wormhole. JCAP, 02, 2019.
- [346] Francisco S. N. Lobo, Manuel E. Rodrigues, Marcos V. de S. Silva, Alex Simpson, and Matt Visser. Novel black-bounce spacetimes: wormholes, regularity, energy conditions, and causal structure. Phys. Rev. D, 103(8):084052, 2021.
- [347] Savvas Nesseris and Juan Garcia-Bellido. Is the Jeffreys' scale a reliable tool for Bayesian model comparison in cosmology? JCAP, 1308:036, 2013.
- [348] Roberto Trotta. Bayesian Methods in Cosmology. In 1701.01467[astro-ph.CO], 1 2017.

- [349] MacKay, David J. C. Information Theory, Inference & Learning Algorithms. Cambridge University Press, USA, 2002.
- [350] H. Jeffreys. Theory of Probability. Oxford, Oxford, England, third edition, 1961.
- [351] Pia Mukherjee, David Parkinson, and Andrew R. Liddle. A nested sampling algorithm for cosmological model selection. Astrophys. J. Lett., 638:L51–L54, 2006.
- [352] M. W. Feast and R. M. Catchpole. The Cepheid period-luminosity zero-point from HIP-PARCOS trigonometrical parallaxes. Mon. Not. Roy. Astron. Soc., 286:L1–L5, 1997.
- [353] Floor van Leeuwen, Michael W. Feast, Patricia A. Whitelock, and Clifton D. Laney. Cepheid Parallaxes and the Hubble Constant. Mon. Not. Roy. Astron. Soc., 379:723–737, 2007.
- [354] A. Conley et al. Supernova Constraints and Systematic Uncertainties from the First 3 Years of the Supernova Legacy Survey. Astrophys. J. Suppl., 192:1, 2011.
- [355] D. M. Scolnic et al. The Complete Light-curve Sample of Spectroscopically Confirmed SNe Ia from Pan-STARRS1 and Cosmological Constraints from the Combined Pantheon Sample. Astrophys. J., 859(2):101, 2018.
- [356] Raul Jimenez and Abraham Loeb. Constraining cosmological parameters based on relative galaxy ages. Astrophys. J., 573:37–42, 2002.
- [357] Michele Moresco, Raul Jimenez, Andrea Cimatti, and Lucia Pozzetti. Constraining the expansion rate of the Universe using low-redshift ellipticals as cosmic chronometers. JCAP, 03:045, 2011.
- [358] M. Moresco et al. Improved constraints on the expansion rate of the Universe up to $z \sim 1.1$ from the spectroscopic evolution of cosmic chronometers. JCAP, 08:006, 2012.
- [359] Michele Moresco, Lucia Pozzetti, Andrea Cimatti, Raul Jimenez, Claudia Maraston, Licia Verde, Daniel Thomas, Annalisa Citro, Rita Tojeiro, and David Wilkinson. A 6% measurement of the Hubble parameter at $z \sim 0.45$: direct evidence of the epoch of cosmic re-acceleration. JCAP, 1605(05):014, 2016.

- [360] Michele Moresco. Raising the bar: new constraints on the Hubble parameter with cosmic chronometers at $z \sim 2$. *Mon. Not. Roy. Astron. Soc.*, 450(1):L16–L20, 2015.
- [361] Yun Wang and Mi Dai. Exploring uncertainties in dark energy constraints using current observational data with Planck 2015 distance priors. *Phys. Rev.*, D94(8):083521, 2016.
- [362] Wayne Hu and Naoshi Sugiyama. Small scale cosmological perturbations: An analytic approach. *Astrophys.J.*, 471:542–570, 1996.
- [363] Yun Wang and Shuang Wang. Distance Priors from Planck and Dark Energy Constraints from Current Data. *Phys. Rev. D*, 88(4):043522, 2013. [Erratum: *Phys.Rev.D* 88, 069903 (2013)].
- [364] Zhongxu Zhai and Yun Wang. Robust and model-independent cosmological constraints from distance measurements. *JCAP*, 1907(07):005, 2019.
- [365] E. Komatsu et al. Five-Year Wilkinson Microwave Anisotropy Probe (WMAP) Observations: Cosmological Interpretation. *Astrophys. J. Suppl.*, 180:330–376, 2009.
- [366] Chris Blake et al. The WiggleZ Dark Energy Survey: mapping the distance-redshift relation with baryon acoustic oscillations. *Mon. Not. Roy. Astron. Soc.*, 418:1707–1724, 2011.
- [367] Chris Blake et al. The WiggleZ Dark Energy Survey: Joint measurements of the expansion and growth history at $z < 1$. *Mon. Not. Roy. Astron. Soc.*, 425:405–414, 2012.
- [368] Shadab Alam et al. The clustering of galaxies in the completed SDSS-III Baryon Oscillation Spectroscopic Survey: cosmological analysis of the DR12 galaxy sample. *Mon. Not. Roy. Astron. Soc.*, 470(3):2617–2652, 2017.
- [369] Daniel J. Eisenstein and Wayne Hu. Baryonic features in the matter transfer function. *Astrophys. J.*, 496:605, 1998.
- [370] Metin Ata et al. The clustering of the SDSS-IV extended Baryon Oscillation Spectroscopic Survey DR14 quasar sample: first measurement of baryon acoustic oscillations between redshift 0.8 and 2.2. *Mon. Not. Roy. Astron. Soc.*, 473(4):4773–4794, 2018.

- [371] Victoria de Sainte Agathe et al. Baryon acoustic oscillations at $z = 2.34$ from the correlations of $\text{Ly}\alpha$ absorption in eBOSS DR14. *Astron. Astrophys.*, 629:A85, 2019.
- [372] Seshadri Nadathur, Paul M. Carter, Will J. Percival, Hans A. Winther, and Julian Bautista. Beyond BAO: Improving cosmological constraints from BOSS data with measurement of the void-galaxy cross-correlation. *Phys. Rev.*, D100(2):023504, 2019.
- [373] Jose Beltrán Jiménez, Lavinia Heisenberg, and Tomi S. Koivisto. The Geometrical Trinity of Gravity. *Universe*, 5(7):173, 2019.
- [374] Jose Beltrán Jiménez, Lavinia Heisenberg, Damianos Iosifidis, Alejandro Jiménez-Cano, and Tomi S. Koivisto. General teleparallel quadratic gravity. *Phys. Lett. B*, 805:135422, 2020.
- [375] Igor Mol. The Non-Metricity Formulation of General Relativity. *Adv. Appl. Clifford Algebras*, 27(3):2607–2638, 2017.
- [376] Laur Järv, Mihkel Rünkla, Margus Saal, and Ott Vilson. Nonmetricity formulation of general relativity and its scalar-tensor extension. *Phys. Rev. D*, 97(12):124025, 2018.
- [377] J.W. Maluf. Hamiltonian formulation of the teleparallel description of general relativity. *J. Math. Phys.*, 35:335–343, 1994.
- [378] Jose W. Maluf. Localization of energy in general relativity. *J. Math. Phys.*, 36:4242–4247, 1995.
- [379] V.C. de Andrade and J.G. Pereira. Gravitational Lorentz force and the description of the gravitational interaction. *Phys. Rev. D*, 56:4689–4695, 1997.
- [380] Uwe Muench, Frank Gronwald, and Friedrich W. Hehl. A Small guide to variations in teleparallel gauge theories of gravity and the Kaniel-Itin model. *Gen. Rel. Grav.*, 30:933–961, 1998.
- [381] Kenji Hayashi and Takeshi Shirafuji. New General Relativity. *Phys. Rev. D*, 19:3524–3553, 1979. [Addendum: *Phys.Rev.D* 24, 3312–3314 (1982)].

- [382] Eckehard W. Mielke. Ashtekar's complex variables in general relativity and its teleparallelism equivalent. Annals Phys., 219:78–108, 1992.
- [383] F. W. Hehl and G. D. Kerlick. Metric-affine variational principles in general relativity. I. Riemannian space-time. General Relativity and Gravitation, 9(8):691–710, August 1978.
- [384] R. Weitzenböck. Invariantentheorie. Noordhoff, Gronningen, 1923.
- [385] Ruben Aldrovandi and José Geraldo Pereira. Teleparallel Gravity: An Introduction, volume 173. Springer, 2013.
- [386] James M. Nester and Hwei-Jang Yo. Symmetric teleparallel general relativity. Chin. J. Phys., 37:113, 1999.
- [387] Ruth Lazkoz, Francisco S. N. Lobo, María Ortiz-Baños, and Vincenzo Salzano. Observational constraints of $f(Q)$ gravity. Phys. Rev. D, 100(10):104027, 2019.
- [388] Jose Beltrán Jiménez, Lavinia Heisenberg, Tomi Sebastian Koivisto, and Simon Pekar. Cosmology in $f(Q)$ geometry. Phys. Rev. D, 101(10):103507, 2020.
- [389] Jose Beltrán Jiménez, Lavinia Heisenberg, and Tomi S. Koivisto. Teleparallel Palatini theories. JCAP, 1808(08):039, 2018.
- [390] Bruno J. Barros, Tiago Barreiro, Tomi Koivisto, and Nelson J. Nunes. Testing $F(Q)$ gravity with redshift space distortions. Phys. Dark Univ., 30:100616, 2020.
- [391] Ruth Lazkoz, Vincenzo Salzano, and Irene Sendra. Oscillations in the dark energy EoS: new MCMC lessons. Phys. Lett., B694:198–208, 2011.
- [392] S. Capozziello, R. Lazkoz, and V. Salzano. Comprehensive cosmographic analysis by Markov Chain Method. Phys. Rev., D84:124061, 2011.
- [393] Matt Visser. Cosmography: Cosmology without the Einstein equations. Gen. Rel. Grav., 37:1541–1548, 2005.
- [394] Celine Cattoen and Matt Visser. The Hubble series: Convergence properties and redshift variables. Class. Quant. Grav., 24:5985–5998, 2007.

- [395] Alexei A. Starobinsky. How to determine an effective potential for a variable cosmological term. JETP Lett., 68:757–763, 1998.
- [396] Takashi Nakamura and Takeshi Chiba. Determining the equation of state of the expanding universe: Inverse problem in cosmology. Mon. Not. Roy. Astron. Soc., 306:696–700, 1999.
- [397] Dragan Huterer and Michael S. Turner. Prospects for probing the dark energy via supernova distance measurements. Phys. Rev. D, 60:081301, 1999.
- [398] Ruth Lazkoz and Elisabetta Majerotto. Cosmological constraints combining $H(z)$, CMB shift and SNIa observational data. JCAP, 07:015, 2007.
- [399] G. R. Dvali, Gregory Gabadadze, and Massimo Porrati. 4-D gravity on a brane in 5-D Minkowski space. Phys. Lett. B, 485:208–214, 2000.
- [400] W. Israel. Singular hypersurfaces and thin shells in general relativity. Nuovo Cimento B Serie, 44(1):1–14, July 1966.
- [401] Pierre Binétruy, Cedric Deffayet, and David Langlois. Nonconventional cosmology from a brane universe. Nucl. Phys. B, 565:269–287, 2000.
- [402] Cedric Deffayet. Cosmology on a brane in Minkowski bulk. Phys. Lett. B, 502:199–208, 2001.
- [403] Ismael Ayuso, Ruth Lazkoz, and Vincenzo Salzano. Observational constraints on cosmological solutions of $f(Q)$ theories. Phys. Rev. D, 103(6):063505, 2021.
- [404] Ruth Lazkoz, Roy Maartens, and Elisabetta Majerotto. Observational constraints on phantom-like braneworld cosmologies. Phys. Rev. D, 74:083510, 2006.
- [405] Alessandro Melchiorri, Luca Pagano, and Stefania Pandolfi. When Did Cosmic Acceleration Start ? Phys. Rev. D, 76:041301, 2007.